Genetic predisposition to genomic instability in cancer.

Thesis

UNRESTRICTED

Genetic Predisposition to Genomic Instability in Cancer

Volume 1 of 2

A thesis submitted for the degree of
Doctor of Philosophy

(Pertaining to the Discipline of Molecular Oncology)

Dr Carina Jayne Vessey
MA, MSc, BM BCh, Dip RCPath

Institute of Molecular Medicine,
Oxford,
Sponsoring Establishment for
The Open University.

Submission date 24/8/98
Date of award 20th October 1998

ProQuest LLC.
789 East Eisenhower Parkway
P.O. Box 1346
Ann Arbor, MI 48106 – 1346

ABSTRACT

Ataxia telangiectasia and Bloom's syndrome are cancer prone genomic instability disorders for which the causative genes *ATM* and *BLM* have only recently been identified. The cellular localisation and biochemical roles of these proteins are currently being defined. ATM shares sequence homology with several lipid and protein kinases but at the outset of this work a kinase function for ATM itself was not established and the extent to which the kinase domain contributed to the cellular phenotype of A-T was unknown. In addition the role of ATM heterozygosity and genomic instability in breast cancer had been suggested but not elucidated.

During the course of this work, the anti-ATM antibody (CN-12) and anti-BLM antibody (IHIC-27), were developed and affinity purified. Antibody CN-12 successfully demonstrated the presence of the 350 kDa ATM protein by immunoblotting and immunoprecipitation in HeLa cells. The protein was largely nuclear in localisation with a minor microsomal fraction but was found to be absent in AT2RO cells which contain a homozygous truncating mutation of ATM. Tumour cell lines provided by the NCI showed varying expression of ATM except for the promyelocytic leukaemia cell line HL60 in which no ATM was detected. Antibody IHIC-27 demonstrated the presence of a 180 kDa protein in HeLa cells which was absent in the Bloom's cell line GM8505. Studies using antibodies directed to the C and N-termini showed BLM instability and cell fractionation studies demonstrated that the protein was nuclear in localisation. Anti-BLM monoclonal antibodies 185a and 32e were able to identify the fusion protein to which they were raised and BLM immunoprecipitated by IHIC-27 but could not identify BLM in whole cell lysates. Neither ATM nor BLM antibodies were useful for immunohistochemical studies with the protocols tested despite successful immunostaining of the positive control.

Studies of immunoprecipitated ATM using a variety of assay conditions with p53 peptides and PHAS-I as substrates did not reveal any serine/threonine protein kinase activity, although low levels of autophosphorylation were identified. H1299 cells transfected with a mutant *ATM* kinase domain did not exhibit a dominant negative phenotype, which curtailed further studies of the cellular function of the domain.

DNA repair in peripheral blood lymphocytes from breast cancer patients and controls was assessed by the comet assay. Although the patients generally showed less DNA repair than the controls at 30 min and 120 min, the difference was not found to be statistically significant.

AIMS

The general purpose of this work was to elucidate the mechanisms underlying the genomic instability seen in ataxia-telangiectasia, Bloom's syndrome and breast cancer by studying the gene products of *ATM* and *BLM* and by investigating the DNA repair capacity in breast cancer patients.

The specific goals are listed below:

1) To raise and characterise polyclonal antibodies versus ATM and BLM proteins which are abnormal in the genetic instability disorders ataxia-telangiectasia and Bloom's syndrome respectively.

2) To determine the levels of expression of these proteins in normal and tumour cell lines and in the tissue from a variety of human tumours.

3) To investigate the putative protein kinase activity of ATM protein with a view to developing an ATM kinase assay for use in determining the integrity of ATM signalling in the lymphocytes of normal women and women with breast cancer. It was hoped that this would enable the development of a test to determine an individuals risk of breast cancer.

4) To investigate the role of the ATM kinase domain in the cellular phenotype of ATM using a dominant negative strategy.

5) To examine the constitutional ability of DNA repair in lymphocytes from normal women and women with breast cancer using the comet assay. The intention was to assess the importance of DNA repair defects as a cause of genomic instability in the aetiology of this disease and to identify differences between the two populations which would be useful as a test of an individuals potential risk of developing breast cancer.

To My Parents

Acknowledgements

Firstly, I would like to thank Chris Norbury for his thoughtfulness and boundless patience as my supervisor throughout my fellowship. I have disturbed him from his desk and bench on innumerable occasions and he has never shown the slightest exasperation. His advice and practical guidance is extremely highly valued by many in the IMM, as evidenced by the frequent queue at his door and I feel very fortunate to have been one of his students. I am also indebted to Adrian Harris for informal discussions and for many helpful suggestions relating to my work which provided me with a new direction in my final year.

Although I fared very well in terms of supervision, I could not have completed this thesis without the support of my laboratory colleagues and friends. To single any one out is difficult but in the early days I relied on Nick Wells and Charles Redwood in particular for hands on advice about the difficulties of recombinant protein production and purification. Later on Sue Houlbrook patiently helped me with the comet assay. When work was at a low point I was extremely grateful for the combined efforts of Ronjon Chakraverty, Richard Isaacs, Dom Moloney, Lisa Williams, Zoe Winters and Nick Watkin for keeping me sane.

I would also like to mention that my breast cancer study would have been impossible to conduct without the help of Margaret Dean, who took the all the blood samples, the Breast Care Sisters, Sarah Babb and Andrea Gamble and all the patients and volunteers in the IMM who participated.

In addition, my thanks extend outside the IMM to Professor Yosef Shiloh, Professor John Lawrence, Dr Andrew Sutcliffe and Dr Michael James for the reagents they generously provided. Mike Bradburn also deserves a special mention for helping me with statistics during my time in Oxford. Through my work, I have also been fortunate enough to meet Louise Izatt who has been both a colleague and a friend since we visited the Baltimore Ataxia telangiectasia conference together in 1997.

Finally I would like to pay tribute to the Medical Research Council for funding me once more, this time as a Clinical Training Fellow. Without their generosity my training in practical science would have been impoverished and I would have missed out on the opportunity of working in this exciting and important field.

Contents

List of Figures

Chapter 1:

Chapter 2:

Chapter 3:

Chapter 4:

Chapter 5:

Chapter 6:

List of Tables

Chapter 1:

Chapter 2:

No tables.

Chapter 3:

Chapter 4:

Chapter 5:

No tables.

Chapter 6:

Abbreviations

ATP	adenosine triphosphate
ADP	adenosine diphosphate
BSA	bovine serum albumin
bp	base pair
cDNA	complementary deoxyribonucleic acid
dNTP	deoxy-nucleotide triphosphate
DMSO	dimethyl sulphoxide
dsb	DNA double strand break
FACS	Fluorescent activated cell sorting
FCS	foetal calf serum
HRP	horse radish peroxidase
IMM	Institute of Molecular Medicine
IR	ionising radiation
kb	kilobase pair
kDa	kilodalton
PCR	polymerase chain reaction
PAGE	polyacrylamide gel electrophoresis
PBL	peripheral blood lymphocytes
PBS	phosphate buffered saline
mRNA	messenger ribonucleic acid
SDS	sodium dodecylsulphate
s	second
min	minute
Gy	Gray
ssb	DNA single strand break
U	unit
µl	microlitre
µg	microgram
UVL	ultra violet light
γ radiation	gamma radiation
M/HDC	moderate to highly damaged comet
rpm	revolutions per minute
2% RPMI	RPMI medium with 2% bicarbonate
v/v	volume for volume
w/v	weight for volume

Thesis Plan

This thesis comprises four results chapters which are broadly related to the theme of genomic instability in cancer but which are quite different in their individual content. The overall plan of the thesis reflects this by the provision of a general introduction concerning genetic predisposition to genome instability in cancer and a general materials and methods section, followed by results chapters with their own specific shorter introductions, additional methods and individual discussions. It is hoped that this format will make the thesis content easier to digest and scrutinise as information specific to each chapter is presented within the chapter itself.

Chapter 1

General Introduction

Genetic predisposition to genome instability in cancer

The studies presented in this thesis are related by the common theme of genomic instability and cancer. This introduction aims to provide an overview of the subject and its involvement in the development of breast cancer in particular. A brief summary of the importance of genomic stability is given followed by a description of the classical cancer prone genomic instability disorders. Specific attention is paid to ataxia telangiectasia, Bloom's syndrome and the molecular biology of breast cancer including genomic instability and DNA repair, as these are the subject of the investigations performed.

The importance of genomic integrity

The stability of an organism's genome is an absolute necessity for faithful transmission of genetic information. This is of prime importance both in mitosis during the lifetime of an organism, so that daughter cells behave and function appropriately, and in meiosis for maintenance of the species as a distinct genetic entity.

The term genomic instability has been used in several different contexts in the literature to describe genetic, cytogenetic and phenotypic changes in the cell. Therefore the endpoints of the studies which have been performed to analyse genomic instability include DNA sequence changes (deletions, insertions, point mutations etc), chromosomal aberrations (gaps, breaks, translocations, chromosomal rearrangements) and cellular transformation respectively. Although ultimately it will be best to consider genomic instability at the genetic level (as chromosomal and cell behavioural abnormalities are ultimately due to genetic change), instability at the

chromosomal level is not necessarily accompanied by sequence instability and vice versa. Therefore cells may be subject to different types of genetic instability , achieved by different molecular pathways.

It has been established over the past few decades that cancer is a genetic disease at the cellular level, and the transformation of a normal cell into a cancer cell is known to be a multistep process. This is well illustrated in sporadic colon cancer which follows the accumulation of mutations in at least 7 different genes (Kinzler and Vogelstein, 1996). This may take some time to occur, in part explaining the emergence of tumours late in life. In view of the requirement for multiple genetic changes, it has been suggested that genetic instability is the driving force behind the acquisition of the multiple mutations required for tumorigenesis (Nowell, 1976), (Loeb, 1991). It would therefore be of considerable interest to discover how common genetic instability is in tumours and whether its presence is essential. This thesis is primarily concerned with the inherited cancer prone disorders which are associated with such gross instability at the DNA and chromosomal level that the instability itself is a defining feature of the syndrome. Such syndromes include ataxia-telangiectasia (A-T), Bloom's syndrome (BS), Nijmegen breakage syndrome (NBS), Fanconi anaemia (FA), hereditary non-polyposis colon cancer (HNPCC) and its variants and finally xeroderma pigmentosum (XP) and its variants. Xeroderma pigmentosum is included because genetic instability is a recognised feature of this syndrome and the defective genes are better characterised in terms of function than the genes involved in the other syndromes. Patients with genomic instability disorders are of great interest to the molecular biologist and oncologist alike because they offer an opportunity

to investigate the molecular mechanisms which are fundamental to the maintenance of genomic integrity and the prevention of cancer.

Likely candidate genes involved in the maintenance of genomic integrity include those required for 1) the fidelity of DNA replication, 2) the detection of and the coordination of the response to DNA damage (this damage may be caused by internally or externally generated agents eg products of oxidative metabolism, irradiation and genotoxic chemicals), 3) pathways of DNA repair, 4) cell cycle checkpoint integrity and 5) appropriate apoptotic responses to deal with cells which are irredeemably damaged.

These processes will be discussed in as far as they relate to known defects in the cancer prone disorders mentioned. There has been considerable interest in this field in recent years and different aspects of the subject have been reviewed previously (Honchel et al., 1995), (Tlsty et al., 1995), (ap Rhys and Bohr, 1996), (Lindahl, 1996), (Sarasin and Stary, 1997), (Miyagawa, 1998).

Ataxia telangiectasia (A-T)

Clinical manifestations

Ataxia telangiectasia is a rare autosomal recessive syndrome with an birth incidence of about 1: 300,000 (Swift et al., 1986), (Woods et al., 1990). It is a pleiotropic disorder affecting many organ systems. The ataxia is cerebellar in nature and is due to death of Purkinje cells in the cerebellum, causing incoordination of eye, head, trunk and limb movement which generally renders the sufferer wheelchair bound by the teenage years. The telangiectasia develops in childhood and tortuous, dilated thin walled blood vessels appear

on the conjunctivae of the eyes and on other sun-exposed areas. α-feto-protein levels are elevated which, along with the ataxia and telangiectasia support the diagnosis.

Infections of the respiratory tract (eg pneumonia) are the most common cause of mortality in A-T patients; These are due to defects in both cell mediated and humoral immunity. There are deficiencies of IgA and IgE together with abnormal T and B cell responses due to problems with lymphocyte maturation and compromised intracellular signal transduction (Lavin and Shiloh, 1996). Approximately 10 % of A-T patients develop malignancy and there is a 250-fold excess risk for lymphomas and a 70-fold excess risk for leukaemias (Morrell et al., 1986). The commonest lymphoid malignancies are mature T-cell leukaemias (Taylor, 1992), although there is also an increased predisposition to B cell tumours. Other tumour types arising in this syndrome include gastric, liver, pancreatic, ovarian, breast and salivary gland cancers (Swift et al., 1987), and malignancy constitutes another major cause of death. Another hallmark of the condition noted when patients first received radiotherapy as treatment for tumours is the dramatic tissue radiosensitivity seen after standard radiotherapy doses (Cunliffe et al., 1975). This can result in severe tissue necrosis with life threatening consequences and has necessitated a reduction in the given dose. This radiosensitivity is also reflected in the reduced clonogenic survival of A-T cells in culture post irradiation. A-T heterozygotes (~1% of the general population) are believed to a have a 3-4 times increased risk of developing cancer. The risk of breast cancer in heterozygote women may be up to five fold greater than that for normal women and this is discussed in more detail later.

Cytogenetic features and predisposition to leukaemias

The dramatically increased cancer risk in homozygotes is at least in part due to genomic instability. Cells from homozygotes show striking chromosomal instability with increased rates of chromosomal aberrations including chromosome losses, gaps, breaks, inversions, translocations, telomere-telomere fusions and increased rates of intrachromosomal recombination. This genetic instability is seen spontaneously presumably as a result of intracellular genotoxic insults, and is exacerbated after treatment of the cells with ionising radiation, radiomimetic chemicals (eg bleomycin, streptonigrin and some restriction enzymes. Cytogenetic studies have shown a significant increase in the number of chromosome breaks in A-T cells post irradiation (Taylor, 1978), (Cornforth and Bedford, 1985). About 10% of all T lymphocytes in A-T patients show translocations and inversions at specific breakpoints involving chromosomes 7 and 14. These include inv(7)(p13q35), t(7;7)(p13;q35), t(7;14)(p13;q11), t(7;14)(q35;q11), t(14;14)(q11;q32), inv(14)(q11;q32) and t(X;14)(q28;q11). Apart from 14q32 and Xq28 these breakpoints are the locations of the T cell receptor (TCR) genes, 14q11 (TCRα/δ), 7q35 (TCRβ) and 7p14 (TCRγ) and in some cases translocations have been proven to occur within them. A-T patients are estimated to have about a 40-fold increase in translocations involving chromosomes 7 and 14 compared with non-A-T individuals but the increase for inv(7) is even greater. Cells with these translocations can proliferate to produce large clones of cells and subsequent clonal selection is associated with the development of leukaemia in young adults. The presence of breakpoints in the TCR genes suggests that

there is a defect in some form of recombination or some aspect of regulation of recombination (Taylor et al., 1996); however the process of V(D)J recombination appears to be qualitatively normal in A-T cells. The presence of cytogenetic abnormalities involving TCR loci is also reflected by the fact that, T cell tumours including T-cell acute lymphocytic leukaemia (T-ALL) and T cell prolymphocytic leukaemia (T-PLL), are seen at a greatly elevated frequency in A-T children when compared with non-A-T children, although B-cell tumours and occasional myeloid leukaemias do occur (Stankovic et al., 1998), (Taylor, 1998). Young adults with A-T are especially susceptible to a mature T-cell leukaemia similar to T-PLL. The latter is a rare leukaemia which is seen sporadically in elderly people from the normal population and which usually shows structural anomalies in *ATM* (Yuille et al., 1998). In T-PLL the most common site involved in the aberrant rejoining during translocation is the *TCL-1* (T-cell leukaemia) locus at 14q32. Two clusters of breakpoints are seen at this locus, between which the *TCL-1* gene has been identified (Virgilio et al., 1994). Activation of *TCL-1* by T cell regulatory elements located upstream or downsteam of *TCL-1* may then occur. Breakpoints in T-PLL are also seen in the Xq28 region within one of two genes *c6.1A* or *c6.1B (MTCP-1).* The latter has four transcripts and one of the protein products shows marked sequence similarity to the TCL-1 protein (Stern et al., 1993). These translocations involving 14q32 and Xq28 are however insufficient for tumorigenesis because large clones can survive for many years before leukaemic transformation. The influence of other genetic changes is presumably required to complete the transformation process.

Cell cycle checkpoint abnormalities

Cell cycle checkpoints activated in response to DNA double strand breaks are also abnormal in A-T. Instead of arresting in G1 post irradiation, A-T cells continue to progress into S-phase therefore allowing replication of DNA on a damaged template. Cells then accumulate at G2/M where most then die. In addition, A-T cells irradiated in S-phase fail to undergo the transient arrest of replication characteristic of normal cells. This phenomenon, termed radioresistant DNA synthesis (RDS), is a defining cellular characteristic of A-T. A-T cells irradiated in G2 also fail to arrest cell cycle progression and initially continue rapidly into the next G1 phase; only at later times after irradiation do the cells become significantly delayed at the G2 boundary. The G1/S DNA damage checkpoint in normal cells is dependent on induction of the tumour suppressor p53 which in turn is a transcriptional activator of the CDK inhibitor p21. p21 inhibits the action of cyclin dependent kinases (CDKs), which are necessary for phosphorylation of the retinoblastoma protein RB. If hyperphosphorylation of RB does not occur, release of E2F, a transcription factor which is required for S-phase progression is prevented and the cells arrest in G1-phase. A-T cells show both delayed and reduced induction of p53 post- irradiation (Lu and Lane, 1993) and reduced p21 responses. The cells cannot perform an adequate G1 arrest post irradiation and continue into S-phase unchecked.

Initially it was thought that the RDS phenotype was responsible for the radiosensitivity of A-T cells, however A-T cell lines exist in which these features are separable. Non-cycling A-T cells are also radiosensitive as shown by the absence of recovery after 'liquid holding' (when the cells are held in a

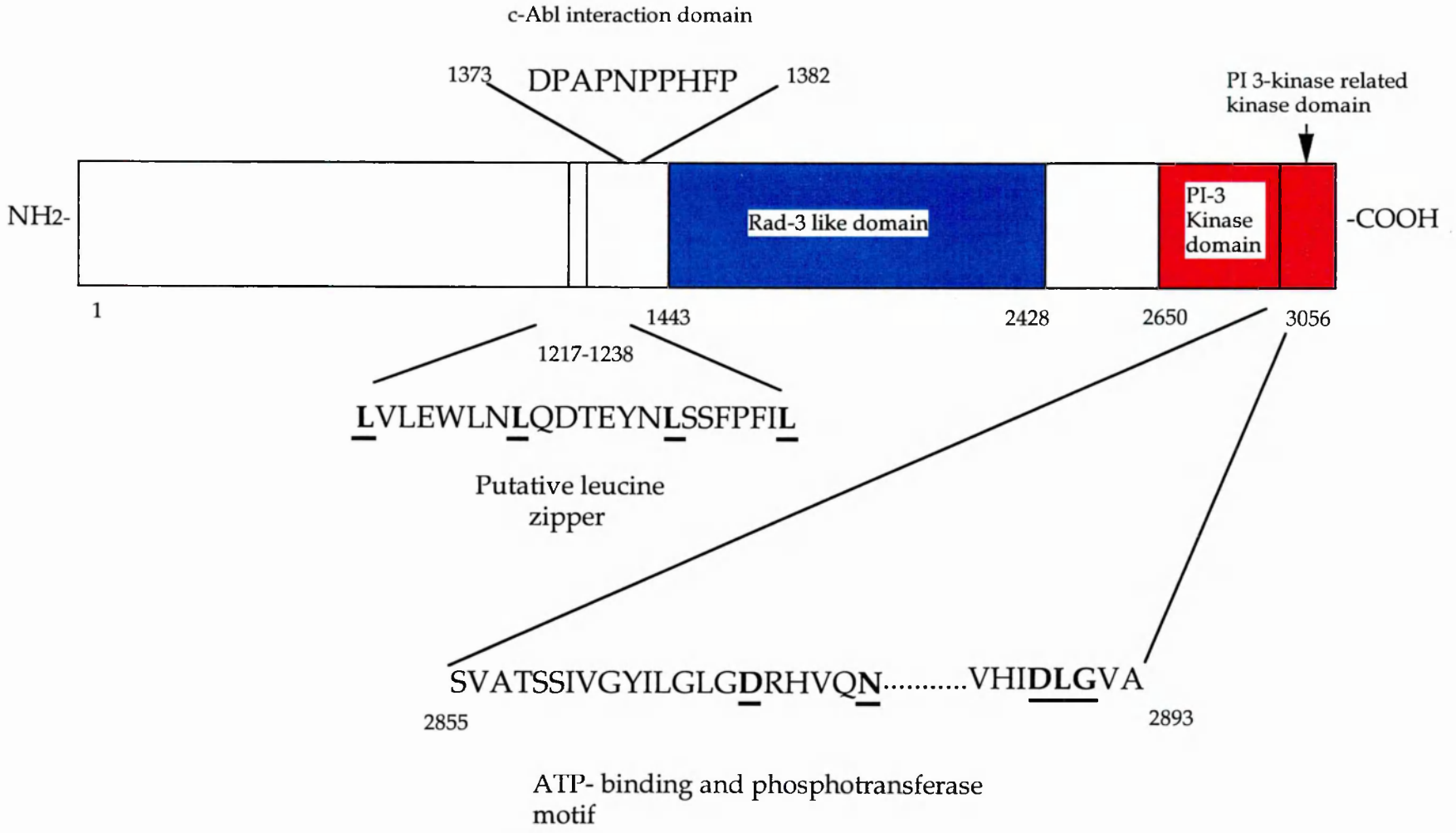

Fig. 1.1

A schematic diagram of the entire ATM protein, amino acid residues 1-3056, showing the recognised domains, the putative leucine zipper motif and the PI-3 kinase signature.

non-proliferating state after irradiation (Cox, 1982)). Therefore any potential explanation for the radiosensitivity ought to be applicable to cells in the G0 phase.

The *ATM* gene

The gene defective in ataxia telangiectasia *ATM* (ataxia telangiectasia mutated) is found on 11q22-23 and was positionally cloned in 1995 (Savitsky et al., 1995). It is 150 kb in size, consists of 66 exons (Uziel et al., 1996) and codes for a major 13 kb transcript which is ubiquitously expressed (there may also be several other transcripts of smaller size resulting from alternative splicing). Binding sites for several factors including E4F1 and E4F2, SP1 and a cAMP and insulin responsive elements have been predicted in the putative promoter region. The promoter is bi-directional and also serves the adjacent *E14 (NPAT/CAND3)* gene (Byrd et al., 1996). The ATM protein comprises 3056 amino acids with molecular weight of 350 kDa (Fig. 1.1). The mutations currently known (~250 in total) are scattered throughout the gene and there are no recognised mutational hotspots (Taylor, 1998). Most mutations create null alleles (ie they lead to premature truncation with destabilisation of the protein product) and the majority of patients are compound heterozygotes carrying different mutations of each allele (Gilad et al., 1996), (Byrd et al., 1996).

ATM is ubiquitously expressed with the highest levels seen in the ovary, testis and spleen (Chen and Lee, 1996). Immunohistochemical studies have shown homogenous nuclear localisation of ATM (Lakin et al., 1996), although some is seen in the cytoplasm associated with unidentified membranous

organelles. The subcellular distribution is different in the ovary where ATM is predominantly seen in the cytoplasm rather than in the nucleus.

Variant A-T phenotypes

Clinically these are patients who show milder features including a later onset of ataxia and cerebellar deterioration with reduced or absent cancer predisposition (McConville et al., 1996), (Gilad et al., 1998). Cells from these patients exhibit levels of radiosensitivity which are intermediate between normals and patients with classical A-T (Taylor, 1998). In contrast to classical A-T patients with truncating mutations which destabilise the protein such that no ATM is detected on Western blotting, in patients with a variant A-T phenotype ATM protein can be found in varying levels. This may represent low amounts of normal protein (formed for example by a degree of normal splicing from a mutation in an intronic sequence resembling a splice donor site), or higher amounts of mutant ATM produced from non-destabilising mutations (eg missense mutations) with some residual function (McConville et al., 1996).

ATM homologues

ATM is related by sequence to several known proteins from organisms as diverse as yeast and mammals (Savitsky et al., 1995), (Zakian, 1995), (Lavin et al., 1995) (Table 1.1 and Fig. 1.2) and these can be classified by their degree of similarity and protein size into two broad groups (Jackson, 1996). The first group comprises large proteins (>270 kDa), of similar size to ATM, which have

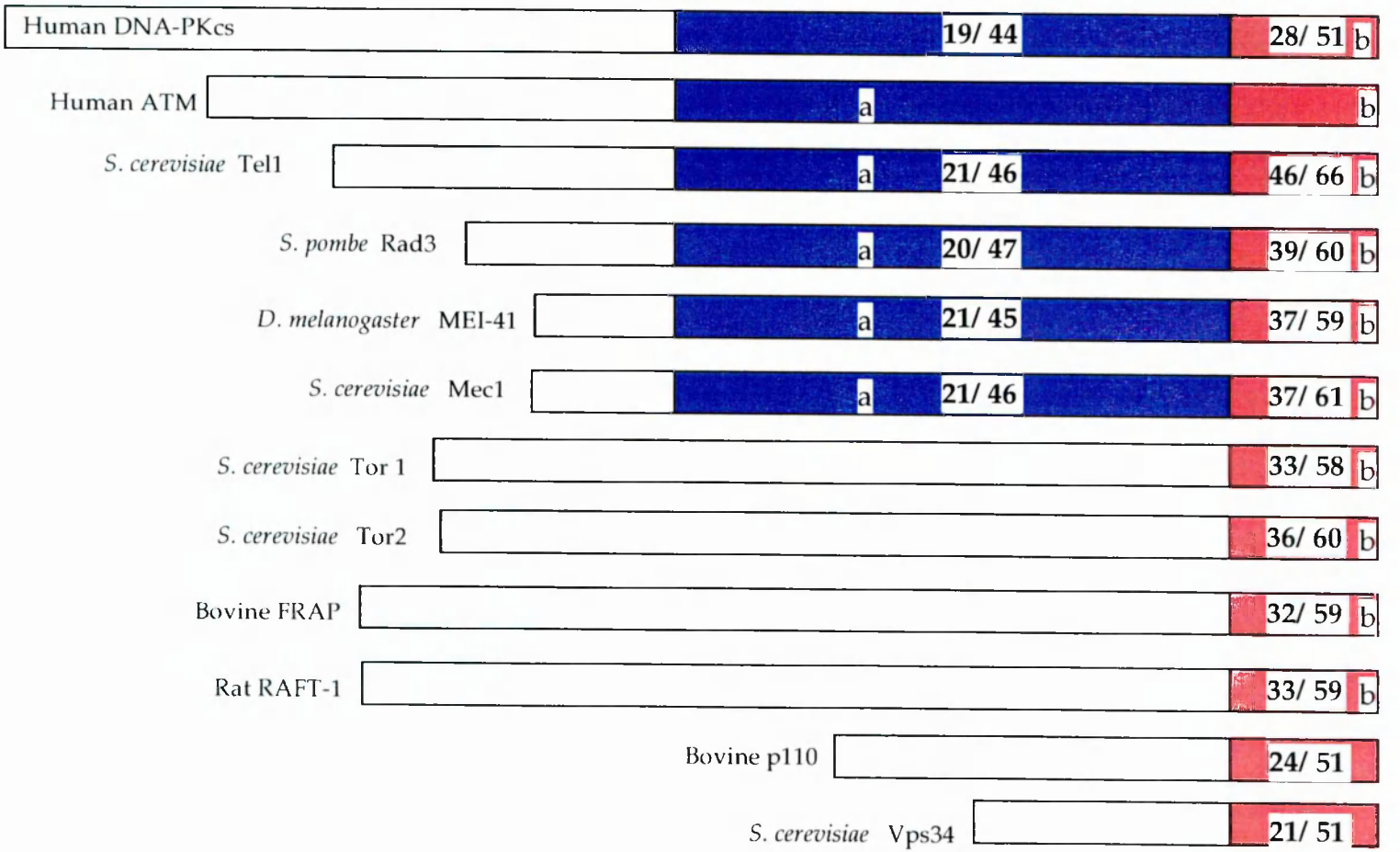

Fig. 1.2

Schematic representation of proteins related to ATM. Percentage amino acid identity and similarity to the ATM protein are included for both domains. Red bar: PI-3 kinase domain, blue bar adjacent, less closely related region of similarity, a: Rad3-like domain, b: PI3-K like kinase domain.

ATM protein Homologue	Species	Function
PI 3-kinase p110 catalytic subunit	mammals	Lipid and protein kinase. Signal transduction
DNA-PK catalytic subunit	human	Serine/threonine protein kinase activated by DNA ends. DNA repair, V(D)J recombination
Vps34	*S. cerevisiae*	Vesicular trafficking
Rad3	*S. pombe*	Cell cycle checkpoint roles in G2 and S in response to damaged or unreplicated DNA
Tor proteins	*S. cerevisiae*	Targets of the immunosuppressant drug rapamycin. Bind the rapamycin/FKB12 complex
FRAP	mammals	" "
RAFT-1	mammals	" "
Mec1/Esr1	*S. cerevisiae*	Cell cycle checkpoint role in G2 and S phase in response to damaged or unreplicated DNA
Tel1	*S. cerevisiae*	Telomere length regulation, mitotic recombination and chromosomal stability
MEI-41	*D. melanogaster*	Cell cycle checkpoint role in S phase and G2/M; DNA repair and meiotic recombination

Table 1.1

ATM homologues in different species and their cellular functions.

a carboxy-terminal phosphatidyl inositol 3-kinase like (PI 3-K) domain. Some of these also feature two other regions of homology, a central Rad-3 like area and PIK-related kinase region (phosphatidyl kinase related kinase region) located at the extreme carboxy-terminus of the protein. This group includes *S. pombe* Rad3 itself, its *S. cerevisiae* homologue Mec1, human DNA dependent protein kinase (DNA-PK), *D. melanogaster* Mei-41, the *S. cerevisiae* proteins Tor1 and Tor2 with their mammalian equivalents Frap-1 and Raft-1 and *S. cerevisiae* Tel1 which is the closest relative of ATM in yeast. The second group of ATM related proteins are much smaller proteins (< 110 kDa) and show less similarity. These include the prototypic p110 protein which is the catalytic sub-unit of PI3-K, *S. cerevisiae* Vps34 and PI4-kinases. The ATM-related proteins with established lipid and protein kinases activity are discussed in greater detail in Chapter 4. Members of the first group seem to show the most functional similarity to ATM at present. Broadly speaking members of this group appear to be important in cell cycle regulation after DNA damage, the maintenance of genomic integrity, and in DNA repair although only *MEC1* is an essential gene.

Schizosaccharomyces pombe rad3 mutants are checkpoint defective in that they fail to arrest in G2 after DNA damage induced by γ-irradiation, ultraviolet light (Seaton et al., 1992) and methanemethylsulphonate (A-T cells are only sensitive to γ-irradiation). They also lose the safeguard which prevents the initiation of mitosis when DNA replication is incomplete (Jimenez et al., 1992). *mec1* mutants also show these two checkpoint losses in addition to defective G1/S and intra-S checkpoints post DNA damage. These mutants also

demonstrate genomic instability and abnormal meiotic recombination as *MEC-1* is required to prevent progress through meiosis when recombination-induced double strand breaks are not rejoined (Lydall 1995). The human protein most closely related to Rad-3/Mec-1 is ATR, which has been shown to be present with ATM along meiotic chromosomes (although ATM is found along synapsing areas and ATR is present along unpaired chromosomal axes), (Keegan et al., 1996).

tel1 mutants were named because they have very short telomeres (Greenwell et al., 1995). *tel1/mec1* double mutants suggest that there may be some functional overlap between *ATM* homologues due to the fact that *tel1* mutations can enhance the radiosensitivity of *mec1* mutants even though *tel1* mutations alone do not confer hypersensitivity to DNA damaging agents. In addition overexpression of Tel1 can complement the phenotype produced by truncated Mec1 protein (Morrow et al., 1995). It is interesting to note that mutants of *tel1* which shows the most marked degree of homology to *ATM* apart from sharing short telomeres and genomic instability otherwise have a quite different phenotype from cells from individuals with A-T. In particular unlike A-T cells, *tel1* mutants have no checkpoint defects, do not show elevated levels of mitotic recombination and as described, are not hypersensitive to DNA damaging agents. It is possible that the amino-terminal region of ATM, which shows no similarity to any other known protein at present but which may allow ATM to interact with other molecules, is responsible for these differences.

The Mei-41 protein is involved in checkpoint control and in the maintenance of genomic stability in *D. melanogaster* (Hari et al., 1995). *Mei-41*

mutants show defects in the G1/S, S phase and G2/M checkpoints together with abnormalities in meiosis, including reduced meiotic recombination with altered frequency and morphology of late recombination nodules. The genomic instability in these mutants is manifest as chromatid and isochromatid breaks.

The yeast Tor (target of rapamycin) proteins (Helliwell et al., 1994) and their mammalian counterparts FRAP and RAFT are targets for the macrolide antibiotic rapamycin which has immunosuppressive properties (Brown et al., 1994). When rapamycin binds to its intracellular receptor FKBP12 and the Tor proteins, or FRAP and RAFT, the target proteins are inhibited and G1 arrest results. The mechanism of cell cycle arrest is believed to be via inactivation of p70 ribosomal protein S6 kinase which is needed for translation of certain mRNAs into proteins required for G1/S progression (Brown et al., 1995). In addition inhibition of cyclin dependent kinases (cyclin D-cdk4 and cyclin E-cdk2) may be important, (Albers et al., 1993). A substantial body of information is now available concerning DNA dependent protein kinase (DNA-PK) which is a further human relative of *ATM* (Jeggo, 1997), (Hartley et al., 1995). DNA-PK is often used as a paradigm for *ATM* although it is known that DNA-PK mutants are not checkpoint defective, unlike A-T cells. Moreover DNA-PK is normal in A-T patients. Therefore these proteins, whilst related, do not have identical roles. However, cells deficient in DNA-PK are similar to A-T cells in that they are radiosensitive. In addition, animals with DNA-PK deficiency (eg mice with severe combined immunodeficiency), are immunodeficient as are individuals with A-T. These observations are common to DNA double strand break (dsb), repair disorders. DNA-PK is a heterotrimeric enzyme,

consisting of a 460 kD catalytic sub-unit and the regulatory subunit Ku (comprising two subunits Ku 70 and Ku 86), which requires DNA ends for its activity (Gottlieb and Jackson, 1993). An extended form of Ku86 called KARP-1 which has potential leucine zipper for protein-protein interactions and a possible basic DNA binding domain may also be important in DNA-PK activity (Myung et al., 1997). Recently KARP-1 induction post irradiation has been shown to be dependent upon ATM and p53 proteins (Myung et al., 1998). Ku binds to DNA ends and when complexed with the catalytic subunit the DNA-PK enzyme is able to perform DNA dsb repair and probably to also inhibit local transcription by phosphorylation of RNA pol II. Attenuation of enzymatic function is regulated by a negative feedback mechanism. DNA-PK phosphorylation of c-Abl results in deactivation of DNA-PK after c-Abl reciprocally phosphorylates it, and DNA-PK is capable of autophosphorylation which causes inhibition of enzyme activity and dissociation of the catalytic subunit from Ku (Kharbanda et al., 1997). DNA dsbs are formed as part of the process of site-specific V(D)J rejoining to generate antibody and T-cell receptor diversity in the immune system. DNA-PK is required for proper repair of the coding joins. If the enzyme is absent coding regions rejoin but deletions are seen, with adverse consequences for immune function. Seeking a parallel with *ATM* , it has been proposed that Ku homologs may be required for *ATM* function but this remains unproven.

The second group of smaller ATM related proteins are involved in signal transduction cascades (eg the PI 3-kinases) (Kappeller and Kantley, 1994). Vps34 also shows PI 3-kinase activity and is important in directing proteins to the vacuole in *S. cerevisiae*. (Schu et al., 1993), (Stack et al., 1995).

Whether ATM in the microsomal fraction of human cells shares related functions remains to be seen. The possibility of defective signal transduction in A-T has been discussed previously (Lavin and Shiloh, 1996). At present the reasons for the association of diabetes mellitus with A-T or for the death of Purkinje cells and granular cells in the cerebellum are unknown but failure to respond to insulin or nerve growth factor may be due to compromised signal transduction. Faulty signal transduction might also underlie the defective mitogenic responses in T and B cells in A-T (O'Connor and Linthicum, 1980), (Khanna et al., 1997). Multiple defects in intracellular signalling post-irradiation have been noted in A-T cells and have been reviewed recently (Rotman and Shiloh, 1997). These include reduced p53 dependent responses, reduced phosphorylation of replication protein A (RPA), failure of activation of poly (ADP-ribose) polymerase (PARP), defective activation of the stress activated protein kinases (SAPK), diminished activation of c-Abl, failure of increased tyrosine phosphorylation of $p34^{cdc2}$ and inhibition of cyclinB/cdc2 kinase activity.

ATM function

The exact role of the *ATM* gene product has not yet been elucidated but cellular A-T phenotypes such as radiosensitivity and genomic instability suggest that a deficiency in the repair of DNA double strand breaks (dsbs) may be responsible. Therefore it has been postulated that ATM protein is involved in either the detection or signalling of DNA damage or in the process of DNA repair itself. For many years DNA repair in A-T cells was thought to be

relatively normal. Reports of increased numbers of residual DNA dsbs post irradiation and deficiency of the fast phase of DNA repair have been made as time has gone on. Many of these studies have only looked at DNA repair in A-T cells in the first couple of hours after treatment with ionising radiation and this may be a highly relevant oversight in the light of new evidence. Recently it has been demonstrated in non- transformed human fibroblast cell lines that the initial phase of DNA dsb repair in A-T cells is better than that seen in normal cells (upto 6 hours). After this the repair curve crosses that of the control cells such that the residual damage at 24 hours is greater in the A-T cells (Foray et al., 1997). Moreover, the number of residual DNA dsbs correlated with the radiosensitivity of A-T cells. This supports the idea that the hypersensitivity in A-T to ionizing radiation is due to the defective repair of dsbs. It has also been shown that a particular type of DNA repair is specifically deficient in A-T cells. Using the shuttle vector pZ189, containing an oxidatively induced dsb, the integrity of DNA repair was studied in one normal and two A-T fibroblast cell lines. Mutation frequencies were twice as high in the A-T fibroblasts and the mutational spectrum was different. The majority of the mutations in all the cell lines were deletions (44-63%). DNA sequence analysis showed that in the normal cells 17 of 17 plasmids with deletion mutations occurred between short direct sequences (removing one of the repeats plus the intervening sequences), suggesting that illegitimate recombination was important in dsb rejoining. Of the 23 deletions in the A-T cells only 3 involved direct repeat sequences and the average deletion size was much shorter than for normals (14 bp versus 71 bp), implicating a defect in the illegitimate recombination pathway (Dar et al., 1997). Such a defect might be in regulation of the process of illegitimate

recombination or within the pathway itself. The relationship between the lethal and the mutagenic sequelae of DNA dsbs is poorly understood but the existence of such an error prone repair mechanism within human cells would suggest that maintenance of cellular viability is likely to be the primary role of this type of repair rather than maintenance of genetic integrity per se.

Role of ATM in meiosis

As previously mentioned A-T is a pleiotropic disorder and other functions of ATM are suggested by the clinical manifestations. A-T sufferers are infertile and a role for ATM is now emerging in meiosis. High levels of ATM are found in normal testis and ovary, and immunohistochemical studies have shown that the molecule is found at the areas of synapsis between homologous chromosomes. Exchange of genetic material takes place at these junctions by a process of homologous recombination which is facilitated by the synaptonemal complex and early and late recombination nodules (RNs). Early RNs are protein complexes involved in homology searches occuring before or at the time of synapsis. Some of these early RNs are converted into late RNs which are the structures involved in the recombination process itself. ATM is a component of the early RNs. In *ATM* knockout mice the synaptonemal complexes fragment at sites of some of the early RNs (Plug et al., 1997) and the infertility that occurs in these animals appears to be due to chromosome fragmentation which leads to meiotic arrest and apoptosis (Keegan et al., 1996). It is possible that in meiosis ATM may monitor strand disruptions that occur during the process of synapsis and recombination. This

could be seen as a germ cell-specific adaptation of a more generalised role for ATM in the processing of dsbs generated by a variety of means.

ATM and telomere metabolism

A-T cells have defects in telomere metabolism and show gross structural abnormalities such as telomere-telomere fusions. These are particularly seen in T-lymphocytes in A-T patients. In these patients a predisposition to accelerated telomere shortening is also seen in T cells at the rate of about 95 +/- 23 base pairs per year. Telomere fusions are not seen in leukaemic cells in A-T patients and there is no evidence that the telomere loss or the telomere fusions per se are involved in the tumorigenesis. However, maintenance of telomere length is thought to be an important factor in cell immortalisation, and indeed immortalised A-T cell lines regain the ability to maintain their telomeres (Sprung et al., 1997). Telomere loss in non-leukaemic A-T lymphocytes is not due to an absence of telomerase as telomerase levels have been shown to be normal in these cells. One of the clinical consequences of accelerated telomere loss may be features of premature aging seen in A-T such as skin atrophy and hyperpigmentation, loss of sub-cutaneous fat and greying of the hair even in children (Metcalfe et al., 1996). As mentioned above, *TEL1*, is also involved in the control of telomere length in *S. cerevisiae* (Greenwell et al., 1995) and mutations in *TEL1* also lead to abnormally shortened telomeres.

In summary, from our present understanding of A-T the cancer-proneness of the disorder at least with respect to the lymphoreticular malignancies is likely to be due to general genomic instability caused by

defective illegitimate recombinational repair. This instability is implicated in the generation of rearrangements in the vicinity of the TCR and Ig genes which activate genes like *TCL-1* to cause leukaemic transformation. These changes may be modulated by other factors as ~90% of A-T patients do not develop leukaemia. For other cancers in A-T sufferers or heterozygotes, other tissue specific mechanisms may be operating but as yet these are poorly elucidated.

Bloom's Syndrome (BS)

Clinical manifestations

Bloom's syndrome (BS) is a rare autosomal recessive disorder with less than 200 cases recognised world wide. It is characterised by a combination of a small but properly proportioned body size, bird-like facies, sun sensitivity with facial erythema, immunodeficiency, premature ageing, male infertility, female subfertility and an increased cancer susceptibility (German and Passarge, 1989), (German, 1993), (German, 1995). The cancer susceptibility is seen for a wide range of human cancers, not just for lymphoma and leukaemia which predominate in ataxia-telangiectasia. Death in BS individuals usually occurs in the mid twenties.

Phenotype of BS cells

BS cells in culture show genomic instability with cytogenetic abnormalities including an increased number of chromatid gaps and breaks in untreated cells. There is also an increased number of sister chromatid exchanges (SCEs), with an elevation in the number of recombinational

exchanges seen between homologous chromosomes which can be visualised after bromodeoxyuridine (BrdU) treatment, indicating an increase in somatic recombination in BS cells. The high number of SCEs seen is pathognomonic of the syndrome and is of use diagnostically. The exchange of genetic material between the two sister chromatids post-BrdU is revealed as a harlequin pattern of staining. Hypermutability is seen at the genetic level at all loci examined and BS is a mutator syndrome, explaining in part the reason for the cancer susceptibility.

The BLM gene

BLM , the gene defective in BS, was first assigned to chromosome 15 after it was discovered that human chromosome 15 could complement the elevated SCE number in BS cells (McDaniel and Schultz, 1992). *BLM* was then regionally mapped by analyzing consanguineous BS kindreds and was found to be closely linked to the oncogene *FES* found at 15q26.1 (German et al., 1994). An ingenious approach called somatic crossover point mapping (SCP) was then used to locate the gene. This relies on the fact that in some BS sufferers a small proportion of their peripheral blood lymphocytes show a low SCE frequency instead of a high SCE frequency suggesting that these cells are functionally wild type. This can be explained if the two *BLM* alleles carry different mutations (ie the patient is a compound heterozygote) and somatic recombination between these within the *BLM* gene results in the generation of a wild type allele. Polymorphic markers were used to assess where the site of recombination had occurred allowing localisation of the *BLM* gene to a 1.3 cM interval on chromosome 15 (Ellis et al., 1995). Identification of further

polymorphic loci enabled mapping of *BLM* to a 250kb region and elimination of *FES* and the adjacent *FUR* as candidate BS genes. A 4437bp cDNA derived from this 250kb region encoded a 1417 aa protein in which were found chain terminating mutations in BS sufferers identifying the corresponding gene as *BLM* (Straughen et al., 1996), (Ellis et al., 1995). Two RNA species at around 4.5kb in size are seen in unaffected individuals. These two bands are either absent or present at reduced intensities in BS sufferers suggesting a destabilizing effect of *BLM* mutations on the RNA species (Ellis et al., 1995).

BLM homologues

BLASTP comparisons of BLM with amino acid sequence databases identified significant similarity from amino acids 649-1041 (which contains seven conserved helicase domains) to the RecQ subfamily of DEXH-box containing helicases, including *E. coli* RecQ, human RECQL, human WRN, *S. cerevisiae* SGS1 and *S. pombe* Rqh1 (Ellis et al., 1995). Helicases are enzymes which can unwind DNA, a process important in both DNA replication and in recombination between DNA molecules. For example, RecQ is a 3'-5' helicase which is a component of the RecF recombination pathway in *E. coli* (Dunderdale and West, 1994). *SGS1*, WRN, Rqh1 and BLM are much larger proteins than RecQ and RecQL because they have extra domains surrounding the region of helicase activity. Between amino acids 588-661 of BLM three short motifs showing some identity to RNA polymerase II are also found and the extreme amino and carboxy-termini of BLM are highly charged and serine-rich. The functions of these terminal regions are as yet unknown but they may

be the site of interaction with other cellular proteins. This may explain why Werner's syndrome, which causes dramatic and premature ageing, has a different clinical phenotype to BS. The causative gene of Werner's syndrome *WRN* contains a similar RecQ helicase domain to *BLM* but it is dissimilar at the N and C-termini.

BLM function

The product of *BLM* has recently been shown to be an ATP dependent 3'-5' DNA-helicase with a requirement for magnesium (Karow et al., 1997). The exact mechanism by which loss of the helicase function results in the observed cellular and clinical phenotypes is not understood, but it has been hypothesized that perturbation of replication or recombinational processes may explain the increased recombination and genomic instability seen in this disorder. Indeed there is some evidence that BLM is involved in replication; a retarded rate of DNA chain elongation is seen in BS cells (Hand and German, 1975), (Giannelli et al., 1977) and the size distribution of DNA replicational intermediates has also been found to be abnormal in BS cells (Lonn et al., 1990). The *S. cerevisiae* homologue of *BLM, SGS1* when mutated is also associated with an elevated recombination frequency (Gangloff et al., 1994), (Watt et al., 1996), and it has been suggested that because many of the mutations seen in BS patients are predicted to inactivate the helicase activity of the molecule (Ellis et al., 1995), the helicase activity itself is required to suppress inappropriate recombination. The *S. cerevisiae* homolog *SGS1* may yield several clues to the function and potential partners of human BLM, as it is likely that the evolutionary conservation in structure is accompanied by conservation of

cellular roles. Sgs1 protein is known to interact physically with two of the topoisomerase enzymes expressed by budding yeast, Top2p (Watt et al., 1995) and Top3p (Gangloff et al., 1994). It is therefore possible that the corresponding human topoisomerases might cooperate with BLM in the execution of its cellular duties. It is clear from the above discussion that much work remains to be done to finally elucidate the exact molecular pathway causing genetic instability in Bloom's syndrome and to relate this to the increased tumour burden that is characteristic of this disease.

Nijmegen Breakage Syndrome (NBS)

Nijmegen breakage syndrome is an autosomal recessive disorder, much rarer than A-T, which is also associated with chromosomal instability. Affected individuals show microcephaly with mental retardation, bird-like facies, developmental delay, short stature, deficiencies in both cellular and humoral immunity and primary ovarian failure. There is also a dramatic 75- fold increase in lymphoreticular malignancies most commonly manifest as B- cell lymphoma which presents at an unusually young age (Wegner et al., 1998). Although the clinical phenotype is dissimilar from A-T, the cellular phenotype shares several key features leading to descriptions of NBS as an 'A-T variant syndrome'. Similarities to A-T include the cytogenetic characteristics of cultured NBS lymphocytes, which show rearrangements most frequently affecting chromosomes 7 and 14 in clusters around the immunoglobulin and T-cell receptor loci. There is also sensitivity to ionising radiation and several groups report that NBS cells are similar in their failure to suppress DNA synthesis post irradiation (radioresistant DNA synthesis or RDS) (Taalman et

al., 1983), (Young and Painter, 1989), (Perez-Vera et al., 1997), (Jongmans et al., 1997), (Sullivan et al., 1997), although the latter observation is contested (Antoccia et al., 1995). This similarity to A-T at the cellular level might suggests either that NBS regulates p53 independently independently of ATM. Alternatively, the *NBS* and *ATM* gene products may interact within the same complex or within the same pathway. One study examining NBS primary fibroblasts and EBV transformed NBS lymphoblastoid cell lines from the same patient treated with 5 Gy of irradiation showed levels of fibroblast radiosensitivity in NBS which was intermediate between normals and A-T fibroblasts. In addition in the NBS lymphoblastoid cells p53 and p21 induction was reduced but there was no significant delay in the p53 response, in contrast to the delayed kinetics of induction seen in A-T cells (Matsuura et al., 1998).The existence of a variant of A-T called A-T_{Fresno} in which the clinical phenotype of both NBS and classical A-T merges (Curry et al., 1989), lends further support to this latter hypothesis. All cases of A-T_{Fresno} examined to date have shown mutations in *ATM* (Gilad et al., 1998) and it is speculated that these may critically alter a putative NBS-ATM interaction domain.

The gene defective in NBS has recently been positionally cloned (Varon et al., 1998). It was initially mapped to 8q21-24 by complementation of radiosensitivity using microcell-mediated chromosome transfer (Matsuura et al., 1997). Linkage analysis of 7 NBS pedigrees in the UK, USA and the Netherlands was used to further localise the *NBS* gene to chromosome 8q21. The NBS consortium conducted a whole genome screen in NBS families mostly of Czech and Polish origin which demonstrated that 30 patients shared a common founder haplotype arising from a mutation in 16th century

Bohemia, which then transferred to Germany and the Netherlands with migration of the Slavic people. This approach lead to localisation of the *NBS* gene to a 1 cM interval on 8q21 (Saar et al., 1997). Linkage disequilibrium associated with this common founder mutation allowed narrowing of the region of interest to less than 300kb. A gene in this area was discovered to have truncating mutations in all NBS patients and was designated *NBS-1* (Varon et al., 1998). *NBS-1* spans over 50 kb of genomic DNA and the cDNA of 4386 bp includes an open reading frame of 2277 bp containing 16 exons. The gene product of the Nijmegen breakage syndrome encodes a protein of 754 amino acids which was called nibrin. Sequence analysis showed that it featured an amino-terminal fork-head associated (FHA) domain (Hoffman and Bucher, 1995), which may mediate interactions with phosphoserine and phosphothreonine. This domain is present in several yeast protein kinases including *S. cerevisiae* Dun1, Rad53 and *S. pombe* Cds1 which are all involved in regulation of the S phase checkpoint. Nibrin also contains a breast cancer carboxy-terminal domain (BRCT) found in a wide variety of proteins which participate in DNA damage checkpoints (Bork et al., 1997). Nibrin was found to be identical to a protein called p95 which was already being studied by another group as a component of the hMre11/hRad50 double strand break repair complex (Carney et al., 1998). In the presence of p95, cells treated with ionizing irradiation show relocalisation of immunologically detected hMre11 and hRad50 into spotty nuclear foci within 30 minutes. This relocalisation does not occur in NBS cells, hence p95/nibrin may be the DNA damage sensor or the transducer of the DNA damage signal from the DNA lesions to the repair complex and to the cell cycle machinery for appropriate checkpoint function.

The mutations described in *NBS-1* so far include the founder mutation 657del5 which results in truncation of the protein beyond both the FHA and BRCT domain and 4 smaller deletions between 1-4 bp and a 1 bp insertion mutation, all of which also result in protein truncation. It remains to be seen whether milder NBS phenotypes share mutations in *NBS-1* or are genetically distinct. Whether the molecular causes of genomic instability in NBS and A-T are related is obviously a key question at present and will be the subject of future research. However, although the final pathway leading to the similar chromosomal rearrangements may be shared, it is likely that the outcome of this genomic instability will be different, because in A-T, T-cell malignancies predominate whereas in NBS, B-cell malignancies are most common.

Fanconi Anaemia (FA)

Fanconi anaemia (FA) is an autosomal recessive disorder with pleiotropic and variable clinical effects. The disease is rare with a prevalence of about 1:200,000. Affected individuals suffer growth retardation and progressive bone marrow failure (pancytopoenia) with onset within the first few years of life. 75% of patients also have other abnormalities including aplasia of the radius and the thumbs, renal and urinary malformations, microcephaly and skin pigmentation. The increased cancer risk is manifest most commonly as an acute myeloid leukaemia (Liu et al., 1994), (Buchwald et al., 1997). FA cells show marked chromosomal instability after exposure to genotoxic agents causing DNA cross-links. These agents include diepoxybutane, cisplatinum and mitomycin C. Somatic cell fusion studies in transformed lymphoblastoid FA cell lines analysed for their cross-linker

sensitivity have identified 8 complementation groups to date: FA groups A-H (Duckworth-Rysiecki et al., 1985), (Strathdee et al., 1992), (Joenje et al., 1997). The clinical diagnosis of FA relies on the characteristic induction by cross linking chemicals of chromosomal aberrations, namely chromatid breaks and chromosome recombination figures. Spontaneous chromosomal damage is also seen in untreated FA cells. This may be due to lesions caused by oxidative damage as several products of oxidative metabolism (eg singlet oxygen, the hydroxyl anion, hydrogen peroxide and the superoxide anion) are known to be able to crosslink DNA and proteins. Indeed, FA cells grown at a low oxygen tension of 5% show suppression of several aspects of the FA cell phenotype (Schindler and Hoehn, 1988), (Joenje and Oostra, 1983). FA cells in culture show poor growth and reduced plating efficiency. FACS analysis demonstrates a greater proportion of cells in the G2 phase of the cell cycle. This may be due to an inherent increase in the length of G2 in FA cells or because of DNA damage of cells in S phase leading to cell cycle checkpoint activation and G2 arrest. The latter may be related to unresolved crosslinks or stalled replication forks preventing completion of DNA replication. Sensitivity to DNA interstrand crosslinks is a consistent hallmark of FA cells, although studies to investigate whether FA cells are deficient in the ability to remove DNA crosslinks have given conflicting results with different complementation groups and different methodologies used (Digweed and Sperling, 1996). Partial removal of interstrand crosslinks to leave adducts on only one strand of the DNA, thus restoring denaturability of the molecule, may explain why in some studies FA cells appear to be proficient at crosslink repair. Persistent interstrand crosslinks might impede the progress of replication forks, reducing

the rate of DNA synthesis in S phase. This has been found for FA-A cells after treatment with crosslinking agents (Moustacchi et al., 1987), (Digweed et al., 1988). It is likely that DNA with interstrand cross-links would be repaired by recombination using a separate undamaged DNA molecule as the template. This would explain the cytogenetic observations in FA cells, as failure of repair of crosslinked damage might lead to chromatid breaks and chromosomal recombination figures as a result of failure to complete the repair process. Defective recombinational repair has been reported in normal and FA-D cells after crosslinking treatment. In FA cells, defective recombination resulted in mutations which were mainly deletions whereas normal cells suffered point mutations (Papadopoulo et al., 1990). Presumably in normal cells, the point mutations are offset by the repair of large tracts of crosslinked unreplicatable DNA. The genes for FA-A and FA-C complementation groups have been cloned and mapped to chromosomes 16q24.3 and 9q3.22 respectively. (Strathdee et al., 1992), (Strathdee et al., 1992), (Pronk et al., 1995), (Lo Ten Foe et al., 1996), (F. A. B. C. Consortium, 1996). FA-A and FA-C encode distinct and novel proteins which interact with each other and form a complex, the biochemical function of which remains elusive. Unbound FA-A and FA-C are found predominantly in the cytoplasm, but the complex is seen in similar quantities in the nucleus and cytoplasm. It is possible that the complex plays a role in repair of DNA with interstrand crosslinks, but this is not yet established (Kupfer et al., 1997). Experiments examining the ability of nuclear extracts to bind crosslinked DNA (Lambert et al., 1992) suggested that a crosslink recognition protein is absent or defective in FA-A cells (Hang et al., 1993). FA-D has been mapped to chromosome 3p22-26 (Whitney et al., 1995).

This multitude of complementation groups indicates the molecular heterogeneity of FA. It is likely that different gene defects giving rise to this disorder act within the same biochemical pathway or within the same multiprotein complex dealing with cross-linker associated DNA damage. Failure of recognition or resolution of crosslink lesions would cause multiple genetic abnormalites which could in turn give rise to leukaemic transformation. Genetic heterogeneity within the disorder may also account for variability of the clinical phenotype and will make the molecular screening for FA more difficult, although it is known that certain complementation groups are commoner in some populations eg FA-A in Ashkenazi Jews (Whitney et al., 1993), (Verlander et al., 1994), and FA-C in Afrikaaners (Pronk et al., 1995) and Italians (Savoia et al., 1996). Epidemiological evidence suggesting that FA heterozygotes may have a higher cancer risk than the general population (Swift, 1971), may mean that identification of all the FA genes and their functions has more relevance than was first appreciated.

Xeroderma Pigmentosum (XP)

Xeroderma pigmentosum is a rare genetic disorder. It is characterised by acute photosensitivity upon sunlight exposure leading to extreme sunburn reactions and later to atrophy and telangiectasia of the affected skin. Affected individuals also have more than a 2000-fold increase in all forms of skin cancer (Kraemer et al., 1987). Tumours appear on sun exposed sites in childhood with a median age of presentation of 8 years. A range of neurological defects including neurodegeneration are seen in up to 40% of cases and a small number show more severe abnormalities with microcephaly and dwarfism.

The syndrome therefore affects multiple systems and is somewhat variable in its phenotype. At the cellular level there is hypersensitivity to ultraviolet light (UVL) and UV-mimicking chemicals with defective DNA repair (Cleaver, 1968). Cell lines derived from XP individuals also show chromosomal instability after exposure to UVL (Parshad et al., 1993), and some have considered XP to be a classical chromosome breakage disorder (Weemaes et al., 1981). XP is now known to comprise two subgroups: classical XP and variant XP. In classical XP, seven different complementation groups have been discovered: XP-A-G. Variant XP is made up of only one additional complementation group, XP-V. In classical XP (80% of cases), the molecular defect lies within the nucleotide excision repair (NER) pathway (Kraemer et al., 1987).

Two overlapping pathways of NER have been identified: transcription coupled repair, which is rapid and which targets the transcribed strand of expressed genes, and the more tardy global genome repair serving the rest of the DNA. Most groups are deficient in both pathways of NER but XP-C apparently only shows a defect in global genome repair. In variant XP the defect is not well characterised but is believed to affect post-replication repair mechanisms which are themselves poorly understood. The gene products corresponding to the XP complementation groups are now being characterised (Table 1.2) and reviewed (Sarasin and Stary, 1997).

Protein	Function
XP-A	DNA damage recognition (Jones and Wood, 1993)
XP-B/ERCC3	ATP-dependent DNA Helicase 3'->5'. Subunit of RNA pol II basal transcription factor BTFII (TFIIH)
XP-C	Role uncertain. May bind damaged DNA and recruit repair machinery
XP-D/ERCC2	ATP-dependent DNA Helicase 5'->3'. p80 subunit of RNA pol II basal transcription factor BTFII (TFIIH), (Schaeffer et al., 1993), (Schaeffer et al., 1994), (Sung et al., 1993).
XP-E	DNA damage recognition (Jones and Wood, 1993).
XP-F/ERCC4	Component of the 5' endonuclease complex
XP-G	3' endonuclease
XP-V	Post replication repair abnormal

Table 1.2

Proteins abnormal in xeroderma pigmentosum and their cellular functions.

TFIIH is probably involved in the local unwinding of the DNA duplex at the site of DNA damage in NER and at the site of the promoter in

transcription initiation, which relies on the DNA-dependent ATPase and DNA helicase activities associated with XPB and XPD.

Interestingly two syndromes, Cockayne's syndrome (CS) and Trichothiodystrophy (TTD) showing overlap with XP are known and also feature UVL sensitivity and defects in NER, although curiously neither CS nor TTD show an elevated cancer risk. CS is characterised by sun sensitivity, severe mental retardation due to dysmyelination, skeletal abnormalities and a wizened facial appearance (Lehmann et al., 1993). The features of TTD include sulphur-deficient brittle hair and nails, and icthyosis (thickened scaling skin) (Itin and Pittelkow, 1990). Growth is also impaired and dysmyelination is seen, as in CS. Classical CS (complementation groups A and B) are defective in transcription coupled repair whereas CS/XP-B, CS/XP-D and CS/XP-G fall into XP complementation groups and are defective in both paths of NER. In TTD 90% of patients are assigned to the same complementation group as XP-D ie TTD/XP-D. Classical TTD (group TTD-A) and TTD/XP-B are in the minority. Although XP-D and TTD/XP-D mutations reside in the same gene, the phenotypic consequences of these mutations are different and the cancer risk is only seen with XP. Analysis of the mutations in the XPD and XPB genes in the different NER syndromes suggests certain mutations are syndrome specific (Broughton et al., 1994), (Broughton et al., 1995), (Takayama et al., 1995), (Takayama et al., 1996). It has been hypothesized that particular mutations may render the transcription role of the complex TFIIH abnormal perhaps affecting expression of a variety of genes leading to TTD (transcription syndrome) whereas others may abolish the NER function leading to genetic instability and tumorigenesis after exposure to UVL.

Hereditary Non-Polyposis Colorectal Cancer (HNPCC)

HNPCC, also known as Lynch syndrome (types I and II), is a major cause of genetic instability-related cancer. It shows autosomal dominant inheritance, affects ~ 1/200 of the population, and poses a considerable health burden as it accounts for 4-13% of all colorectal cancer in industrialised nations (Lynch et al., 1993). The syndrome is defined clinically by the occurence of tumours in at least 3 family members in 2 generations or more, at least one of whom should have been diagnosed below the age of 50 years (Vasen et al., 1991). Affected individuals develop intestinal tumours, usually of the colon (Lynch type I). In Lynch type II, there is also a predisposition to extraintestinal cancers including transitional cell tumours of the urinary tract and gynaecological malignancies eg endometrial carcinoma. A clue to the mechanism underlying HNPCC was found several years ago when it was demonstrated that some colonic tumours from HNPCC patients showed dramatic changes in microsatellite sequences termed microsatellite instability (MIN) (Aaltonen et al., 1993) (Peltomaki et al., 1993). Microsatellites are sequences consisting of 10-50 repeats of 1-6 bp elements. The length of a given sequence is often polymorphic and heritable. Whilst they have no definite attributed function they have been implicated in recombination, as promoter sequences, as possible binding sites for DNA topoisomerases (Honchel et al., 1995) and they have been used to demonstrate the presence of loss of heterozygosity (LOH) in human tumours. In addition to LOH, some tumours studied were shown to have expansion or contraction of the repetitive element within microsatellites when compared to DNA from non-tumorous tissue. MIN is now known to be a feature of some sporadic cancers and it is present

in about 80% of colonic and extracolonic HNPCC tumours. Intriguingly when MIN occurs in tumours it tends to be associated with tumour diploidy, indolent clinical behaviour and improved patient survival. In contrast tumours which lack MIN but which show high degrees of LOH tend to be aneuploid, suggesting that there may be different overall genetic mechanisms which may both encourage tumorigenesis. At the molecular level there seem to be three different types of MIN. One type where there is a single repeat difference with a slightly higher than normal new mutation rate, a second type which again shows a single repeat difference but this time with a higher mutation rate and a third type which features marked expansion or contraction in multiple microsatellites (Honchel et al., 1995). Mapping of the genes involved in HNPCC was begun when linkage of HNPCC to chromosome 2p was found in 2 large kindreds (Peltomaki et al., 1993) although no LOH was demonstrated on chromosome 2 suggesting that the observed MIN was caused by something other than loss of tumour suppressor gene activity. The elucidation of the molecular defects underlying HNPCC was largely guided by earlier work on mutants of *E. coli* which showed elevated frequencies of instability in regions of simple repeat sequences, reminiscent of MIN in humans. These bacterial strains bore mutations in the genes *mutS* and *mutL*, which are involved in DNA mismatch repair (Levinson and Gutman, 1987). Investigation of similar instability in repeat tracts in the yeast *S. cerevisiae* was shown to be due to mutations in yeast homologues of the bacterial genes of mismatch repair named *MLH1* (*MutL* homologue 1), *MSH2* (*MutS* homologue 2) and *PMS1* (Post meiotic segregant 1). Two groups quickly identified a human gene *hMSH2* (human *mutS* homolog 2) on chromosome 2p, which was mutated in

some patients with HNPCC (Fishel et al., 1993)(Leach et al., 1993). However some kindreds of HNPCC showed linkage to chromosome 3p and also exhibited MIN. This led to the identification of *hMLH1*, which is a human homologue of bacterial *mutL* and yeast *MLH1* genes. Whilst *hMSH2* and *hMLH1* mutations are thought to account for most of the cases of HNPCC, two other susceptibility genes on chromosomes 2q and 7 have now been discovered and are called *hPMS1* and *hPMS2* after their *S. cerevisiae* counterparts. Interactions between these mismatch repair proteins are now being described and their functions are being further elucidated. The gene product of *hMSH2* associates with hMSH3 or hMSH6 as a heterodimer. No mutations have been found in *hMSH3* or *hMSH6* in HNPCC so far, perhaps because these complexes overlap in function (Acharya et al., 1996), (Risinger et al., 1996). Recently it has been shown that the hMSH2-hMSH6 complex is an ATPase which binds mismatched nucleotides in the ADP-bound form whilst ADP->ATP exchange results in dissociation of the complex. ATP hydrolysis then allows recovery of mismatch binding (Gradia et al., 1997). This recognition step may serve to initiate further downstream events in the repair pathway. The importance of mismatch recognition may also explain why the most conserved region of the mutS homologues contain a helix-turn helix domain associated with a "Walker-A"-type adenine nucleotide and magnesium binding motif. Mutation of conserved amino-acid residues within the adenine nucleotide binding domain results in a dominant mutator phenotype in bacteria and yeast. Defective mismatch repair may cause cancer by causing mutations in oncogenes and tumour suppressor genes. Alternatively, the resulting MIN near or within certain genes may alter their function is such a way as to promote more

generalised genomic instability, or other aspects of the transformed phenotype. There is no clear explanation yet of the differences at the genetic level that explain the distinction between the Lynch type I and type II phenotypes. It is possible that other genes modify expression of the phenotype or perhaps different mutations give rise to different clinical entities. This may be the case for the Muir-Torre Syndrome, in which affected patients present with at least one sebaceous gland tumour and a minimum of one internal malignancy (usually colorectal carcinoma). MTS patients also show MIN, and genetic linkage to DNA markers on Chromosome 2 linked to HNPCC kindreds has been demonstrated (Hall et al., 1994). It is tempting to speculate therefore that MTS is another phenotypic variant of HNPCC, although this requires further elucidation.

Breast cancer

Breast cancer is a major cause of death in females in the UK with a provisional incidence rate for England and Wales in 1997 of 109.6/100,000 women and a mortality rate (1996) of 45.3/100,000 women (personal communication from the Office for National Statistics). About 80% of breast cancer cases are sporadic due to acquired mutations, with a peak incidence in the peri-menopausal years, whereas in 20% there is a family history of the disease. Some of the familial cases are clusters which have occurred by chance because breast cancer is so common. In others the clusters are related to exposure to common environmental agents or shared lifestyle patterns and the rest are due to inherited genetic causes. In hereditary breast cancer (5% of the total), the age of onset is younger and bilaterality is more common.

Prediposing factors for breast cancer include sex (only 1% of cases occur in males), age (99% of cases occur over the age of 30), prolonged exposure to hormones causing proliferation of breast tissue (early age of menarche, late maternal age at the birth of the first child, late menopause, use of the oral contraceptive pill or of hormonal replacement therapy, breast feeding), obesity, high dietary fat intake, smoking, exposure to ionising irradiation, country of residence and a previous history of breast disease or a family history of breast cancer. The latter may be seen in patients with a family history of a breast and ovarian cancer or as breast cancer alone. Certain syndromes also carry an increased risk eg Li-Fraumeni syndrome, Lynch syndrome (type II), Cowdens disease, Peutz-Jegher syndrome, Ruvalcaba-Myresmith and Klinefelters syndrome (Hodgson and Maher, 1993).

Studies of the cytogenetics of breast cancer may reveal chromosomal regions which are important in the pathogenesis of this disorder. Some have commented that there are no consistent karyotypic abnormalities in breast cancer (Bodmer, 1988), although there have been many reports of allelic losses or rearrangements most notably of chromosomes 11, 13 and 17 (Bieche and Lidereau, 1995). These have been associated with mutations in *Tp53* (17p13.1), *BRCA-1* (17q21), *BRCA-2* (13q12.13), *ERB-B2* (17q12), *NM23* (17q22) and *ATM* (11q22-23) (Kerangueven et al., 1997), (Plummer et al., 1997) and allele losses are even seen in pre-invasive disease and good prognosis grade I tubular carcinomas (Man et al., 1996).

At the molecular level, breast cancer may be due to mutations in rare but highly penetrant genes, mutations in more common but low penetrance genes, and/or polygenic effects which perhaps modulate the expression of

either of the former. Overall, defects in low penetrance genes may account for more cases of breast cancer in the population than those due to the highly penetrant genes (Ponder, 1990).

Several genes have been implicated in the development of hereditary breast cancer including *BRCA1, BRCA2, Tp53, ATM* and the androgen receptor and oestrogen receptor genes. The latter have an obvious role in hormonal signal transduction within the nucleus and p53 is important in checkpoint integrity after DNA damage and the induction of apoptosis. It is likely that BRCA1 and 2 and ATM are involved in the cell response to DNA damage and in DNA repair mechanisms but their exact functions are not fully elucidated.

BRCA-1

The human *BRCA1* gene was identified by positional cloning in 1994 (Miki et al., 1994). The gene is thought to function as a tumour suppressor and mutations in it confer a marked predisposition to breast and ovarian cancer. Women who inherit a mutant *BRCA1* allele have a 90% lifetime risk of developing breast cancer (Ford et al., 1994), indicating high penetrance. The mutated gene is found in 45 % of families with inherited breast cancer and 80-90 % of families with an inherited susceptibility to breast and ovarian cancer. The gene is composed of 24 exons, 22 of which code for a protein of 1863 amino acids. Most of the exons are small but exon 11 is very large making up ~60% of the coding region. The function of BRCA1 is unknown but database searches reveal an amino terminal C3H4C4 motif, characteristic of RING finger zinc-binding domains which interact with DNA or proteins. Other regions of interest include a bipartite nuclear localisation signal (NLS) encoded by exon

11 and two BRCT domains in the carboxy terminus which may function as transactivators of transcription (Chapman and Verma, 1996). The latter may have a role in the regulation of gene expression as the ability of artificial and genomic reporter constructs to activate p53-responsive elements is reduced if the second BRCT element is mutated (Ouichi et al., 1998). A role in activation of the WAF-1 promoter has also been reported independent of p53 activation (Somasundaram et al., 1997). The BRCT domain has also been identified in the cell cycle checkpoint proteins p53-binding protein-1 and *S. pombe* Rad4, the DNA repair protein XRCC1 and the retinoblastoma protein pRb. Involvement of BRCA1 in the regulation of gene transcription is also suggested by its association with RNA polymerase II (Scully et al., 1997). In terms of molecular partners, BRCA1 has been found in a multiprotein complex with hRad51 (Scully et al., 1997), a protein which catalyzes ATP-dependent DNA strand exchange reactions and is a homologue of *E. coli* recombination and DNA repair protein RecA. Additional support for the hypothesis that BRCA1 is involved in the response to DNA damage is suggested by the fact that DNA damage is associated with BRCA1 hyperphosphorylation and altered nuclear co-localisation of BRCA1 with hRad51 (Scully et al., 1997).

BRCA2

The *BRCA2* gene was mapped to chromosome 13q12-13 in 1994 and was recently identified (Wooster et al., 1995), (Tavtigian et al., 1996). In contrast to *BRCA1*, both female and male *BRCA2* heterozygotes are susceptible to breast cancer with a lifetime risk of ~80-90% for women and ~ 6% for men (Stratton, 1996). In addition, *BRCA2* confers susceptibility to other tumours including

carcinomas of the ovary, colon, pancreas, larynx and prostate. Genetic inactivation of both alleles appears to be associated with tumorigenesis and *BRCA2* therefore seems to behave as a tumour suppressor gene (Stratton, 1996), (Collins et al., 1995), (Gudmundsson et al., 1995).

The *BRCA2* gene is composed of 27 exons, 26 of which code for a large protein of 3814 amino acids (Tavtigian et al., 1996), with no strong resemblance to any other known proteins. It is a nuclear protein and *in vitro* transactivation assays suggest that its amino terminus is involved in the transcriptional regulation of genes, the identities of which are unknown at present (Milner et al., 1997). BRCA2 has been found to associate with hRAD51 via direct binding through at least two binding sites, one at the amino-terminal end of the region encoded by exon 11 and one at the carboxy-terminus (Scully et al., 1997), (Sharan et al., 1997), (Wong et al., 1997). It is thought to exist in a multiprotein complex with BRCA1 on the basis that BRCA1 has also been shown to colocalize with hRAD51 (although BRCA1 does not bind to hRAD51 directly) (Sharan et al., 1997), (Wong et al., 1997), (Mizuta et al., 1997). This suggests that BRCA2 may have a role in RAD51 mediated recombination or DNA dsb repair, a hypothesis which is supported by a number of other lines of evidence: BRCA2 is found in ovary and testis where recombination occurs in meiosis, BRCA2 knock-out blastocysts are sensitive to X-irradiation (Sharan et al., 1997) but show embryonic lethality as seen with hRAD51 and BRCA-1-knock outs. Mice with alleles coding for a truncated BRCA2 molecule (encoding the amino-terminus alone with its putative transactivation domain) survive but show marked growth retardation and their cells suffer a progressive failure of cellular proliferation associated with increased p53 and p21 levels. The cells are

markedly sensitive to UVL and the alkylating agent methylmethanesulphonate and moderately sensitive to γ irradiation, but apoptosis and checkpoint function seem to be intact. In addition there is spontaneous genetic instability with increased numbers of chromatid breaks, quadriradials and triradials together with polyploidy. DNA dsb repair in V(D)J recombination, which occurs predominantly in G1 phase, is grossly intact. The authors suggest a role for BRCA2 in recombination or recombinational repair rather than in DNA dsb repair (Patel et al., 1998), although they comment that due to lack of a suitable antibody they cannot confirm the presence of truncated BRCA2 in their mutants. The animals develop thymic lymphomas (as described for *ATM* mutant mice) but no mammary gland carcinomas are reported.

Mice homozygous for *BRCA2* truncations which retain the amino-terminal putative transactivation domain and the amino-terminal RAD51 interaction domain have also been generated (Connor et al., 1997). They possess a similar overall phenotype to those described by Patel et al, but homozygous mutant mouse embryonic fibroblasts (MEFs) showed reduced DNA dsb repair after 40Gy of X-irradiation compared with wild type and heterozygous MEFs assessed by the neutral comet assay. These authors therefore concluded that BRCA2 is required for DNA dsb repair, although, as in the other study, they could not verify the expression of truncated BRCA2 due to lack of suitable reagents.

p53

p53, encoded by the *Tp53* gene is now a well established tumour suppressor, mutation of which is the commonest alteration seen in human cancer. Women with the rare Li-Fraumeni syndrome who carry a germline mutation in p53 are highly predisposed to breast cancer although many other tumour types are also seen including soft tissue sarcomas, osteosarcomas, leukaemias, brain tumours and adrenocortical carcinomas. p53 is known to be important in the maintenance of genomic integrity and is involved in gene regulation, cell cycle checkpoint control, DNA repair, cellular senescence and apoptosis all of which have an impact on tumorigenesis (Harris, 1996). p53 germ-line mutations have also been identified in patients with sporadic breast cancer (Andersen, 1996), (Prosser et al., 1992), (Sideransky et al., 1992). A p53 splice site mutation has also been identified in a family with hereditary breast and ovarian cancer (Jolly et al., 1994).

The sex hormone receptors

A mutation of the androgen receptor gene which affects the DNA binding portion of the receptor has been found in a several cases of male breast cancer, a subset of which are characterised by partial androgen insensitivity (Andersen, 1996). It is also possible that mutations at the oestrogen receptor (ESR) locus are associated with breast cancer susceptibility and there is a report of cosegregation of an ESR haplotype and breast cancer in a late-onset family (Andersen, 1996), (Zuppan et al., 1991).

Other genes

A variety of other genes including c-myc, which encodes a nuclear transcription factor, c-erb-B2 (HER2/neu) and NM-23 have been implicated in breast cancer and show amplification and correlation with poor prognosis (Callahan and Campbell, 1989).

ATM

The reported association of an increased risk of cancer in A-T heterozygotes (Swift et al., 1976), has resulted in a surge of interest in this area although no overall increase in deaths from breast cancer was seen in this non-molecular study of 27 families of patients with A-T comparing blood relatives to spouse controls. Subsequent studies also suggested that A-T heterozygotes were predisposed to breast cancer (Swift et al., 1987), (Swift et al., 1991), (Pippard et al., 1988), (Borresen et al., 1990). The lack of an over-representation of breast cancer amongst A-T sufferers appears puzzling if the heterozygotes are at increased risk and has been explained on the basis that death in A-T usually occurs prior to the age of susceptibility to breast cancer. In support of this hypothesis, there are reports of breast cancer in A-T patients who reach an older age than usual in this condition, but it is also of note that only one *ATM* mutation (7271T->G) has been statistically proven to confer an increased risk of breast cancer (Stankovic et al., 1998) which may complicate the picture. If heterozygotes really are at increased risk of the disease then knowledge of a woman's genetic status with respect to the *ATM* gene becomes important in terms of breast cancer screening. This is doubly relevant as X-ray exposure for mammography is part of the current breast cancer screening programme, yet

ATM heterozygotes are theoretically more sensitive to the harmful effects of ionising irradiation. These include early and late radiation reactions and possible genetic effects leading to oncogenesis. Several investigators have now addressed the question of breast cancer risk and *ATM* status using different study designs. Those in association and agreement with Swift include (Athma et al., 1996) who have traced *ATM* in 99 A-T families using the closely linked markers D11S1778 and D11S1819 which flank *ATM* . They found 33 women with invasive breast cancer; 25 were A-T heterozygotes compared with the expected number of 14.9. For all breast cancers in the sample the odds ratio, estimating the relative risk of carriers compared to non-carriers, was 3.8 (95% confidence limits 1.7-8.4). This risk is similar to that of 3.9 for all ages found by an analysis of previously mentioned studies of breast cancer risk in mothers and other close relatives of A-T cases (Easton, 1994). For the 21 women under the age of 60 the odds ratio was 2.9 (95% CI: 1.1-7.6) and for the 12 women over the age of 60 it was 6.4 (95% CI: 1.4-28.8), suggesting that A-T heterozygotes are predisposed to breast cancer. Based on an estimated heterozygote frequency in the USA of 1.4% and the estimated relative risks before and after age 60, 6.6% and 8.3% of all breast cancers in the USA were estimated to occur in A-T heterozygotes in the younger and older age groups respectively. It is notable that the risk in this study appeared greater in older rather than younger women. This is in direct contrast to results of previous studies (Easton, 1994) and observations in other cancer predisposition syndromes. The incidence of bilaterality was not increased in the heterozygotes either, although this is increased in other familial breast cancer cases. Other investigators have criticised Swift's earlier studies (Swift et al., 1987) and (Swift

et al., 1991), on the basis that there was an unexpectedly low incidence of breast cancer in the controls used (Fitzgerald et al., 1997). This team conducted a germ-line mutational study of the *ATM* gene in a group of 401 women with early onset breast cancer (aged 40 or below), compared with 202 healthy individuals with no history of cancer. A cDNA-based protein truncation test was used to detect chain terminating mutations (these account for 90% of mutations in cases of A-T). Chain terminating mutations were detected in 2/401 (0.5%) of women with breast cancer and 2/202 (1%) of controls. Although this screening method cannot identify missense or regulatory region mutations, whilst identifying pre-mRNA splicing variants, it suggests that there is no significant correlation between *ATM* heterozygosity and the development of early onset breast cancer (Fitzgerald et al., 1997). It is conceivable that if the risk of breast cancer in carriers of *ATM* gene does increase with age then they might have failed to detect the effect in a younger age group. An independent statistical analysis (Bishop and Hopper, 1997) of (Athma et al., 1996) and (Fitzgerald et al., 1997) has commented that the higher estimate of the 95% confidence interval of the Fitzgerald study allows for up to a 7-fold increased risk to be consistent with the observed data, therefore allowing the results to be consistent with those of (Athma et al., 1996).

The role of A-T heterozygosity in familial breast cancer has been examined in 100 Swedish families (two or more cases of breast cancer in the family regardless of age of onset) not suffering from germ-line mutations in *BRCA-1* or *BRCA-2* (Chen et al., 1998), using the protein truncation test to look for germ-line *ATM* mutations in peripheral blood lymphocytes. One germ-line mutation was found, consistent with the expected carrier frequency for A-T of

1%. They also studied 4 paraffin embedded breast tumours together with non-tumour tissue from patients with familial breast cancer harbouring known germline mutations of *ATM*. None showed a Knudson 'double hit' of the *ATM* gene in the tumour tissue; indeed the mutated allele rather than the wild type allele had been lost in one case. Although this is only a small sample size it suggests that the *ATM* gene is not responsible for the tumour development and is not acting as a classical tumour suppressor in these cases. Two other studies have also shown an absence of linkage to the A-T locus in familial breast cancer (Wooster et al., 1993), (Cortessis et al., 1993).

As can be seen from the preceding discussion, the conflict in the literature is as yet unresolved, largely due to the relatively small study sizes in relation to the assumed frequency of heterozygosity within the general population, and the lack of exact information regarding this frequency. It is doubtful that *ATM* plays a major role in sporadic breast cancer in the general population, although it may be relevant in a proportion of women with familial breast cancer. This is given further weight by the fact that recently, a particular *ATM* mutation 7271T->G has been shown to be significantly associated with an increased risk of breast cancer in both homozygote and heterozygotic carriers (Stankovic et al., 1998). This mutation allows production of a full length ATM protein which may have residual activity as it is associated with a milder clinical A-T phenotype. This mutation may provide a tool which in the future may be used to investigate the molecular mechanism of breast cancer association with A-T.

DNA repair and breast cancer

The repair of DNA damage suffered by a cell is of critical importance to survival and several DNA repair systems exist to deal with different DNA lesions. Damage on a single strand can be repaired by base excision repair, nucleotide excision repair and mismatch repair pathways already mentioned. DNA double strand breaks can be repaired by several different pathways including homologous recombinational repair (where extensive homology is required between the region with the double strand break and the sister chromatid or homologous chromosome being used as the template), and non-homologous recombinational repair which requires very little or no homology on the ends of the strands being rejoined. A more detailed review of these repair pathways is beyond the scope of this thesis and for further information the reader may refer to the following articles (ap Rhys and Bohr, 1996), (Barzilay and Hickson, 1995), (Camerini-Otero and Hsieh, 1995), (Hendrickson, 1997), (Belmaaza and Chartrand, 1994).

One of the risk factors for the development of breast cancer is radiation exposure (Goss and Sierra, 1998). DNA damage if left unrepaired can cause mutations directly, and unrepaired breaks may be converted into chromosomal breaks allowing translocations with abnormal gene position and regulation effects and the creation of gene fusions, all of which may be oncogenic.

Constitutional DNA repair has been studied in breast cancer patients by analysing the frequency of chromatid breaks after G2 phase X-irradiation in phytohaemaglutinin (PHA)- stimulated lymphocytes (Scott et al., 1994). These authors found that 21 of an unselected series of 50 women with sporadic breast cancer showed an abnormally high frequency of breaks and suggest that these

women have defects in the processing of DNA damage. In a similar study chromatid breaks were quantified in PHA stimulated lymphocytes after either X-irradiation or UV-C exposure, with or without post-treatment with a DNA-repair inhibitor, 1-b-arabinofuranosylcytosine (ara-C), to examine the contribution of DNA repair to the results. 6 out of 7 cases of women with breast cancer and a family history of breast cancer and 6 out of 11 cases of sporadic breast cancer were found to be deficient in the repair of radiation induced DNA damage; these showed greater numbers of chromatid breaks per 100 metaphases compared with normal controls with no personal or family history of breast cancer (Parshad et al., 1996). Scott's group have since published another study using high dose or low dose rate γ-irradiation and a micronucleus assay on G0 lymphocytes from breast cancer cases and normal volunteers including some spouses of breast cancer patients. With the high dose rate protocol they found 31% (12 out of 39) of breast cancer patients compared with only 5% (2 out of 42) controls showed elevated micronucleus induction (Scott et al., 1998). A variety of different mechanisms may be responsible for the elevated chromosomal radiosensitivity described. These include defective DNA repair (Parshad et al., 1983), perturbations in cell cycle checkpoint control (Little and Nagasawa, 1985), (Wang et al., 1996), failure of the apoptotic elimination of cells with damaged chromosomes (Schwartz et al., 1995), (Wang et al., 1996) or defects related to those which lead to the classical chromosome fragility disorders (ataxia-telangiectasia, Bloom's syndrome, Fanconi's anaemia and Nijmegen breakage syndrome) already discussed. Consideration of the molecular defects underlying rare disorders, therefore,

may help to elucidate the mechanisms of genomic instability which are important in the evolution of common human malignancies.

Chapter 2

Materials and Methods

2.1 Chemicals

Unless otherwise stated, all chemicals used were purchased from Sigma Chemical Company. All tissue culture media, PBS, EDTA, trypsin and L-glutamine were supplied by Tissue Culture Services, Clare Hall, UK. Bacterial media were supplied by ICRF Central Stores, Clare Hall. All radioisotopes were supplied by Amersham, UK Ltd. Protease inhibitors and Polyacrylamide mixes were purchased from Boehringer Mannheim.

2.2 Enzymes

Unless otherwise stated, all enzymes used were purchased from Boehringer Mannheim. DNA-dependent Protein Kinase was purchased from Promega.

2.3 Plasmids

The bacterial expression vector pET-14b was purchased from Novagen and plasmid pQE-32 (Qiagen) strains 1 and 2 containing histidine sequence-tagged-5' inserts of *ATM* cDNA were received as a gift from Dr Andrew Sutcliffe in the form of M15 stab cultures (CRC Laboratories, Birmingham , UK). pET-14b with histidine sequence tagged PHAS-I insert was received as a gift from Professor John Lawrence (University of Virginia). The mammalian expression vector pCD2-CMV was described previously (O'Connell et al., 1994). pCR-Script was purchased from Stratagene.

2.4 Bacteriophages

Lambda phage λ CEV-29 containing the AT_{7-9} clone was received as a gift from Professor Yosef Shiloh (Tel Aviv University).

2.5 *E. coli* strains

BL21 (F^-*ompT hsdS*$_B$ ($r_B^-m_B^-$) *gal dcm* (DE3)pLysS (cam^R), an E. coli B strain with DE3, λ prophage carrying the T7 RNA polymerase gene was used for expression of recombinant proteins cloned into pET-14b. The bacteriophage DE3 transferred chromosomal copy of the T7 RNA polymerase gene is under *lacUV5* promoter control. Addition of IPTG (isopropyl-β-D-thiogalactopyranoside) stimulates expression of the polymerase which allows expression of recombinant His-tagged protein downstream of the T7 promoter of pET-14b. A small amount of T7 lysozyme encoded by a plasmid in BL21 pLysS binds T7 polymerase and inhibits it ensuring very low levels of expression from the T7 promoter in the absence of IPTG (which might be useful if the target product is mildy toxic).

DH10β (F^-*ara* D139 Δ(*ara, leu*)7697Δ*lac* X74 *gal* U *gal* X *mcr* A Δ (*mrr-hsd* RMS-*mcr* BC) *rps* L*dor* f80d*lac* ZDM15 *end* A1 *nup* G *rec* A1) was used as an electrocompetent strain for transformations.

LE392 ($e14^-$(McrA$^-$)*hsdR514 supE44 supF58 lacY1*) was used as a host for the lambda phage λ CEV-29 containing the AT_{7-9} clone.

M15 (F^- *lac* Z DM15 *ara*$^-$ *gal*$^-$ *mtl*$^-$ *rec*A^+ *uvr*$^+$ *lon*$^+$ (Km^r Str^s)), (Hoffmann-La Roche Ltd.), was used as the host for pQE-32.

2.6 Preparation of competent *E. coli*

To prepare supercompetent DH10β 3ml of Luria Broth (LB) was innoculated with a single bacterial colony and grown overnight at 37°C in a shaking incubator. 2ml of this overnight culture was then innoculated into 200ml of LB and incubated at 37°C until the OD_{600} was (0.5-0.8). The culture was then allowed to shake on ice for 30 minutes before centrifugation at 4,200 rpm for 10 minutes at 4°C (Beckman J-6B). The bacterial pellet was then washed twice in 200ml of ice cold sterile water, prior to repeat centrifugation and resuspension of the bacterial pellet in 20ml of 10% glycerol. After this, a final centrifugation was performed as described above and the bacteria were resuspended in 2ml of 10% glycerol and aliquoted into 50µl samples for storage at -70°C. A transformation efficiency of at least 10^8 colonies/µg plasmid was aimed for.

2.7 Transformation of competent *E. coli*

Aliquots of competent cells were thawed at room temperature. 0.7µl of plasmid DNA was taken directly from the ligation reaction and was added to 50µl of electrocompetent DH10β and mixed gently. The bacteria were then transferred to a cuvette and electroporated at 2.5kV, 25µF, 400Ω using a

BIORAD electroporator. 150µl of SOC medium containing 2% Bacto Tryptone, 10mM NaCl, 2.5mM KCl, 10mM $MgCl_2$, 0.5% Bacto yeast extract, 10mM $MgSO_4$ and 20mM glucose was then added to the cuvette and the sample was divided into two aliquots for spreading onto duplicate agar plates (made with LB and 100 µg/ml Ampicillin).

2.8 Agarose gel electrophoresis

DNA samples were electrophoresed through 0.7% agarose gels containing 0.25 µg/ml ethidium bromide in TBE buffer (90mM Tris, 90mM boric acid, 2.5mM EDTA), using a horizontal gel apparatus (Pharmacia). DNA samples containing 1/5 volume of DNA sample buffer (30% (w/v) sucrose, 100mM EDTA, 0.01% (w/v) Bromophenol Blue), were electrophoresed at 100mA until the dye had reached the desired distance. DNA was visualised by exposure to UV light from a high intensity, long range wavelength transmitter (Fotodyne). A photograph of the gel was taken using by an MP-4 Polaroid camera following the manufacturer's instructions.

2.9 Restriction digests

Closed circular plasmid DNA was digested with the appropriate restriction enzyme(s) according to the manufacturers instructions assuming that 1µg of DNA is digested by 1 unit of enzyme in 1 hour at 37°C. The mixture was normally made up to a volume of 30µl, including the appropriate buffer and incubated at 37°C for 90 minutes.

2.10 Small scale preparation of plasmid DNA from *E. coli*

A single bacterial colony containing the plasmid of interest was resuspended in 3 ml of medium (LB/100µg/ml Ampicillin) and incubated overnight in a shaking incubator at 37°C.

The following morning the cells were collected from 1.5 ml of the culture by centrifugation at 14,000 rpm for 30s in a benchtop centrifuge. Most of the medium was then poured off and the bacteria were resuspended in the remaining 50-100 µl. 300 µl of TENS (10 mM Tris pH 8, 1 mM EDTA, 0.5% SDS and 0.1M NaOH), was added to this to lyse the bacteria, and the mixture was vortexed for 2-3 s prior to the addition of 150 µl of 3M Na acetate (pH 5.2) which precipitates the protein and the denatured chromosomal DNA. The mixture was vortexed again briefly and centrifuged for 2 min as before. The pellet contains most of the chromosomal DNA, SDS-protein complexes and cellular debris. The supernatant which contains the plasmid DNA was removed to a fresh tube and precipitated with 0.9 ml of absolute ethanol. This was then centrifuged again for 2 min to pellet the plasmid DNA, washed in 70% ethanol and allowed to dry before being resuspended in 30 µl of TE (10 mM Tris.Cl pH 8.0, 1 mM EDTA, pH 8.0), containing 20µg/ml of RNAase A. 3µl of the resulting solution was cut with the appropriate restriction enzymes to release the cloned insert from the plasmid. The sizes of the cut vector and insert were then verified by agarose gel electrophoresis.

2.11 Large scale preparation of plasmid DNA from *E. coli*

A 2 l flask with 400ml of LB medium containing 100µg/ml Ampicillin was inoculated with 1 ml of a fresh overnight culture of *E.coli* containing the plasmid of interest. The culture was incubated overnight at 37°C with vigorous shaking (250 rpm). The cells were harvested by centrifugation for 10 minutes at 9Krpm in a JA10 rotor in a J2-21 centrifuge. The pellet was resuspended in 10 ml of DISH-1 (50 mM glucose, 25 mM Tris pH 8 and 10 mM EDTA). To this 30 ml of freshly prepared TENS (10 mM Tris pH 8, 1 mM EDTA, 0.5% SDS and 0.1M NaOH),was added and mixed in by swirling. 15 ml of 3M Na acetate pH 5.2 was then added to the above mixture to precipitate the denatured protein and chromosomal DNA. The mixture was centrifuged again as previously and the supernatant containing the plasmid was poured off carefully through a sterile gauze into a clean 250 ml centrifuge tube and precipitated with 90 ml of absolute ethanol. The precipitated plasmid was then pelleted by centrifugation at 9Krpm for 10 min in the JA-10 rotor. The supernatant was discarded and the pellet was drained by inverting the bottle on tissues for 10 min. After this exactly 8 ml of TE (10 mM Tris.Cl pH 8.0, 1 mM EDTA, pH 8.0), was added to dissolve the pellet. CsCl/ethidium bromide density gradient purification allows separation of the plasmid DNA from the contaminant chromosomal DNA due to their different capacities to bind the interclating agent ethidium bromide which reduces the density of the DNA. Plasmid DNA binds less and is therefore more dense, appearing as the lower band after CsCl gradient centrifugation: Exactly 8 g of the dissolved DNA solution was added to 8.4 g of CsCl in a plastic universal and vortexed briefly

to dissolve the CsCl. 0.4 ml of ethidium bromide solution (10 mg/ml) was then added to the universal and mixed. The resultant DNA/CsCl/ethidium bromide solution was then divided between two vTi tubes placed in the vTi90 rotor and centrifuged at 70Krpm overnight at 25°C. After separation of the DNA on the CsCl gradient the band corresponding to the plasmid DNA was removed using a 1 ml syringe and a 19 g needle. The plasmid solution was then transferred to a 15 ml tube (Falcon) and the ethidium bromide was extracted sequentially with CsCl-saturated isopropanol until the solution was completely colourless. The plasmid DNA was then precipitated by the addition of 2 volumes of water and 7 volumes of absolute ethanol and the DNA harvested by centrifugation at 4Krpm for 15 min in a JA-20 rotor. After this the DNA was washed in 70% ethanol, dried and resuspended in 1 ml TE (10 mM Tris.Cl pH 8.0, 1 mM EDTA, pH 8.0) and stored at -20°C.

2.12 Ligation of plasmid DNA

Ligations were carried out using 50ng of vector and ~500ng of insert DNA (unless otherwise indicated), which had previously been purified using the GeneClean kit (BIO 101). 1 unit of T4 DNA ligase and 1 µl of ligase buffer, was added to the DNA for ligation to a total volume of 10µl. For sticky end ligations, reactions were incubated at 16°C for 16 hours. Ligation reactions were then transformed into competent bacteria as described. A control ligation and vector only control for transformation were always included.

2.13 Preparation of oligonucleotides

These were all made at ICRF Oligonucleotide Service (Clare Hall, UK). On receipt, the dried oligonucleotides were precipitated by addition of 20µl of 3 M Na acetate, 180µl of distilled H_2O, 2µl of 1 M $MgCl_2$ and 600µl of absolute ethanol with incubation on ice for 10 min. The mixture was then centrifuged at 14Krpm for 10 min in a benchtop centrifuge 5415C (Eppendorf) and the precipitate was resuspended in 1ml of sterile water resulting in a final concentration of ~40µM.

2.14 DNA Sequencing

This was performed on an ABI PRISM 377 DNA sequencer. The template sequence to be analysed was first amplified using the ABI Prism Dye Terminator Cycle Sequencing Core Kit with fluorescent-tagged deoxynucleotides which block the progression of the Amplitaq DNA polymerase (Perkin- Elmer). Manufacturers instructions were followed. The sequence was analysed using Sequence Navigator (ABI Prism) and Sequencher (Gene Codes Inc.), software.

2.15 Preparation of whole cell extracts for Western blotting

Cells growing in tissue culture were washed once with phosphate buffered saline (PBS), (137 mM NaCl, 2.7 mM KCl, 4.3 mM $Na_2HPO_4.7H_2O$, 1.4 mM KH_2PO_4, pH 7.3) and removed from the tissue culture plate using PBS with 2.5mM EDTA. Cell number was determined using a haemocytometer and approximately 1-5 $x10^6$ cells were lysed in 200µl 2X SDS buffer (60mM Tris-

HCl, pH 6.8, 1% (w/v) SDS, 5% (v/v) glycerol, 0.001% (w/v) Bromophenol Blue and 1% (v/v) 2-mercaptoethanol). Chromosomal DNA was sheared by passing the extract through a 25-G needle 3 times and the sample was boiled for 5 minutes before storage at -20°C.

2.16 Protein gel electrophoresis

Single dimensional separation of proteins by polyacrylamide gel electrophoresis was always performed under denaturing and reducing conditions ie in the presence of SDS and 2-mercaptoethanol, using the discontinous buffer system of Laemmli (Laemmli, 1970). Prior to electrophoresis, cell lysates or protein samples were boiled for 3 minutes in 2X SDS sample buffer (60mM Tris-HCl, pH 6.8, 1% (w/v) SDS, 5% (v/v) glycerol, 0.001% (w/v) Bromophenol Blue and 1% (v/v) 2-mercaptoethanol). Gels were made up using an acrylamide/bisacrylamide (37.5:1) solution (Boehringer Mannheim), in the presence of a catalyst (10% Ammonium persulphate and TEMED (N,N,N',N'-tetramethylethylenediamine). The resolving gels were prepared in 375mM Tris-HCl, pH 8.8, 0.1% (w/v) SDS, while the stacking gels (6% polyacrylamide) were prepared with a buffer containing 125mM Tris-HCl, pH 6.8, 0.1% (w/v) SDS. The electrophoresis running buffer contained 190mM glycine, 25mM Tris and 0.1% (w/v) SDS. For analysis of ATM and BLM, samples were resolved by SDS-PAGE on 7.5% gels. Recombinant fragments of ATM, BLM and β-tubulin were resolved on 13% gels.

Unless otherwise stated all SDS-polyacrylamide gels were prepared on the BIORAD miniprotean vertical gel electrophoresis apparatus (Hoefer). A

large format gel apparatus was used with 7.5% gels when resolution of high molecular weight and lower molecular weight proteins was required from the same sample.

For detection of unlabelled proteins following electrophoresis, gels were stained with 0.1% (w/v) Coomassie Blue in 10% acetic acid and 50% methanol. Gels were destained by washing in 10% acetic acid, 10 % methanol. Samples were compared against molecular weight standards. Coomassie Blue stained gels were then dried onto Whatman 3MM paper using a Hoefer slab gel dryer, model SE1160.

For detection of ^{32}P-labelled proteins after drying as described, gels were exposed to X-Ray film (Kodak X-OMAT AR) at -70°C in a cassette with intensifying screens for autoradiography.

If required, transfer of proteins to Immobilon-P membrane (Millipore) for Western blotting was achieved using the semi-dry technique. The membrane was pre-wetted in 100% methanol and then placed in the transfer buffer containing 10% (v/v) methanol and 1mM CAPS (3-[cyclohexylamine]-1-propane sulphonic acid) in deionised water (Milli-Q). The membrane was then laid onto the gel, taking care to exclude any air bubbles and 2 pieces of 3MM Whatman blotting paper, pre-soaked in transfer buffer, were placed on both sides. This sandwich was then placed into the Semi-Phor transfer tank (Hoefer) with the gel side uppermost, before being electrophoresed at 9V for 45 minutes.

2.17 Western blotting

This was performed according to the method given in (Ausubel et al., 1997). Samples were electrophoresed on polyacrylamide gels and semi-dry protein transfer was performed as described. The membrane was incubated in a blocking solution of PBS containing 5% Marvel dried milk powder (MDMP) for 1 hour. The appropriate primary antibody was then added to PBS/0.3% (v/v) Tween-20, 5% MDMP to the appropriate dilution and spotted on the membrane for incubation for 1 hour at room temperature or overnight at 4°C. The membrane was then washed for 10 minutes x3 in PBS/0.3% (v/v) Tween-20 and then incubated for 1 hour with the appropriate secondary HRP-conjugated antibody. The membrane was then washed for 10 minutes x3 with PBS containing 0.3% (v/v) Tween-20. Detection of HRP-labelled conjugates was achieved using ECL Western blotting detection reagents (Amersham Life Science). The interaction of peroxidase with luminol and an enhancer in the supplied developing solutions causes the emission of light which can be detected using Kodak Scientific Imaging Film X-OMAT AR (Kodak).

2 18 Mammalian cell culture

Cell lines, culture conditions and media

HeLa-S3 cells, (a non A-T cell line), SV40-transformed human cervical carcinoma cell line, 2% RPMI medium, 15% FCS.

GM4724 (ATM+/+), human lymphoblastoid cells, 2% RPMI medium, 15% FCS.

GM2782a (ATM-/-), human lymphoblastoid cells, 2% RPMI medium, 15% FCS.

AT5BIVA (ATM-/-), SV40-transformed human AT5BI fibroblasts, alpha medium, 20% FCS.

AT2RO (ATM-/-), human fibroblasts, not cultured. Cell lysates were donated by Dr M. James.

GM8505 (BLM -/-), human fibroblasts, alpha medium, 20% FCS.

MRC5, a wild type human fibroblast line, alpha medium, 20% FCS.

NCI-H1299 cells (p53 null), a human non-small cell lung carcinoma line, 2% RPMI medium, 10% FCS.

Human peripheral blood lymphocytes. 2% RPMI medium, 15% FCS.

(3 mM L-glutamine was added to all media prior to use and cells were cultured at 37°C in an atmosphere of 5% CO_2).

2.19 Preparation of phage DNA

Multiple attempts to isolate the *ATM* cDNA by PCR and by hybidization from several different human libraries proved unsuccessful and are not discussed here. A source of the AT7-9 clone in λCEV-29 was gratefully received as a gift from Professor Y. Shiloh (Tel Aviv University). Amplification of the phage containing the insert was achieved by culture of the phage in host LE392 bacteria using a phage plate lysate protocol: A single colony of LE392 was inoculated into 3 ml of TB medium containing 5g NaCl/L, 10g bactotryptone/L, 10mM $MgSO_4$ and 10mM maltose and incubated overnight at 37°C in a shaking incubator. To 0.5ml of the overnight LE392 culture, 2-3x10^5 c.f.u. of phage were added and incubated at 37°C for 15 minutes. 15 ml of TOP agarose containing 0.7% agarose in NZY broth (5g NaCl, 2g

$MgSO_4.H_2O$, 5g yeast extract, 10g NZ amine (casein hydrolysate)/l), was added to the culture, gently mixed and poured onto the top of NZY/agarose plates and incubated at 39°C for exactly 8 hours for optimum bacterial growth and phage induced bacterial lysis. After this time had elapsed, each plate was overlayed with 10ml of phage buffer containing 5.8g NaCl, 2g $MgSO_4.H_2O$, 50ml 1M Tris-HCl, pH 7.5, 5ml 2% gelatin/L and 0.5ml of chloroform and allowed to elute the phage with gentle shaking overnight at room temperature. The following day, the eluate was collected from the plates and purification of the phage DNA was achieved using a Lamda DNA purification WIZARD kit (Promega) following the manufacturers instructions.The purified AT7-9 clone insert in the λCEV-29 DNA was digested with the restriction enzyme Sal1 to obtain the AT7-9 insert which was originally cloned into the phage Sal1 site (Fig. 2.1).

2.20 Flow cytometry

Cells were harvested and fixed for 30 minutes in ice cold 70% ethanol/30% PBS, collected by centrifugation and treated with RNAase A (100μg/ml final concentration) and propidium iodide (40μg/ml) in PBS for 30 minutes at 37°C. Cell cycle distribution was then determined using a FACScan (Becton-Dickinson) and Lysis II software with the assistance of Dr Chris Norbury.

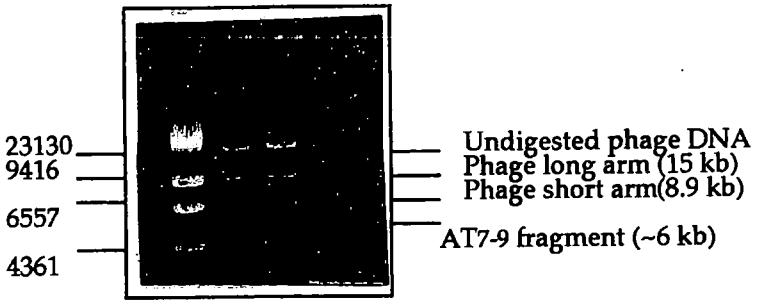

Fig. 2.1

Treatment of a preparation of λCEV-29 DNA with the restriction enzyme Sal1 releases the AT7-9 clone.

2.21 Subcellular fractionation protocol

The protocol followed for analysis of the subcellular localisation of ATM and BLM proteins was modified from (Watters et al., 1997). 2 x 10^8 HeLa cells or GM8505 cells were obtained as pellets on dry ice from ICRF Cell Services (Clare Hall, UK). These were resuspended in 2ml ice-cold homogenisation buffer (25 mM HEPES, 0.25 M sucrose, 1 mM EGTA, 5 MM $MgSO_4$, 50 mM NaF, 1 mM DTT). N.B. All solutions used also contained a cocktail of serine and cysteine protease inhibitors (Boehringer Mannheim) together with the aspartic protease inhibitor pepstatin. The cell suspension was then homogenised for 50 strokes in a type A Dounce Homogeniser, placed in a 15ml Falcon tube and centrifuged at 3000 rpm in a Beckman GPR centrifuge for 15 min to pellet the nuclei.

The supernatant was carefully pipetted off, placed in 11 x 34 polyallomer tubes (Beckman) and centrifuged in a TLA-100 rotor at 58,000 rpm for 40 min to pellet the microsomal fraction, leaving the cytosolic extract as the supernatant. The microsomal pellet was resuspended in 100µl of 2x protein sample buffer. The cytosolic extract was resuspended in an equal volume of 2x protein sample buffer.

The nuclear pellet was lysed in 500µl of lysis buffer (50 mM Tris-HCl, 150 mM NaCl, 2 mM EGTA, 2 mM EDTA, 25 mM NaF, 25 mM ß-glycerophosphate, 0.1 mM sodium vanadate, 0.2% Triton X-100, 0.3% NP-40 including protease inhibitors as described). After incubation on ice for 30 min, the debris was removed by centrifugation at 16,000 rpm for 15 min in a JA-20

rotor, yielding the nuclear extract as supernatant. The nuclear extract was resuspended in an equal volume of 2x protein sample buffer. All extracts in sample buffer were then boiled for 3 min, sheared and stored at -20°C until required. 25µg of protein was loaded per track for analysis by Western blot.

2.22 Protein immunoprecipitation from nuclear isolates

Nuclear isolates were obtained from batches of 2 x 10^8 HeLa cells received from Cell Production Clare Hall, ICRF, using a gentler protocol (Kroll and Rowe, 1991). The cell pellet from each batch was washed once in ice-cold PBS and then resuspended in 3.6 ml of nuclear isolation buffer (30 mM Tris-HCl pH 7.5, 1.5 mM $MgCl_2$, 10 mM KCl, 20% v/v glycerol together with a protease inhibitor cocktail and the phosphatase inhibitors, 1mM β-glycerophosphate and 1 mM sodium vanadate. The plasma membrane of the cells was lysed by adding 400µl of 10% Triton X-100, briefly vortexing and incubating the lysate on ice for 5 min. After centrifuging at 1000 rpm (Beckman GPR centrifuge), for 90 s the supernatant was pipetted off and the nuclear pellet was resuspended in 3.6 ml of nuclear isolation buffer (30 mM Tris-HCl, 1.5 mM $MgCl_2$, 10 mM KCl, 20% v/v glycerol with protease and phosphatase inhibitors and 0.35 M NaCl to elute the nuclear proteins). After a 30 min incubation on ice, the eluate was centrifuged at 12,000 rpm (JA-20 rotor), to eliminate the debris. The resultant supernatant was then divided for use in subsequent immunoprecipitations:

Pre-clearing of nuclear extracts was achieved by incubating the extracts with pre-swollen protein A-Sepharose beads (Sigma) on a rocker for 60 min at

4°C. After this time the beads and non-specifically bound proteins were pelleted by centrifuging at 10,000 rpm for 10 seconds (Eppendorf centrifuge 5415C), and the supernatant (ie the pre-cleared extract), was taken for further use.

The pre-cleared extract was added to an equal volume of immunoprecipitation buffer (100 mM Tris-HCl pH 8.0, 500 mM NaCl, 0.75% v/v Triton X-100, 10 mM EDTA, 0.02% (w/v) NaN_3, and protease inhibitors as described. The required immunoprecipitating antibody was then added to the extracts at the appropriate dilution.

The antibody and extract were incubated at 4°C for 1 hour on a rotating wheel prior to addition of 50µl of preswelled protein-A-Sepharose beads. The mixture was then incubated for a further 1 hour under the same conditions to allow binding of the beads to the antibody with the precipitated protein. After this time the beads were pelleted as previously and washed three times with immunoprecipitation buffer containing 0.1% SDS, prior to a final wash of 10 mM Tris-HCl pH 7.5. The beads with attached antibody and immunoprecipitated protein were then ready for Western analysis or in the case of ATM for use in the autophosphorylation, p53 peptide or PHAS-I ATM kinase assays. Western analysis simply required boiling of the pelleted beads in 30 µl of 2X SDS sample buffer for 5 minutes before loading onto a protein gel.

Chapter 3

Production and Characterisation of Antibodies versus ATM and BLM Proteins

3.1 Introduction

Antibodies are potentially very powerful investigative tools which can be used for many biological studies including definition of the sub-cellular localisation, the cell cycle distribution, the tissue specific or tumour related expression and the biochemical actions and interactions of the protein of interest. When a novel gene is described therefore, much of the initial effort is directed toward raising antibodies against the gene product .

Polyclonal antibodies can in theory be raised against any immunogenic protein. At the outset of this thesis, no commercial antibodies against ATM or BLM were available and strategies for the expression of full-length epitope tagged cDNAs were still being planned. As no source of full length ATM was available for use as an immunogen, ATM peptides were designed and recombinant partial ATM constructs were expressed with the aim of presenting these as immunogens in rabbits for the development of polyclonal anti-ATM antisera. Whilst polyclonal antibodies with their range of epitope specificities are particularly useful for some purposes eg. immunoprecipitation, their source is finite. Development of hybridomas as a source of monoclonal antibodies with single epitope specificity is potentially the most useful for investigations in the long term as the supply of monoclonals is theoretically infinite.

3.2 Additional materials and methods

3.2.1 Production of anti-ATM antibodies

Several different recombinant ATM fragments were sent for rabbit immunisation. These included:

A) 4 biochemically synthesized ATM peptides designed by myself and made by the Peptide Synthesis Laboratory, Lincoln's Inn Fields, ICRF. These were conjugated to Keyhole Limpet Haemocyanin (Sigma) as a carrier molecule to improve the immunological response to the peptide.

B) Two recombinant ATM proteins were generated from plasmids pQE-32 strains 1 and 2, received as a generous gift from A. Sutcliffe (Birmingham CRC unit). These comprised ATM protein sequence from amino acids 288-524 (strain 1) and from amino acids 992-1144 (strain 2). The proteins expressed from both of these strains proved to be considerably insoluble and primarily present in the cell pellet. Therefore both proteins had to be sent in the form of purified inclusion bodies and they were also sent in the form of an acrylamide gel slurry derived from unstained protein gels from which the appropriate band was dissected. The production of these is described below:

A) ATM peptide production and KLH conjugation

A variety of ATM peptides were designed and entered into the SHARQ database (Alex Whittaker, Lincoln's Inn Fields, ICRF) to identify similarities with known proteins. Those without any marked similarities with known proteins were then used as potential immunogens for anti-ATM antibody production.

These comprised ATM protein sequence

Peptide 1: VDIMRASQDNPC (amino acid 1629-1639)

Peptide 2: PRFDKENPFEGC (amino acid 1778-1789)

Peptide 3: ERKKEVEKFKRLIRC (amino acid 22-45)

Peptide 4: EVESMEDDTNGNLMEVEC (amino acid 834-850)

(the carboxyterminal cysteine residues are added for coupling of the peptide via sulphydryl groups).

Each peptide was resuspended in distilled water to a concentration of 1mg/ml. The carrier protein Keyhole Limpet Haemocyanin (Sigma Immunochemicals) was dissolved in PBS to a concentration of 10mg/ml and the coupling agent MBS (m-maleimidobenzoyl-N-hydroxysuccinimide ester), (ICN biomedicals Inc.) was dissolved in dimethylformamide to a final concentration of 25mg/ml. 100µl of this MBS solution was added to 1ml of KLH (10mg/ml), mixed and allowed to incubate at room temperature for 1 hour. The KLH-MBS was then desalted using the technique of FPLC (fast protein liquid chromatography), on a 10ml Sephadex G25 column: Firstly the column and the coil were washed with 0.1 M phosphate buffer pH 6.0, then 1ml of the KLH-MBS solution was injected. The elution of protein was determined by A_{280} and eluted fractions were collected in glass tubes. The KLH-MBS caused an initial sharp peak of absorbancy. A second broader peak was due to the MBS/dmf which absorbs significantly at ~280nm.

After desalting, 300µl of the peptide of interest (1mg/ml) was added to 1ml of the KLH-MBS conjugate and incubated at room temperature overnight on a rotating wheel. The following day the peptide-KLH conjugate was

desalted on a 10ml Sephadex G25 column by FPLC as described above. The concentration of the peptide conjugate was then estimated using the BCA assay (Pierce) against bovine serum albumin standards at A562 nm, according to the manufacturer's instructions.

The suggested dose of antigen to be used per injection in the rabbit immunisation schedule was 50-1000μg. 100 μg per injection was sent to ICRF Biological Resources (Clare Hall), for rabbit immunisation.

B) Overexpression and purification of recombinant fragments of ATM protein from *E. coli*

After failure of expression of ATM fragments cloned into several different vectors (pET-14b, Bluescript, pMal, pCR-Script), stab cultures of *E. coli* M15 (Qiagen) containing the pQE-32 vector with a recombinant *ATM* insert were gratefully received from A. Sutcliffe (Birmingham CRC unit). The recombinant *ATM* fragments were $(His)_6$-tagged and cloned into the BamH1 site of the vector. Two strains were sent including strain 1: *ATM* bp 866-1573 and strain 2: *ATM* bp 2976-3434. These strains have been also been used to generate the polyclonal antibodies FP14 and FP-8 respectively (Stankovic et al., 1998).

Expression of the *ATM* fragments was achieved using the following method: Each M15 culture was streaked out on agar plates containing 100 μg/Ampicillin and 50 μg Kanamycin/ml. After overnight incubation at 37°C, a single colony from each M15 strain was picked, inoculated into 3 ml of LB

containing 100 μg Ampicillin and 50 μg Kanamycin/ml and incubated in the shaking incubator at 37°C overnight.

The next day, 0.5 ml of miniculture was inoculated into 20 ml of prewarmed LB/Amp/Kana (100 μg/Ampicillin and 50 μg Kanamycin/ml) and incubated in the shaking incubator at 37°C until the OD_{600} reached 0.6 after which pre-induction samples were taken. 200 μl of culture was pelleted by centrifugation and resuspended in 40 μl of 2X protein sample buffer and recombinant *ATM* fragment expression was induced by addition of 2 mM isopropyl-β-D-thiogalactopyranoside (IPTG) for 2 hours at 37°C. Post-induction samples were taken after 2 hours and were subjected to SDS-PAGE on 13% gels, along with pre-induction samples (25 μl of each sample was used with a ratio of post/pre induction culture amounts of 1/4 to account for bacterial growth). The gels were then stained with Coomassie Blue and destaining revealed successful induction of both recombinant ATM proteins, strain 1 (~30 kDa, expected size 26 kDa) and strain 2 (21 kDa, expected size 17 kDa, Fig. 3a). Larger scale inductions were then prepared: For each strain, two 2l flasks each containing 400 ml of pre-warmed LB/Amp/Kana were inoculated with 4ml of an overnight miniculture and incubated at 37°C in a shaking incubator until the OD_{600} reached 0.6. Pre-induction samples were then taken as before and ATM fragment expression was then induced by the addition of IPTG (2 mM) with incubation for a further 2 hours at 37°C. Post-induction samples were taken at this point (SDS-PAGE was duly performed at a later time, as before to check protein induction). The flasks were then placed on ice for 10 min prior to transfer of the cultures to eight 50 ml tubes (Falcon)

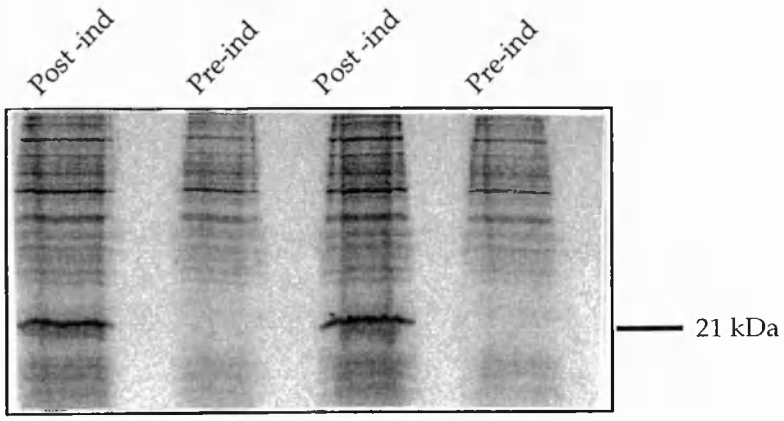

Fig. 3a

Induction of a 21 kDa recombinant ATM protein in pQE-32 (strain 2) whole bacterial lysate. Whole bacterial lysates were made from pre and post induction cultures of pQE-32 (strain2) with induction conditions of 2 mM IPTG at 37 C for 2hr. 20 µl of each lysate (post induction samples were diluted 1:4 to ensure equal protein loading) was then subjected to SDS-PAGE and stained with Coomassie Blue.

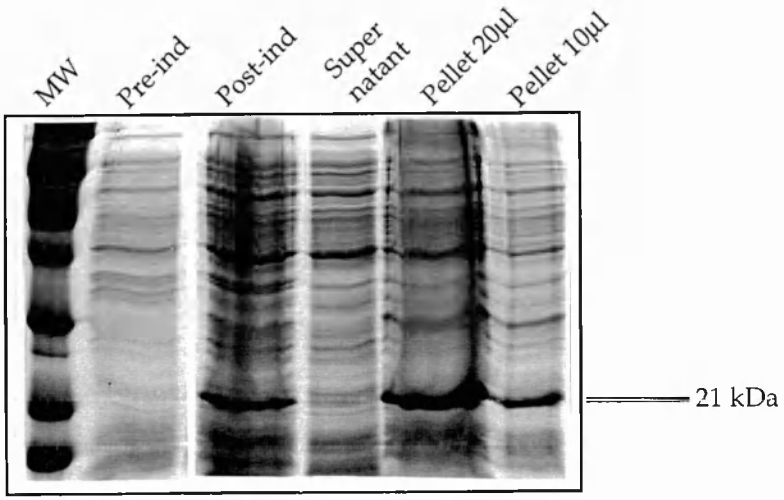

Fig. 3b

The 21 kDa recombinant ATM protein induced in pQE-32 (strain 2) is insoluble and predominantly seen in the cell pellet. Whole bacterial lysates were made from pre and post induction cultures of pQE-32 (strain 2) with induction conditions of 2 mM IPTG at 37 C for 2hr. 20 µl of each lysate, the lysate supernatant and cell pellet were then subjected to SDS-PAGE and stained with Coomassie Blue. (Post induction samples were diluted 1:4 to ensure equal protein loading).

and centrifugation at 4.2 krpm (in a Beckman GPR centrifuge) for 5 min at 4°C to pellet the cells. The supernatant was then discarded and the equivalent of 200 ml of culture was resuspended in 4 ml of ice cold binding buffer (5 mM imidazole, 0.5 M NaCl, 20 mM Tris-HCl, pH 7.9). The cells were then sonicated (Soniprep 150, MSE), to lyse them and shear the DNA, in 30s bursts on ice until the viscosity fell. The lysate was then centrifuged in a pre-cooled SW-55ti rotor at 39 krpm for 20 min at 4°C.

A His-Bind metal chelation column was then prepared in the cold room using 4ml of His-Bind resin (Novagen) which settles to a 2 ml column. The column was then washed with 6 ml of sterile distilled water, then 10 ml of charge buffer (400 mM $NiSO_4$), followed by 6 ml of binding buffer. The supernatant from the bacterial extract was then loaded onto the column. After this the column was again washed with 25 ml binding buffer followed by 15 ml of wash buffer (60 mM imidazole, 0.5 M NaCl, 20 mM Tris-HCl, pH 7.9). The expressed His-tagged protein was then eluted with elution buffer (1 mM imidazole, 0.5 M NaCl, 20 mM Tris-HCl pH 7.9), and collected in 1 ml fractions. Pre and post induction whole lysates and post induction supernatant samples were subjected to SDS-PAGE on a 13% gel, alongside each of the eluted fractions (50 µl of each fraction was mixed with 50 µl of 2X protein sample buffer and 25 µl of each sample was run). The gel was then stained with Coomassie Blue and destained in 10% methanol, 10% acetic acid, before gel drying.

Very little of either protein was found to be present in the supernatant and the eluates from the His-Bind columns. Both proteins were found to be predominantly insoluble and were largely present in the cell pellet after

induction (for strain 2 see Fig. 3b). Only small amounts of recombinant protein were extractable from the cell pellet using 0.25% Tween 20/ 0.1 mM EGTA which can help to extract proteins loosely associated with cell membranes. Therefore, further purification of the proteins was achieved by isolating the inclusion bodies (insoluble protein aggregates), from post-induction cell pellets stored at -70°C: Each pellet was resuspended in 5 ml of freshly made lysis buffer (25% sucrose, 50 mM Tris-HCl pH 8, 2 mM EDTA, 2 mM EGTA, 2 mM dithiothreitol, 0.5 mM Phenylmethyl-sulphonyl fluoride (PMSF, a serine protease inhibitor), and 10 μg/ml each of L-1-Chloro-3-[4-tosylamido]-7-amino-2-heptanone-HCl (TLCK.HCl, a trypsin, serine and cysteine protease inhibitor) and N-α-p-tosyl-L-arginine methyl ester (TAME.HCl an inhibitor of trypsin and other proteases). 5 mg/ml of lysozyme was admixed and the lysate was incubated on ice for 15 min after which $MgCl_2$ (to 10 mM) and DNAase I (50 μg/ml) were added. Following reincubation on ice for 15 min, the lysate was mixed with 2 volumes of inclusion body preparation solution (200 mM NaCl, 1% Na deoxycholate, 1.6% NP-40, 2 mM EDTA, 20 mM Tris-HCl pH 7.5) and centrifuged at 20Krpm in a JA-20 rotor for 20 min. The lysis supernatant was then decanted and the pellet was washed three times by resuspension in 25 ml of 0.5% Triton X-100 with 0.1 mM EDTA prior to recentrifugation at 20Krpm in a JA-20 rotor for 10 min. The inclusion bodies were resuspended in 1 ml of PBS. In order to determine whether inclusion bodies containing recombinant ATM fragments had been purified from the pellet, 1/50 of the final preparation was mixed with 40 μl of 2X sample buffer, boiled for 5 min and 20 μl was resolved on a 13% protein gel (Fig. 3c).

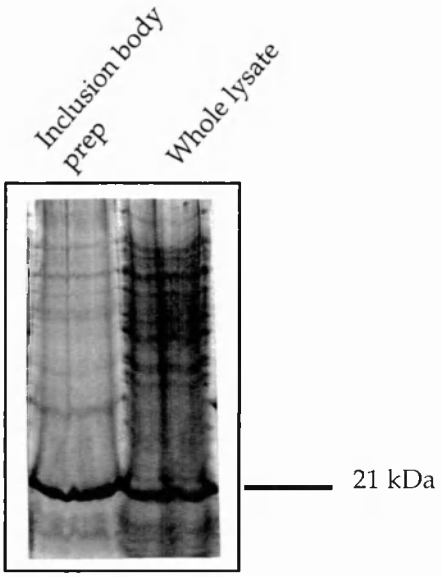

Fig. 3c

The 21 kDa ATM recombinant protein from pQE-32 (strain 2) can be partially purified by isolating inclusion bodies from the cell pellet. Equivalent amounts (20 µl) of a whole cell lysate and an inclusion body preparation from an induced culture of pQE-32 (strain 2), (induction conditions of 2 mM IPTG, 37 C for 2hr) were subjected to SDS-PAGE. Proteins were detected by staining the gel with Coomassie Blue.

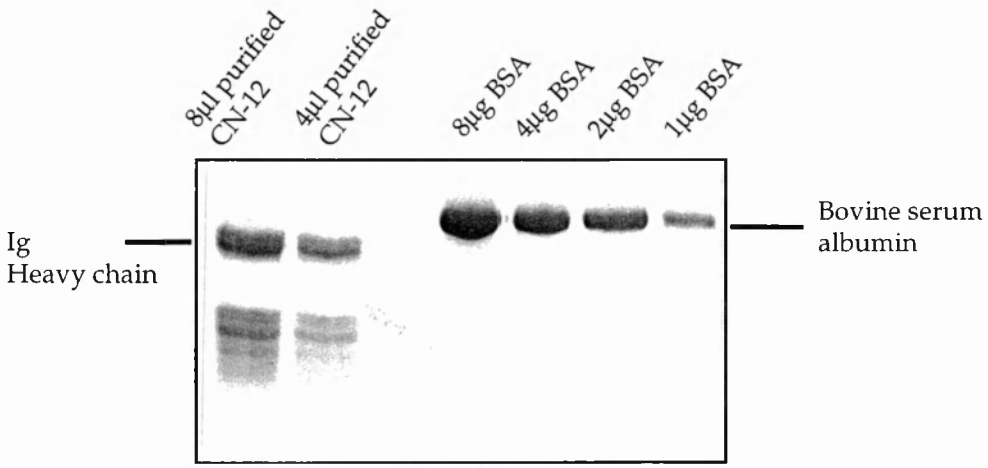

Fig. 3d

Titration of affinity purified CN-12 antibody against BSA standards. (8µl of antibody is equivalent to 2µg of protein). Aliquots of affinity purified polyclonal antibody CN-12 in sample buffer were subjected to SDS-PAGE alongside bovine serum albumin standards. Proteins were detected by staining the gel with Coomassie Blue.

Gel purification of the insoluble proteins was also performed by resuspending the induced cell pellet in 2X SDS sample buffer, boiling for 5 min and shearing the DNA by forcing the sample through decreasing needle gauges using a 1 ml syringe.

For each protein sample a large format 13% polyacrylamide gel was prepared with a single large well and two smaller wells at the edge. The large wells were loaded with 1 ml of induced pellet lysate for each pQE-32 strain. The gel was run at 4W for sufficient time to allow adequate separation of the recombinant proteins. After this time a thin horizontal strip of gel was cut 1cm above and below the predicted position of the induced protein of interest. This gel strip was then sheared by forcing it through needles of decreasing gauges using a firmly held 1 ml syringe to produce an acrylamide gel slurry enriched for the protein of interest (~1mg protein/ml of slurry). It is possible to use such slurries for direct injection of rabbits as the procedure is well tolerated and the acrylamide acts as an immunological adjuvant.

3.2.2 Rabbit immunisation

This was performed by Biological Resources at Clare Hall, ICRF using their standard rabbit immunisation protocol. The pre-bleeds, test bleeds and final bleeds were sent to this laboratory frozen on dry ice.

3.2.3 BLM antibody production and purification

As a continuation of work performed by Christine Addison in the laboratory I was given the anti-BLM rabbit polyclonal antibody IHIC-27 to affinity purify. IHIC-27 was raised against an amino-terminal recombinant BLM fragment (amino acid residues 300-500) fused to maltose binding protein (BLM-MBP).

Due to the lack of purified recombinant BLM, affinity purification of IHIC-27 was carried out by affinity chromatography in two steps: firstly maltose binding protein specific antibodies from the crude serum IHIC-27 were removed by adsorption on an affinity column to which MBP was bound. Secondly the BLM specific fraction from the eluate of the first column was obtained by adsorption onto an affinity column to which the fusion protein BLM-MBP was bound.

To prepare the first column, 2mg of MBP was coupled to cyanogen bromide-activated sepharose beads 4B (Sigma). (Sepharose is a bead formed agarose gel and when activated by CNBr which binds to the hydroxyl groups of sepharose, ligands containing primary amino groups react with the cyanate ester groups to form isourea linkages to the gel). To form the sepharose gel the beads were initially swelled (1g of freeze dried beads swell to a gel volume of ~3.5 ml), and washed in 200ml/g of 1mM ice cold HCl. (HCL preserves the activity of the reactive groups which hydrolyze at high pH). The final aliquot of HCL was removed until cracks appeared in the gel. 5mg of MBP was then dissolved in 2ml of coupling buffer ($NaHCO_3$ 0.1 M, pH 8.3, NaCl 0.5 M), and rocked gently with 1 ml of gel overnight at 4°C. After this time the coupled slurry was then transferred to the column. The remaining active groups were

then blocked by amino residues provided by exposing the column to an excess of 0.2 M glycine pH 8.0 for 2 hours. Excess adsorbed protein was then washed away with 4 rounds of alternate washes with acetate buffer (Na acetate 0.1M, NaCl 0.5 M) and coupling buffer. The column was then cleared of blocking agent by another wash with coupling buffer. The column was then prepared for the serum by washing in turn with: 1) 10 ml of 10 mM Tris pH 7.5, 2) 10 ml of 100 mM glycine pH 2.5, 3) 10 ml of 10 mM Tris pH 8.8, after which the column pH was checked and then 4) 10 ml of freshly made triethylamine pH 11.5, and 5) 10 mM Tris pH 7.5 until the pH reached 7.5. The serum was then diluted 1:10 with 10 mM Tris pH 7.5 prior to loading (10 ml of IHIC-27 were loaded in 100 ml of the above). The antibody solution was then passed over the column three times to ensure binding to the MBP. The final flow through was collected as it contained IHIC-27 depleted for MBP specific antibodies and this was used to load onto the second column. 2 mg of BLM-MBP fusion protein was bound to the second column using the method described above. After the second column had been washed as described the flow through from the first column was loaded onto the BLM-MBP column and reloaded twice to ensure binding of remaining BLM specific antibodies to the fusion protein. The column was then washed with 20 ml of 10 mM Tris pH 7.5 followed by 20 ml of 500 mM NaCl, 10 mM Tris pH 7.5.

Acid-sensitive anti-BLM antibodies were then eluted with 2.5 ml of 100 mM glycine pH 2.5. The column eluate was collected in 0.5 ml fractions into separate tubes containing 0.5 ml of 1 M Tris pH 8.0 to neutralise the solution. The column was then washed in 10 mM Tris pH 8.8 until the pH reached 8.8. Base-sensitive antibodies were then eluted using 2.5 ml of freshly prepared

triethylamine pH 11.5. The column eluate was collected in 0.5 ml fractions into separate tubes containing 0.5 ml of 1 M Tris pH 8.0 to neutralise the solution. The column was then washed in 10 mM Tris pH 7.5 until the pH was 7.5 and then the column was stored at 4°C. The amount of protein in the various fractions was then checked against the buffers they were collected into by measuring the A_{280}.

3.2.4 Testing of polyclonal rabbit sera raised against ATM

The pre-bleed, test bleeds and final bleed of each immunized rabbit (Table 3.1), were screened for their ability to detect a ~350kDa ATM band by Western blotting against a series of positive and negative (ataxia-telangiectasia cell line AT2RO) control human cell line lysates .

The crude serum was used as the primary antibody (at a dilution of 1/500) and the secondary layer was a peroxidase conjugated anti-rabbit antibody (Sigma Immunochemicals), also used at a dilution of 1/500. Western blotting was performed as described earlier. Although sera from all the rabbits CN-3-CN12 were tested, only rabbit CN-12 showed a protein band of of ~350 kDa (the correct size for ATM). Data for the other rabbits are not shown as the blots had very high background.

3.2.5 Affinity purification of CN-12 by Western blotting

A large format 13% polyacrylamide gel was prepared with a single large well and two smaller wells at the edge. The large well was loaded with 1 ml of induced whole cell lysate of bacteria expressing pQE-32 strain 2 (ie the portion

Antibody	Immunogen
CN-3	ATM peptide 1
CN-4	ATM peptide 2
CN-5	ATM peptide 3
CN-6	ATM peptide 3
CN-7	ATM peptide 4
CN-8	ATM peptide 4
CN-9	Inclusion bodies of recombinant ATM polypeptide (aa 288-524)
CN-10	Gel slurry containing recombinant ATM polypeptide (aa 288-524)
CN-11	Inclusion bodies of recombinant ATM polypeptide (aa 992-1,144)
CN-12	Gel slurry containing recombinant ATM polypeptide (aa 992-1,144)

Table 3.1

Description of immune sera raised against ATM with details of the immunogens used.

of the ATM protein to which CN-12 antibody was originally raised). The gel was run at 4W for sufficient time to allow adequate separation of the recombinant portion of ATM which runs at 21kDa alongside the 21kDa protein size marker. After this time a thin horizontal strip of gel was cut, 1cm above and below the 21kDa markers and the recombinant ATM protein was transferred from this to Immobilon-P membrane using the semi-dry method as described previously.

The membrane was then incubated in blocking buffer (PBS containing 0.1% Tween and 5% Marvel low fat milk), for 1 hour. The membrane was then removed and transferred to a 50 ml Falcon tube to which was added 2 ml of blocking solution and 2 ml of crude CN-12 serum. This was then incubated overnight at 4°C on a rotating wheel. The following day the membrane with bound antibody was washed three times in PBS/0.1% Tween for 10 min. The membrane was then transferred to a new 50 ml tube (Falcon) and elution of bound antibody was achieved by addition of 1 ml 0.1 M glycine.HCl pH 2.5 and incubation on a rotating wheel for 5 min. The membrane was then removed and the remaining eluate was neutralised by the addition of 45µl of 3M Tris.HCl pH 8.0.

A 13% acrylamide gel was then run with different amounts of purified antibody, alongside a set of BSA standards to determine the amount of purified antibody generated (Fig. 3.d).

3.2.6 Antibodies

Anti-ATM antibodies:

Affinity purified CN-12: a polyclonal rabbit antibody raised to the amino-terminus of ATM (bp 2976-3434, amino acid residues 992- 1,144), used at 2μg/ml unless stated otherwise.

ATM.B: a rabbit polyclonal antibody (the generous gift of Dr N.Lakin), was used at a dilution of 1/1000.

Anti-BLM antibodies:

IHIC-27 rabbit polyclonal antibody used at 1/250 unless otherwise indicated.

185a mouse monoclonal, neat culture supernatant used.

32e mouse monoclonal, neat culture supernatant used.

Other antibodies used:

Anti- HA tag antibody 12CA5, used at 1μg/ml (Boehringer Mannheim).

Anti His_6-tag mouse monoclonal antibody clone 13/45/31-32 (Dr H. Zentgraf, DKFZ, Germany) used at a dilution of 1/10.

Monoclonal mouse anti-beta tubulin supplied by Amersham Life Science was used at a dilution of 1/300.

IHIC-7 anti-topoisomerase IIα, rabbit polyclonal used at 1/500 dilution for immunohistochemistry.

Secondary layers: Peroxidase conjugated anti-rabbit IgG and peroxidase conjugated anti-mouse IgG were supplied by Sigma immunochemicals and were diluted by 1/500 in incubation solution prior to use.

All antibodies were preserved in 0.02% Na azide and stored at 4°C.

3.2.7 Investigation of the expression of ATM protein in the National Cancer Institute cell panel

The National Cancer Institute has compiled a panel of 60 tumour cell lines spanning a range of human malignancies. A database now exists for these cell lines which contains information regarding several different aspects of cellular behaviour. Apart from documenting cell line sensitivity to various drugs, information regarding key cellular mediators eg p53, p21 and checkpoint function has been collated. It is now possible to obtain these cell lines for experimental purposes and compare the results obtained with information already present in the NCI database to identify possible relationships between the parameters studied. Therefore an investigation of ATM expression in these cell lines was conducted.

Equivalent amounts (25 µl) of protein equalized cell lysates from a 27 cell lines in the panel were subjected to SDS-PAGE in duplicate on 7.5 % gels. ATM protein was subsequently detected by Western blotting using the affinity purified antibody CN-12. A U2OS cell lysate (an osteosarcoma line not included in the panel) and later on HCC-2998 lysates were used as positive internal standards to allow comparison of ATM protein expression levels between different gels. (Representative gels are shown Fig. 3.6-3.10). ATM protein levels were then quantitated by band intensity analysis using the Bioimage™ Whole Band Analyser System (Millipore) and corrected using the internal standards to allow comparison of protein levels across all the samples studied. Comparison of the ATM protein levels with: reported p53 mutations (assessed by preparing and sequencing the cDNA), p53 protein levels (assessed

by Western blotting), γ irradiation (6.3 Gy) induced G1 arrest capacity (quantitated as the percent of the G1 population that remained in G1 phase 17 hours after irradiation and incubation with nocodazole) and X-ray induction of WAF-1, MDM-2 and gadd45 (measured by RNA isolation and dot blot hybridization) for each cell line was performed using the COMPARE programme of the NCI Human Tumour Cell Screen Molecular Database (http://epnws.1.ncifcrf.gov:2345/dis3d/java/user_compare.html).

3.2.8 Immunohistochemical analysis of ATM and BLM proteins

MRC5 (wild type fibroblasts) (Huschtscha and Holliday, 1983), and AT5BIVA (SV40-transformed AT fibroblasts) (Savitsky et al., 1995) cells were cultured in the appropriate media on microscope slides with 4 wells (Becton-Dickinson). Before the cells reached confluence, the medium was washed off and cells were fixed for 5 min in 70% ethanol or other fixative (see below). (Alternatively, cytospin specimens of these cell lines were used). The slides were then microwaved in 0.01M Na citrate buffer pH 6.0 for 5 mins x2 and allowed to cool in dH_2O prior to blocking in 10% FCS/PBS for 30 min. After a brief wash in PBS the slides were incubated with the relevant primary antibody: CN-12 (2μg/ml), anti-BLM monoclonals: 185a or 32e (neat), or IHIC-7 (anti-Topo IIα 1/500) as a positive control, overnight at 4°C. The following day they were rinsed three times for 5 min in PBS and the appropriate peroxidase conjugated anti-rabbit or anti-mouse secondary layer was applied (at a dilution of 1/500) for 1 hour at room temperature. After a final rinse in PBS, the reaction product was developed using the vector® AEC Substrate Kit

for Horseradish Peroxidase (Vector) according to the manufacturers instructions. A positive reaction is indicated by the development of a red-brown reaction product after 30 min (a water based mountant such as Apathy's mounting medium was used as the reaction product is soluble in alcohol).

Alternative protocols eg including a protease (0.1% Trypsin) digestion step, and pre-treatment with a detergent (0.2% Triton X-100) to reveal nuclear epitopes were tried as were alternative fixation methods eg: no fixation, air drying, 3.7 % Formalin/PBS, 3% paraformaldehyde/2% sucrose in PBS and 100% acetone fixation.

IHIC-27 staining of alcohol fixed cytospin specimens was also investigated by Helen Turley (ICRF, Department of Cellular Science), in dilutions from 1/100 to 1/1500 using the diaminobenzidine reaction method to develop the slides which gives a brown reaction product. All slides were lightly counterstained with haematoxylin.

3.3 Results

3.3.1 Immune serum from rabbit CN-12 recognises a protein of ~350 kDa in U2OS cell extracts

When polyclonal antisera from immunized rabbits were tested, only one antiserum, that from rabbit CN-12 was found to recognise a band in the osteosarcoma cell line, U2OS of similar size to ATM (~350 kDa). No distinct bands were seen in this region using preimmune serum from this rabbit as a

negative control (Fig. 3.1). After affinity purification of CN-12 the band recognised in U2OS and HeLa cells appeared much sharper (Fig. 3.2).

3.3.2 Affinity purified CN-12 antiserum can immunoprecipitate a protein of ~350 kDa from HeLa cell nuclear extracts

Affinity purified CN-12 immunoprecipitated and recognised a protein of ~350 kDa in HeLa cell nuclear extracts (Fig. 3.3), which was the same size as the band recognised a U2OS whole cell lysate. Two other fainter bands of ~140 and 160 kDa and ~80 kDa were also recognised in the HeLa immunoprecipitates. The intense band at ~350 kDa was not seen in nuclear extracts immunoprecipitated with preimmune serum from CN-12 and 'no antibody' negative controls.

3.3.3 The polyclonal antibodies CN-12 and ATM.B both recognise a protein of ~350 kDa in HeLa whole cell lysates which is not present in an ataxia-telangiectasia cell lysates

Affinity purified CN-12 (raised to ATM amino acid residues 992-1144) and the anti-ATM antibody ATM.B, (a gift from Dr N. Lakin, which was raised to ATM amino acid residues 1980-2338 (Lakin et al., 1996)), recognised a protein of ~350 kDa protein in HeLa cell lysates but not in the ataxia-telangiectasia fibroblast cell line AT2RO lysates (Fig. 3.4). AT2RO cells are homozygous for the mutation ATM 5539 del 11 which is predicted to truncate ATM protein at codon 1847 (Gilad et al., 1996). If the truncated protein was stable its estimated molecular weight would be ~211 kDa. ATM.B was raised to a portion of the

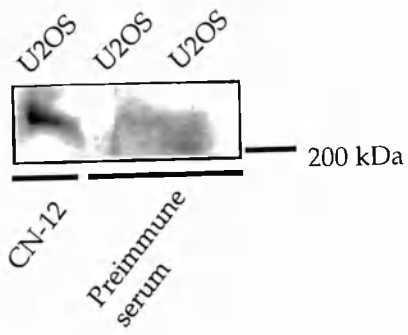

Fig. 3.1

Immune serum (polyclonal antibody CN-12) but not preimmune serum recognises a protein of ~ 350 kDa in U2OS cells. Whole cell extracts were prepared from U2OS cells and 25µl of these extracts (equivalent to 125,000 cells) were subjected to SDS-PAGE. ATM was then detected by Western blot analysis using CN-12 or preimmune serum (sera were used at a dilution of 1/250).

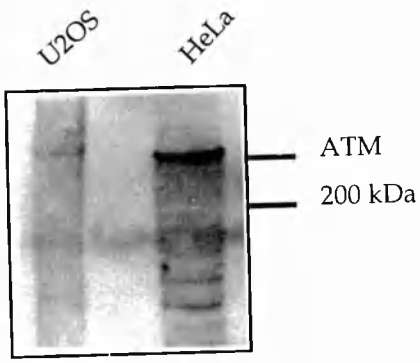

Fig. 3.2

Affinity purified CN-12 recognises a protein of ~350 kDa in U2OS cells. A whole cell lysate was prepared from U2OS cells and 25 µl of this (equivalent to 125,000 cells), and 15µl of a HeLa cell nuclear extract (equivalent to 0.8 million cells), were subjected to SDS-PAGE. ATM protein was then detected by Western blot analysis using affinity purified CN-12 (2µg/ml).

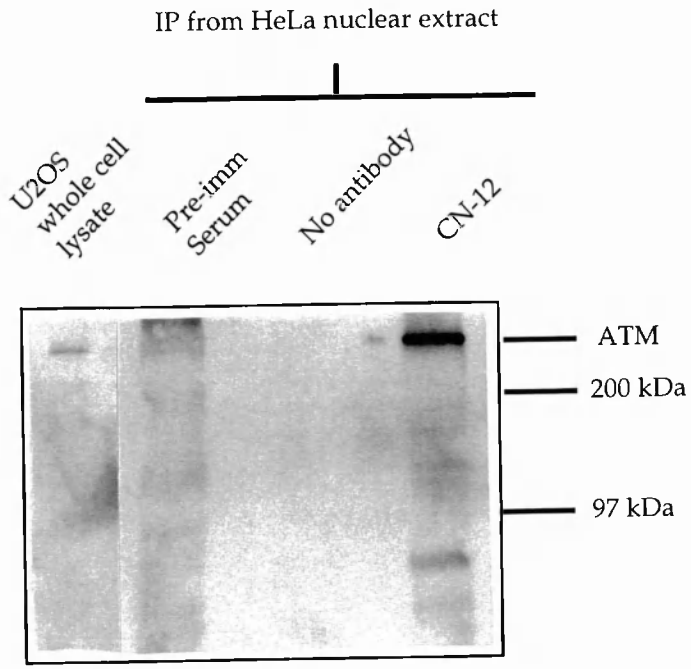

WB: CN-12

Fig. 3.3

Affinity purified CN-12 is able to immunoprecipitate ATM protein from a HeLa cell nuclear extract (50 million cells/sample). HeLa cell nuclear extracts were immunoprecipitated with or without affinity purified CN-12 (2 µg/ml) or preimmune serum and equivalent amounts (23 million cells per immunoprecipitate) were then subjected to SDS-PAGE. 25µl of U2OS whole cell extract (equivalent to 125,000 cells) was included as a positive control. ATM protein was subsequently detected by Western blot analysis using affinity purified CN-12 (2 µg/ml).

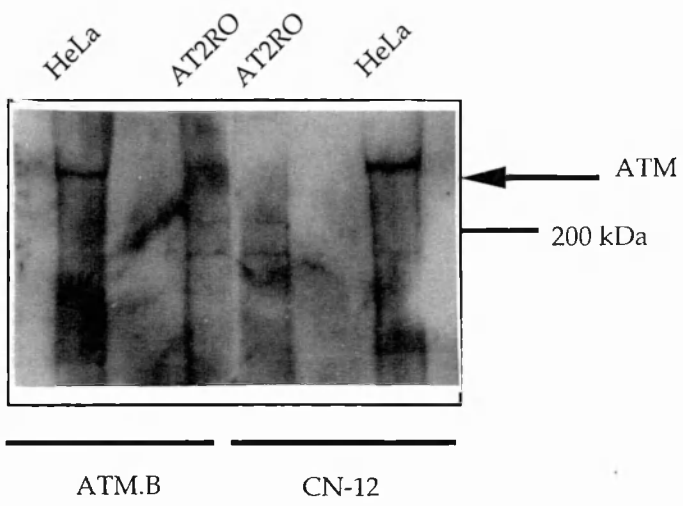

Fig. 3.4

Affinity purified CN-12 and ATM.B both recognise a protein of ~350 kDa in HeLa cells but this protein is not present in ataxia telangiectasia AT2RO cells. 25 µl (equivalent to 125,000 cells) of HeLa and AT2RO whole cell lysates were subjected to SDS-PAGE. ATM protein was detected by Western blot analysis using anti-ATM antibody ATM.B 1/1000, (a gift from N. Lakin), and affinity purified CN-12 (2µg/ml).

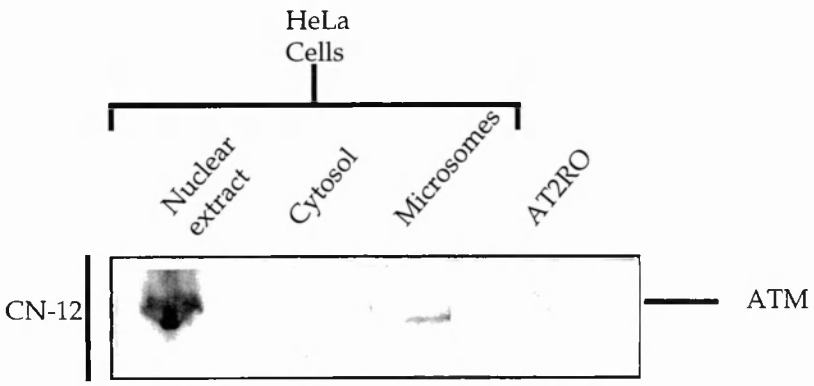

Fig. 3.5

ATM protein is present in HeLa nuclear and microsomal extracts but is not identified in HeLa cytosol nor in an AT2RO cell lysate. Equivalent amounts (100µg protein), of HeLa cell nuclear, cytosolic and microsomal extracts, and 25µl (equivalent to 125,000 cells) of an AT2RO lysate were subjected to SDS-PAGE. ATM was then detected by Western blot analysis using affinity purified CN-12 (2 µg/ml).

ATM protein distal to this truncation therefore as expected, ATM.B did not identify a protein of this size in AT2RO lysates. The fact that no proteins of ~211 kDa were seen with CN-12 suggests that the truncated ATM protein in AT2RO cells is unstable.

3.3.4 Investigation of the subcellular localisation of ATM

Affinity purified CN-12 was used to determine the subcellular localisation of ATM in HeLa cell nuclear, microsomal and cytosolic extracts by Western blotting. An AT2RO whole cell lysate was used as a negative control. ATM was found to be a predominantly nuclear protein, although small amounts were also identified within the microsomal fraction. ATM was not detected in the cytosol of HeLa cells nor in the AT2RO whole cell lysate (Fig. 3.5).

3.3.5 Affinity purified CN-12 can be used to determine the expression of ATM in tumour cell lines.

Affinity purified CN-12 was used to investigate the expression of ATM in a variety of tumour cell lines from the National Cancer Institute Cell Panel (Fig. 3.6 to Fig. 3.10). U2OS cell and later on HCC-2998 lysates were used as positive internal controls to allow comparison of different gels. Expression of full length ATM was seen in 26 of 27 cell lines from this panel including leukaemia cell lines (CCRF-CEM and RPMI-8226), breast cancer cell lines (BT-549, MCF7-ADR-RES), ovarian cancer cell lines (OVCAR-3, OVCAR-5, OVCAR-8 and SK-OV-3), non-small cell lung cancer lines, (EKVX, HOP-62, NCI-H226, and NCI-H322M), colonic cancer cell lines (COLO-25, HCC-2998 and HCT-116), renal

Western blot of cell line lysates from National Cancer Institute Cell Panel

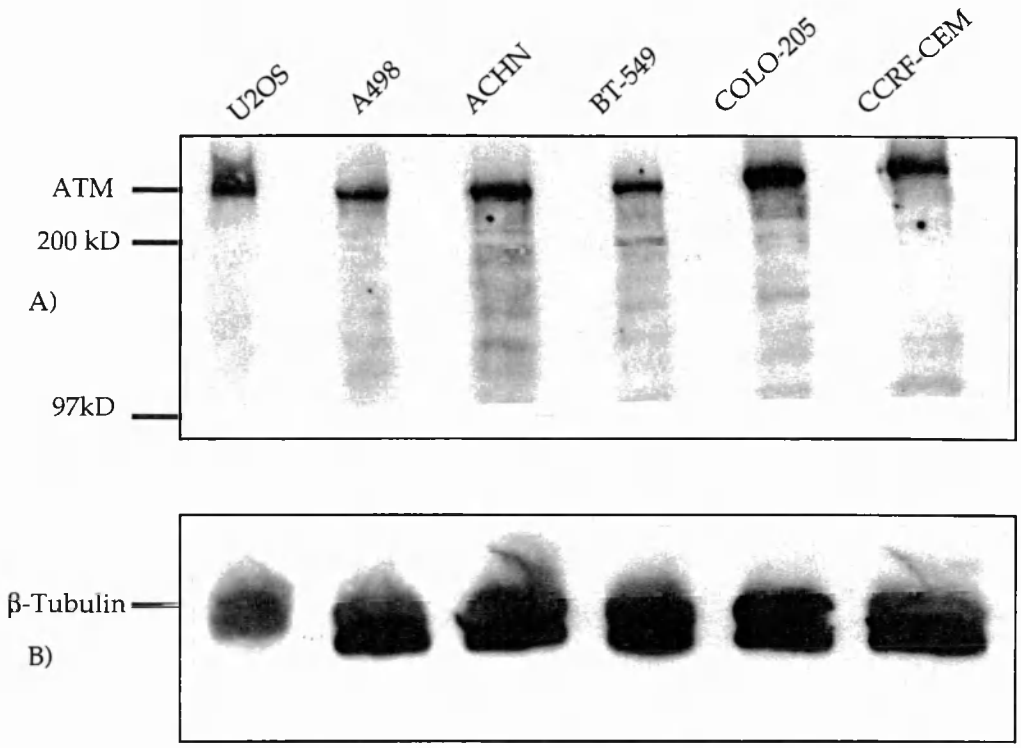

Fig. 3.6

A) Equivalent amounts (50μg) of protein equalised whole cell lysates of U2OS, A498, ACHN, BT-549, COLO-205, and CCRF-CEM cell lysates were subjected to SDS-PAGE. ATM protein was detected by Western blot analysis using affinity purified CN-12 antibody (2μg/ml). B) The above lysates were also Western blotted with β-tubulin antibody (1/300) to monitor protein loading.

Western blot of cell line lysates from National Cancer Institute Cell Panel

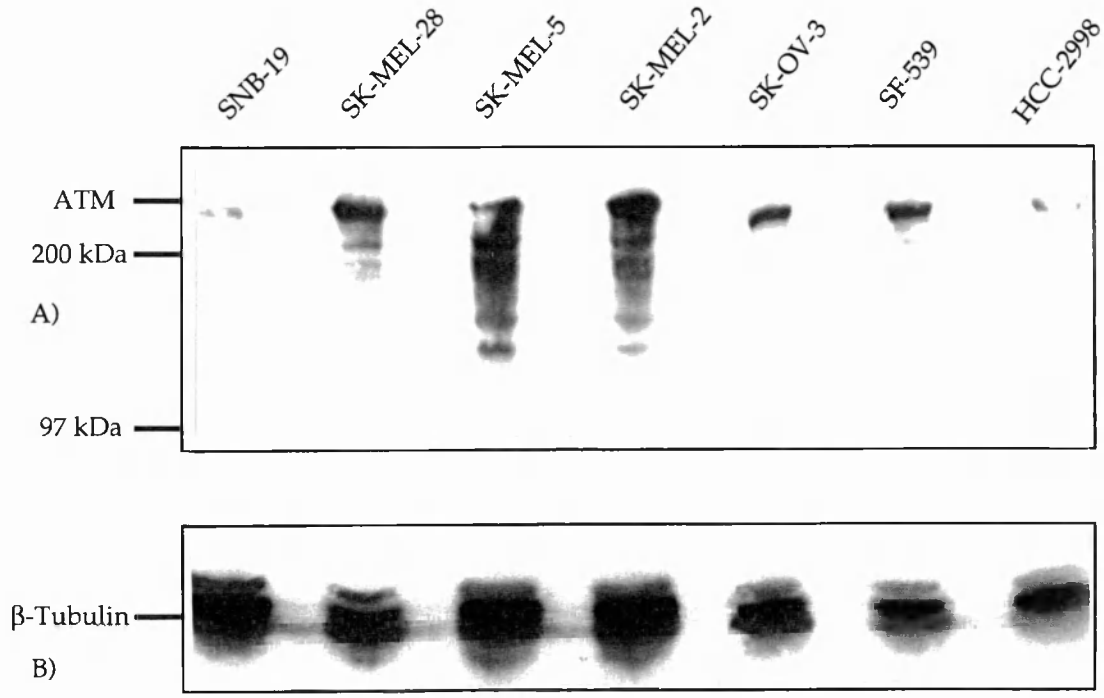

Fig. 3.7

A) Equivalent amounts (50μg) of protein equalised whole cell lysates of SNB-19, SK-MEL-28, SK-MEL-5, SK-MEL-2, SK-OV-3, SF539 and HCC-2998 cell lysates were subjected to SDS-PAGE. ATM protein was detected by Western blot analysis using affinity purified CN-12 antibody (2μg/ml). B) The above lysates were also Western blotted with β-tubulin antibody (1/300) to monitor protein loading.

Western blot of cell line lysates from National Cancer Institute Cell Panel

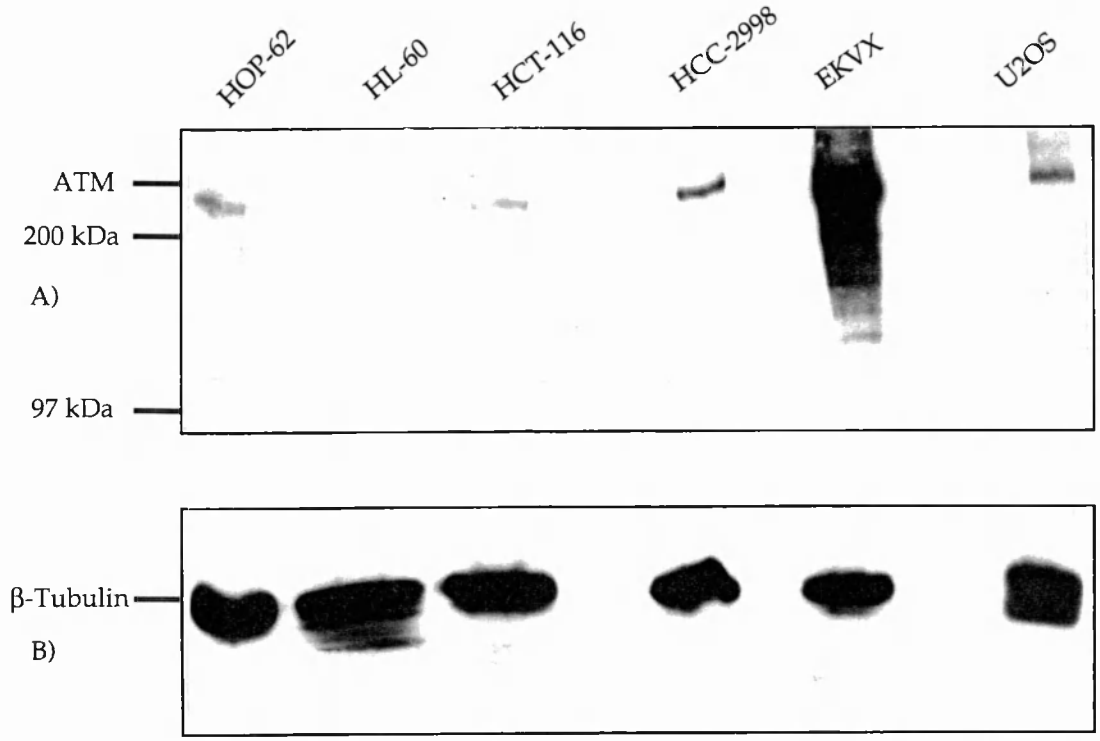

Fig. 3.8

A) Equivalent amounts (50μg) of protein equalised whole cell lysates of HOP-62, HL-60, HCT-116, HCC-2998, EKVX, and U2OS cell lysates were subjected to SDS-PAGE. ATM protein was detected by Western blot analysis using affinity purified CN-12 antibody (2μg/ml). B) The above lysates were also Western blotted with β-tubulin antibody (1/300) to monitor protein loading.

Western blot of cell line lysates from National Cancer Institute Cell Panel

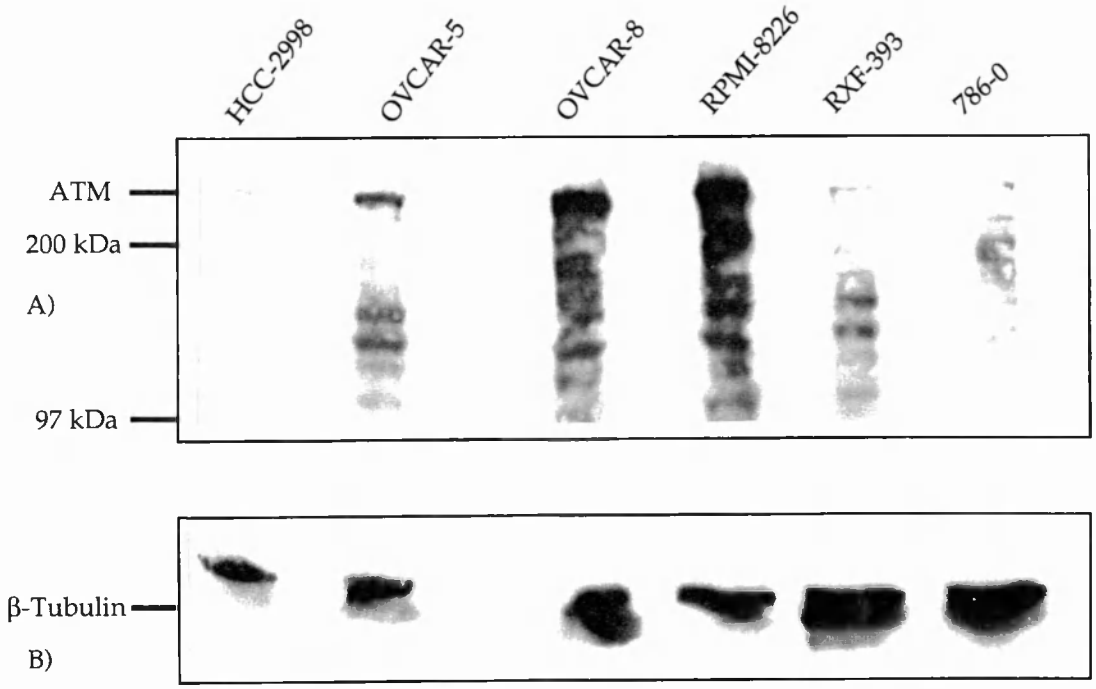

Fig. 3.9

A) Equivalent amounts (50μg) of protein equalised whole cell lysates of OVCAR-5, OVCAR-8, RPMI-8226, RXF-393, 786-0 and HCC-2998 cell lysates were subjected to SDS-PAGE. ATM protein was detected by Western blot analysis using affinity purified CN-12 antibody (2μg/ml). B) The above lysates were also Western blotted with β-tubulin antibody (1/300) to monitor protein loading.

Western blot of cell line lysates from National Cancer Institute Cell Panel

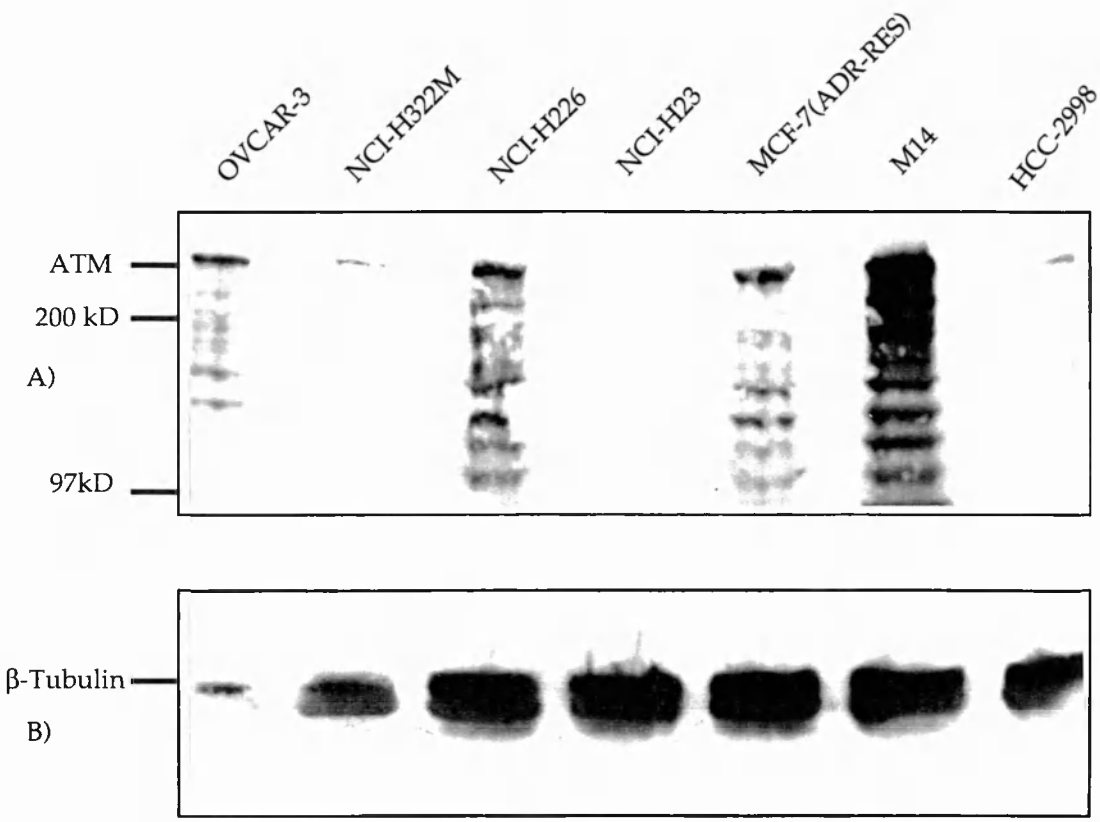

Fig. 3.10

A) Equivalent amounts (50μg) of protein equalised whole cell lysates of OVCAR-3, NCI-H322M, NCI-H23, MCF-7(ADR-RES), M14 and HCC-2998 cell lysates were subjected to SDS-PAGE. ATM protein was detected by Western blot analysis using affinity purified CN-12 antibody (2μg/ml). B) The above lysates were also Western blotted with β-tubulin antibody (1/300) to monitor protein loading.

tumour cell line (RXF-393, 786-0, ACHN and A498), melanoma lines (M14, SK-MEL-2, SK-MEL-28 and SK-MEL-5), brain tumour cell lines (SF-539 and SNB-19). ATM was absent from HL-60 (Fig. 3.8), a promyelocytic leukaemia cell line, very low in NCI-H23 a non-small cell lung cancer cell line (Fig. 3.10) and low in seven other cell lines: HOP-62, HCT-116, HCC-2998, SNB-19, NCI-H322M, RXF-393 and 786-0 although equivalent amounts of the cell lysates were loaded. In the positive cell lines, several other bands were also seen, most notably at ~200 kDa, and two further bands between 200 kDa and 97 kDa. In the negative cell line no prominent bands of lower molecular weight were seen which might have represented truncated mutant ATM protein.

Pearson correlation coefficients for ATM levels versus parameters for these cell lines in the NCI database were as follows: p53 mutation: 0.141, p53 protein level: 0.2, X-ray induction of WAF-1: 0.219, X-ray induction of MDM-2: 0.072, X-ray induction of gadd45: 0.002, G1 arrest post 6.3 Gy of γ radiation: -.041 ie no significant correlations with any of the parameters chosen was identified. (+1 would represent a perfect positive correlation and -1 a perfect negative correlation).

3.3.6 Polyclonal antibody IHIC-27 identifies BLM protein

Western blot analysis of pure recombinant BLM protein, and MRC5 (wild type) and GM8505 (a Bloom's cell line) whole cell lysates was performed using the affinity purified polyclonal antibody IHIC-27. IHIC-27 recognised full-length recombinant BLM and a protein of the same molecular weight (~180 kDa) in MRC5 cells. This protein was not present in the Bloom's cell line GM8505. Three other prominent protein bands of approximate molecular weights of 110

and 90 kDa and 69 kDa and a weaker band of 160 kDa are detected in both MRC5 and GM8505 using this antibody (Fig. 3.11). The BLM mutation in GM8505 is not published but is reported to be a missense mutation which, if stable, would result in a protein of ~80 kDa. However expression is unlikely as only small amounts of the mRNA are detected due to mRNA instability (personal communication, Nathan Ellis).

3.3.7 Affinity purified IHIC-27 identifies BLM protein in a variety of cell lines

Western blot analysis of pure recombinant BLM protein and whole cell lysates from MRC5 and U2OS (wild type cell lines), GM8505 and GM2932 (Bloom's cell lines) was performed using the affinity purified polyclonal antibody IHIC-27. IHIC-27 recognised full-length recombinant BLM (~180 kDa) and a protein of the same molecular weight in U2OS and MRC5 cells Fig. 3.12). This protein was not present in the Bloom's cell line GM8505 but a weak band was identified at this molecular weight in GM2932 cells. Numerous other proteins were also recognised by IHIC-27 in wild type and Bloom's cells including bands already identified at ~110 kDa and 90 and 69 kDa, which differed in intensity from one cell line to another.

3.3.8 BLM is a nuclear protein

Affinity purified IHIC-27 was used to investigate the subcellular localisation of BLM in HeLa cell nuclear, microsomal and cytosolic extracts by Western blotting (Fig. 3.13). A Bloom's whole cell lysate (GM8505) was used as a

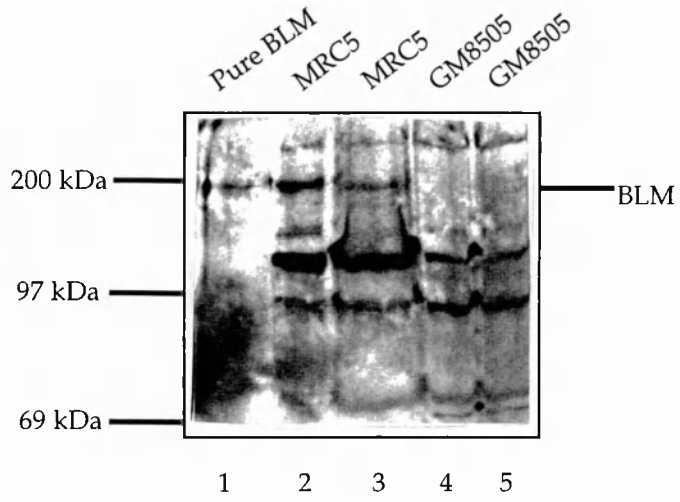

Fig. 3.11

BLM is absent in Bloom's cells but present in MRC5 cells. Protein extracts from: 1) 0.5µg of purified full length recombinant BLM , and 30 µl (equivalent to 150,000 cells) of 2) and 3) MRC5 cells (BLM +/+) (3 was an older lysate), and 4) and 5) GM8505 cell lysates (BLM-/-) were subjected to SDS-PAGE. BLM protein was detected by Western blot analysis using affinity purified IHIC-27.

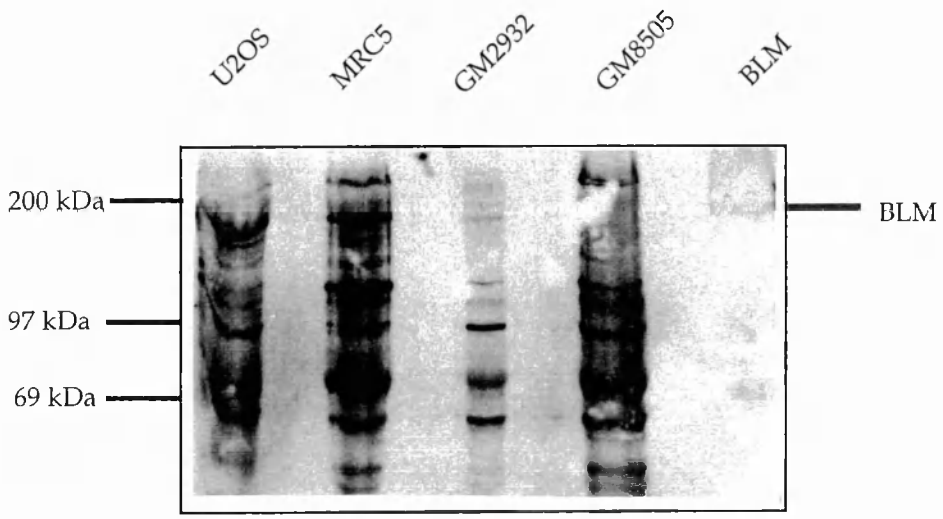

Fig. 3.12

Affinity purified IHIC-27 recognises multiple proteins in wild type and Bloom's cells. 25 µl (equivalent to 125,000 cells) of the wild type cell l ines U2OS and MRC5, the Bloom's cell lines GM2932 and GM8505, and 0.15µg of pure recombinant BLM protein were subjected to SDS-PAGE on a 7.5% gel. Western analysis was then performed and BLM protein was identified using affinity purified IHIC-27.

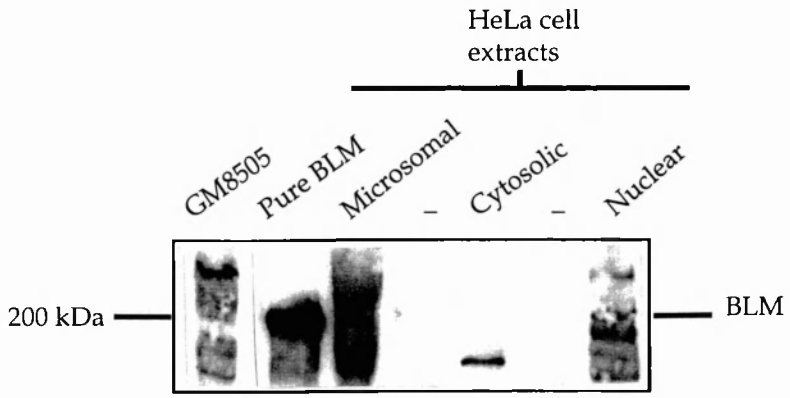

Fig. 3.13

BLM is a nuclear protein. A whole cell extract was prepared from GM8505 cells (BLM -/-) and nuclear, cytosolic and microsomal extracts were prepared from confluent HeLa cells (BLM +/+). Equivalent amounts (25 μg) of these protein extracts and 0.2μg of purified recombinant BLM (positive control), were subjected to SDS-PAGE. BLM was detected by Western blot analysis using affinity purified IHIC-27.

negative control. BLM was found to be a nuclear protein and no band corresponding to full-length BLM was identified in HeLa cytosolic or microsomal fractions or in the Bloom's cell line GM8505 whole cell lysate, although bands were seen above and below 180 kDa. The nuclear, cytosolic and microsomal fractions tested were representative of these cellular compartments as evidenced by their relative expression of ATM which was investigated concurrently (Fig. 3.5).

3.3.9 Monoclonal antibody 185a recognises recombinant BLM protein

Samples of BLM-MBP fusion protein, yeast lysates expressing recombinant BLM (both uninduced and induced) and purified recombinant BLM were subjected to SDS-PAGE. (The yeast lysates described and the purified recombinant BLM protein were provided by J. Karow). Western blot analysis was then performed using the monoclonal antibody 185a raised against BLM-MBP (Fig. 3.14a). 185a recognised both the fusion protein against which it was raised, recombinant BLM expressed by induced yeast cultures and purified recombinant BLM. However, as expected, no BLM protein was detected in the uninduced yeast cultures. When HeLa cell nuclear extracts were prepared (with or without subsequent immunoprecipitation with IHIC-27) and separated by SDS-PAGE along with an induced yeast culture lysate expressing BLM, the monoclonal antibody 185a only recognised the recombinant yeast BLM and BLM in the immunoprecipitated nuclear extracts (Fig. 3.14b).

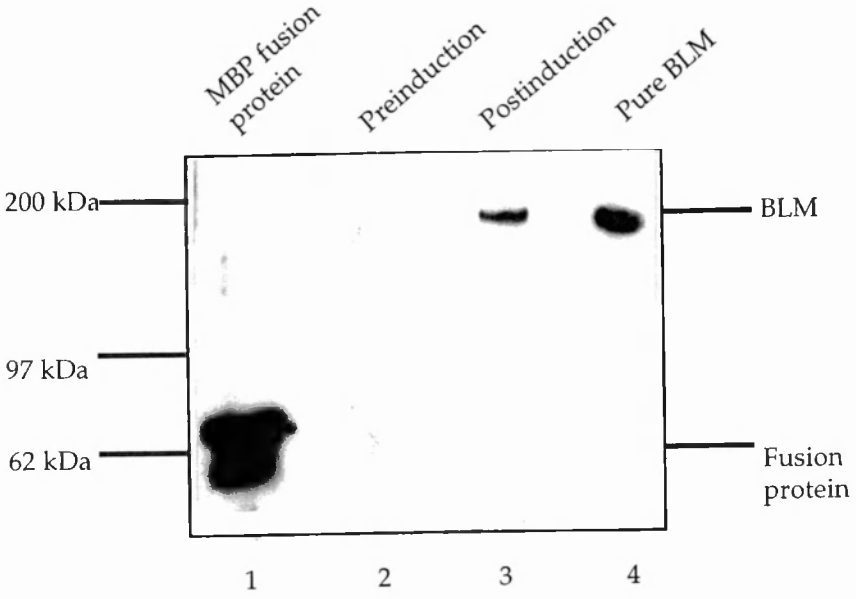

Fig. 3.14a

Monoclonal antibody 185a recognises the portion of BLM against which it was raised (amino acid residues 300 - 500) and full length BLM. 20 µg of 1) a partial length BLM-MBP fusion protein, equivalent amounts (7.5 µl) of crude lysate from 2) uninduced yeast and 3) induced yeast expressing 0.15 µg of full length recombinant BLM and 0.5 µg of 4) purified full length recombinant BLM were subjected to SDS-PAGE. BLM was then detected by Western blot analysis using monoclonal antibody 185a.

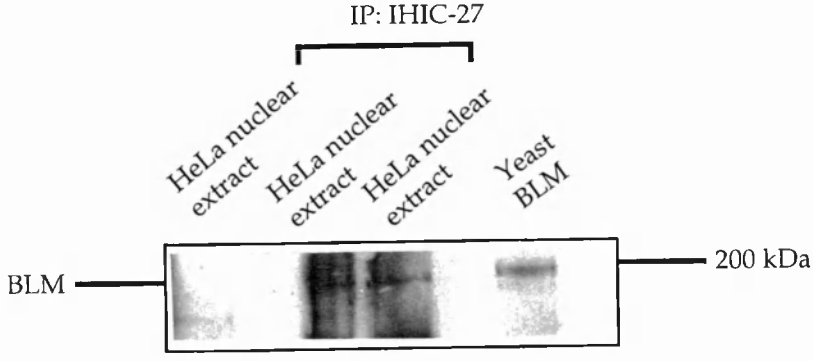

Fig. 3.14b

Monoclonal antibody 185a recognises BLM in HeLa cell nuclear extracts only after immunoprecipitation with the anti-BLM poly clonal antibody IHIC-27. A HeLa cell nuclear extract equivalent to ~30 million cells, 15 µl (equivalent to 14 million cells) of 2 HeLa cell nuclear extracts immunoprecipitated with IHIC-27 and 0.15µg of recombinant BLM expressed in yeast were subjected to SDS-PAGE on a 7.5% gel. BLM protein was detected by Western analysis using monoclonal antibody 185a.

3.3.10 BLM protein is unstable

Purified BLM (with a His-tag at the carboxy-teminus) was subjected to Western analysis and blotted with either the anti-BLM monoclonal antibody 185a (raised to the amino-terminus of BLM) or an anti-His tag antibody (Fig. 3.15a). Both antibodies identified full-length BLM at 180 kDa but an additional protein of molecular weight ~75-90 kDa was identified using the anti-His antibody. This extra lower molecular weight protein, presumably carboxy-terminal BLM, was not recognised by 185a. Interestingly no protein of ~90-105 kDa, corresponding to the amino-terminal portion of BLM was identified by 185a either. This may be due to further proteolytic processing of the amino-terminus. As shown previously, additional lower molecular weight proteins have been identified by IHIC-27 in Western blots of cell lysates, some of which appear more intense the longer the lysate is kept (Fig. 3.11). In addition, when recombinant BLM from induced yeast lysates and MRC5 cell lysates were separated by SDS-PAGE, BLM protein was detected by Western analysis using either the anti-BLM monoclonal antibody 185a or the anti-His tag antibody. Full length BLM protein was identified in all lysates but a second smaller protein >97 kDa was also identified in the yeast lysate expressing BLM. Both of these proteins were also seen much more faintly in the MRC5 lysates, however the smaller protein was not identified using the anti-His tag antibody (Fig. 3.15b).

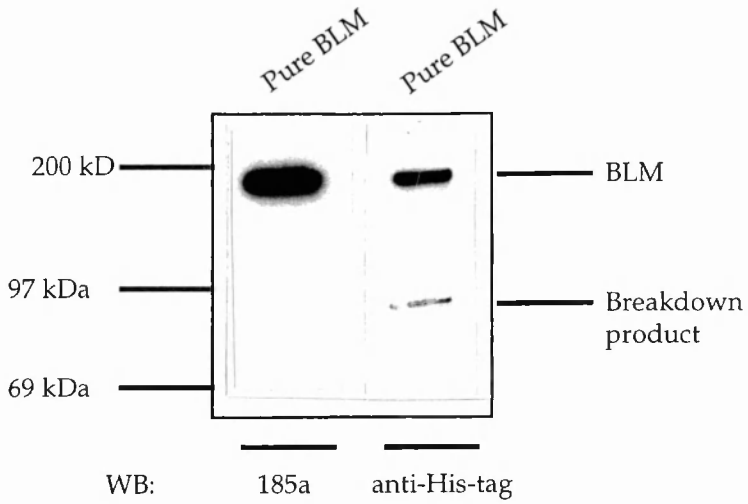

Fig. 3.15 a

BLM protein is susceptible to breakdown. 0.5 µg of purified His-tagged recombinant BLM was subjected to SDS-PAGE. BLM was detected using either a monoclonal antibody 185a directed against the amino-terminus or with an anti His-tag antibody directed against the carboxy-terminus.

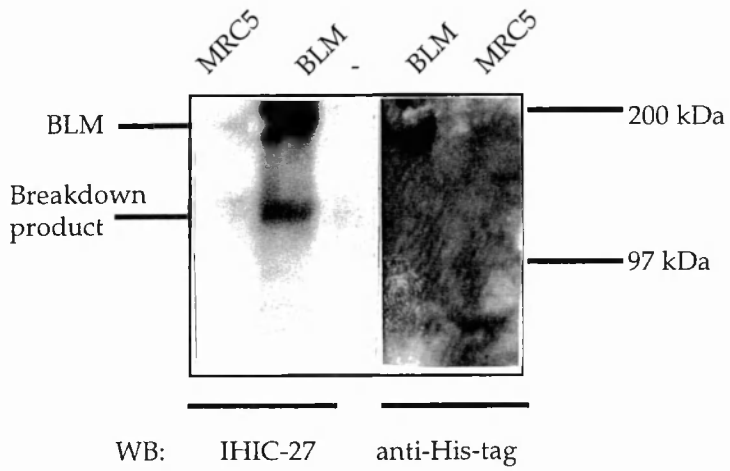

Fig. 3.15 b

BLM is susceptible to breakdown. (25 µl) of an MRC5 cell lysate (equivalent to 125,000 cells) and 0.15µg of recombinant BLM from a yeast lysate were subjected to SDS-PAGE on a 7.5% gel. BLM protein was detected by Western analysis using the polyclonal antibody IHIC-27 directed against the amino terminus of BLM or an anti-His tag antibody directed against the carboxy terminus of BLM.

3.3.11 Monoclonal antibody 32e recognises wild type and recombinant BLM protein

Nuclear isolates prepared from HeLa cells and immunoprecipitated with affinity purified IHIC-27 were subjected to SDS-PAGE together with an induced lysate from yeast expressing BLM as a positive control. Western analysis using the monoclonal anti-BLM antibody 32e to detect BLM was then performed (Fig. 3.16). 32e recognised a band of 180 kDa in the HeLa cell nuclear isolate immunoprecipitated with IHIC-27 and in induced yeast cultures expressing BLM. No BLM was detected by 32e when the immunoprecipitating antibody IHIC-27 was omitted.

3.3.12 Immunostaining of cells with anti-ATM and anti-BLM antibodies

As described above immunostaining for ATM and BLM was attempted in a variety of different ways with the same result. Representative examples of the immunostaining for both are included here (Fig. 3.17 to Fig. 3.19).

Although immunostaining for Topoisomerase IIα (the positive control) using the polyclonal rabbit antibody IHIC-7 was successful, (a red-brown reaction product stained the metaphase chromosomes of both AT5BIVA (Fig. 3.17A) and MRC5 fibroblasts (Fig. 3.17B)), immunostaining of formalin fixed AT5BIVA (Fig. 3.17C) and MRC5 cells (Fig.3.17D) using CN-12 (2 μg/ml) was negative.

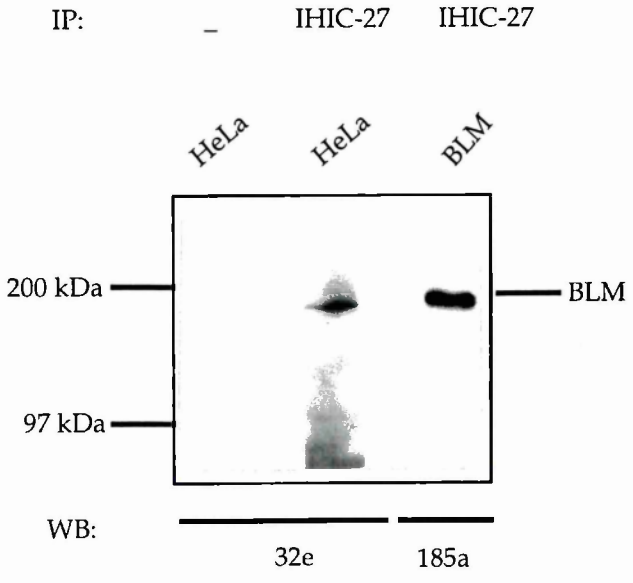

Fig. 3.16

Monoclonal antibody 32e recognises BLM protein in HeLa cell immunoprecipitates. Nuclear isolates were prepared from HeLa cells and immunoprecipitated with affinity purified antibody IHIC-27. 20µl of the immunoprecipitated proteins (equivalent to 18 million cells) and 0.15µg of full length recombinant BLM protein (from a yeast lysate) were then subjected to SDS-PAGE. BLM protein was detected by Western blot analysis using anti- BLM monoclonal antibodies 185a and 32e.

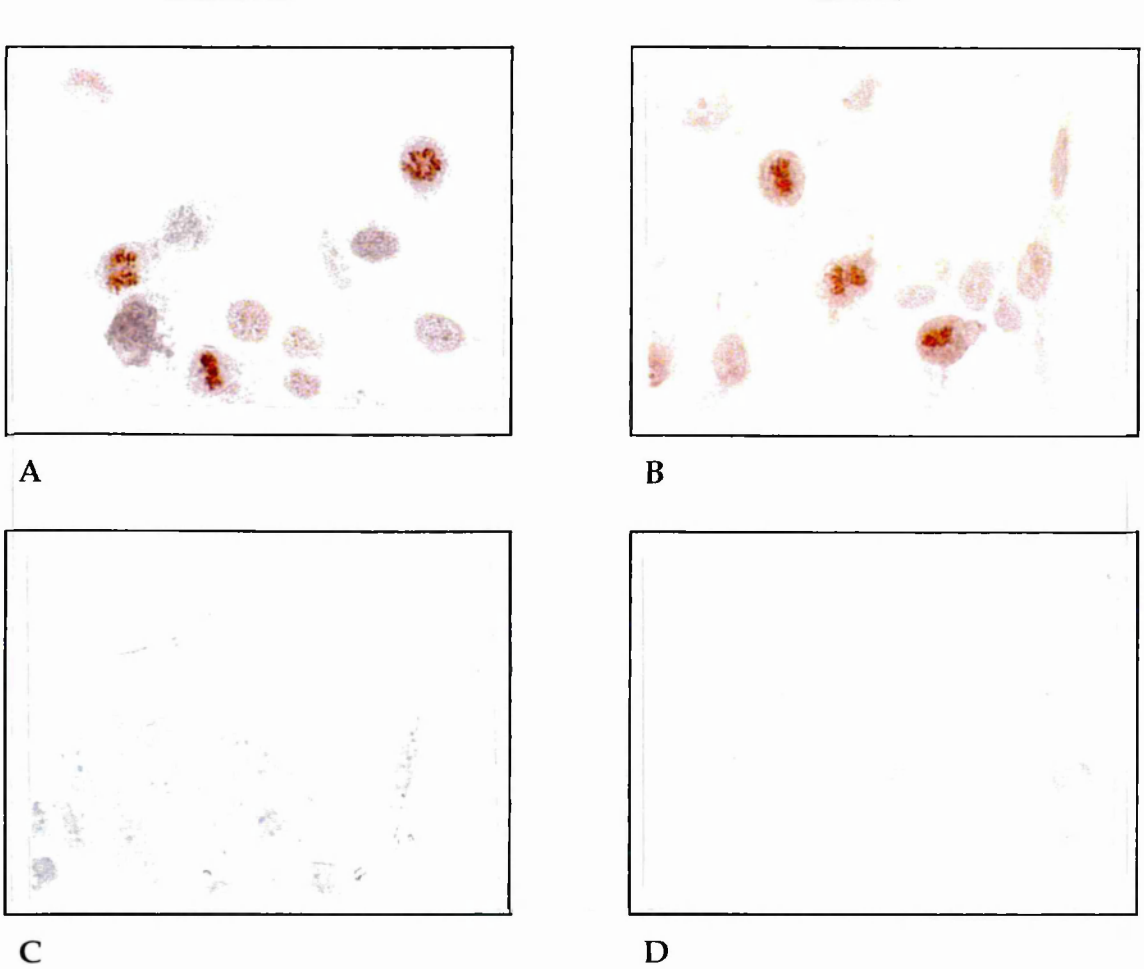

Fig. 3.17

The anti-ATM polyclonal antibody CN-12 is not useful for detection of ATM by immunohistochemistry: AT5BIVA (ataxia telangiectasia fibroblasts) and MRC5 (wild type fibroblasts) were analysed by immunohistochemistry for the presence of Topoisomerase II α using IHIC-7 (A and B respectively) and ATM protein using CN-12 (2μg/ml), (C and D respectively), after fixation in formalin/PBS. In this experiment the vector AEC substrate kit was used and the formation of a red-brown reaction product indicates a positive result.

GM8505 MRC5

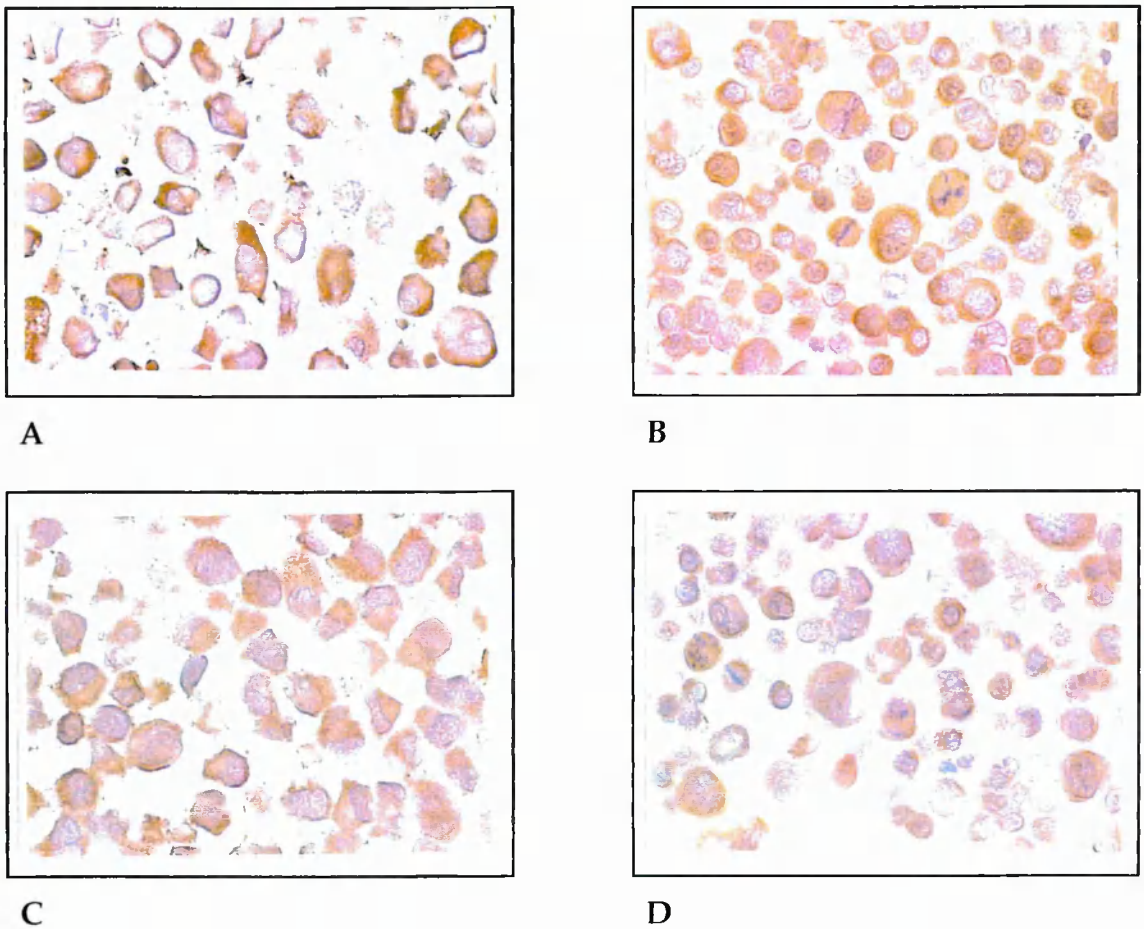

Fig. 3.18

The polyclonal anti-BLM antibody IHIC-27 is not useful for immunohistochemistry: GM8505 (a Bloom's cell line), (A and C) and MRC5 cells (B and D) were analysed by immunohistochemistry using the polyclonal antibody IHIC-27 at 1/100 (A and B) and 1/200 (C and D) for the presence of BLM protein. The DAB reaction was used for development and the formation of a brown reaction product indicates a positive result.

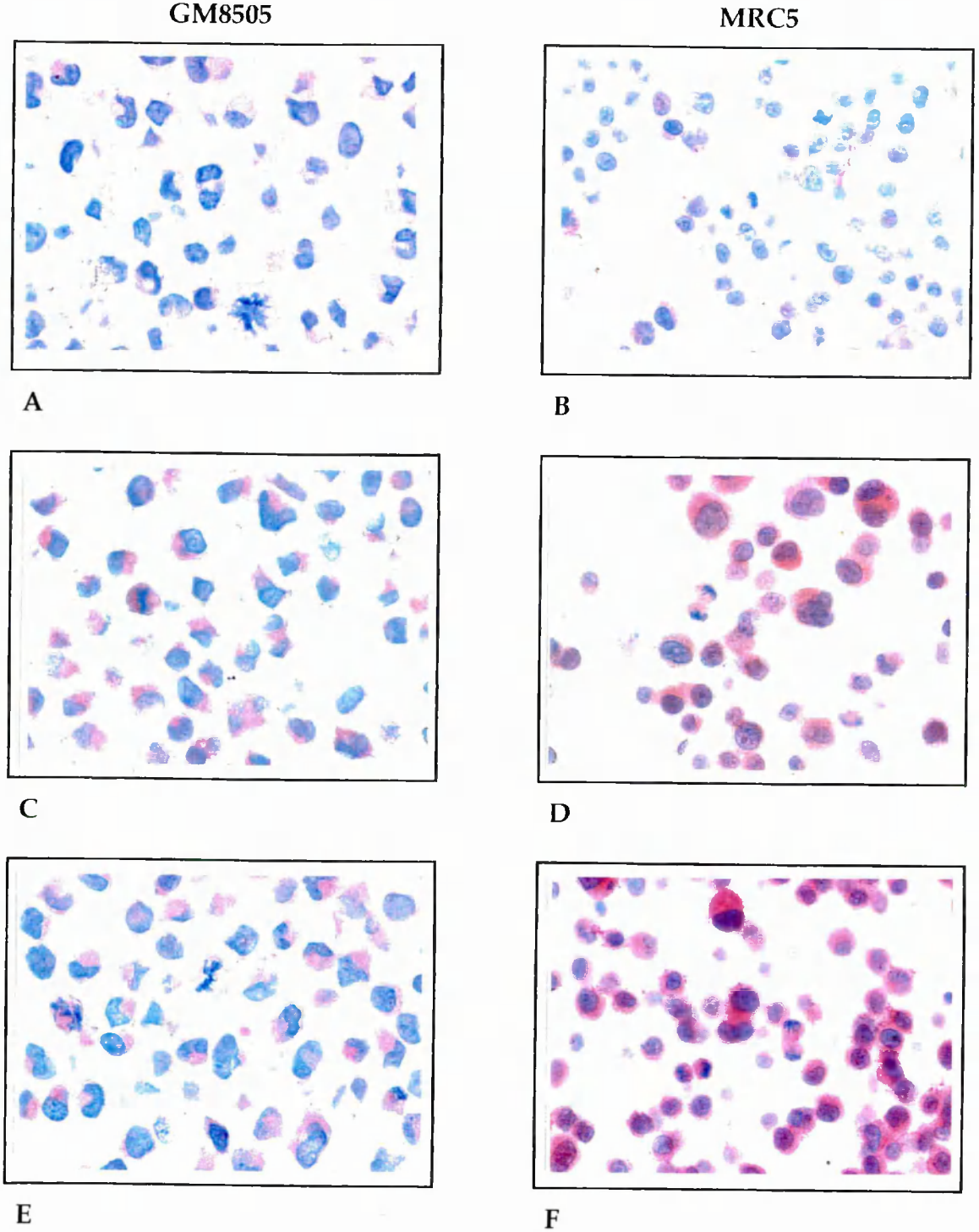

Fig. 3.19

The monoclonal anti-BLM antibodies 185a and 32e are not useful for the detection of BLM by immunohistochemistry: GM8505 (Bloom's cells), (A, C and E) and MRC5 cells (B, D and F) were analysed by immunohistochemistry using the mouse monoclonal antibodies 185a (C and D) and 32e (E and F) for the presence of BLM protein. In A) GM8505 and B) MRC5 cells, the primary antibody was omitted. The vector AEC substrate kit was used and the formation of a red-brown reaction product indicates a positive reaction.

When immunostaining for BLM was attempted using alcohol fixed cytospin specimens of GM8505 cells and MRC5 cells using the polyclonal rabbit antibody IHIC-27 at dilutions of 1/100 and 1/200 a pale brown reaction product was seen in the cytoplasm of both cell types at all dilutions (Fig. 3.18). No specific nuclear staining of any type was identified. A negative control omitting the primary antibody was negative; a positive control showed Topoisomerase IIα staining of lymphocytes in lymph node sections (not shown).

Cytospin specimens of GM8505 cells and MRC5 cells were also used for immunostaining with the monoclonal anti-BLM antibodies 185a and 32e (Fig. 3.19). Weak reddish-brown staining of the cytoplasm was seen in GM8505 with both monoclonals 185a and 32e (Fig. 3.19 C and E) and this cytoplasmic staining was noted to be slightly stronger in MRC5 cells (Fig. 3.19 D and F). (This additional cytoplasmic staining is not due to detection of full length BLM protein as this is not cytoplasmic in location Fig. 3.13) . No specific nuclear staining of any type was identified. Primary antibody was omitted as negative control and revealed pale pink cytoplasmic staining in both GM8505 and MRC5 cells (Fig. 3.19 A and B).

3.4 Discussion

The polyclonal antibody CN-12 recognises a ~350 kDa protein which is not present in ataxia telangiectasia cell lines and which is the same size as a

protein detected by the polyclonal antibody ATM.B despite the fact that the regions of ATM these antibodies were raised against are dissimilar and do not overlap. It was therefore concluded that the 350 kDa protein recognised by CN-12 was ATM. The identity of the other weaker bands seen in cell line immunoprecipitates and whole cell lysates (including the NCI panel), remains speculative. They may represent as yet unidentified cross-reacting proteins which show sequence similarities to the region of ATM against which CN-12 was raised (although CN-12 recognises the amino-terminus of ATM which does not show any similarity with any other known proteins at present). It is possible that some of the additional bands may represent ATM breakdown products retaining the region to which CN-12 is directed. Whilst a range of transcript sizes from 2-12 kb has been observed in several different tissues (Savitsky et al., 1995), no alternative splicing has been identified in the coding region of *ATM* (Savitsky et al., 1997), implying that these are not splice variants of ATM protein.

Most *ATM* mutations are null (Gilad et al., 1996) and as mentioned, protein instability may explain why no truncated ATM protein is detected in AT2RO cell lysates which could potentially express a protein of 211 kDa. This has been documented for many other truncation mutants of ATM previously (Brown et al., 1997), (Stankovic et al., 1998) and is therefore not an unexpected finding.

The subcellular localisation of ATM was described in 1996 (Lakin et al., 1996). The finding that it is a predominantly nuclear protein is in keeping with its putative role as a sensor of DNA damage and in the transduction of DNA damage response pathways, including DNA repair. Immunohistochemical

studies have since shown colocalisation of ATM with replication protein A (RPA), at the synapsing areas on homologous chromosomes in meiosis and a role in recombination has been suggested (Hawley and Friend, 1996), (Keegan et al., 1996), (Plug et al., 1997). The discovery of ATM in as yet indeterminate microsomal structures raises the possibility of a role for ATM in cytoplasmic signalling (Lavin and Shiloh, 1996), as seen for some of its homologues eg phosphatidyl inositol 3-kinase or the yeast Vps proteins which are also membrane associated. It is possible that derangement of cytoplasmic ATM-related effects may account for some aspects of the pleiotropic nature of the disorder.

CN-12 is a relatively good antibody for Western blotting and detected apparently full-length ATM protein in 26/27 of the cell lines in the NCI tumour cell line panel examined, although the levels were rather variable. The underlying molecular defects in the range of tumour cell lines tested are likely to differ from one cell line to another and variability in the levels of ATM protein detected may reflect differences in regulation or degradation of the protein in the context of these tumour cell lines (whereas in normal cells ATM does not show upregulation after γ or UV irradiation (Lakin et al., 1996), (Brown et al., 1997)). It is possible that Western blotting may underestimate the true number of *ATM* mutations in these tumour cell lines as missense mutations, extreme carboxy-terminal truncations and small in frame deletions not associated with protein instability may be overlooked as they may not alter the apparent size of the protein. *ATM* heterozygotes may also be missed for similar reasons, although it is possible that tumour lines showing reduced levels of ATM may be A-T heterozygotes with one allele coding for an unstable

truncated protein or one or both alleles featuring mutations generating potential splice sites or missense mutations, where a small proportion of the full length protein may be expressed.

The complete lack of ATM expression seen in the promyelocytic leukaemia cell line HL-60 is of interest because of the association of *ATM* mutations and T-cell leukaemias (as described in Chapter 1). Clustering of *ATM* missense mutations (rather than the more common null mutations) particularly in the kinase domain of *ATM* has been shown in the tumour DNA from patients with sporadic T-prolymphocytic leukaemia (Vorechovsky et al., 1997), which is similar to the leukaemia seen in A-T patients. Missense mutations can give rise to mutated full length *ATM* protein so it is doubtful that such a mutation is present in HL-60. The lack of expression of ATM in HL60 probably results from truncation mutations leading to unstable protein. A case of acute myeloid leukaemia has been documented in A-T previously in association with ATM protein expression from 2125del126nt which deletes 42 amino acids from the full length ATM protein. The mutation on the second allele in this case was unknown (Stankovic et al., 1998). The marked reduction in ATM levels in the non-small cell lung cancer cell line NCI-H23 and the less marked reduction in HOP-62 and NCI-H322M is surprising, as lung cancer is not noted to be one of the more common tumours in patients with AT or their relatives (Swift et al., 1987), (Morrell et al., 1986). The reduction of ATM levels observed in the colonic carcinoma cell lines HCT-116 and HCC-2998 and the renal carcinoma cell lines RXF-393 and 786-0 is not reflected in a particular predisposition to these tumours in AT, although the brain tumour cell line SNB-19 showed reduced levels of ATM and brain tumours are recognised in

the spectrum of non-lymphoreticular tumours seen in A-T (Morrell et al., 1986). It is possible that ATM is reduced in these lines due to protein regulatory changes or due to secondary mutations in one or both *ATM* alleles. The significance of reduced levels of ATM is difficult to ascertain because it is not clear what absolute level of functional ATM is required under normal circumstances for appropriate regulation of the cell processes it influences. In this respect a functional assay of the protein or gene sequencing would be more useful. ATM protein levels of from 1-100% of normal have been documented in AT variants with a milder AT phenotype (Gilad et al., 1998), (Stankovic et al., 1998). Milder variant A-T phenotypes are associated with mutations generating functional splice sites from cryptic splice sites (aberrant splicing signals can then create mutant products but may also alternatively allow production of small amounts of wild type protein (McConville et al., 1996)) or with missense mutations which allow expression and some residual degree of ATM function. The missense mutation 7271T->G results in the amino acid substitution V2424G and is associated with full length stable mutated ATM protein. This mutation confers a milder A-T phenotype, especially in homozygote rather than compound heterozygote A-T individuals, suggesting it has some residual wild type activity (although it is associated with an increased risk of breast cancer (Stankovic et al., 1998)). Therefore protein function cannot necessarily be inferred from protein levels unless no protein at all is detected. This may explain why no significant correlation of ATM levels with downstream effectors (p21 induction, p53 levels and G1 arrest capacity after 6.3 Gy of γ irradiation) was found in the NCI Database correlation screen.

In addition other defects in the cell lines tested may intefere with normal cellular transduction pathways thus obscuring expected associations.

The polyclonal antibody IHIC-27 recognises a protein of molecular weight ~180 kDa in cells which are wild type for BLM (HeLa, U2OS and MRC5 cells), however no band is seen in the Bloom's fibroblastic cell line GM8505. IHIC-27 also recognises purified recombinant BLM with a molecular weight of ~180 kD, although the predicted molecular weight for the BLM gene product is ~156 kDa. On this basis, the protein identified by IHIC-27 is believed to be BLM. A weak band corresponding to a protein of the same size as BLM was identified by IHIC-27 in GM2392 cell lysates (Bloom's cells). This may represent mutated but near full-length BLM or alternatively, this may be a revertant clone of GM2392 although no details of the recent phenotype of this cell line were available. Further characterisation of the mutation in this cell line and an examination of the phenotype is required before any other conclusions can be drawn.

Cellular fractionation of HeLa cells and Western blotting with IHIC-27 was used to demonstrate that BLM is a nuclear protein. This is consistent with its proposed role as a 3'-5' DNA helicase (Karow et al., 1997). Unfortunately this antibody was of limited use despite affinity purification because of the recognition of multiple other bands both in wild type and Bloom's cells (Fig. 3.12). The additional bands may represent proteins cross reacting with BLM or maltose binding protein, as even the affinity purified IHIC-27 was known to contain MBP-specific antibodies (data not shown). Alternatively explanations include splice variants or breakdown products of BLM. The fragility of BLM, possibly due to a protease sensitive site, was suggested by the identification of

smaller sized products, derived from His-tagged recombinant BLM, by the His-tag antibody (Fig. 3.15a) and native BLM by IHIC-27 (Fig. 3.15b). These products were of different sizes ~85-90 kDa (carboxy-terminus) and ~110 kDa (amino-terminus) respectively which may represent two fragments from breakdown of BLM~180 kDa at a single site (whether these products are functional is not known). The reason for failure of 185a to identify the smaller breakdown product (Fig. 3.15a) in comparison with IHIC-27 (Fig. 3.15b) may relate to alteration of the epitope recognised by monospecific 185a in the processed fragment. Newly prepared recombinant BLM does not show the smaller product of BLM which may explain why it is not detected by the anti-His-tag antibody (Fig. 3.15b). Storage of the protein in 25% glycerol at -70°C was found to improve BLM stability (J. Karow, personal communication). The 180 kDa BLM band was difficult to distinguish from these additional bands and therefore monoclonal antibodies were developed against the BLM-MBP fusion protein (Helen Turley, ICRF) in the hope of improving the specificity.

Several monoclonal antibodies were tested of which monoclonal 185a recognised purified recombinant BLM, recombinant BLM expressed in yeast with a molecular weight of ~180 kD and the BLM-MBP fusion protein (62 kDa). Unfortunately this did not recognise BLM protein in whole cell lysates of wild type cell lines (data not shown). This may be due to low abundance of the protein or low affinity of the antibody as BLM was recognised in HeLa cells immunoprecipitated with IHIC-27 and Western blotted with 185a (Fig. 3.14b). The same was true for monoclonal 32e (Fig. 3.16), which again limits the usefulness of these antibodies. CN-12, IHIC-27 and 185a and 32e were not useful for immunohistochemistry with the protocols attempted. No differences

in staining could be seen in wild type cells compared to mutant cells. This prevented studies of the precise localisation of the gene products in normal tissues and studies of their expression in tumours. Other groups have had similar problems and have developed epitope tagged ATM and BLM (P. North, personal communication), to study the localisation of the recombinant proteins within cells. The lack of cellular staining seen when CN-12 was used in immunohistochemical studies may be due in part to the absence of post-translational modification of the immunogenic polypeptide due to induction in a bacterial expression system. It is possible that induction of the protein in a eukaryotic expression system, (eg a yeast or baculovirus system), might have provided an immunogen closer in this respect to the native ATM protein and improved the immunohistochemical performance of the antibody. Refinement of the immunostaining detection method and further studies of the ATM negative cell line HL60 will be conducted as detailed in Future Directions.

Genetic Predisposition to Genomic Instability in Cancer

Volume 2 of 2

A thesis submitted for the degree of
Doctor of Philosophy

(Pertaining to the Discipline of Molecular Oncology)

Dr Carina Jayne Vessey
MA, MSc, BM BCh, Dip RCPath

Institute of Molecular Medicine,
Oxford,
Sponsoring Establishment for
The Open University.

Submission date 24/8/98

Chapter 4

Investigation of the Putative Protein Kinase Activity of ATM

4.1 Introduction

At the outset of this thesis, although the phenotype of cells lacking ATM had been characterised, the precise biochemical function of ATM itself remained a unclear. In the hope of elucidating a putative enzymatic role for ATM, a considerable amount of interest was focused on the carboxy-terminus of the protein because it contained a conserved DXXXXN and DLG protein kinase motif (Taylor et al., 1992) and it featured significant homology with the catalytic subunit of phosphatidyl inositol 3-kinase (Savitsky et al., 1995), (Zakian, 1995), (Jackson, 1996) (Fig. 1.1), an enzyme known to function as a lipid kinase which is important in the generation of phosphatidyl inositol derived second messengers (Kappeller and Kantley, 1994). Other ATM homologues including Vps34 were also established as PI 3-kinases (Keith and Schreiber, 1998). In addition to these lipid kinases, DNA-PK, an enzyme of similar size to ATM, also featuring the PI3-kinase domain described above does not appear to function as a lipid kinase but is known to be a Serine/Threonine protein kinase dependent on DNA ends for its activation (Jackson, 1996), (Hartley et al., 1995). Some homologues are able to phosphorylate both proteins and lipids eg Vps34 (Stack and Emr, 1994) and the p110 catalytic subunit of mammalian PI 3-K which phosphorylates its own p85 regulatory subunit (Carpenter et al., 1993).

However, at the time these studies were undertaken, there was no incontrovertible evidence that ATM possessed either protein or lipid kinase activity. The possibility that ATM is able to autophosphorylate and thereby perhaps modulate its own function has been suggested because activated DNA-PK shows autophosphorylation. This causes dissociation of the catalytic

from the Ku regulatory subunit and a reduction in DNA-PK activity (Chan and Lees-Miller, 1996). FRAP, another mammalian ATM homologue is also capable of autophosphorylation (Keith and Schreiber, 1998). Indeed, phosphorylation of a protein the same size as ATM (~350 kD), has been documented *in vitro* in cell lysates of the human lung fibroblast cell line MRC5 immunoprecipitated with the anti-ATM antibody 6076 (Keegan et al., 1996). Mouse ATM was shown to be phosphorylated using metabolic ^{32}P labelling followed by immunoprecipitation (Chen and Lee, 1996). In the light of this suggestive evidence therefore, an attempt to demonstrate ATM autophosphorylation in HeLa cells was made.

In addition two other ATM kinase assays were designed. In order to choose a substrate for each of these assays, parallels with DNA-PK, RAD-3 and the TOR family were drawn. A variety of candidate substrates have been suggested as targets for phosphorylation by ATM, partly because they are known to be substrates of DNA-PK. These include p53, c-Abl, SP-1, cJun, cFos, cMyc and Ku (Jeggo, 1997). As described in Chapter 1, ATM acts upstream of p53 and since DNA-PK is an ATM homologue, synthetic p53 peptides were designed to include DNA-PK phosphorylation sites, p53 serine 15 and p53 threonine 18 and used as potential ATM substrates in the ATM/p53 peptide kinase assay, (Table 4.1) (Shieh et al., 1997), (S. Jackson personal communication).

The translation initiation factor e1F4E binding protein, PHAS-I (Lawrence and Abraham, 1997), (which has properties of heat and acid stability) was also chosen as another potential ATM substrate for use in the ATM/PHAS-I kinase assay for several reasons. PHAS-I has been reported to be

p53 Peptide	Sequence
wild type = p53$_{10-19}$	BIO-N-eahx-**VEPPLSQETF**
p53 Ser 15	BIO-N-eahx-**PPL<u>S</u>QEAFSDLW**
p53 Thr 18	BIO-N-eahx-**PPLAQE<u>T</u>FSDLW**
p53 Ala/Ala	BIO-N-eahx-**PPL<u>A</u>QE<u>A</u>FSDLW**

Table 4.1

p53 peptides used in the ATM/p53 kinase assay.
(BIO-N-eahx indicates the N-terminal biotinylation with an eahx spacer linking this to the p53 peptide used).

phosphorylated by ATM homologues including mTOR (Brunn et al., 1997) and Rad3 (Tamar Enoch personal communication), (Fig. 4.1). Hypophosphorylated PHAS-I is a repressor of translation inititiation as it blocks the binding of e1F4E (which is the protein responsible for recognition of the mRNA cap) to e1F4G. PHAS-I and e1F4G compete for the same binding site on e1F4E. This interaction prevents the formation of a complex containing e1F4E and e1F4G which is necessary for efficient binding and proper positioning of the 40S ribosomal subunit on the mRNA. Phosphorylation of PHAS-I, which occurs after transduction of signals from insulin or growth factors binding at the cell surface, allows e1F4E release, complex formation and initiation of translation. The phosphorylation of PHAS-I can be inhibited by factors affecting ATM homologues (eg rapamycin which also inhibits the TOR protein family) and by inhibitors of PI3-kinase (eg wortmannin and LY294002). This suggests that a PI3-kinase or PI3-kinase homologues, possibly including ATM, contribute to regulation of PHAS-I.

4.2 Additional materials and methods

4.2.1 ATM autophosphorylation assay

Pelleted protein-A-Sepharose beads bound to CN-12 with immunoprecipitated ATM were washed in kinase buffer (25 mM HEPES pH 7.5, 75 mM KCl, 10 mM $MgCl_2$, 0.2 mM EGTA, 0.1 mM EDTA, freshly added 1 mM dithiothreitol and unlabelled ATP to a final concentration of 10 μM).

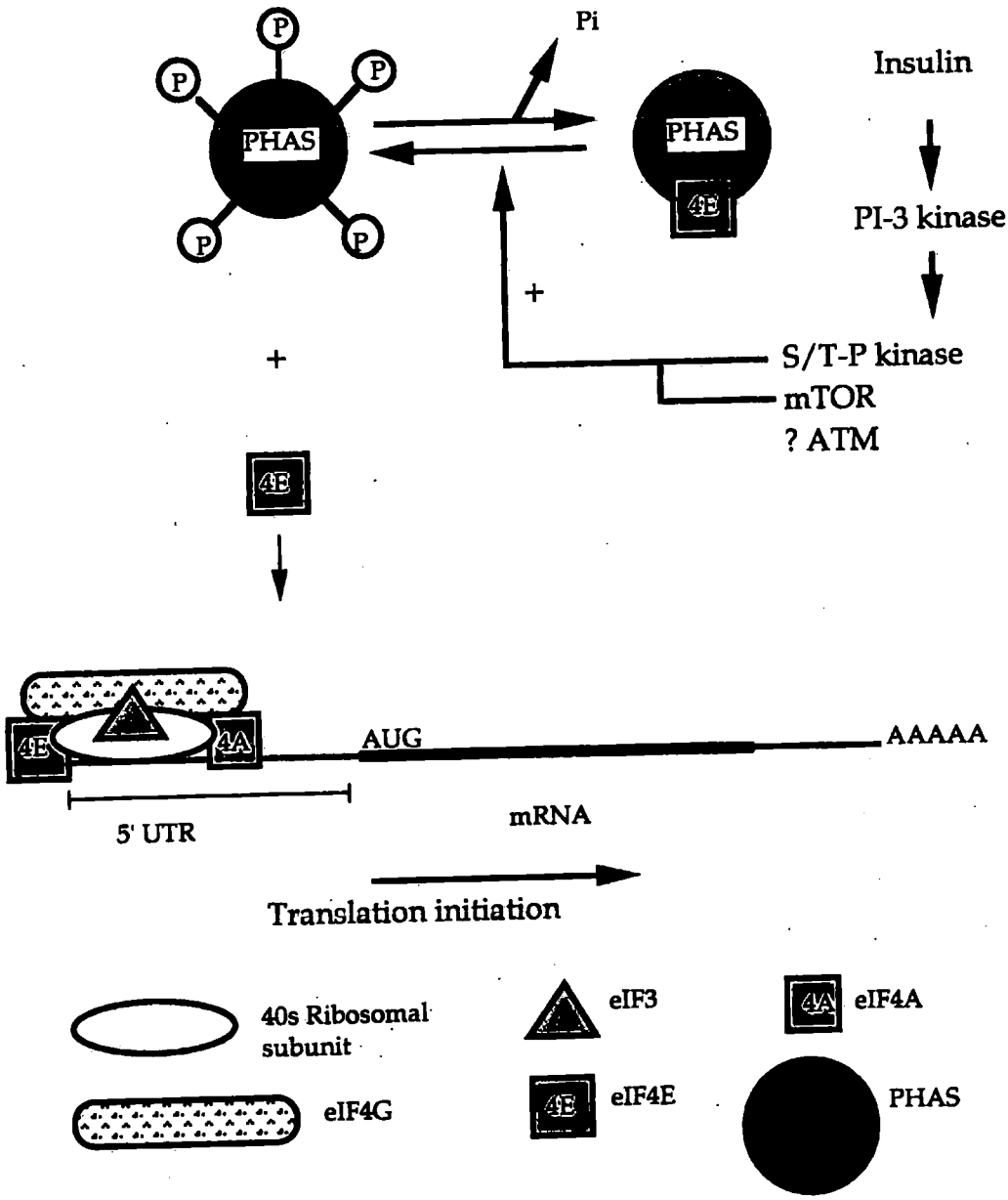

Fig. 4.1

Pathways controlling PHAS-I phosphorylation. In vivo the protein kinases which phosphorylate PHAS-I include mTOR and Phosphatidylinositol 3-kinase. Others have not yet been identified but as the phosphorylation sites in PHAS-I have the (S/T)-P motif, they are likely to be proline directed. Mitogen activated kinase also phoshorylates PHAS-I but only in vitro. The upstream pathways activating PI-3 kinase and mTOR are not known in detail but they are both involved in the transduction of insulin growth signals. The PI-3 kinase pathway can be blocked by wortmannin and LY294002 as can mTOR although higher concentrations of wortmannin are required to inhibit the latter. mTOR can also be inhibited by rapamycin.

Following repelleting of the beads, kinase buffer containing [γ^{32}P]ATP sufficient to provide each sample with 2.5 μCi of [γ^{32}P]ATP in a volume of 15 μl was prepared and carefully mixed into each pellet. Each kinase sample was allowed to incubate at 37°C for 15 min. After this time the reaction was stopped by the addition of an equal volume of 2X SDS sample buffer. The samples were then boiled for 5 min and separated by SDS-PAGE on a 7.5% gel. When optimal separation of the protein markers was achieved the gel was fixed in a mixture of 50% methanol and 10% acetic acid for 30 min prior to gel drying. The dried gel was then exposed to X-OMAT AR X-ray film (Kodak) to reveal the position of [^{32}P]-labelled proteins.

4.2.2 ATM kinase assay using p53 peptides as substrates

ATM was immunoprecipitated from 50x10^6 HeLa cells per sample, lymphoblastoid cell line GM4724 (5x10^6 cells/ sample) or A-T lymphoblastoid cell line GM2782a (5x10^6 cells/ sample) and the pelleted beads were resuspended in kinase buffer with unlabelled ATP and repelleted as described previously. At this stage 15μl of kinase buffer containing [γ^{32}P]ATP to provide 2.5 μCi per sample, the required p53 peptide ($p53_{10-19}$, p53 serine 15, p53 threonine 18 or the p53 alanine15/alanine18 which were synthesized in the Peptide Synthesis Laboratory, ICRF, Lincoln's Inn Fields, Table 4.1) to a final concentration of 0.2 mM and 100ng of restriction enzyme treated pCR-Script (Stratagene) to provide a potentially activating source of DNA with double strand breaks were added to each sample including the negative control immunoprecipitated with preimmune serum from rabbit CN-12 and the

positive control containing 10 units of DNA-dependent protein kinase (Promega). The DNA-PK sample was prepared last as DNA-PK is known to autophosphorylate and deactivate itself. (The DNA double strand break source and the DNA-PK positive control were not used in initial experiments with $p53_{10-19}$). The samples were then incubated at 37°C for 15 min and after this the reactions were stopped by addition of 500µl per sample of 5 mM EDTA in PBS which chelates the Mg^{2+} required for kinase action.

As the p53 peptides were biotin labelled they were collected on 200 µl of streptavidin coated para-magnetic beads (Sigma), by mixing the streptavidin coated beads and the sample at 4°C for 15 min. The beads were then collected on a magnetic stand (Dynal). After the first collection, the beads were washed in PBS and recollected three times in PBS. After the final wash the beads were resuspended in 50µl of PBS and each sample was transferred to small squares of Whatman 3MM paper on parafilm. These were allowed to dry in the fume hood and once they were dry they were transferred to 5 ml of scintillation fluid in scintillation vials and counted (Beckman LS 5000CE).

4.2.3 Production of recombinant PHAS-I protein

A recombinant His-tagged PHAS-I cDNA in the expression vector pET-14b (Novagen), was provided as a generous gift by Professor John Lawrence. The plasmid was transformed into chemically competent *BL21 (de3) pLysS E. coli* (Novagen), using the heat shock method: 0.15 µg of the above plasmid was added to 100 µl of the bacteria and mixed gently. The mixture was left on ice for 15 min and was then subjected to a heat shock at 42°C for 90 s before being

replaced on ice to cool. After this the bacteria were plated out on selective LB/AMP plates to select for transformants (a no DNA control was also included). The plates were incubated at 37°C overnight and the following morning 3 ml minicultures in LB/AMP were made from colonies picked from the pET-14b transformed plate (No colonies were seen on the negative control plate, ~300 were seen on the test plate). The minicultures were incubated in the shaking incubator at 37°C overnight and the following day, bacterial minipreps were made from the minicultures as previously described. 3µl of each miniprep was then digested simultaneously with the restriction enzymes Xba1 and EcoRV. Aliquots of the digests were then subjected to 0.7% agarose gel electrophoresis to check that the bacteria were carrying the plasmid and that the plasmid and the insert sizes were correct. When this was verified, test inductions of the colonies with the correct sized insert were prepared (colonies A-B): Fresh minicultures were made by adding 10 µl of the old miniculture from the chosen colonies to 3 ml of LB/AMP and incubated in the shaking incubator at 37°C overnight. The next day, 0.5 ml of miniculture was inoculated into 20 ml of prewarmed LB/AMP and incubated in the shaking incubator at 37°C until the OD_{600} reached 0.6 after which pre-induction samples were taken (200 µl of culture was pelleted by centrifugation and resuspended in 40 µl of 2X protein sample buffer) and PHAS-I expression was induced by addition of either 0.4 mM or 2 mM isopropyl-β-D-thiogalactopyranoside (IPTG) for 2 hours at 37°C. Post-induction samples were taken after 2 hours and were subjected to SDS-PAGE on a 13% gel, along with pre-induction samples (25 µl of each sample was used with a ratio of post/pre

induction culture amounts of 1/4 to account for bacterial growth). One such gel was then stained with Coomassie Blue and destained in 10% methanol, 10% acetic acid, before gel drying (Fig. 4.2). Another was transferred using the semi-dry technique and subjected to Western analysis; anti-His tag antibodies were used to identify His-tagged PHAS-I protein (Fig. 4.3).

4.2.4 Purification of PHAS-I protein

Two 2l flasks each containing 400 ml of pre-warmed LB/AMP were inoculated with 4ml of an overnight miniculture of colony B and incubated at 37°C in a shaking incubator until the OD_{600} reached 0.6. Pre-induction samples were then taken as before and PHAS-I expression was then induced by the addition of IPTG (0.4 mM) with incubation for a further 2 hours at 37°C. Post-induction samples were taken at this point (SDS-PAGE was duly performed at a later time, as before to check protein induction). The flasks were then placed on ice for 10 min prior to transfer of the cultures to eight 50 ml tubes (Falcon) and centrifugation at 4.2 Krpm (in a Beckman GPR centrifuge) for 5 min at 4°C to pellet the cells. The supernatant was then discarded and the equivalent of 200 ml of culture was resuspended in 4 ml of ice cold binding buffer (5 mM imidazole, 0.5 M NaCl, 20 mM Tris-HCl, pH 7.9). The cells were then sonicated (Soniprep 150, MSE), to shear the DNA in 30s bursts on ice until the viscosity fell. The lysate was then centrifuged in a pre-cooled SW-55ti rotor at 39Krpm for 20 min at 4°C.

The His-Bind metal chelation column was then prepared in the cold room using 4ml of His-Bind resin (Novagen) which settles to a 2 ml column.

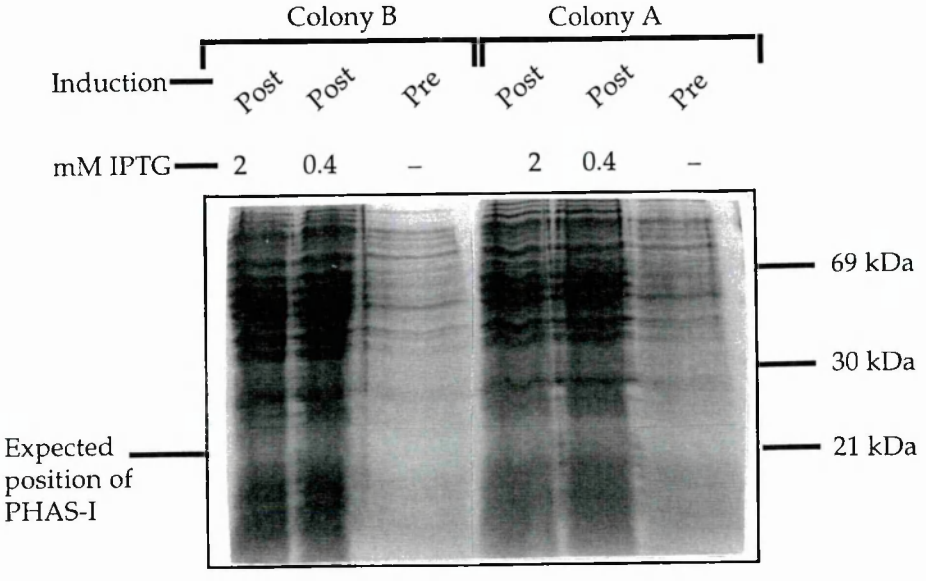

Fig. 4.2

Lack of visible recombinant PHAS-I expression in BL21 DE3 pLys S strain on a Coomassie Blue stained gel (induction conditions 0.4/2mM IPTG, 2 hours at 37 C). 20 µl of bacterial lysate was loaded per lane and subjected to SDS-PAGE on a 13% acrylamide gel . Proteins were detected by staining with Coomassie Blue.

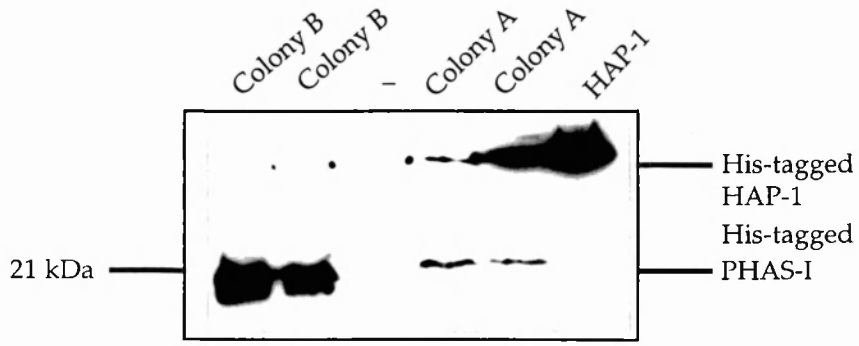

Fig. 4.3

Recombinant His-tagged PHAS-I protein is expressed by BL21 DE3 pLys S strain (induction conditions : 2 hour incubation, 0.4 mM IPTG at 37 C). 20 µl of bacterial lysate was loaded per lane and run on a 13% acrylamide gel. The PHAS-I protein was detected by Western blot analysis using anti-His-tag antibodies. A bacterial lysate expressing His-tagged HAP-1 protein was used as a positive control.

The column was then washed with 6 ml of sterile distilled water, then 10 ml of charge buffer (400 mM $NiSO_4$), followed by 6 ml of binding buffer. The supernatant from the bacterial extract was then loaded onto the column. After this the column was again washed with 25 ml binding buffer followed by 15 ml of wash buffer (60 mM imidazole, 0.5 M NaCl, 20 mM Tris-HCl, pH 7.9). The expressed His-tagged protein was then eluted with elution buffer (1 mM imidazole, 0.5 M NaCl, 20 mM Tris-HCl pH 7.9), and collected in 1 ml fractions. Pre and post induction whole lysates and post induction supernatant samples were subjected to SDS-PAGE on a 13% gel, alongside each of the eluted fractions (50 µl of each fraction was mixed with 50 µl of 2X protein sample buffer and 25 µl of each sample was run). The gel was then stained with Coomassie Blue and destained in 10% methanol, 10% acetic acid, before gel drying (Fig. 4.4). PHAS-I fractions 2-5 were then pooled and aliquoted for storage at -70°C prior to use, (25 µl of stored eluate was roughly equivalent to 5 µg of PHAS-I protein).

4.2.5 ATM kinase assay using PHAS-I as a substrate

Immunoprecipitates were prepared for Western analysis and for the kinase assay, using affinity purified CN-12 (anti-ATM) and pre-immune serum from rabbit CN-12 as previously described but using the following cell lines: 20 x 10^6 cells GM4724 human lymphoblastoid cell (ATM +/+), 28 x 10^6 cells GM2782a human lymphoblastoid cells (ATM -/-) and 2 x 10^8 HeLa S3 cells. (For Western blotting this resulted in the immunoprecipitate in the 30µl loaded per track being derived from 5, 7 and 50 x 10^6 cells respectively. A HeLa

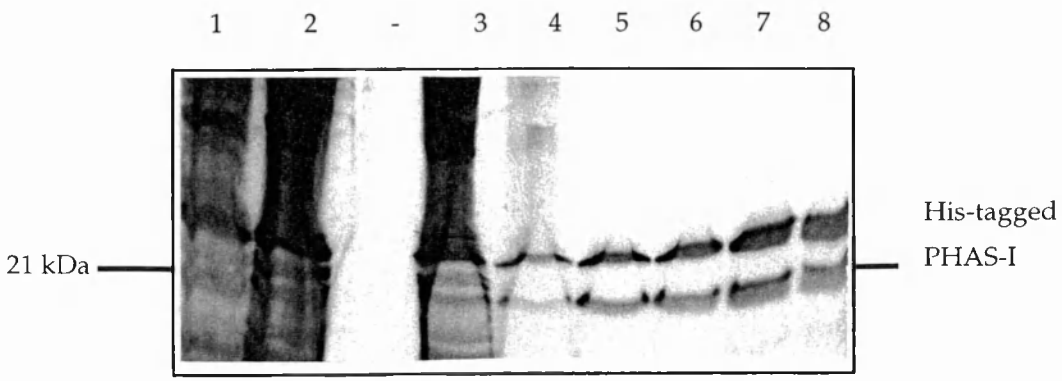

Fig. 4.4

His-tagged recombinant PHAS-I protein can be purified over a His Bind column. Recombinant PHAS-I expression was induced in BL21 DE3 pLys S strain after 2 hours incubation at 37 C with 0.4 mM IPTG . 25µl of bacterial lysate was loaded in lanes 1) preinduction: whole cell lysate , 2) 2 hour post induction: whole cell lysate, and 3) 2 hour post induction bacterial supernatant. PHAS-I protein was purified by passing the supernatant over a His-Bind column. 12.5 µl of eluted PHAS-I protein (resuspended in an equal volume of 2X protein sample buffer) from the first five collected fractions was loaded in lanes 4-8 respectively. The samples were subjected to SDS-PAGE on a 13% acrylamide gel and proteins were detected after staining with Coomassie Blue.

sample containing 10 x 10^6 cells was also included to determine if cell number was limiting in terms of ATM immunoprecipitated.

The samples for the ATM/PHAS-I kinase assay were treated as described above for the autophosphorylation assay but with addition of 10µl of purified PHAS-I (~1µg of PHAS-I protein) and 100ng of restriction enzyme treated pCR-Script per sample, as a source of DNA with dsbs, to the [γ^{32}P]ATP containing kinase buffer. DNA-PK was used as a positive control (as described in the p53 peptide assay). The samples were incubated and processed as before prior to PHAS-I (~21 kDa) separation by SDS-PAGE on a 13% gel. The gel was fixed, stained in Coomassie Blue for 10 min then destained for 30 min to check PHAS-I localisation prior to gel drying. The blot was then wrapped in Saran wrap and exposed to X-OMAT AR film (Kodak) to determine the amount of PHAS-I phosphorylation in each sample including the DNA-PK positive control.

4.3 Results

4.3.1 Immunoprecipitated ATM from HeLa cell nuclear extracts phosphorylates associated proteins of MW ~ 350 kDa and ~ 200-97 kDa

The ability of ATM to phosphorylate co-immunoprecipitated proteins in HeLa nuclear extracts was investigated. Proteins were isolated using the affinity purified anti-ATM antibody CN-12 and analysed using the ATM kinase assay followed by Western blot analysis and autoradiography (Fig. 4.5A and B).

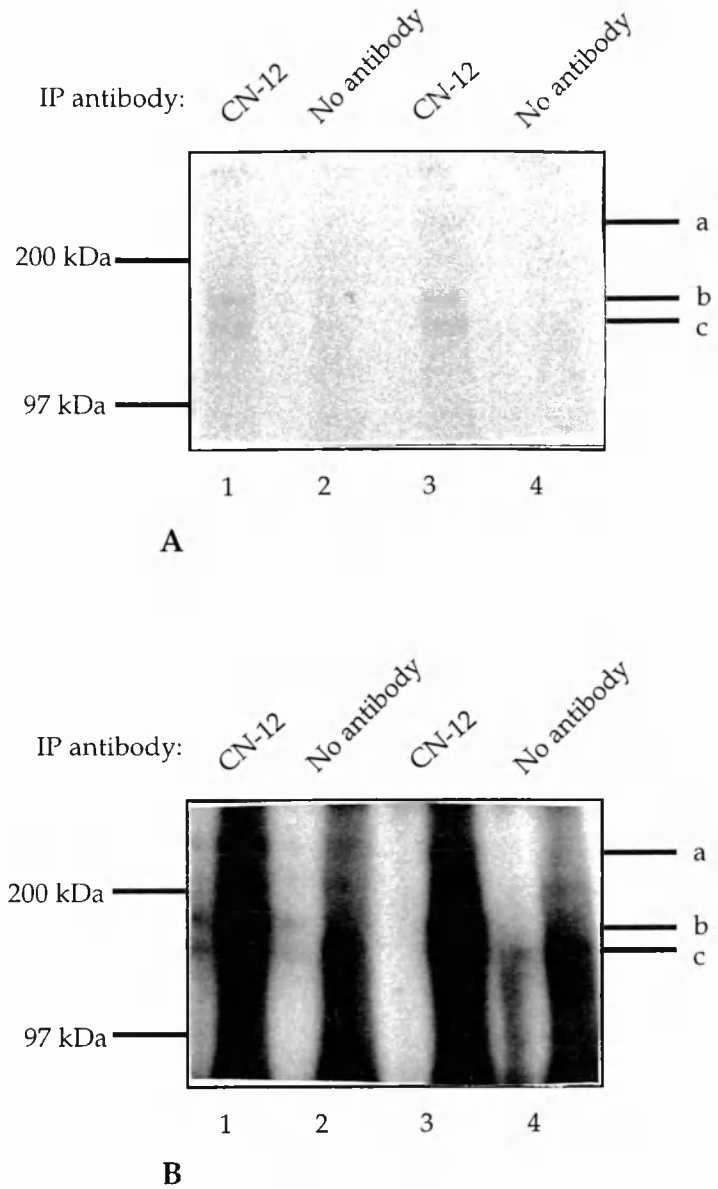

Fig. 4.5

Protein species phosphorylated by immunoprecipitated ATM in HeLa cells. ATM from HeLa cell nuclear extracts was immunoprecipitated with affinity purified antibody CN-12 (samples 1 and 3). CN-12 was omitted in samples serving as negative controls (samples 2 and 4). A kinase assay was then performed as previously described. Subsequently, 30µl of phosphorylated HeLa cell nuclear extract (equivalent to 20 million cells per sample) was loaded in each lane of a 7.5% acrylamide gel and subjected to SDS-PAGE. Subsequent auto-radiographic exposure of the fixed and dried gel of three days (4.5A) or one week (4.5B), revealed three phosphorylated protein species of the following molecular weights: a) 350 kDa, b) and c) between 200-97 kDa.

After a three day exposure, phosphorylation of two protein species of molecular weights ~ 160 kDa and 140 kDa was detected (Fig. 4.5A). Longer exposures, identified two other phosphorylated protein species of molecular weight ~200 and 350 kDa, (Fig. 4.5B) in the CN-12 immunoprecipitated samples although the background was increased. A discrete ~ 140 kDa band and faint indistinct bands at ~200 kDa and ~ 350 kDa were also seen in the 'no antibody' negative control.

4.3.2 Immunoprecipitated ATM from HeLa cell nuclear extracts does not phosphorylate the p53 peptide 10-19

The ability of immunoprecipitated ATM from HeLa nuclear extracts to directly phosphorylate the p53 peptide $p53_{10\text{-}19}$ was investigated using the affinity purified antibody CN-12 to immunoprecipitate ATM followed by analysis with the ATM/p53 kinase assay and measurement of $p53_{10\text{-}19}$ [γ ^{32}P] incorporation in a scintillation counter. The experiment was performed on two separate occasions with [γ ^{32}P]ATP of a different activity date, hence the results are presented separately (Fig. 4.6 and Fig. 4.7). In the first experiment, the highest mean $p53_{10\text{-}19}$ [γ ^{32}P] incorporation was greatest for the sample immunoprecipitated with affinity purified CN-12 immune serum (Fig. 4.6) and in the second experiment, the highest mean $p53_{10\text{-}19}$ [γ ^{32}P] incorporation was greatest for the preimmune serum negative control (Fig. 4.7). However, there was an overlap in the range of the $p53_{10\text{-}19}$ [γ ^{32}P] incorporation for the samples immunoprecipitated with CN-12 and the preimmune serum negative

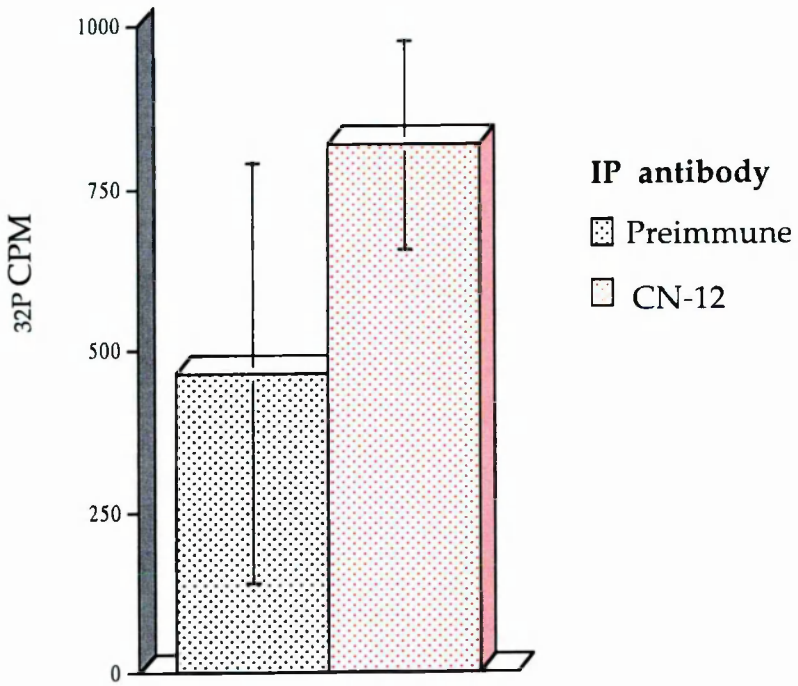

Fig. 4.6

Immunoprecipitated ATM does not phosphorylate the p53 peptide p5310-19. HeLa cell nuclear extracts (50 million cells/sample) were immunoprecipitated with preimmune serum (black bar, n=2), or affinity purified CN-12 (red bar n=2). The ATM/p53 peptide kinase assay was then performed using [γ32]-ATP. Biotinylated p53 was then collected on streptavidin beads and associated [γ32P] activity was measured in a scintillation counter. (The height of each bar represents the mean and the vertical error bars the range of the two readings).

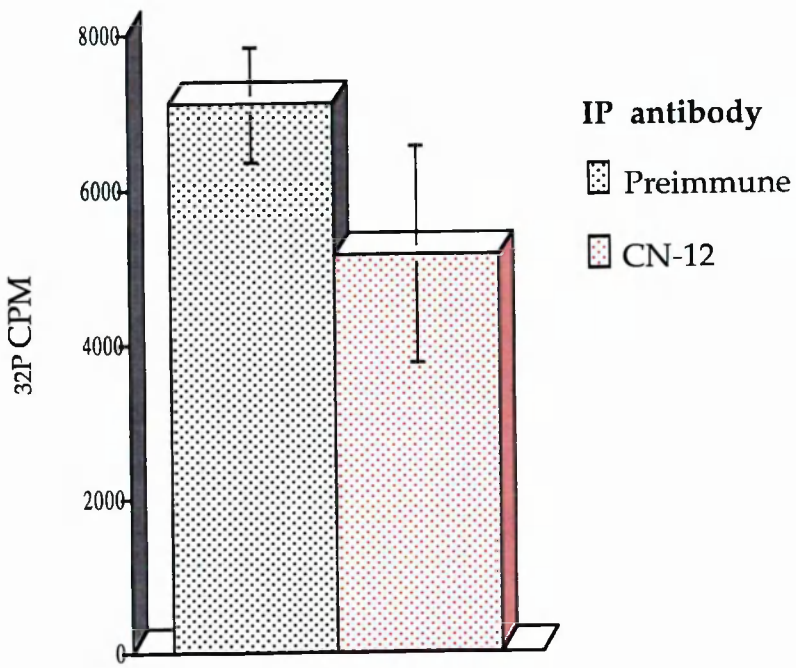

Fig. 4.7

Immunoprecipitated ATM does not phosphorylate the p53 peptide p5310-19. HeLa cell nuclear extracts (50 million cells/sample) were immunoprecipitated with preimmune serum (black bar, n=2), or affinity purified CN-12 (red bar n=2). The ATM/p53 peptide kinase assay was then performed using [γ32]-ATP. Biotinylated p53 was then collected on streptavidin beads and associated [γ32P] activity was measured in a scintillation counter. (The height of each bar represents the mean and the vertical error bars the range of the two readings).

control on both occasions indicating lack of significant phosphorylation above background by immunoprecipitated ATM.

4.3.3 Immunoprecipitated ATM from HeLa cell nuclear extracts does not phosphorylate the p53 peptides p53 Ser 15 or p53 Thr 18

The ability of immunoprecipitated ATM to directly phosphorylate the p53 peptides p53 Ser 15 and p53 Thr 18 was investigated in two separate experiments, using the affinity purified antibody CN-12 to immunoprecipitate ATM from HeLa cell nuclear extracts. The ATM/p53 kinase assay was then performed with a source of potentially activating DNA double strand breaks (DNA dsbs) followed by measurement of p53 peptide [γ^{32}P] incorporation in a scintillation counter. Negative controls included immunoprecipitations with preimmune serum and assessment of [γ^{32}P] incorporation in the p53 peptide Ala15/Ala18 which cannot be phosphorylated on these residues (Table 4.2, Fig. 4.8). Phosphorylation of the p53 peptides by an external source of DNA-PK was used as a positive experimental control. The level of [γ^{32}P] incorporation for each sample was displayed as a percentage of that observed for the p53 Ser peptide by DNA-PK. This corrected for the difference in the [γ^{32}P]ATP activity dates between the experiments and allowed the results to be combined (Table 4.2, Fig. 4.8): DNA-PK phosphorylates the p53 Ser15 peptide to the greatest extent followed by the p53 Thr18 peptide. No phosphorylation of the negative control p53 Ala15/Ala18 peptide could occur due to replacement of the serine and threonine with non-phosphorylatable alanine. Levels of phosphorylation of this peptide therefore represent non-specific background effects. Although

Sample	[γ^{32}P] Incorporation Expt 1/Expt2	% of DNA-PK /p53 Ser Incorporation Expt1/Expt2	Mean % [γ^{32}P] Incorporation
DNA-PK/p53 Ser	63,798/250,709	100/100	100
DNA-PK /p53 Thr	30,936/-	48.5/-	48.5
DNA-PK /p53 Ala	4,308/-	6.75/-	6.75
Hela/p53 Ser Preimmune	643/807	1.007/0.322	0.665
Hela/p53 Ser CN-12	1,884/1,101	2.953/0.439	1.696
Hela/p53 Thr Preimmune	453/1080	0.710/0.431	0.571
Hela/p53 Thr CN-12	769/1136	1.205/0.453	0.829
Hela/p53 Ala Preimmune	844/1,108	1.323/0.442	0.883
Hela/p53 Ala CN-12	598/1,689	0.937/0.674	0.806

Table 4.2

p53 peptide [γ^{32}P] incorporation in the ATM/p53 peptide kinase assay using preimmune serum or CN-12 immunoprecipitates from 50x10^6 HeLa cells per sample.

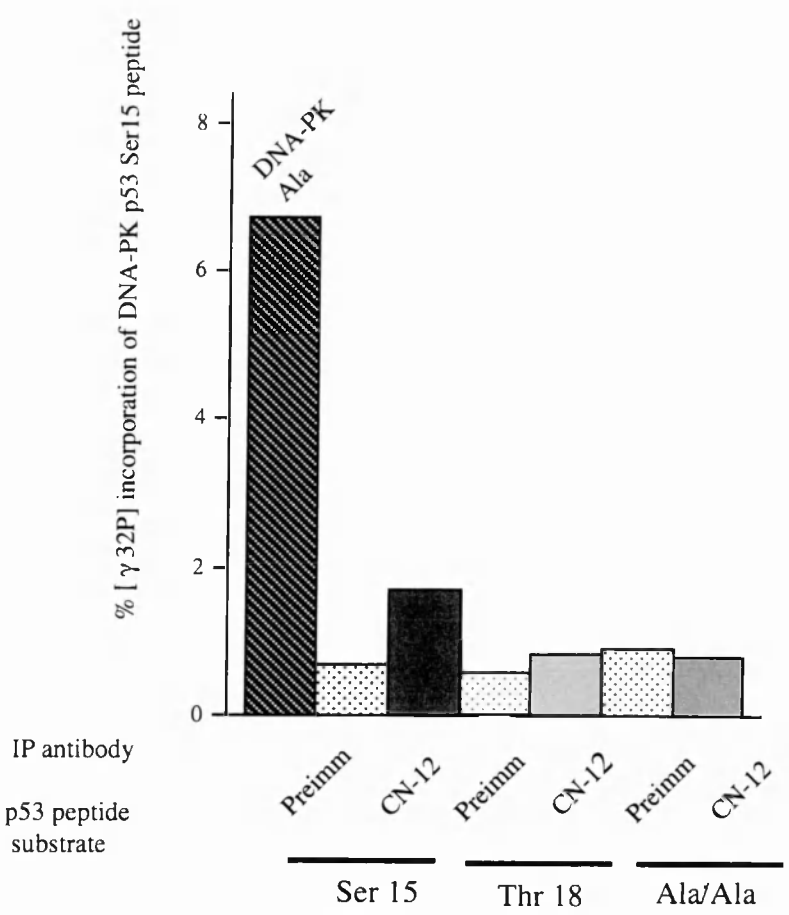

Fig 4.8

Immunoprecipitated ATM protein does not phosphorylate the p53 peptide substrates: p53 Ser 15 or p53 Thr 18. HeLa cell nuclear extracts (50 million cells /sample) were immunoprecipitated with preimmune serum or affinity purified CN-12. The ATM/ p53 peptide kinase assay was then performed . Biotinylated p53 from each sample was subsequently collected on streptavidin beads and the associated [γ 32P] activity was measured in a scintillation counter. The experiment was performed twice. Results are presented as a percentage of the DNA-PK p53 Ser 15 peptide positive control. (The bar height is the mean of the two readings taken in Table 4.2).

there was some variation in the p53 peptides tested, all showed phosphorylation levels of less than 2% of the positive DNA-PK p53 peptide Ser15 (ie less than that seen for the negative control (DNA-PK Ala15/18) described above), indicating lack of specific phosphorylation of these p53 peptides by ATM immunoprecipitated from HeLa cells.

4.3.4 Immunoprecipitated ATM from HeLa and GM4724 cell nuclear extracts does not phosphorylate the p53 peptides p53 Ser 15 or p53 Thr 18

The ability of immunoprecipitated ATM to directly phosphorylate the p53 peptides p53 Ser15 and p53 Thr18 was investigated in two separate experiments, using the affinity purified antibody CN-12 to immunoprecipitate ATM from HeLa, GM4724 (wt) and GM2782a (ataxia telangiectasia) cell nuclear extracts. The ATM/p53 kinase assay was then performed as described above (Fig. 4.9). Negative controls included assessment in each cell line of [γ ^{32}P] incorporation in the p53 peptide Ala15/18. Phosphorylation of the p53 peptides by an external source of DNA-PK was again used as a positive experimental control. (The peptide p53 Thr 18 was not tested in the second experiment). The level of [γ ^{32}P] incorporation for each sample was again displayed as a percentage of that observed for the p53 Ser peptide by DNA-PK. This corrected for the difference in the [γ ^{32}P]ATP activity dates between the experiments and allowed the results to be combined (Table 4.3, Fig. 4.9).

Although there was some variation in the mean % [γ ^{32}P] incorporation for each p53 peptide in each cell line the highest level of incorporation was still

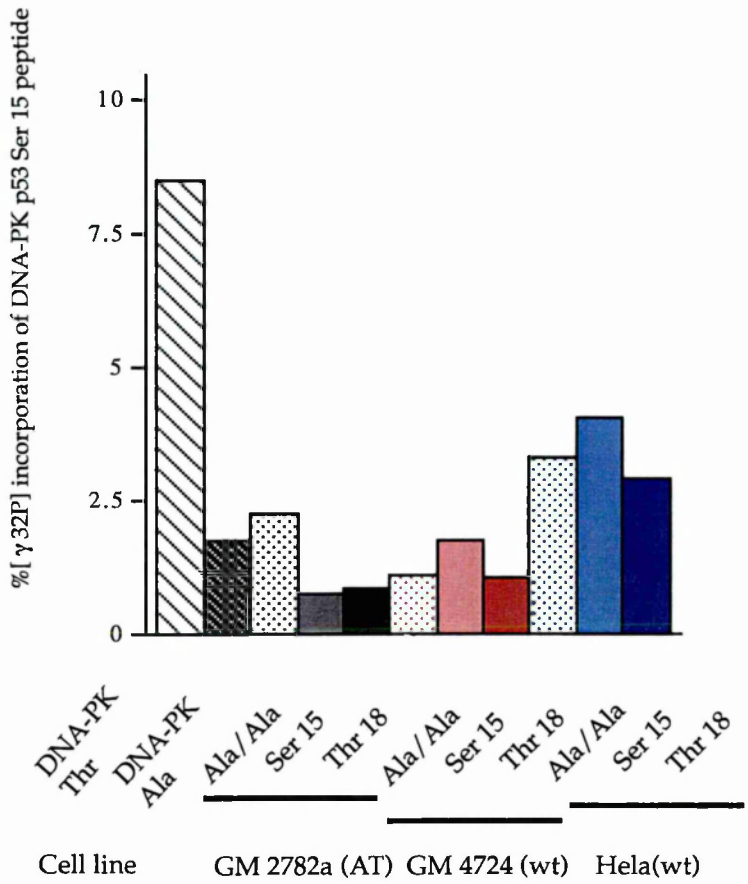

Fig. 4.9

Immunoprecipitated ATM protein does not phosphorylate the p53 peptide substrates: p53 Ser 15 or p53 Thr 18. Nuclear extracts from HeLa cells (50 million cells sample), GM 2782a and GM 4724 cells (5 million cells / sample), were immunoprecipitated with affinity purified CN-12.The ATM / p53 peptide kinase assay was then performed using for each of the p53 peptides shown. Biotinylated p53 from each sample was collected on streptavidin beads and the associated [γ32P] activity was measured in a scintillation counter. Excluding the p53 Thr 18 peptide, the experiment was performed twice. Results are presented as a percentage of the DNA-PK p53 Ser15 peptide positive control. (The bar height represents the mean of the two readings taken, as shown in Table 4.3).

Sample	[γ^{32}P] Incorporation Expt 3/Expt 4	% of DNA-PK /p53 Ser Incorporation Expt 3/Expt 4	Mean % [γ^{32}P] Incorporation
DNA-PK/p53 Ser	190,393/224,464	100/100	100
DNA-PK /p53 Thr	16,119/-	8.466/-	8.466
DNA-PK /p53 Ala	3,266/-	1.715/-	1.715
2782a/p53 Ser IP:CN-12	2,396/7,241	1.258/3.226	2.242
2782a/p53 Thr IP:CN-12	1,355/-	0.712/-	0.712
2782a/p53 Ala IP:CN-12	1,874/1,468	0.984/0.654	0.819
4724/p53 Ser IP:CN-12	2,070/2,430	1.087/1.083	1.085
4724/p53 Thr IP:CN-12	3,253/-	1.709/-	1.709
4724/p53 Ala IP:CN-12	2,507/1,680	1.317/0.748	1.033
Hela/p53 Ser* IP:CN-12	11,175/1,547	5.869/0.689	3.279
Hela/p53 Thr* IP:CN-12	7,634/-	4.010/-	4.010
Hela/p53 Ala* IP:CN-12	10,312/822	5.416/0.366	2.891

Table 4.3

p53 peptide [γ^{32}P] incorporation in the ATM/p53 peptide kinase assay using CN-12 immunoprecipitates from ~5x10^6 ataxia telangiectasia lymphoblastoid cells (GM2782a), ~5x10^6 GM4724 (wt) lymphoblastoid cells and * 50x10^6 HeLa cells per sample.

only 4.01% (HeLa p53 Thr18), that of the positive control*. The greatest measurement in GM2782a and GM4724 combined was for p53 Ser15 [γ^{32}P] incorporation in GM2782a of 2.242%, indicating background or non-ATM related [γ^{32}P] incorporation levels. Levels of [γ^{32}P] incorporation in all peptides with HeLa precipitated ATM were greater than that seen for both p53 Ser15 [γ^{32}P] incorporation in GM2782a and the DNA-PK p53Ala15/Ala18 negative control. This observation was abolished on correcting for the effect of cell number (*the HeLa immunoprecipitates were made from ten times as many cells) and after considering the mean for DNA-PK negative control in experiments 1 and 3 (4.233%). In addition values of [γ^{32}P] incorporation in HeLa cells show small inter-experimental variations: If the % [γ^{32}P] incorporation in the p53 Ser15 peptide is averaged across experiments 1-4 (ie mean = 2.315%) it can be seen that this value is very close to the internal AT cell line (2782a) p53 Ser15 peptide negative control from experiments 3 and 4 (mean = 2.242%) even without correcting for the increased cell number used in the HeLa cell immunoprecipitates. This is evidence that [γ^{32}P] incorporation levels for all peptides in the cell lines examined can be accounted for by non-specific background rather than ATM-related effects.

4.3.5 Immunoprecipitated ATM from HeLa and GM4724 cell nuclear extracts does not phosphorylate PHAS-I

The affinity purified antibody CN-12 immunoprecipitates ATM from HeLa cells (Fig. 4.10, lanes 2 and 4), and GM4724 lymphoblastoid cells (Fig. 4.11, lane

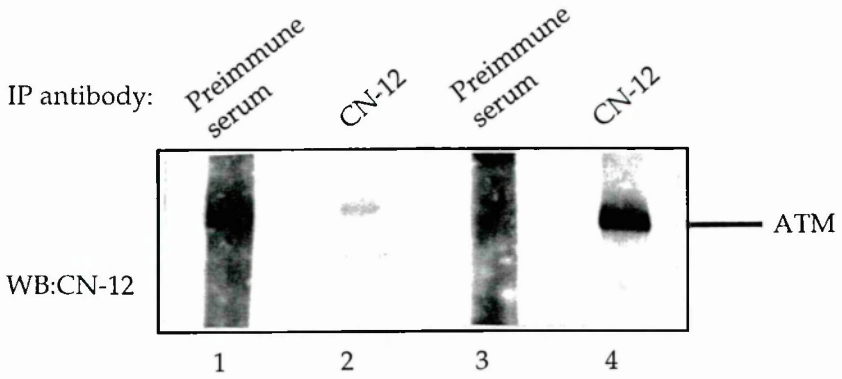

Fig. 4.10

ATM protein can be immunoprecipitated from HeLa cells. Immunoprecipitation of ATM from HeLa cell nuclear extracts containing 2) 25 million cells per sample and 4) 5 million cells per sample, was performed using affinity purified CN-12. Immunoprecipitation using pre-immune serum from rabbit CN-12 was also performed in samples 1) and 3) respectively as negative controls. The total immunoprecipitated nuclear extract (30 µl), for each sample was loaded on a 7.5% acrylamide gel and subjected to SDS-PAGE. Subsequent Western blotting was performed with CN-12 antibody (1 µg/ml). These samples were prepared in parallel with the paired kinase samples (Fig. 4.12).

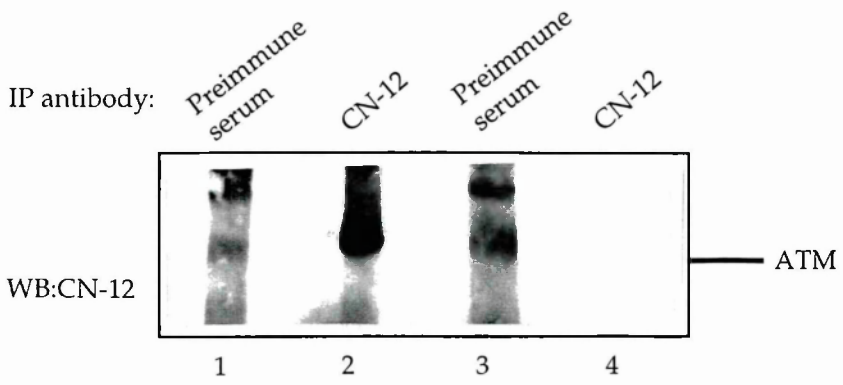

Fig. 4.11

ATM protein can be immunoprecipitated from lymphoblastoid cell line GM4724 (ATM +/+) but not from the A-T lymphoblastoid cell line GM2782a (ATM-/-). Attempted immunoprecipitation of ATM from 2) GM4724 and 4) GM2782a cell nuclear extracts was performed using affinity purified CN-12. Immunoprecipitation using pre-immune serum was also performed in 1) GM4724 and 3) GM2782a cell lines for negative controls. 30 µl of extract (equivalent to 5 million cells per sample) was loaded in each lane of a 7.5% acrylamide gel and subjected to SDS-PAGE. Subsequent Western blotting was performed with CN-12 antibody (1 µg/ml). These samples were prepared at the same time as the paired kinase samples (Fig. 4.13).

2) but not from the A-T lymphoblastoid cell line GM2782a (Fig. 4.11, lane 4). Preimmune serum immunoprecipitates an indistinct band from HeLa cells, GM4724 and GM2782a cells which is of a slightly lower molecular weight than ATM (Fig. 4.10 and 4.11). (NB less ATM is immunoprecipitated from 25 million HeLa cells in comparison with 5 million HeLa cells Fig. 4.10 lane 2 versus lane 4. This may be due to inefficient cell lysis when 5 fold more cells are used). Paired samples for each of the above immunoprecipitates were subjected to the ATM/PHAS-I kinase assay, to investigate if immunoprecipitated ATM is a protein kinase capable of phosphorylating PHAS-I. Immunoprecipitates from the A-T cell line and immunoprecipitates using preimmune serum served as negative controls. Phosphorylation of PHAS-I by an external source of DNA-PK served as a positive control. PHAS-I [γ ^{32}P] incorporation for each sample was determined by Western analysis and autoradiography of the transferred proteins (Figs. 4.12 and 4.13). A three day exposure was used to detect PHAS-I phosphorylation potentially caused by ATM and a 30 min exposure was used to detect PHAS-I phosphorylation caused by added DNA-PK. Weak phosphorylation of a band equivalent to the lower band of purified PHAS-I (Fig. 4.4), was seen with HeLa cell, GM4724 and GM2782a immunoprecipitates (Fig.4.12 and 4.13). As GM2782a is an AT cell line, any phosphorylation of PHAS-I detected with GM2782a immunoprecipitates cannot be due to ATM. The likelihood of such phosphorylation being due to non-specific effects is increased by the fact that the PHAS-I phosphorylation seen was greater in GM4724 and HeLa (25 million cell derived sample) with non-affinity purified preimmune serum (Fig. 4.13, lane 4 and Fig. 4.12 lane 5). Non-affinity purified preimmune serum was known to contain more non-specific antibodies (data

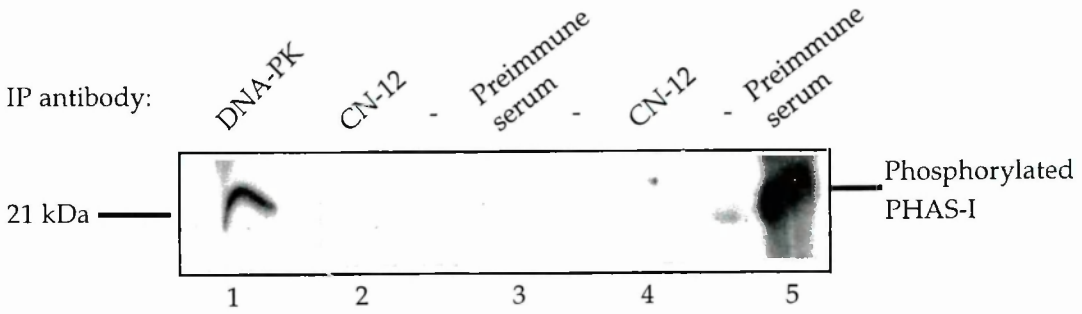

Fig. 4.12

Phosphorylation of PHAS-I in immunoprecipitates from HeLa cell nuclear extracts. ATM was immunoprecipitated from 2) a HeLa cell nuclear extract (equivalent to 5 million cells) and 4) a HeLa cell nuclear extract (equivalent to 25 million cells) using the affinity purified antibody CN-12. Pre-immune serum was used as the immunoprecipitating antibody as a negative control for 2) and 4) in 3) and 5) respectively. The ATM/PHAS-I kinase assay was then performed on the extracts as described previously. The total nuclear extract of 30 µl from each kinase reaction was then loaded onto a 13% acrylamide gel. 1) Phosphorylation of purified PHAS-I protein by DNA-PK was used as a positive control. Subsequent radiographic exposure of the gel for 3 days revealed the phosphorylated protein bands in each extract. The DNA-PK/PHAS-I positive control band was excised from the dried gel and exposed for 30 minutes only.

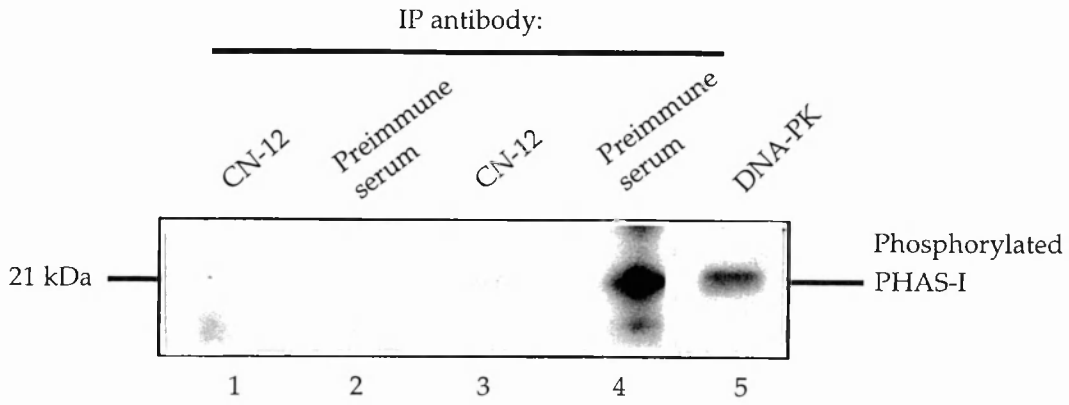

Fig. 4.13

Phosphorylation of PHAS-I in ATM immunoprecipitates from a lymphoblastoid cell line GM4724 (ATM+/+) and an A-T lymphoblastoid cell line GM2782a (ATM-/-). ATM was immunoprecipitated from 1) GM2782a and 3) GM4724 nuclear extracts using affinity purified antibody CN-12. Pre-immune serum from rabbit CN-12 was used as the immunoprecipitating antibody as a negative control in 2) GM2782a , and 4) GM4724 respectively. The ATM/PHAS-I kinase assay was then performed on the extracts as described previously. 30 µl of nuclear extract (equivalent to 5 million cells) from each kinase reaction was then loaded onto a 13% acrylamide gel. 5) Phosphorylation of purified PHAS-I protein by DNA-dependent protein kinase was used as a positive control. Subsequent radiographic exposure of the gel for three days revealed the phosphorylated protein bands in each extract. The DNA-PK/PHAS-I positive control band was excised from the dried gel and exposed for 30 minutes only.

not shown) perhaps capable of immunoprecipitating proteins which might phosphorylate PHAS-I. In addition although more ATM protein was immunoprecipitated from 5 million than from 25 million HeLa cells, no corresponding difference in the level of PHAS-I phosphorylation was seen between these two samples (Fig. 4.12 lane 2 versus lane 4) which also suggested that the weak phosphorylation of PHAS-I seen was ATM-independent.

4.4 Discussion

Several assays using different substrates and a variety of modifications have been employed to investigate whether ATM has a protein kinase function. Preliminary 'autophosphorylation assay' results showed phosphorylation of a protein of similar size to ATM, together with proteins of 160 and 140 kDa. It was tempting to speculate that the observed 350 kDa phosphoprotein represented autophosphorylated ATM and the 160 and 140 kDa proteins were co-immunoprecipitated, phosphorylated substrates of ATM. However, this could not be stated with certainty for two reasons. Firstly a further study of the phosphoproteins was not possible because additional attempts at the assay proved unsuccessful. Secondly, the possibility of non-specifically co-purifying proteins in the immunoprecipitates was raised by the presence of much weaker bands of similar size (~350, 160, 140 kDa) with the negative (no immunoprecipitating antibody) control, potentially due to non-specific protein carry over on the protein-A-Sepharose beads. Pure, active ATM obtained by biochemical fractionation is extremely difficult to prepare and even with this source of ATM, the possibility of co-purifying proteins

perhaps including kinases has to be considered (S. Jackson, personal communication). Related problems may also apply to the use of immunoprecipitation to provide an ATM source as anti-ATM antibodies may also precipitate other known or unknown homologous proteins.

The lack of demonstrable ATM-dependent phosphorylation of p53 peptides and PHAS-I seen in the other assays may be explained in several ways: It is possible that ATM does not function as a protein kinase, at least under the conditions used, the substrates or the portion of the substrate chosen may have been inappropriate or perhaps unknown co-factors are required for ATM kinase function which were not included in these experiments. In the later assays, a source of restriction enzyme treated plasmid DNA was chosen to mimic radiation induced DNA damage instead of using cell irradiation to activate ATM, however this modification of the assay still did not result in detectable specific kinase activity.

The extent to which the observed levels of phosphorylation achieved were truly non-specific and not related to ATM function was investigated by including ataxia-telangiectasia cell immunoprecipitates as a negative control in the later experiments. These showed phosphorylation levels of a similar order to the non-AT cell lines tested which provided further evidence that the phosphorylation observed in the samples was not ATM-dependent.

The attempts to demonstrate an ATM protein kinase function described above were either negative or inconclusive. However, there has been considerable interest in this area recently and other groups investigating the putative protein kinase function of ATM have published positive results. His tagged full-length *ATM* cDNA has been cloned into a baculovirus vector and

the recombinant protein expressed (Scott et al., 1998). Despite a very low yield (nanogram quantities) of recombinant ATM, autophosphorylation activity was observed in baculovirus infected Sf9 insect cell lysates immunoprecipitated with an anti-His tag antibody. Interestingly more than one phosphorylated band was seen (as for the autophosphorylation assay described previously). This observation might indicate ATM-dependent phosphorylation of co-immunoprecipitated proteins or breakdown products of ATM itself. The smaller phosphorylated proteins are unlikely to be due to internal splice variants of ATM protein because although alternative splicing of upstream and downstream regions of *ATM* mRNA occurs, splicing affecting the coding region has not been described (Savitsky et al., 1997). Amongst other potential ATM targets which have been investigated, evidence for c-Abl as an ATM substrate has also been provided: a c-Abl interaction domain has recently been characterised between amino acids 1366-1466 of ATM using a yeast 2 hybrid system (Shafman et al., 1997). This may be functionally important as stimulation of the c-Abl tyrosine kinase activity has been found to occur after ionising radiation in ATM wild type cells but does not occur in cells from AT patients nor in cells from ATM knockout mice. Ectopic co-expression of a functional ATM kinase domain and c-Abl in abl null 3T3 cells activates the tyrosine kinase activity of c-Abl to a similar maginitude to that stimulated by ionising irradiation. This c-Abl activation did not occur with expression of a mutated ATM kinase domain nor if the co-expressed c-Abl was mutated (S465A). Therefore, ATM appears to phosphorylate c-Abl on Ser 465 *in vitro* and activate its tyrosine kinase activity (Baskaran et al., 1997).

ATM has also been reported to phosphorylate IκB-α (Jung et al., 1997), an inhibitor of the nuclear factor NF-κB transcritional activator. It is possible that aberrant regulation of IκB-α and NF-κB contribute to the A-T cellular phenotype because a cDNA encoding a truncated form of IκB-α has been shown to correct the radiosensitivity and radioresistant DNA synthesis defect post irradiation in SV40 immortalised ataxia telangiectasia fibroblasts (Jung et al., 1995).

Interest has always focused on p53 as a possible direct downstream target of ATM, hence the attempted development of ATM/p53 peptide kinase assays, but recent investigations have suggested that the ATM-p53 interaction may be more indirect. These studies have shown that ionising radiation causes dephosphorylation of p53 on Ser 376 which allows binding of 14-3-3 proteins to p53 to enhance its sequence-specific DNA binding. Interestingly, Ser 376 dephosphorylation and 14-3-3 binding of p53 do not occur in A-T cells which exhibit delayed and reduced p53 responses (Waterman et al., 1998). It was therefore proposed that ATM might be responsible for the activation of a phosphatase to dephosphorylate p53 on residue Ser 376 to transduce the radiation response, although the target phosphatase is not known. If this hypothesis is true it would provide an explanation for the lack of phosphorylation seen in the p53 peptide assays described above and direct attention towards other regions of p53 and the development of ATM kinase assays incorporating preparations of ATM with additional enzymes or co-factors.

The use of p53 peptides in these experiments, rather than full length recombinant or immunoprecipitated p53 may also have created problems if carboxyterminal regions of p53 are important in p53/ATM interactions required for ATM kinase activity. Therefore in theory, these assays could be improved upon by the use of a full length substrate. Since the submission of this thesis however there have been two reports of DNA damage dependent phosphorylation of short p53 peptides on p53 Ser15 (p53 residues 1-47, and p53 residues 1-24) and PHAS-I by ATM (Banin et al., 1998), (Canman et al., 1998). ATM activation in these studies was due to DNA damage caused by neocarzinostatin or 5 Gy of ionising irradiation. It is of considerable importance that in contrast to DNA-PK, the protein kinase activity of ATM was dependent on the presence of 4-10mM of Mn^{2+} ions and it was also noted that an external source of DNA double strand breaks was ineffective in the activation of ATM (Canman et al., 1998). The lack of Mn^{2+} ions and the use of restriction enzyme cut plasmid to provide an activating source of DNA dsbs in the current study provide sub-optimal conditions for ATM activation and may largely explain the negative results obtained.

My original intentions were to develop and use an ATM kinase assay for estimation of the functional integrity of ATM in women with breast cancer. Due to problems with the development of such an assay I decided to perform a study of the DNA repair capacity in the peripheral blood lymphocytes I had collected from these patients. This study is described in Chapter 6.

Chapter 5

Construction of a Potentially Dominant Negative Mutant of the ATM Kinase Domain

5.1 Introduction

The *S. cerevisiae VPS34* (vacuolar protein sorting) gene is related by sequence to the human ATM gene and has PI 3-kinase activity (Stack et al., 1995) (Fig. 5.1). When active, the serine/threonine protein kinase Vps15 recruits Vps34 to the membranes of yeast golgi apparatus and stimulates Vps34 PI 3-kinase activity. This then activates the sorting of proteins eg. carboxypeptidase Y, to the yeast vacuole. Mutant *vps34* alleles which differ from the wild type sequence in certain critical regions of the conserved kinase motif, if over-expressed in a wild type strain display a dominant negative phenotype with a reduction in PI 3-kinase activity and missorting of soluble vacuolar proteins. This effect appears to be due to the mutant Vps34 titrating active Vps15 away from wild type Vps34 protein as over-expression of the wild type *VPS34* allele suppresses the dominant negative phenotype. One such *vps34* mutant allele creates the protein coding change D749E in the kinase motif (Schu et al., 1993). Therefore it was reasoned that by creating an identical mutation in the conserved kinase motif of human *ATM* (D2889E) and overexpressing this in a human cell line it might be possible to abolish any kinase activity of wild type ATM protein in a dominant negative fashion. The role of ATM kinase activity might then be elucidated by studying aspects of the resulting cellular phenotype. Of particular interest was the putative role of ATM kinase activity in the response to DNA damage and cell survival post γ irradiation.

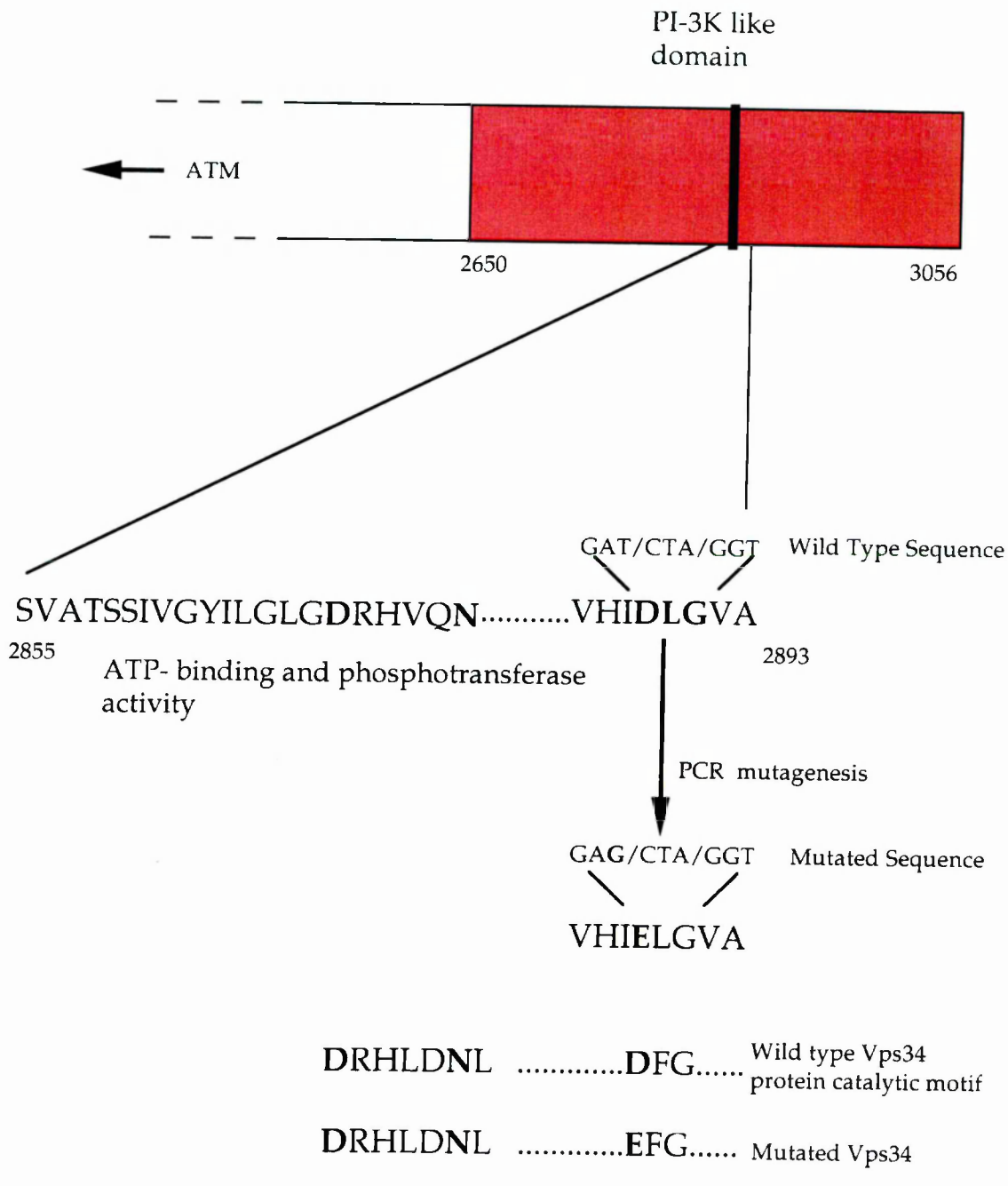

Fig. 5.1

Schematic diagram showing the construction of the ATM kinase domain T8667G mutation by PCR mutagenesis. The wild type and mutated Vps34 catalytic motif is shown below for comparison.

5.2 Additional materials and methods

5.2.1 Cloning of a putative ATM dominant negative kinase domain by PCR-site directed mutagenesis

The purified AT7-9 fragment released from the phage DNA by Sal1 digestion (Chapter 2, Fig. 2.1), was amplified and mutated using a modified polymerase chain reaction that relies on a first round PCR amplification of two fragments, one 5' and one 3' which overlap in the region where the mutation is to be generated. (The internal primers of these reactions were designed to include the required mutation).

The two fragments from the first round were then used as the template for the second round PCR which is a simple amplification reaction using the external primers. 8081s was designed to include a Sal1 site (GTCGAC) and a Haemagglutinin (HA) tag sequence (YPYDVPDYA). (Homology with the ATM sequence begins at the *. 9171r includes the ATM stop codon (TCA) ie 5'TGA and a Not1 site (GCGGCCGC). Base changes creating the mutation at bp 8667 are denoted in bold.

5' ->3' Primer 8081s (external):

G/AGA/GTC/GAC/ACC/ATG/TAC/CCC/TAC/GAC/GTG/CCC/GAC/TAC/GCA*/GGA/GGT/GTA/AAT/TTA/CC

5'->3' Primer 8651s (internal):

GAA/CTT/GTA/CAT/ATA/GA**G**/CTA/GGT/GTT/GCT

3'->5' Primer 8679r (internal):

AGC/AAC/ACC/TAG/CTC/TAT/ATG/TAC/AAG/TTC

3'->5' Primer 9171r (external):

AGA/GGC/GGC/CGC/*TCA/CAC/CCA/AGC/TTT/CCA/TCC/TGG

First Round PCR

For each reaction, 1µg of the purified AT7-9 SalI fragment was used as a template, 2.5 µl of each 40 µM primer (For reaction 1 primers 8081s and 8679r were used and for reaction 2, primers 8651s and 9170r were used), 0.5 µl of Pwo DNA polymerase (Boehringer Mannheim), 10 µl of 10X Pwo buffer with Mg^{2+} and 10 µl of 2.5 mM dNTPs were used with dH_2O to a final volume of 100 µl. A drop of mineral oil was then placed on top of the mixture to prevent evaporation. PCR was performed in an Omnigene PCR machine (Hybaid), for 15 cycles of the following: Denaturation at 95°C for 30s, Annealing at 55°C for 45s and extension at 72°C for 1min. The entire reaction mixture was then extracted with an equal volume of phenol isoamylalcohol/CCl_4 (24:1:24). The aqueous phase was taken off and precipitated with a 0.1X volume of 3 M Na acetate pH 5.2 and 2.2X volume of 100% ethanol. The mixture was vortexed and incubated on ice for 10 min centrifuged (14,000 rpm, 10 min), followed by a wash in 70% ethanol. The pellet was then resuspended in 10 µl of dH_2O. The DNA from each reaction was then subjected to 0.7% agarose gel electrophoresis and bands of the appropriate size were visualised under a low intensity UV light and excised. Both gel slices were then allowed to freeze on a glass plate over dry ice before being placed in a single spin column (made from a 1ml blue pipette tip with the upper end cut off, placed in a 1.5 ml tube) and

being spun in a microcentrifuge (Eppendorf) at 6000rpm for 45 s. Prolonged spinning should be avoided as the agarose can inhibit subsequent reactions. ~ 15 µl of combined DNA from PCRs 1 and 2 was obtained off the column. This was used as the template for the second round PCR.

Second Round PCR

The entire combined DNA from reactions 1 and 2 was used as the template for this reaction together with 0.5 µl of Pwo DNA polymerase, 2.5 µl of the 40 µM external primers 8081s and 9170r, Pwo buffer with Mg^{2+} and 10 µl of 2.5 mM dNTPs were used with dH_2O to a final volume of 100 µl. After covering the reaction mixture with a drop of oil, the PCR was performed for 15 cycles of the following: Denaturation at 95°C for 30s, Annealing at 37°C for 45s and extension at 72°C for 1min. 5 µl of the reaction product was then subjected to 0.7% agarose gel electrophoresis to check that a band of the appropriate size was produced. 15 µg of the mutated fragment was then digested with the restriction enymes Sal1 and Not1 and the digest was then extracted with an equal volume of phenol isoamylalcohol/CCl_4. The aqueous phase was taken off and precipitated with a 0.1X volume of 3 M Na acetate pH 5.2 and 2.2X volume of 100% ethanol. The mixture was vortexed and incubated on ice for 10 min followed by a wash in 70% ethanol. The pellet was then resuspended in 10 µl of dH_2O to concentrate it. Meanwhile the expression vector pCD2-CMV (O'Connell et al., 1994), was also digested with Sal1 and Not1 and 1 µg of the cut vector and 2 µg of the $AT_{8081\text{-}9170}$ fragment were ligated at 16 °C overnight using 0.5 µl T4 DNA ligase and 0.5 µl ligase buffer in a final reaction volume of 4 µl. Vector only and alternative insert controls were

also included as well as a control with neither vector nor insert. 0.7 µl of each reaction product was then used to transform *E.coli* DH10β by electroporation as decribed previously. Transformed bacteria were then plated on LB/AMP plates and incubated overnight at 37°C. No colonies were seen on the negative control plate, 1 was seen on the vector only control plate and 400 colonies were seen on both insert plates. Colonies were picked from the $AT_{8081-9170}$ insert plate from which bacterial minicultures and then plasmid minipreps were made. Restriction digests with Sal1 and Not1 and 0.7% agarose gel electrophoresis confirmed the presence of the vector with the 1.1 kb insert in the 10 minicultures tested. Large scale preparation of plasmid DNA was then performed and the resultant plasmid DNA was sequenced using the external primers 8081s, 9170r and several other primers including:

8804r(5019r):

CCTGAGAGTTTCTCATCACTTCC

8286s(4501s):

GCGAAGTGGTGTTCTTGAATGGT

CMV T7 lead in primer: AATACGACTCACTATAG

Sequencing was performed and analysed as described previously.

The wild type AT7-9 clone DNA from the phage had been previously sequenced by myself during earlier cloning attempts and deviated from the published sequence (Savitsky et al., 1995), by two base changes: G9093A which was a silent change (Glut->Glut), and G9007A which resulted in Asp>Asn. Professor Yosef Shiloh agreed that the changes were present in the clone he

sent me but wondered if they were specific to that clone or if they were rare polymorphisms. Both of these sequence anomalies have, however been identified subsequently in normal and A-T individuals (personal communication from Dr Louise Izatt) and they may represent the true wild type sequence in this region.

5.2.2 Transient transfection and clonogenic assay of H1299 cells expressing a mutant ATM kinase domain

Transient transfection of human non-small cell lung carcinoma NCI-H1299 cells with a mammalian expression vector pCD2-CMV containing a mutated ATM kinase domain (pCD2-CMV-ATELG) or the empty vector pCD2-CMV), was achieved using the calcium phosphate method (Graham and Eb, 1973): The H1299 cells were cultured until they were in the log phase of growth and then seeded at 0.5-1 x 10^6 cell/9cm Falcon tissue culture plate (Becton Dickinson) 24 hours before transfection. They were then refed with medium 2 hours before adding the precipitate. The following solutions were then made up: 2X Hepes buffered saline (Hepes 10g/l, NaCl 16g/l pH to 7.10 ± 0.05 with NaOH and filter sterilised), 100XPO_4 (35 mM Na_2HPO_4, 35 mM NaH_2PO_4,) and 2M $CaCl_2$, filter sterilised. To make a precipitate of 1.1 ml/9 cm dish, 550 µl of 2XHBS was added to 11µl of 100XPO_4 in a falcon tube, while 20 µg of DNA (pCD2-CMV-ATELG, or pCD2-CMV) was diluted in dH_2O with 125 mM $CaCl_2$ to a total volume of 539 µl in a separate tube. The DNA/$CaCl_2$ was then mixed in dropwise to the HBS/PO_4, while air was bubbled through the latter using a pipettor and a pasteur pipette. The precipitate was then allowed to

stand for 30 min at room temperature and finally mixed with a vortex before 1 ml of the precipitate was added dropwise over the surface of each 9cm dish. The cells were returned to the incubator for 16 hours after which they were washed once with PBS, 2.5 mM EDTA to chelate excess calcium and refed with medium. (Transient expression of the mutated kinase domain should peak 48 hours later). Anti-CD2 bearing magnetic beads (Dynal M.450) were then used to harvest transfected cells which were then transferred to separate 15 cm Falcon tissue culture plate (Becton Dickinson) and were re-fed before being incubated at 37°C for 48 hours prior to harvesting in PBSA/2 mM EDTA and resuspending cells from each 10 cm plate in 100µl of 2X SDS protein sample buffer. 40µl of each H1299 transfectant lysate was then subjected to SDS-PAGE on a 12% gel. After protein transfer as described previously, haemagglutinin-epitope bearing proteins were detected by Western blot analysis using anti-HA tag antibody. The expected size of the HA-tagged mutated ATM kinase domain was ~40 kD.

For clonogenic study H1299 cells transiently transfected with empty vector or pCD2-CMV-ATELG were harvested as described above, resuspended in culture medium in 15 ml tubes (Falcon) and irradiated at a rate of 0.3 Gy/min to a total of 0.5 Gy, 1 Gy, 2 Gy, 3 Gy, 4 Gy and 6 Gy. Cells from each timepoint were subsequently plated in triplicate on 9 cm tissue culture plates in DMEM medium with 10% FCS and left undisturbed for 10 days prior to fixation in 2:1 methanol : acetic acid and cell staining for 30 min with Crystal Violet (1 mg/ml in H_2O) followed by colony counting (n.b a colony was defined as a group of 50 or more cells). Numbers of colonies were adjusted

according to the plating ratio of unirradiated empty vector: pCD2-CMV-ATELG transfectants.

5.3 Results

5.3.1 Creation of the T8667G mutation in the *ATM* kinase domain

Automated sequencing of both the wild type AT7-9 clone and the *ATM* kinase domain (after PCR site directed mutagenesis), was performed (Fig. 5.2). This confirmed the presence of the desired mutation (T8667G) in the mutant *ATM* fragment and showed an intact lead-in sequence from the CMV promoter. Comparison of both of the above with the published sequence also revealed the presence of the two other base changes G9007A and G9093A which probably represent the true wild type sequence as previously described. No other mutations were detected.

5.3.2 Expression of the mutant *ATM* kinase domain in H1299 pCD2-CMV-ELG transfectants

Western blotting of H1299 cell pCD2-CMV-ATELG transfectants and subsequent detection using an anti-HA tag antibody confirmed the presence of an HA-tagged protein of ~40 kDa (the expected size of the mutant kinase domain). This protein was not detected in H1299 cell lysates transfected with the empty pCD2-CMV vector alone (Fig. 5.3). Multiple other heavier proteins were detected in both samples and probably represent anti-CD2 antibody chains non-specifically detected by the secondary antibody layer. HA-tagged

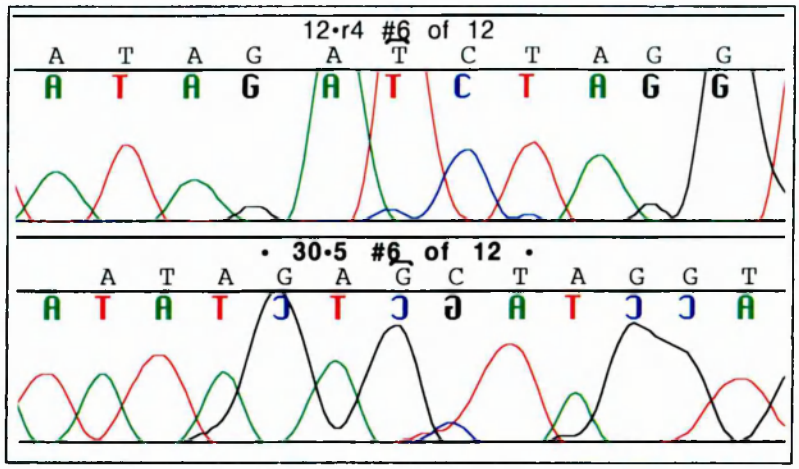

Fig. 5.2

Chromatograms to demonstrate the wild type sequence of the ATM gene (upper panel) and the T8667G mutation generated by PCR mutagenesis (lower panel). The lack of alignment of the chromatograms is due to base spacing differences as these samples were sequenced on different gels.

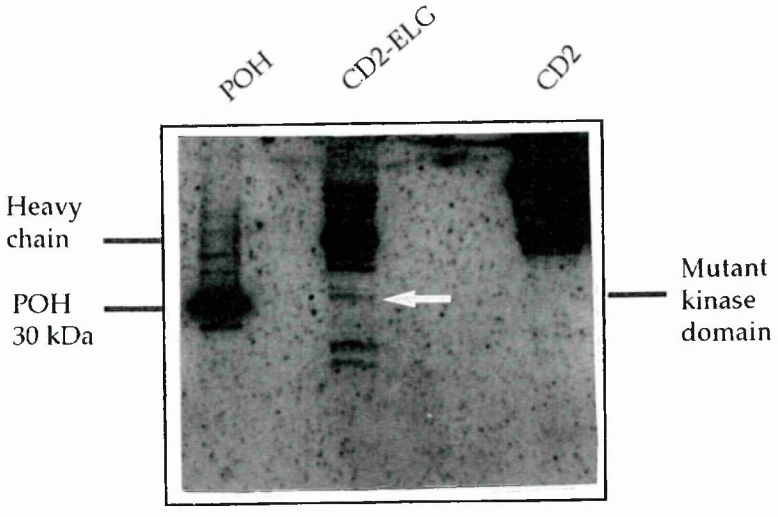

Fig. 5.3

H1299 cells transfected with pCD2-CMV-ATELG express the mutant ATM kinase domain. 40 µl (equivalent to 120,000 cells) of H1299 cells transfected with the empty vector pCD2-CMV (CD2), or vector with the mutant ATM kinase domain (CD2-ELG), were subjected to SDS-PAGE. The HA-tagged mutant ATM kinase domain was detected by Western blot analysis using anti-HA antibody. HA-tagged POH was used as a positive control.

POH protein was provided as a positive control for the anti HA-tag antibody and the proteins of larger molecular weight described above were not identified in this sample.

5.3.3 Effect of the mutant *ATM* kinase domain on H1299 pCD2-CMV-ELG clonogenic survival

An assay of clonogenic cell survival was performed in triplicate on H1299 cells transfected with pCD2-CMV-ATELG or the empty vector for a range of different doses of γ radiation (0, 0.5, 1, 2, 3, 4 and 6 Gy). There was no difference between these two cell populations except at the 4 Gy dose point where the mutant ATM kinase domain transfectants showed a reduced clonogenic cell survival (26.18% vs 46.11% for the empty vector transfectants). This difference was not maintained at the 6 Gy dose point (Fig. 5.4).

5.4 Discussion

The mutant ATM kinase domain which was apparently expressed in H1299 transfectants did not cause an A-T cell phenotype in terms of cellular radiosensitivity (measured here by clonogenic survival after IR) which would have been expected if the mutant domain impeded the activity of the wild type protein in a dominant negative manner. Several explanations may account for the observations made. Firstly, there is the unlikely possibility that the 40 kDa protein identified in the pCD2-CMV-ATELG transfectants by Western blotting may have represented a protein other than the recombinant ATM kinase domain. As no anti-ATM kinase domain antibodies were available for use at

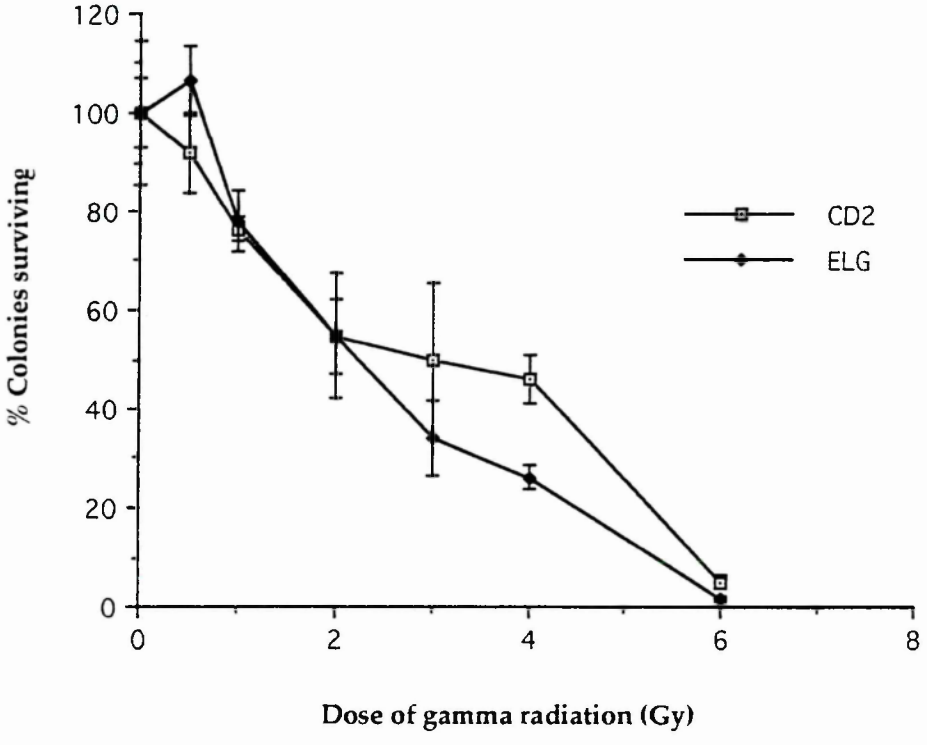

Fig. 5.4

Graph to illustrate the relative clonogenic survival of H1299 cells transfected with the empty vector pCD2-CMV (CD2) and vector containing the mutated ATM kinase domain pCD2-CMV-ATMELG (ELG), with increasing dose of γ radiation. (The experiment was performed in triplicate and the sample means are presented).

the time of this study, the identity of the presumed recombinant protein could not be verified. This was of importance because ~15 bp at the extreme 3' end of the mutant construct was not sequenced and the presence of the native stop codon was not confirmed. Secondly, the small mutant kinase domain expressed may have lacked the relevant protein-protein interaction sites required to inhibit the wild type protein in a dominant negative fashion. This possibility was entertained prior to conduction of this work but attempts at cloning larger fragments of the AT7-9 clone 5' to the mutant kinase domain were unsuccessful due to difficulties with the secondary stage PCR reactions (data not included).

The importance of upstream regions in ATM function is suggested by the fact that expression of ATM fragments containing the ATM leucine zipper motif enhanced the radiosensitivity and chromosomal breakage and abrogated the S-phase checkpoint after γ radiation in a human RKO colorectal carcinoma cell line (Morgan et al., 1997). Moreover, in 1996 a "kinase-dead" mutant of Rad3 (Rad3 D2249E) resulted in a phenotype with increased radiosensitivity (Bentley et al., 1996). Even more recently, a kinase inactivated mutant of the *ATR* (ataxia telangiectasia and rad3$^+$ related) gene has been described in which the equivalent conserved residue in the DFG motif in the kinase domain was altered by site directed mutagenesis such that the conserved D (aspartic acid) at residue number 2494 was substituted by an E (glutamic acid), as for the ATM kinase domain described in the current study and the Rad3 mutant described above. The expression of constructs containing this substituted ATR kinase domain in an SV40-transformed human fibroblast cell line resulted in

increased radiosensitivity and reduced colony forming ability consistent with a dominant negative effect of the kinase-inactive form. In support of this hypothesis, expressed mutant kinase domain constructs were found to form part of a larger protein complex when analysed by gel filtration, consistent with their presumed ability to titrate other important proteins from active ATR kinase species (Wright et al., 1998).

The H1299 cell transfectants in the current study were p53 null and to investigate whether this explained their lack of increased radiosensitivity after IR, Dr Weg Ongkeko, a PhD student in the laboratory performed some additional work using the mutated ATM kinase domain. Dr Ongkeko stably transformed the plasmid pCD2-CMV-ATELG, into H1299 cells bearing a temperature sensitive p53 allele. Two resulting clones AT6 and AT11 and two empty vector pCD2-CMV controls were treated with 0, 1, 2, 4, or 7 Gy of γ irradiation and each treatment group was replated in triplicate and incubated at 32°C (p53 active) or 37°C (p53 inactive) for 48 hours. The plates were then allowed to incubate at 37°C for 10 days prior to colony staining and counting. No differences in clonogenic survival were observed between any of the cell lines tested (data not shown), although all the clones were CD2 positive by flow cytometry.

As discussed, the small size and lack of extensive upstream regions of the protein kinase domain used for these studies may have prevented interactions necessary for the dominant negative effect however the technique could also have been improved upon by performing assays of expression of the recombinant kinase domain over the timecourse of the experiment. Short

term assays eg the comet assay could also have been used to estimate the amount of DNA damage due to apoptosis and inadequate DNA repair at different timepoints in the experiment rather than just using the final clonogenic survival post irradiation, which is remote from the transient expression period, as an index of ATM function.

For these reasons and because increased radiosensitivity which is a hallmark of absent ATM kinase activity was not observed in the transfectants investigated in the current study, this project was not developed any further.

Chapter 6

Investigation of the Constitutional DNA Repair Capacity of Patients with Breast Cancer using the Alkaline Comet Assay

6.1 Introduction

The following investigation into the constitutional DNA repair capacity of lymphocytes from women with breast cancer using the comet assay was embarked upon because of an interest in genome instability in the aetiology of the disease. This was stimulated by reports of the association of *ATM* heterozygosity and breast cancer (Swift et al., 1976), (Swift et al., 1987), (Pippard et al., 1988), (Borresen et al., 1990), (Swift et al., 1991), as discussed in Chapter 1 and secondly by the finding of elevated chromosomal radiosensitivity in lymphocytes from breast cancer patients compared with normals (Scott et al., 1994). An introduction to the comet assay together with the reasons for its suitability for this study is given below. A detailed review of breast cancer, genome instability and DNA repair is provided in Chapter 1.

6.1.1 The comet assay

The single cell gel electrophoresis SCGE assay otherwise known as the comet assay was developed in 1986 (Singh and Stephens, 1986), (Singh et al., 1988), based on an assay to detect DNA damage which had been designed previously (Ostling and Johanson, 1984), (Rydberg and Johanson, 1978). It has been of considerable value in investigating cellular responses to DNA damage, in animal and *in vitro* studies of genotoxicity and more recently in human toxicity biomonitoring (Collins et al., 1997). Many variations of the comet assay now exist and have recently been reviewed (Fairburn et al., 1995). When performed under alkaline conditions, the assay is an extremely sensitive indicator of DNA damage due to single strand breaks (a major component of

DNA damage due to γ rays), and alkali-labile sites. About 50 single-strand breaks per cell (equivalent to 0.05 Gy), can be resolved using the method described below. DNA double strand breaks can also be also detected under these conditions (Collins et al., 1997).

The technique relies on a suspension of single cells (with damaged or undamaged DNA), being embedded in agarose and then lysed under alkaline conditions using high salt to extract the proteins. Cell lysis with detergent causes the nucleus of the cell to be converted into a non-membrane bound, 'nucleoid' (comet head), containing non-nucleosomal supercoiled DNA. Under alkaline conditions, which assist the detection of DNA single strand breaks, the supercoiled DNA within the nucleoid is relaxed and denatured into negatively charged broken single strands which then migrate toward the anode during electrophoresis to form the comet tail. The alkali also converts alkali-labile sites, such as apurinic/apyrimidinic (AP) sites created when bases are lost, into DNA breaks (weakly alkaline conditions are less able to do this than is strong alkali). The high salt enhances the rate of strand separation which allows extended comet tails to form. To estimate the number of DNA double strand breaks formed post DNA damage, the electrophoresis can be performed under neutral conditions. Under these conditions DNA loops are formed and extend out from the nucleoid to create more solid, elongated comets (McKelvey-Martin et al., 1993). Both the neutral and alkaline comet assays detect DNA single strand breaks (Ostling and Johanson, 1984), (Singh et al., 1988), although this is often overlooked in the literature as described by (McKelvey-Martin et al., 1993). After the electrophoresis stage of the assay, a

fluorescent dye such as propidium iodide which binds to DNA is used to reveal the comets when viewed with a flourescence microscope.

The relative intensity of fluorescence in the comet tail is dependent on the frequency of DNA breaks. This can be measured using a variety of comet parameters eg comet tail length, % comet tail DNA, and the tail moment. The tail moment is most often quoted and is the product of the amount of DNA in the tail and the mean distance of DNA migration in the tail. Because the comets from a population of single cells can be observed, this method is able to detect whether all cells within a population are able to tolerate or process DNA damage equally or whether particularly sensitive sub-populations exist.

Apart from genotoxicity testing, the assay can also be used to measure DNA repair. In this case the cells are allowed varying amounts of time to recover from DNA damage prior to performing the comet assay. The kinetics with which cells perform DNA repair can then be measured (Singh, 1996), (Collins et al., 1997). This is a major advance because until the advent of the comet assay no tests were suitable or sensitive enough to monitor DNA repair differences between individuals. Now the constitutional (although perhaps lymphocyte specific), ability to repair various lesions (eg single or double strand breaks) can be determined by performing the comet assay on peripheral blood lymphocytes from the individual in question. Differences in human DNA repair processes have been implicated as a predisposing factor in the development of malignancy and several papers examining DNA repair and the occurrence of particular human cancers including lung cancer (Wei and Spitz, 1997), and breast cancer (Jaloszynski et al., 1997), have recently been published.

Despite the popularity and obvious applications of the comet assay, few studies have concentrated on the reliability and validity of results obtained. Those studies which have been performed (Collins et al., 1997), (Visvardis et al., 1997), suggest that whilst there is considerable inter-individual variability in DNA damage responses, samples taken from the same individual prepared on different slides or at different times after cryopreservation do not differ statistically in the assay results. However initial DNA damage can vary on an intra-individual basis and this can be seen when the same individuals donate cells on two different occasions for testing (Collins et al., 1997). This may represent real physiological variations with time related for example to changes in the amount of oxidative stress, genotoxic burden or dietary antioxidant profiles. Environmental genotoxins (eg tobacco smoke) may produce DNA damage, probably due to the effect of tar derivatives and such factors should be considered in study design (Piperakis et al., 1998), (Collins et al., 1997). Allowing for such caveats, the comet assay now offers a valuable opportunity to investigate the phenomenon of genome instability caused by faulty DNA repair processes.

Genomic instability in peripheral blood lymphocytes of women with breast cancer has been investigated previously (Scott et al., 1994), (Parshad et al., 1996) and was described in Chapter 1. In these studies chromatid breaks were used as a measurement of genomic instability as unrepaired DNA strand breaks are processed to chromatid breaks which can be detected at the susequent metaphase (Natarajan et al., 1980). Other end-points such as aberrations in metaphase chromosomes and micronucleus formation have also been used as indicators of genome instability. Apart from the fact that the

analysis of such endpoints required skilled observers and was extremely time-consuming, the endpoints themselves are indirect and somewhat removed from the damaging and reparative processes. The comet assay is relatively easy to perform and analyse and the endpoint reflects the level of DNA damage itself which is more closely related to causative factors. It can also be modified to investigate particular types of DNA lesions (Collins et al., 1997).

Investigation of the DNA repair capacity of peripheral blood lymphocytes from breast cancer patients and healthy controls may help to further elucidate the role which DNA repair defects play in predisposition to the disease. If a clear association with defective repair is found, the comet assay might provide a means of selecting women for more intensive breast cancer screening.

6.2 Additional materials and methods

6.2.1 Collection of blood samples

10ml blood samples were collected in EDTA tubes by Margaret Dean, phlebotomist for the local breast surgery unit, from patients with breast cancer who had given prior informed and signed consent after discussion with the Breast Care Sisters, Sarah Babb and Andrea Gamble. Treatment response data, family histories and information on smoking were collected from the clinical notes and the Breast Cancer Database at the Churchill and John Radcliffe Hospitals, Oxford. Control samples of 10ml of blood were collected from

women volunteers working in the Institute of Molecular Medicine, who had no history of breast cancer in first degree relatives and who were non-smokers.

6.2.2 Separation of mononuclear cells from blood

Samples of peripheral lymphocytes were prepared within 4 hours of phlebotomy by first diluting the blood 1/3 with 2% RPMI medium prior to gently laying this over 10mls of Lymphoprep (Nycomed). Studies of the effects of storage conditions on human blood suggest that samples are suitable for use in the comet assay for up to four days after collection when stored at 4°C or at room temperature (Anderson et al., 1997). Samples were then centrifuged at 2000 rpm for 20 minutes (Beckman GPR centrifuge) to achieve density gradient separation of lymphocytes from the plasma and the erythrocytes. The leukocyte layer was then gently pipetted off and washed once by placing into 10 mls of 2% RPMI and recentrifuging at 1000rpm for 10 minutes. The supernatant was then discarded and the cell pellet was resuspended in 1ml of 10% DMSO in 2% RPMI in a cryotube. The samples were then taken to a temperature of -70°C at a rate of 1°C/minute and transferred to a liquid nitrogen storage facility as soon as possible. When required, cells were thawed quickly in a 37°C water bath and resuspended slowly in 10mls of 2% RPMI. Samples were then centrifuged at 1000 rpm for 10 minutes and the cell pellet was resuspended in 10mls of 2% RPMI supplemented with 3mM glutamine and 20% FCS. The cells were cultured overnight at 37°C in a humidified atmosphere of 5% CO_2 to allow recovery from freeze-thaw and to allow cell disaggregation. A cell count was performed on each sample at this stage and

lymphocyte number was found to range from 0.2-1x10^6 with a viability, assessed by trypan blue exclusion, of >95%. Cells from each sample were then subjected to 4Gy of ionising radiation on ice or at room temperature (or mock irradiation) before harvesting at timepoints of 0, 30, and 120 minutes post treatment, by centrifugation at 1000 rpm for 10 minutes. (The samples irradiated at room temperature were immediately placed on ice for 10 min prior to the t=0 timepoint to allow time for samples to be transferred from the radiation source back to the laboratory for harvesting. The remaining samples were then allowed to incubate at 37°C in a waterbath prior to harvesting at the 30 and 120 min timepoints). After this cell pellets were resuspended in 1 ml of ice cold 10% DMSO in PBS and stored at -70°C prior to alkaline single cell gel electrophoresis (comet assay).

6.2.3 Comet assay

Lymphocyte samples from each subject and time point were analysed in batches including 1-2 controls and 4-5 patient samples (controls and patient samples had previously been coded so as to be indistinguishable during the assay and subsequent analysis). After rapid thawing, the 1ml stored samples were added to 1ml of PBS and then this mixture was added to 2ml of molten 2% low melting point agarose. The resulting cell suspension was then quickly layered onto a poly-L-lysine slide (BDH) which had been previously coated with 0.3% agarose (the agarose coated slides were edged with an immunohistochemistry pen (Dako), to help prevent the gels slipping off during the assay). This was performed in duplicate for every timepoint analysed.

Samples were allowed to dry briefly and for subsequent stages slides were kept under foil to exclude DNA damage induced by UV light. The slides were then transferred into freshly prepared cell lysis buffer containing 1M NaCl, 30mM NaOH, and 0.1% N-lauroyl sarcosine for 1 hour at room temperature. Slides were then washed twice for 30 minutes each in buffer containing 30mM NaOH and 2mM EDTA prior to electrophoresis. Electrophoresis was performed in buffer containing 30mM NaOH and 2mM EDTA at 40mA for 25 minutes in a horizontal tank (Pharmacia). After this, slides were transferred into a solution of 2μg/ml propidium iodide for 30 minutes to stain the DNA. Slides were stored under foil at 4°C prior to image analysis of 60 cells per timepoint (ie 30 cells/slide in duplicate), which was performed with a fluorescence microscope (Zeiss Axioskop), using Komet 3.1 software (Kinetic Imaging, UK).

6.2.4 Ionising radiation

Cells were irradiated in suspension in 15 ml centrifuge tubes (Falcon) using a Gammacell 1000 ^{137}Cs γ-irradiator (Atomic Energy Corporation, Canada) at a dose rate of 3 Gy/minute.

6.3 Results

6.3.1 Patient and control populations

Clinical information on the patients and controls entered into this study is given in Tables 6.1 and 6.2. All patients and controls studied were female. The

Category	Patients (n=33)	Controls (n=25)
Sex	Female	Female
Age range	37-83 years	~22-55
Median age	55 years	~28
History of Smoking:	11/30,	None
Current smokers:	8/30, 2 NR	None
Family History of breast cancer	5/30 3 NR	None
Tumour type	IDC (G1) 10* (G2) 7 (G3) 16 Colloid Ca 1 ILC 1(a) Tubulo-lobular 1(b)	-
Tumour size: Range and Median size (cm)	Range 0.8-5cm, Median size 1.8cm	-
Nodal involvement	12/29 cases 4 NR	-

Table 6.1

Summary of the clinical information on patients and controls entered into the comet assay study.

* One was a Colloid carcinoma

(a) Patient 10 had two primary tumours,

(b) Patient 19 had two primary tumours, see Table 6.2

NR: not recorded in the clinical notes.

Table 6.2

Clinical information on the breast cancer patients in the current study

(AR) Adverse reaction, N (none), Y (yes), G (tumour grade), DCIS (ductal carcinoma in situ), ADH (atypical ductal hyperplasia), CMF (Cyclophosphamide, methotrexate, 5-fluorouracil), CAF (Cyclophosphamide, doxorubicin, 5-fluorouracil), ATAC trial (Tamoxifen or Arimidex (Anastrazole) alone), MEGACE Megesterol acetate, Ov Ca (ovarian carcinoma).

(a) Local oedema.
(b) The patient's mother also had a history of ovarian carcinoma.
(c) Reddening of the skin.
(d) Soreness of the nipple.
(e) Reddening of the skin.
(f) Soreness of the nipple
(g) Mother and father both had gastric cancer.
(h) Peeling of the axillary skin.
(i) Mother had breast cancer. Father died of gastric cancer.
(j) Reddening of the skin.
(k) Soreness of the skin with ulceration.
(l)'Skin reaction'.

No.	Age	Pathology	Family History	Smoker	Therapy	(AR)
1	58	2cm, G2 Ductal, DCIS, 1/8 nodes +ve	Mother (age 70) and 2 aunts	N	Radiotherapy Tamoxifen	N
2	67	1.8cm, G2 Ductal, DCIS, 0/7 nodes, vascular invasion seen	N	20 yr ago	Radiotherapy ATAC	N
3	45	1.1cm, GI Ductal, 0/6 nodes	N	1/day	Radiotherapy Tamoxifen	N
4	41	1.6cm, G3 Ductal, DCIS, 0/12 nodes	N	15/day	Radiotherapy	N
5	69	5cm, G3 Ductal, DCIS, 13/13 nodes +ve	Sister (age 50)	1 year ago	Radiotherapy Tamoxifen CMF	N
6	47	2.5cm, G3 Ductal, 0/8 nodes	N	N	Radiotherapy	Y (a)
7	50	4.2cm, G2 Ductal + lobular, 2/15 nodes +ve	Mother (age 77) (b) Aunt (age 80)	N	Radiotherapy Tamoxifen CMF	N
8	52	3.4cm, G3 Ductal, DCIS, 0/1 nodes, vascular invasion seen	N	N	Radiotherapy Tamoxifen CAF	N

Table 6.2

Continued overleaf.....

No.	Age	Pathology	Family History	Smoker	Therapy	(AR)
9	55	1.2cm, G2 Ductal, DCIS, 0/9 nodes	N	N	Radiotherapy ATAC	N
10	62	1)1.7cm, G1 Ductal, DCIS 2) 1.3cm, Lobular Ca, LCIS, 0/14 nodes	N	N	Radiotherapy Tamoxifen	N
11	35	3.6cm, G3 Ductal, DCIS, 5/16 nodes +ve	N	8/day	Radiotherapy Chemo-therapy	N
12	75	4.4cm, G3 Ductal, 0/7 nodes Breast Ca 1978 other side	N	N	1978 Surgery+ Radiotherapy 1998 Radiotherapy ATAC	Y(c)
13	49	1.2cm, G3 Ductal, 0/14 nodes	N	8/day	Radiotherapy	Y(d)
14	73	1cm, G1 Ductal, DCIS, 0/14 nodes	Aunt (age 80)	N	Radiotherapy	Y(e)
15	39	1.5cm, G3 Ductal 1998, 2/2 nodes +ve, Previous lobular Ca, 1989	N	20/day	1989: Radio-therapy + CMF 1998: Tamoxifen	N

Table 6.2

....Continued overleaf.....

No.	Age	Pathology	Family History	Smoker	Therapy	(AR)
16	58	2.1cm, G3 Ductal, DCIS, 0/6 nodes	N Ov Ca 1985	N	Radiotherapy Tamoxifen	N
17	70	1.5cm, G2 Ductal, 0/6 nodes	N	20 years ago	Radiotherapy MEGACE	Y(f)
18	59	2cm, G3 Ductal, DCIS, 0/12 nodes	N (g)	N	Radiotherapy ATAC	N
19	43	1996: 2.6cm, G2 Ductal, DCIS, 1/7 nodes +ve, 0.7cm tubulo-lobular Ca, 1997: 4.5cm G2 Ductal + lymphatic inv.	N	10 years ago. Now 1 /month	Radiotherapy Tamoxifen CMF	Y(h)
20	51	1.1cm, G1 Ductal, DCIS, 2/8 nodes +ve	No	No	Radiotherapy CMF Tamoxifen	N
21	61	0.8cm, G1 Ductal, DCIS, 0/1 nodes	N	N	ATAC	N
22*	60	1.5cm, G3 Ductal, 4/5 nodes +ve, previous Ca	N	N	Radiotherapy Tamoxifen CAF	N
23	67	0.8cm, Colloid Ca, DCIS, ADH	N	15/day	Radiotherapy Tamoxifen	N
24	83	1.2cm, G1 Ductal, 3/21 nodes +ve	N	N	Arimidex	N

Table 6.2

....Continued, (* excluded from statistical analysis as t=0 damage at 0 Gy > 4 Gy).

No.	Age	Pathology	Family History	Smoker	Therapy	(AR)
25	57	2.2cm, G3 Ductal, DCIS, 0/7 nodes	N	N	Tamoxifen	N
26	47	1.8cm, G3 Ductal, DCIS, + Previous tumour	Mother (i)	Y	Radiotherapy Tamoxifen	Y(j)
27	48	1cm, G1 Ductal, DCIS	N	N	Radiotherapy Tamoxifen	N
28	47	2.1cm, G1 Ductal, DCIS, 0/8 nodes	N	N	Radiotherapy Tamoxifen	Y(k)
29	70	2.8cm, G3 Ductal, DCIS, 2/9 nodes +ve	N	?	Radiotherapy ATAC	Y(l)
30	49	1992: Previous tumour. 1998: 2.4cm, G3 Ductal, DCIS, lymphatic invasion.	N	N	1992: Radiotherapy 1998: Recurrence: CMF	N
31*	50	1.9cm, G3 Ductal, DCIS, 0/7 nodes	N	?	Radiotherapy Tamoxifen	N
32	48	4cm, G2 Ductal, DCIS, 2/4 nodes +ve	N	N	Radiotherapy Tamoxifen CMF	N
33	82	G1 Mucinous Carcinoma, Vascular invasion	N	N	Tamoxifen	N

Table 6.2
(* excluded from statistical analysis as t=0 damage at 0 Gy > 4 Gy).

median age of the patients was noted to be older than the controls (55 versus 28 years). Although occupational information is not provided the patients came from a variety of backgrounds whereas all the controls studied worked at the Institute of Molecular Medicine, Oxford and twenty of these worked in a laboratory environment. None of the controls had a personal history of smoking nor of breast cancer in a first degree relative as they were selected as controls on this basis. Eleven of the thirty one patients in which the information was recorded had a history of smoking and eight of these continued to smoke. Four gave a history of breast cancer in a first degree relative (mother or sister). In addition the mother of patient 7 also had a history of ovarian carcinoma and patient 14 had an aunt with breast cancer. Other tumours mentioned in the clinical notes in first degree relatives include fatal gastric cancer in the father of patient 26 (whose mother had breast cancer) and a history of gastric carcinoma in both parents of patient 18. Four patients had previous history of breast cancer or recurrent tumour and two patients had two separate tumours diagnosed at the time of presentation. The median age for primary presentation was 55 years with a range of 35-83 years and the median tumour size was 1.8cm. Most patients had Grade 3 invasive ductal carcinoma (IDC) of the breast, followed in frequency by Grade 1 and Grade 2 tumours. One had a variant of IDC (Colloid carcinoma). One patient had invasive lobular carcinoma of the breast (ILC) and another has a variant of this tumour called Tubulo-lobular carcinoma (Millis et al., 1994). Of the patients who underwent axillary nodal dissection (29/33) by the time of completion of this study, twelve were found to have positive lymph nodes.

6.3.2 4 Gy of ionising irradiation damages lymphocyte DNA and leads to comet formation after alkaline single cell gel electrophoresis.

DNA from unirradiated, undamaged single cells which were subjected to the comet assay and stained with propidium iodide formed bright, round 'nucleoids' with a symmetrical narrow halo lacking a tail (Fig. 6.1).

In contrast some cells irradiated with 4 Gy ionising radiation (IR) sustained considerable levels of DNA damage and were termed highly damaged comets (HDCs). The nucleoid of such comets was small and faint and appeared detached from the tail of the comet which was broad, long and very faintly staining (Fig. 6.2). Cells with intermediate levels of damage were seen most often after 4 Gy IR. The comet nucleoids were bright but smaller than those of undamaged cells and the presence of a broad moderately bright tail gave each comet a 'fried egg' shape (Fig. 6.3 and 6.4). In some individuals HDCs and more moderately damaged comets were observed after 4 Gy of IR, resulting in a dual population with respect to the amount of damage detected (Fig. 6.5).

6.3.3 Individual control and patient comet assay results

The results of the comet assay are displayed for each control and patient, in the form of 1): simple line graphs of tail moment versus time for irradiated and unirradiated samples and 2): a tail DNA frequency histogram for the different timepoints of irradiated and unirradiated samples. The tail DNA is presented in 'bins' of <0%, 1-10%, 11-20%, 21-30%, 31-40%, 41-50% and >50% to show the

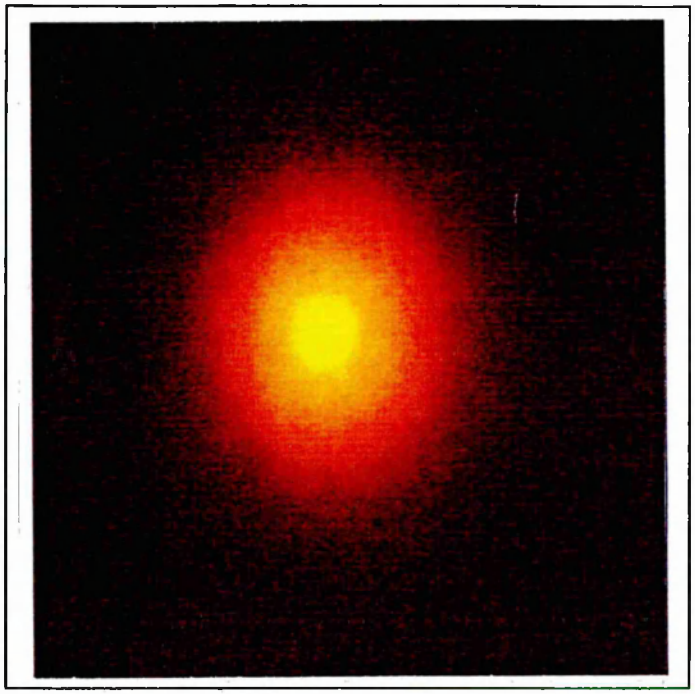

Fig. 6.1

An undamaged comet from patient 25. In this case 99% of the DNA is present in the large round comet head, (t= 0 min, 0 Gy).

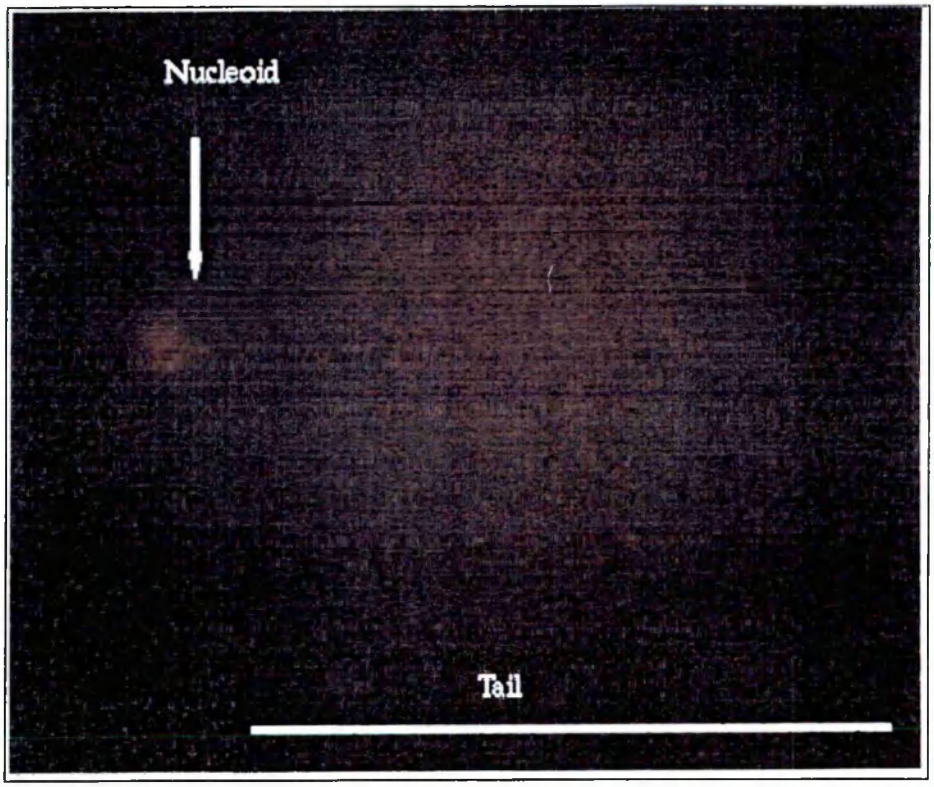

Fig. 6.2

A highly damaged comet is shown with tail DNA 75%. The majority of the DNA is present in the broad tail which is slightly detached from the undamaged DNA in the head which is represented by the small nucleoid.

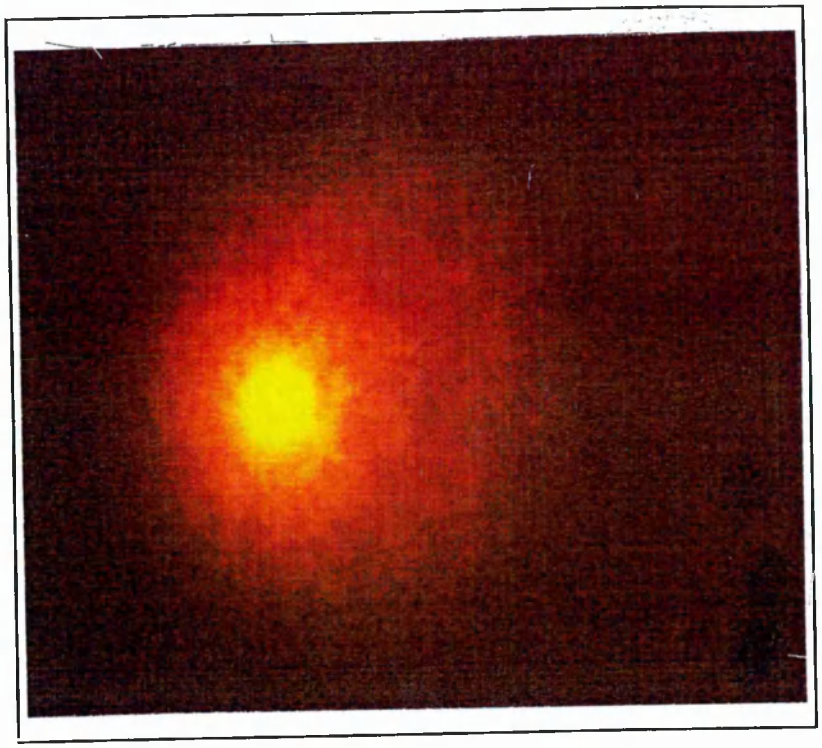

Fig. 6.3

Comet with 14 % tail DNA from patient 25, (t=0 min, 4 Gy).

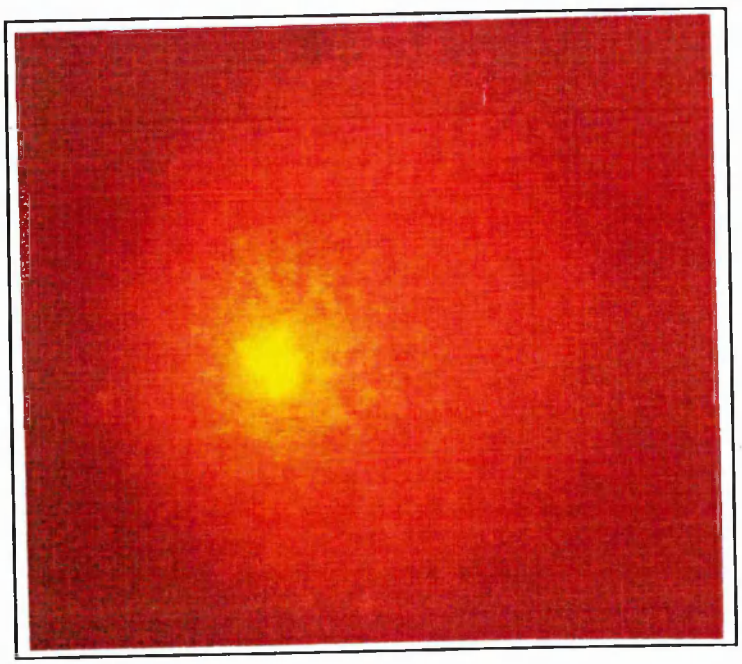

Fig. 6.4

Comet with 20 % tail DNA from patient 25, (t=0 min, 4 Gy).

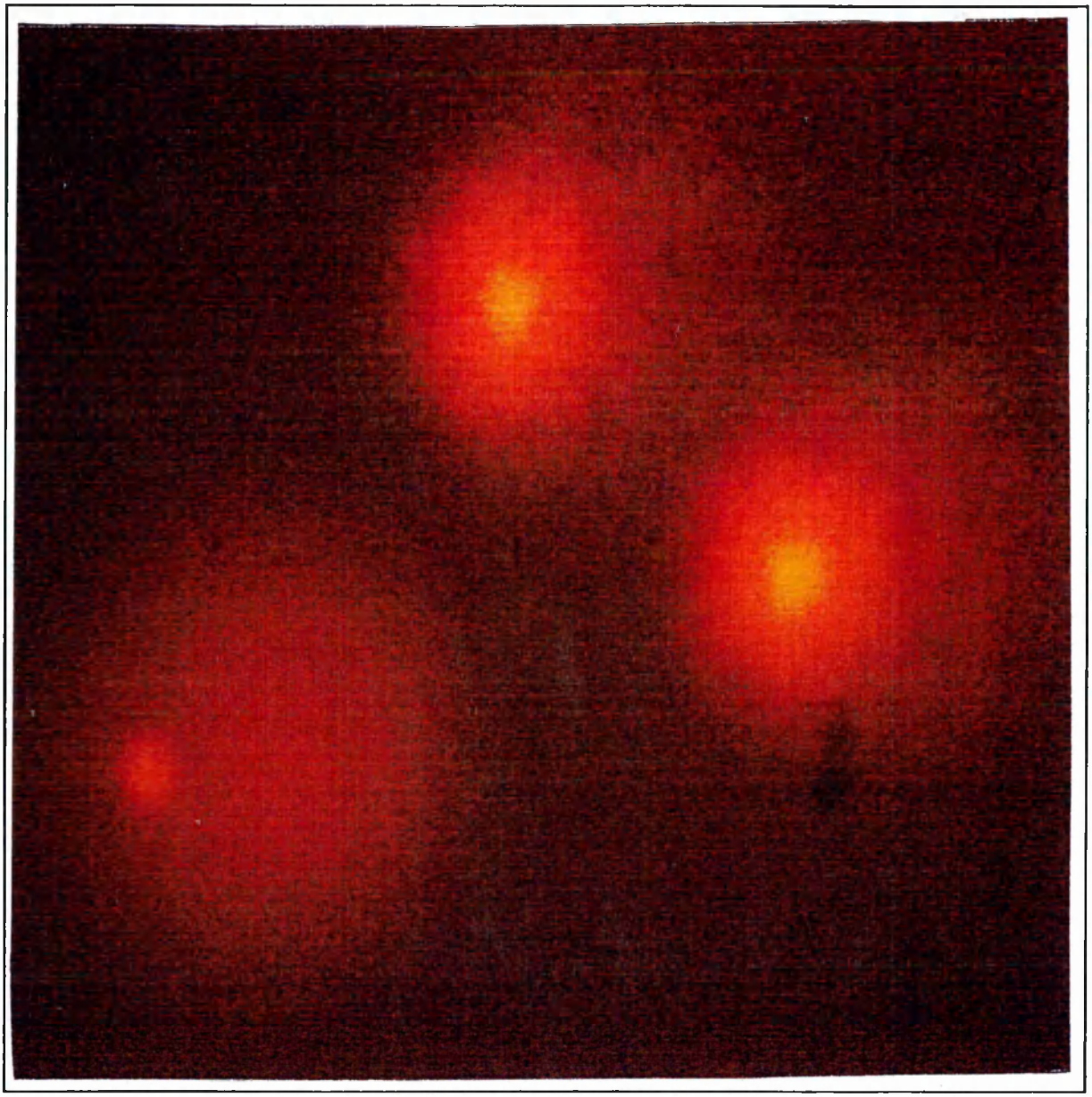

Fig. 6.5

Two populations of comets from patient 26, which vary in the amount of tail DNA, (t=0 min, 4 Gy) .

profile of DNA damage in the lymphocyte population at each timepoint, (see Appendix 1, presented at the end of Chapter 6).

6.3.4 Assessment of the numbers of moderate to highly damaged comets

Some of the samples tested showed initial diminution of DNA damage, at t=30 min post IR followed by a marked increase in DNA damage at the later t=120 min timepoint (See Appendix 1 controls 8, 11, and 16 and patients 3, 4, 6, 11, 24, 30 and 33). Fragmented DNA in apoptotic cells can be detected in the comet assay and contributes to the apparent DNA damage. Therefore in order to discover if cell death was a potential cause of the increase in DNA damage, the number of comets with tail DNA over 40% were also counted for each sample, treatment and timepoint as an indication of the number of apoptotic cells present (Table 6.3). Samples in which >10% of the cells (ie >6 comets) showed DNA damage over 40% included two of the controls (controls 7 and 8) and nine of the patients (patients 3, 4, 6, 16, 21, 23, 30, 31 and 32). Some comets with tail DNA exceeding 40% were seen in other patients eg patient 26, alongside the more usual DNA damage levels seen after 4 Gy of IR (Fig. 6.5).

6.3.5 Examination of levels of initial DNA damage sustained

Some of the cases tested in the comet assay showed very low initial damage levels at 4 Gy compared with the 0 Gy level (eg control 5 and patient 22, see Appendix 1). Because the samples were treated (IR or mock IR) at room temperature, DNA repair enzymes would have been functional and some

No.	Controls (0 Gy),			Controls (4 Gy),			Patients (0 Gy),			Patients (4 Gy),		
	t=0	30	120	t=0	30	120	t=0	30	120	t=0	30	120
1	0	0	0	2	2	0	2	1	1	1	1	-
2	3	1	0	3	4	3	3	1	0	3	4	3
3	0	0	1	2	0	0	0	1	1	5	6	13
4	0	0	2	1	1	3	1	8	9	6	4	22
5	1	0	0	0	2	3	0	0	5	0	3	-
6	0	0	1	1	1	1	6	2	14	17	9	23
7	7	4	3	6	7	8	0	2	0	1	0	0
8	6	6	4	2	1	10	2	3	3	2	3	2
9	4	1	1	3	2	3	2	2	0	1	2	1
10	2	3	1	2	1	1	5	1	2	2	0	4
11	1	4	3	3	1	2	2	3	1	4	2	6
12	3	0	1	1	3	1	0	2	0	1	0	1
13	0	0	2	1	0	0	0	1	0	0	1	1
14	0	2	0	1	1	0	3	0	1	3	1	0
15	0	0	0	1	0	1	0	0	0	0	0	1
16	0	0	0	0	0	1	1	5	3	13	14	9
17	1	0	0	1	0	0	3	2	0	1	1	0
18	2	3	4	4	5	3	3	3	2	2	3	3
19	1	0	1	1	0	0	2	1	4	1	1	2
20	1	4	4	1	0	3	1	2	4	2	2	2
21	0	0	0	0	2	0	3	7	3	6	3	5
22	0	0	0	0	0	0	2	1	1	0	0	0
23	0	0	0	0	0	0	3	0	0	7	0	0
24	0	0	0	0	0	0	0	0	0	0	0	1
25	0	0	0	0	0	0	1	0	1	1	0	0
26							3	1	4	1	5	6
27							2	0	2	3	2	3
28							2	2	0	3	0	0
29							2	0	4	2	2	2
30							15	9	8	11	7	11
31							11	5	3	2	4	9
32							3	0	9	2	0	0
33							0	0	0	1	0	0

Table 6.3

Number of comets with tail DNA > 40% in control and patient samples at timepoints t=0, 30 and 120 min after 0 or 4 Gy IR.

DNA damage could be repaired by the cells during the 1.3 min it took to deliver the full 4 Gy dose. Therefore a possible explanation for this phenomenon was that very fast DNA repair occured in these samples in the 1.3 minutes prior to the t=0 timepoint. To investigate this possibility, a study of the remaining cases was conducted with an additional sample kept at 4°C (to inhibit DNA repair enzymes), just prior to and during irradiation. An unirradiated control at 4°C was also included. Results for control and patient cases with these additional samples are presented in Table 6.4. As expected in a proportion of cases of both the controls and the patients the initial damage was increased at 4°C (after both IR and mock IR), at t=0. However, the unexpected finding was that in some the initial damage was less than the level measured at t=0 for the equivalent samples treated at room temperature (25°C) eg control 14 and patient 9.

6.3.6 Comparison of control and patient DNA repair capacity at 30 and 120 min post 4 Gy of ionising radiation

The combined results for controls and patients are presented in Table 6.5 and graphically as a scatter plot of % DNA repair for each irradiated group studied (ie controls and patients after exposure to 4 Gy of IR at 30 and 120 min at room temperature; Fig. 6.6). The corrected DNA damage at each timepoint was taken as the damage at 4 Gy minus the damage at 0 Gy. Values for repair at t=30 min and t=120 min, were calculated as the percentage diminution of DNA damage from 100% at t=0. Patients 22 and 31 were excluded from the analysis because the damage at t=0 was greater in the mock irradiated than in the irradiated

Initial Damage at 4°C compared with 25°C	Controls	Patients
4 Gy	(n=16)	(n=19)
Increased	9	8
Reduced	7	11
0 Gy	(n=14)	(n=16)
Increased	8	7
Reduced	6	9

Table 6.4

Difference in the initial damage seen after irradiation or mock irradiation at 4°C compared with 25°C in patient and control samples.

No.	% DNA Repair Control (t=30)	% DNA Repair Control (t=120)	% DNA Repair Patient (t=30)	% DNA Repair Patient (t=120)
1	87.3	99	-163.5	gels slipped off
2	115.3	65.1	78	79.5
3	90.6	93.1	20.8	-21.6
4	72.1	88.3	124.3	25.5
5	-10.6	-33.6	44.5	gels slipped off
6	77.7	103.3	59.4	76.5
7	-94	-124.3	82.5	107.4
8	19.5	-53.7	91	108.9
9	25.8	28.9	98.8	72.1
10	112.5	90.9	-51.2	-47.4
11	103	85.7	49.3	24.4
12	49.1	78.9	138.4	70.2
13	98.6	116.1	65.7	75.5
14	113.4	98.5	66.9	98.4
15	54.6	79.6	35.9	58.3
16	99.4	31.1	60.6	70
17	72	69.4	98.6	69
18	46.4	125	74.9	76.2
19	97.9	114	49.7	129.1
20	129.3	95.9	66.8	83.8
21	63.7	113.3	104.7	79.8
22	93.2	117.8	*	*
23	105.9	94.02	96.5	104.8
24	81.4	82.9	91.9	33
25	79.3	96.8	76.9	106.6
26			-58.1	64.1
27			68.3	66.8
28			81.9	101.1
29			55.5	94.8
30			22.4	-64.1
31			*	*
32			109.3	114.1
33			110	89.3

Table 6.5

Percentage repair of DNA in peripheral blood lymphocytes of controls and breast cancer patients after 4 Gy of IR, (* excluded from statistical analysis as damage at t=0 0Gy > 4 Gy).

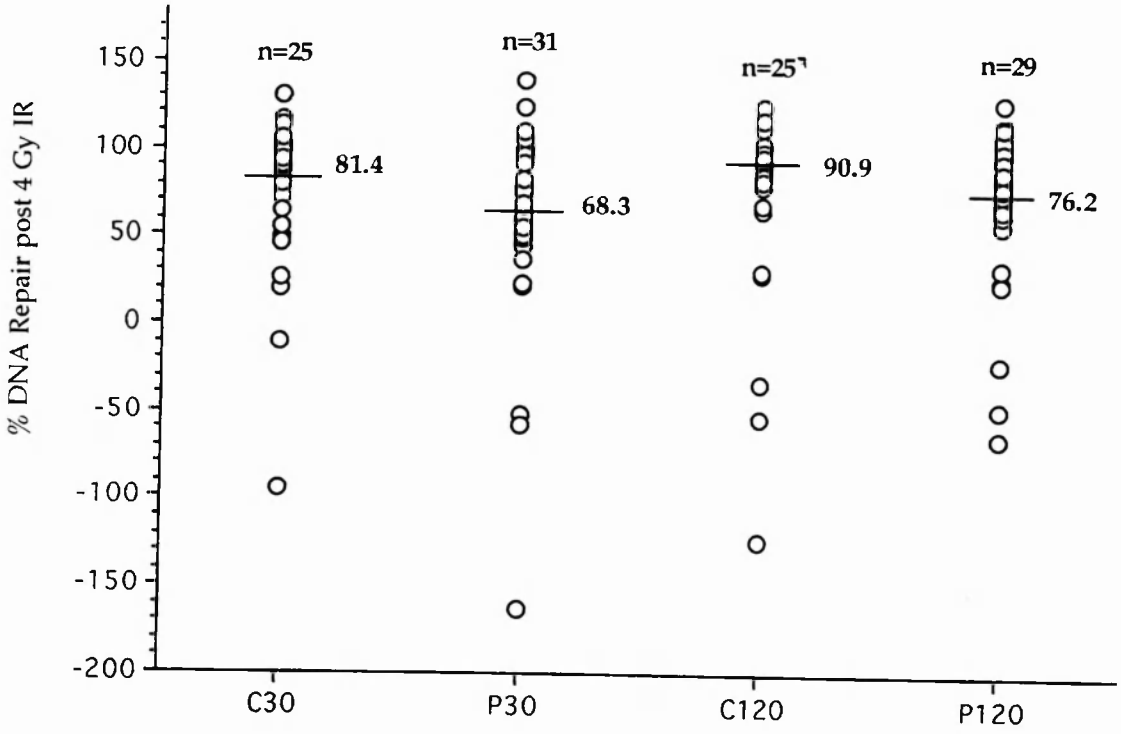

Fig. 6.6

Percentage DNA repair in peripheral blood lymphocytes of a group of controls (C30 and C120) and breast cancer patients (P30 and P120) at 30 and 120 min after 4 Gy of ionising radiation. (Numbers in bold indicate median % values for repair).

sample. In patient 22 this was not due to increased numbers of highly damaged cells (Table 6.3) but the possibility of fast repair was not excluded as the cause. In patient 31, there was a predominance of highly damaged comets in the mock irradiated sample at t=0 for unknown reasons and the results obtained at 4°C suggest that this patient was performing very fast repair. As can be seen there was considerable inter-individual variability in the amount of DNA repair within each group tested (ie DNA repair at: 30 min in controls, 120 min in controls, 30 min in patients and 120 min in patients). Within each group examples of very high repair and very low repair could be found at both timepoints. Overall however, the median values for repair were higher at both timepoints in the control compared with the patient samples (81.4% versus 68.3% at t=30 min) and (90.9 versus 76.2% at t=120 min) respectively however, this observed difference was not statistically significant using the Mann-Whitney *U*-test (with the assistance of Mike Bradburn, ICRF, Medical Statistics Group, Oxford). The results of this are presented in Table 6.6.

6.3.7 DNA repair capacity and radiosensitivity in breast cancer patients treated with radiotherapy.

Nine of nineteen patients who were treated with radiotherapy for breast cancer suffered an adverse reaction sufficient to be recorded in their clinical notes. These were patients 6, 12, 13, 14, 17, 19, 26, 28 and 29 (see Table 6.2 for details). These reactions ranged in severity from sore or reddened skin, through to skin ulceration. Six of the nine had % DNA repair values at 30 min which were below the medians for both the control and the patient groups. At 120 min,

	Median % DNA Repair (range)		
Time	Controls	Patients	p
30 min	**81.4** (-94.0, 129.3),	**68.3** (-163.5, 138.4)	0.36
120 min	**90.9** (-124.3, 125.1)	**76.2** (-64.1, 114.1)	0.26

Table 6.6

Summary statistics for comparison of the % DNA repair between controls and breast cancer patients measured using the alkaline comet assay at time =30 min and 120 min (using the Mann-Whitney *U*- test).

only three had % DNA repair values which were below the medians for both the control and the patient groups. Of the nine, only one (patient 6), showed >10% of the damaged cells with DNA damage >40% (possibly representing apoptotic cells).

6.4 Discussion

In studies of potential risk factors for common malignancies including breast cancer, the choice of controls is hampered by the fact that despite using individuals without a personal or family history of the tumour it is impossible to avoid the potential presence in the control population of individuals who will subsequently develop the disease. In a control population of 25 women (as used in this study), it is estimated that two to three will become breast cancer patients at some stage in their lives. This inevitably reduces the differences measured between these two groups from the levels which might have been observed if the comparison group behaved as true controls and all remained disease free.

In setting the criteria for 'normal' controls for this study other factors which might adversely affect the comet assay itself (eg the smoking of cigarettes (Piperakis et al., 1998)), also had to be considered and excluded, especially as this is a minor risk factor for the development of breast cancer (Goss and Sierra, 1998). A review of the literature reveals a variety of additional conditions and environmental agents which affect levels of DNA damage and which can be detected in the comet assay. These include older age (Piperakis et al., 1998), diet (including foods rich in genotoxins or antioxidants eg β-carotene (Collins et al., 1997), (Collins et al., 1997), (Sheng et al., 1998),

ascorbic acid and vitamin E (Taj and Nagarajan, 1994)), drugs (including Tamoxifen used to treat oestrogen-receptor positive breast cancer (Taj and Nagarajan, 1994)) and occupational exposure to genotoxins (Collins et al., 1997), which would be very difficult to control for. In criticism of the study design, the volunteer controls were younger than the patient group studied, no effort was made in this study to control for diet and drug exposure and the nature of the laboratory work environment might have subjected most of the controls to a risk of genotoxin exposure above that for the general population.

Thirty three breast cancer patients and 25 female controls were entered into the study. This number is slightly larger than that seen in the previous investigation of breast cancer and DNA repair using the comet assay (Jaloszynski et al., 1997). The latter study included volunteer healthy female controls and 26 women with breast cancer (the control group was younger than the patient group in this study also). The breast tumour type and grade were not documented in Jaloszynski's study and so cannot be commented upon but the group of patients in the current study are not perfectly representative of breast cancer patients in general, in that although the commonest tumour is invasive ductal carcinoma as expected, grade three tumours rather than grade 2 tumours predominate. This may be the result of chance due to the relatively small number of patients studied.

During the current study, several observations were made which required explanation and therefore further investigation. Firstly, in some cases after initial damage and repair, evidence of increased DNA damage was seen at the 120 min timepoint. There are a number of possible explanations of this phenomenon. The number of apoptotic cells might be increasing and making

the DNA repair appear to decrease. Alternatively, excision repair pathways might be creating single strand breaks which were then slowly or inadequately processed and revealed in the assay (Collins et al., 1997). It is already established that apoptotic cells which digest their DNA into small fragments (~180 bp), can be detected and quantified in the comet assay (Olive et al., 1993) and appear as highly damaged comets (HDCs), (Singh, 1996). In necrotic cells, the cell membrane integrity is lost before degradation of the DNA occurs and therefore no increase in tail moment (and by implication tail DNA) is seen with this mode of death (Olive et al., 1993). For this reason cells which have undergone necrotic death prior to conduction of the assay are not detected. Because the comet assay is such a sensitive indicator of DNA fragmentation, cells in the first stages of apoptosis were detectable earlier by the comet assay than by flow cytometry and were visualised using the former method between two and twenty four hours after irradiation of peripheral blood lymphocytes. Analysis of lymphocytes from a small number of subjects by FACS prior to the current study only revealed a sub-G1 population (representing apoptotic cells) six hours after 4 Gy of IR (data not shown). The later stages of apoptosis, when the DNA is highly fragmented, are much more difficult to detect because of the extreme faintness of the comets (Olive et al., 1993) (Fig. 6.2). The effect of apoptosis on the comet assay may be problematic in genotoxicity testing, as dead or dying cells may give false positive responses due to cytotoxicity (Henderson et al., 1998). To determine the extent to which excessively damaged apoptotic cells were contributing to the increase in DNA damage/reduction in DNA repair seen, comets with tail DNA >40% were counted for each timepoint. The choice of the 40% tail DNA cut off value was

based on the observation that in the cases analysed the % tail DNA seen after 4 Gy IR at time=0 was usually less than 20%. In addition, although HDCs with tail DNA of ~90% or tail moments of ~30 are said to be apoptotic (Olive et al., 1993), non-apoptotic cells had tail moments of <2 or <20% (Schwartz et al., 1995). Given that early apoptotic cells may be detected, and the fact that it was important not to underestimate the number of apoptotic cells, the value of 40% tail DNA appeared reasonable to use for this purpose and these cells were described as moderate to highly damaged comets (M/HDCs). Whilst nine of thirty three of patients showed a timepoint where >10% of their tail DNAs were >40%, only two of the twenty five controls did, suggesting that the patients were more susceptible to this sort of DNA damage. It is interesting to note that in a few of the cases (control 11, patient 6 and patient 33), the increasing damage at the later timepoints is seen for both the irradiated and unirradiated samples. This may indicate a greater degree of susceptibility to apoptosis possibly caused by other experimental conditions superimposed on the radiation damage.

In five cases (control 8 and patients 3, 4, 6 and 30) the increasing DNA damage after initial repair was associated with increased numbers of M/HDCs. In the five other cases showing increasing damage (control 11 and 16 and patients 11, 24, and 33), M/HDCs were not seen in large numbers. This might be due to the fact that the increasing damage in these cases is contributed to by greater numbers of comets in bins corresponding to lower levels of damage than those assessed here. Whether or not such cases are distinguished due to cells that are in extremely early apoptosis is impossible to say as additional morphological criteria for, and other assays of, apoptosis

were not performed on these samples. In patients 16, 21, 23, 31 and 32, M/HDCs of >10% total cell number at a particular timepoint were observed but this was not associated with rising DNA damage levels overall. In these cases it is possible that the extreme damage in some cells was masked by the levels of repair found in these samples (Table 6.5). In control 7 good repair cannot account for this phenomenon but at every timepoint in this individual (IR or mock IR), comets with >50% tail DNA damage are found (also see the tail DNA frequency histogram relating to this case in Appendix 1). It is possible that a discrete population of very highly damaged comets might explain these results.

It is also important to mention that DNA strand migration can occur not only due to DNA damaging agents and apoptosis as invoked above but also as a consequence of DNA strand breakage during the excision repair processes themselves. The incision step of base and nucleotide excision repair has been found to be very fast and is even active at 4°C (Klaude et al., 1996). If repair is slow or stops at this point these strand breaks can be detected in the comet assay (Collins et al., 1997). Further processing can generate large stretches of single stranded DNA around the original lesion and the damage may be greater if these processes are inadequate or faulty than if they were absent altogether. Thus the interpretation of comet assay results may not be entirely straightforward, as repair processes themselves generate transient DNA damage that, if incompletely processed due to interruption or aberration, can be detected in the assay. Whether apoptosis or a faulty type of repair is the true explanation of the rising DNA damage seen in the cases mentioned is not clear

because individual pathways of DNA strand break repair and alternative assays of apoptosis were not included in this investigation.

The second cause for concern during the early phases of this study was the finding of cases in which the initial level (ie at t=0) of DNA damage sustained after 4 Gy of irradiation appeared rather low (eg control 5 and patient 23), in comparison to the others studied. The absolute amount of direct DNA damage sustained due to the ionising radiation should be equivalent in all the cases, however the possibility was entertained that in these cases the low initial damage might be accounted for by more rapid repair occurring during the timeframe of irradiation such that the remaining damage at t=0 was lower than expected. To investigate this possibility additional samples (IR and mock IR) were treated on ice to reduce the activity of the repair enzymes. As described in the results higher values of initial damage were then attributed to some of these samples, in keeping with the hypothesis outlined above (Table 6.4). However a similar number showed exactly the opposite effect with a reduction in the initial damage recorded. This effect was not expected but it may be explained by the relative levels of direct and indirect damage to DNA that occurs due to ionising irradiation. Ionising radiation (frequency $>10^{15}$ Hz) including diagnostic and therapeutic X-rays contains sufficient energy to break chemical bonds directly creating single and double strand DNA breaks and base damage. Deposition of energy from the radiation also results in the formation of reactive oxygen species (ROS) eg the superoxide anion (O_2^-), and hydrogen peroxide (H_2O_2), from water in the cell. The hydroxyl radical ($OH\cdot$) is formed from H_2O_2 and O_2^- via the Haber-Weiss reaction. This reaction is

slow and in biological systems it is usually catalysed by transition metal ions, a process called the Fenton reaction. Ferrous iron (Fe^{2+}) appears to be the major intracellular mediator of the Fenton reaction, although the precise source and form of the iron is unknown. The ROS cause oxidative damage to the cellular macromolecules including lipid peroxidation, the oxidation of cysteine residues and amino groups in proteins and strand breaks and oxidation of guanosine residues in DNA. The amount of indirect oxidative damage caused by IR is dependent on the activity of the enzymes catalysing the above reaction and the cellular antioxidant reserves eg glutathione. These may vary on an individual to individual basis dependent on genetic and environmental factors including the level of antioxidants found in the diet. Therefore the levels of initial DNA damage may reflect the sum effect of all of the above. At room temperature, a high level of initial DNA damage may be due to poor antioxidant status, more active oxidative systems, or slower repair processes, whereas low levels of initial damage may reflect high antioxidant levels, less active oxidative systems and faster repair processes.

If both the irradiated and the mock irradiated samples are kept on ice just prior to and during treatment, the level of activity of the enzymes of both repair and oxidative metabolism will be reduced and in theory, the initial damage should approximate to the level of direct DNA damage sustained. This maybe greater than or less than the value obtained for initial damage at room temperature. However, subsequent incubation at 37°C to allow the removal of DNA damage restores the activity of the repair enzymes and the enzymes generating and dealing with the reactive oxygen intermediates, complicating the picture once again.

In the analysis of the levels of DNA repair the measurements obtained after treatment of the samples at room temperature, rather than those on ice were used (Table 6.5 , Table 6.6 and Fig. 6.6) but where available the results of the latter were provided graphically (Appendix 1). This decision was made on the basis that *in vivo,* the impact of direct and indirect DNA damage is important and will influence inter-individual differences in DNA damage. Clearly this modification of the comet assay as a DNA repair assay cannot be simply interpreted, but in this study it was considered important to identify individuals in whom DNA damage was persistent after the original insult.

The overall results of the study show that in most individuals the greatest reduction in DNA damage post irradiation is seen in the first 30 minutes. This compares well with the kinetics of repair documented in other studies (Olive et al., 1990). There was marked inter-individual variability in the DNA repair recorded in both the control and the patient group. This is a phenomenon which has been previously documented in studies of lymphocyte DNA damage or repair using the comet assay (Collins et al., 1997), (Jaloszynski et al., 1997). This fact alone would preclude the use of the assay as an indicator of potential breast cancer risk in individual patients. Median % values for DNA repair were found to be higher for the controls at both the 30 min and the 120 min timepoints however the statistical analysis described generated p values of 0.36 and 0.26, suggesting that the observed differences between the controls and the patients in repair at both timepoints was no greater than that expected by chance alone (Table 6.6). This is in contrast to the findings of the previous study into DNA repair and breast cancer which showed that breast cancer subjects appeared to be significantly more sensitive to exposure to the

radiomimetic drug bleomycin those of healthy control subjects. Breast cancer patient lymphocytes were shown to have higher levels of DNA damage and a weaker DNA repair capacity which was statistically significant by the Mann-Whitney *U*-test (Jaloszynski et al., 1997). The latter study differs in a number of ways from the current study in that the DNA damaging agent was Bleomycin rather than IR, the study was smaller, the cells were treated on ice prior to incubation and a visual scoring method was used to assign the comets to 5 categories of damage rather than an image analysis package as used in the current study. Computerised image analysis gives a precise result for each comet detected and the mean comet tail moment and other parameters can be statistically calculated for each sample and timepoint tested. Visual scoring methods have been shown to correlate well with image analysis packages in the past (Collins et al., 1997), but this may not be the case when low levels of damage are generated and slightly different populations of comets are present in the same sample. In some respects however, the findings of these studies are somewhat similar especially in the inter-individual variability and the fact that in many cases, the calculated repair exceeded 100% implying that once stimulated by bleomycin or IR, the cells were capable of reparing other procedure related and spontaneous DNA lesions. It is possible that the difference in the overall results reflects the marked inter-individual variability in the results of the assay and that with such variation much larger patient and control groups may be required to satisfactorily test the hypothesis.

Additional information on the relationship between radiosensitivity reactions in breast cancer patients and the capacity for DNA repair was also provided by the current study. About 5% of patients undergoing therapeutic

cancer radiotherapy sustain severe normal tissue damage after standard radiotherapy regimens (Norman et al., 1988), (Ribeiro et al., 1993). A test to identify such susceptible patients prior to treatment would be very welcome both to avoid the morbidity associated with adverse reactions and to produce dosage schedules for non-sensitive patients which can be increased to maximize their efficacy. Interest in the possible causes of radiosensitivity reactions was stimulated by the finding that A-T sufferers receiving the usual radiotherapy doses for cancer therapy have demonstrated severe normal tissue necrosis with life threatening consequences (Gotoff et al., 1967), (Cunliffe et al., 1975), (Abadir and Hakami, 1983) and cells from both A-T homozygotes and A-T heterozygotes show *in vitro* radiosensitivity, the latter being intermediate in degree between normals and homozygotes (Paterson et al., 1979), (Arlett and Priestley, 1985). As A-T heterozygotes may have an increased cancer susceptibility compared with normal controls, it has been suggested that subjects who have cancer and who display marked sensitivity post-radiotherapy might be A-T heterozygotes (Dahlberg and Little, 1995), (Jones et al., 1995). If this is the case then screening for the *ATM* gene could be used to identify highly radiosensitive patients prior to radiotherapy. To date only a few studies have addressed the question of the role of *ATM* heterozygosity in adverse radiotherapy reactions *in vivo*. One study did not detect any mutations in the *ATM* gene in 16 breast cancer patients and 7 patients with other cancer types all of whom had severe radiotherapy reactions (Appleby et al., 1997). The restriction endonuclease fingerprinting assay which only identifies about 70% of the mutations was used in this study but provided that the assumed proportion of cancer patients who were A-T carriers (4%) and the likelihood

that *ATM* mutations will lead to radiation reactions after radiotherapy (100%), were correct, some mutations would have been expected. Apart from the controversy regarding cancer risk in A-T heterozygotes discussed in Chapter 1, the issue of whether A-T carrier status leads to radiosensitivity *in vivo* has not yet been clarified. Anecdotally at least, A-T heterozygosity does not seem to be associated with radiosensitivity, (Swift, 1994). No large studies focussing on this subject are available but incidental information has come to light from investigations of *ATM* and breast cancer. Out of 3 *ATM* mutation carriers with breast cancer identified in two separate studies only one showed a mild skin reaction with minimal late effects following radiotherapy while the other 2 showed no reaction (Ramsay et al., 1996), (Fitzgerald et al., 1997). It is possible that the wild type allele is able to obviate the radiation sensitivity or perhaps the specific genetic or epigenetic background found in different patients makes a difference. Indeed, other factors must be relevant in adverse radiation responses because the 2 patients in the latter study who did have an adverse reaction to radiotherapy sufficient to interrupt treatment did not have *ATM* mutations. Clearly this subject has profound clinical implications and merits further investigation. Although outcome of radiotherapy was not consistently commented upon in the clinical notes and the numbers of patients with unacceptable adverse reactions were low, one patient in this study was said to have sustained ulcerated skin due to radiotherapy (patient 28). This patient gave no family history of breast cancer and had DNA repair values above that seen for the median % DNA repair value for the control group at both timepoints (81.9% at t=30 and 101.1% at t=120 respectively) and very few M/HDCs. Eight others, two of whom had a positive family history of breast

cancer (patients 14 and 26), suffered minimal clinically irrelevant radiotherapy reactions which might not always be commented upon. All showed at least one timepoint of repair which was below the median % repair of both the controls and the patients. Only one (patient 6), showed high levels of M/HDCs. *ATM* sequence and ATM protein expression was not investigated in these patients and therefore their *ATM* status cannot be commented upon. The considerable inter-individual variability in patients and controls suggests that levels of persistent DNA damage post IR are unlikely to be useful in the prediction of adverse responses to radiotherapy.

Four patients (patients 1, 5, 7 and 26), gave a history of breast cancer in a first degree relative (mother or sister). Three of these showed % median repair values which were below those observed for the controls at both timepoints but patient seven showed no obvious repair defect. A larger study of such cases would be required to determine if defective DNA repair is associated with a close family history of breast cancer.

To summarize, no significant association was found between DNA repair capacity and breast cancer in this study. Closer analysis suggests that the differences in DNA damage revealed by the comet assay cannot be accounted for solely by inter-individual differences in DNA repair. Other contributory factors including apoptosis may have to be taken into account.

FUTURE DIRECTIONS

Several lines of future work arise from the studies described. Firstly given the experience of others it would seem possible to refine the immunostaining protocols employed for ATM eg by using fluorescently labelled secondary antibodies and visualisation with confocal microscopy to improve subtle antigen detection. In addition, now that many non-commercial ATM antibodies are available, some of these may be used in the future to investigate ATM localisation in a range of normal and tumour tissues including breast cancers. The antibody CN-12 will be used to complete the study of ATM in the cell lines of the NCI panel for which there are currently no results.

The complete absence of ATM protein in the human promyelocytic leukaemia cell line HL60 is of considerable interest and merits further investigation. In particular sequencing of the ATM gene in this cell line will be undertaken to determine if it is mutated and the protein destabilised as predicted. Following on from this, a study of ATM expression in a variety of sporadic human lymphomas and leukaemias including promyelocytic leukaemia should now be conducted.

Given the recent success of (Canman et al., 1998) and (Banin et al., 1998) in demonstrating the protein kinase activity of ATM against p53 Ser 15 and PHAS-I, using Mn^{2+} containing buffers and effective methods of ATM activation it is now theoretically possible to assess the integrity of signalling via ATM in human peripheral blood lymphocytes. Considering the interindividual variability usually seen in this type of study, large numbers of individuals should be entered to obtain meaningful results. It would also be worthwhile investigating ATM function in markedly radiosensitive patients to elucidate the relationship of this phenotype with a compromised ATM pathway rather than ATM protein defects per se.

Appendix 1

Appendix 1

DNA damage profiles (Tail moment versus time) and comet tail DNA frequency histograms are presented for all individuals studied (controls and patients).

DNA damage profiles:

The black line represents the mock irradiated sample and the red line represents the samples treated with 4 Gy IR at room temperature. The green point and the blue points represent samples mock irradiated or treated with 4 Gy IR at 4 ^{o}C respectively.

Comet tail DNA frequency histograms:

The coloured bars represent the following treatments,

Red bars: 0 Gy, t=0 min
Green bars: 0 Gy, t=30 min
Dark blue bars: 0 Gy, t=120 min

Pink bars: 4 Gy, t=30 min
Yellow bars: 4 Gy, t= 0 min
Pale blue bars: 4 Gy, t=120 min

(Two 4 Gy t=120 min timepoints are missing due to gel loss during the assay).

DNA damage profile

Tail DNA frequency histogram

Control 1

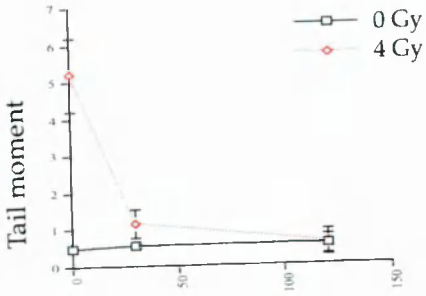

Time (min)

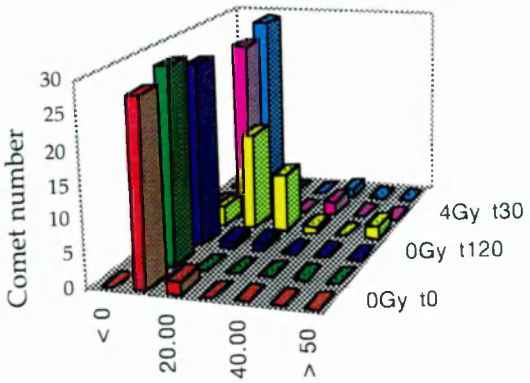

% Tail DNA

Control 2

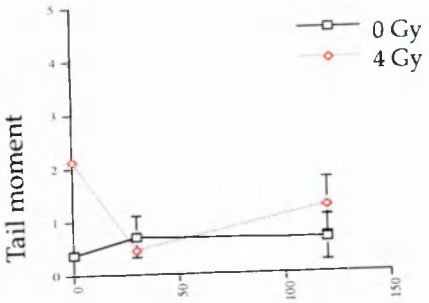

Time (min)

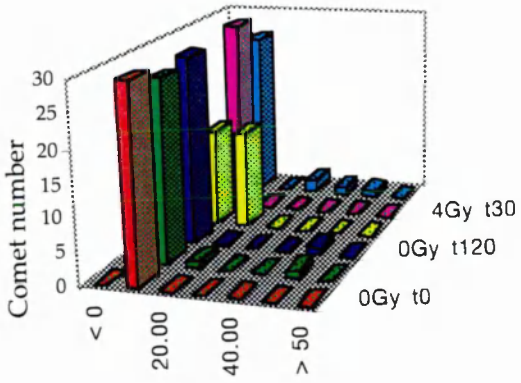

% Tail DNA

Control 3

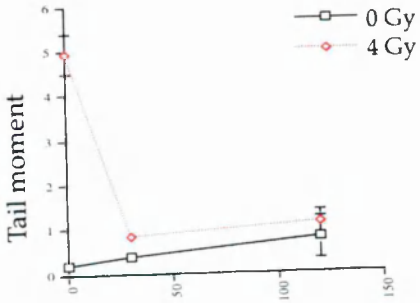

Time (min)

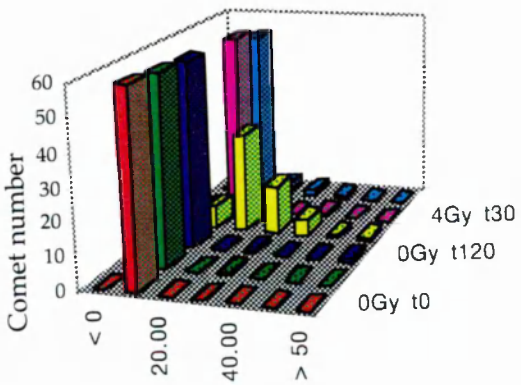

% Tail DNA

DNA damage profile

Tail DNA frequency histogram

Control 4

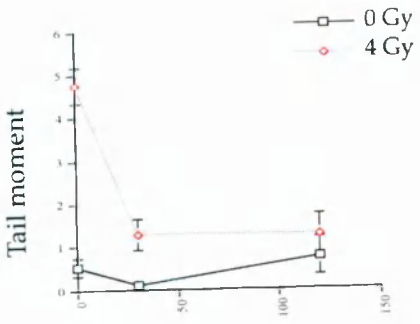

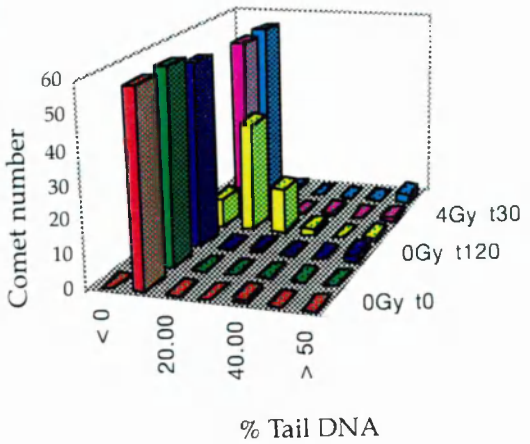

Control 5

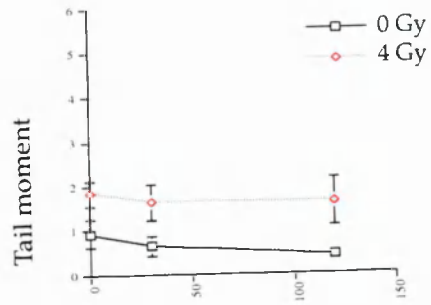

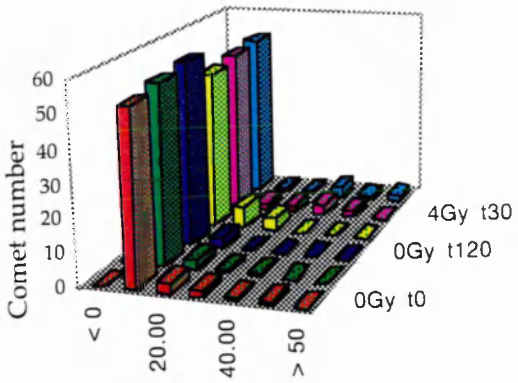

Control 6

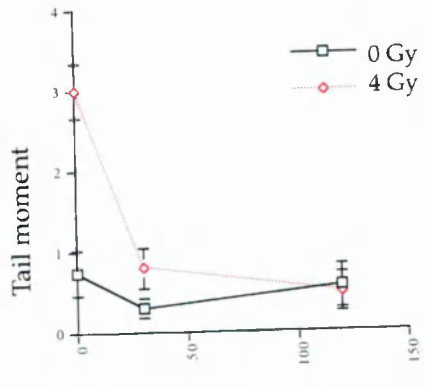

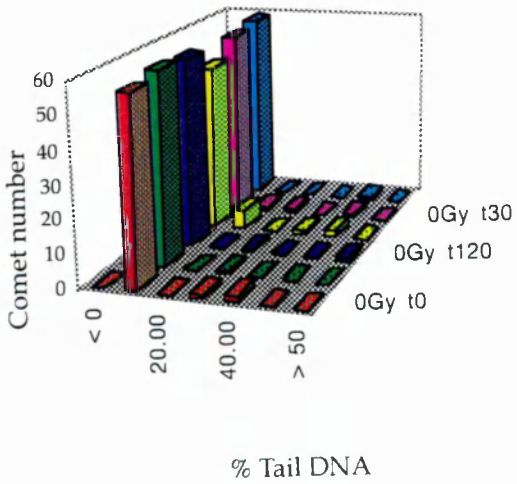

DNA damage profile

Tail DNA frequency histogram

Control 7

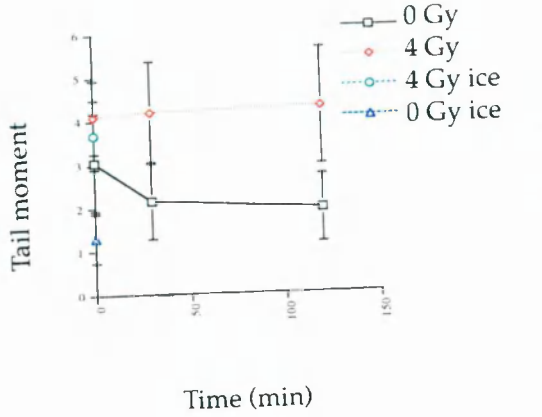

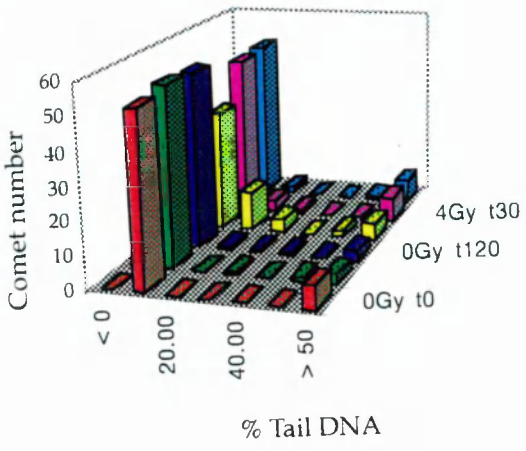

Control 8

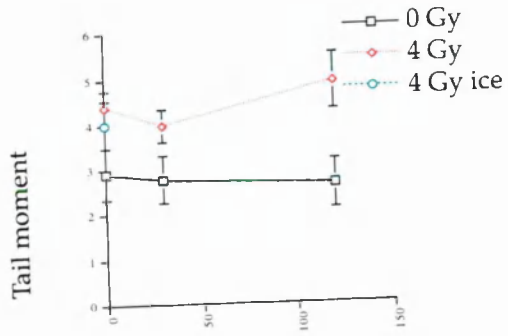

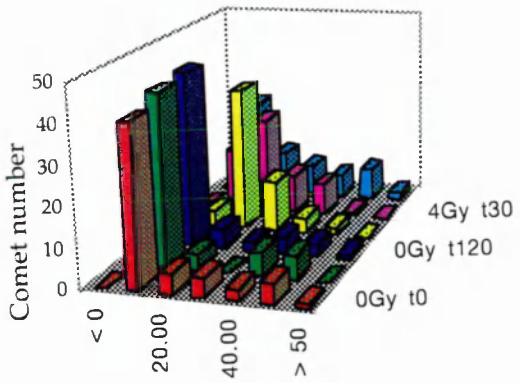

Control 9

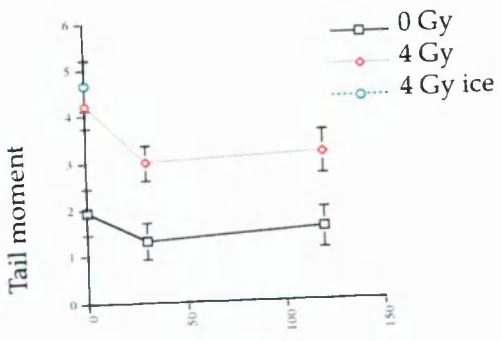

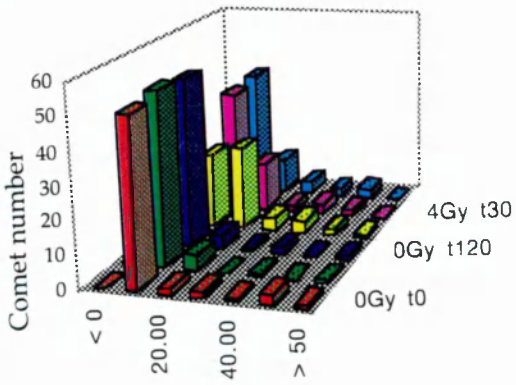

DNA damage profile

Tail DNA frequency histogram

Control 10

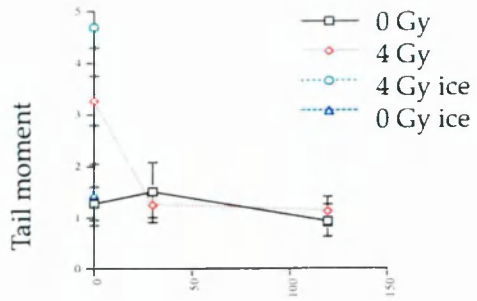

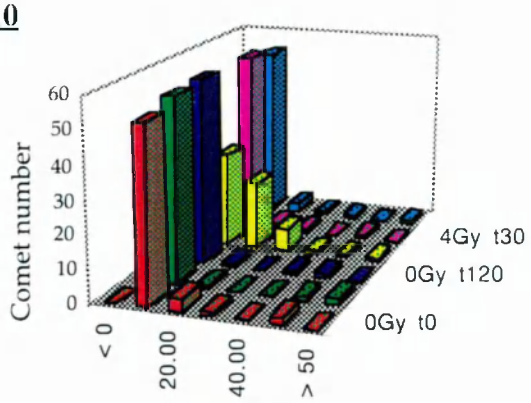

Control 11

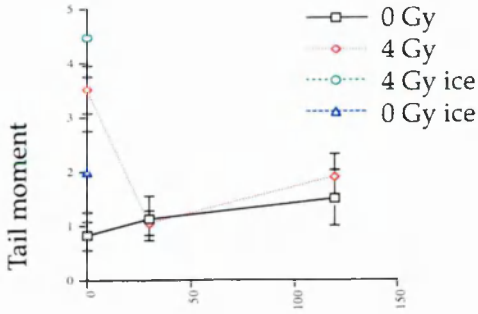

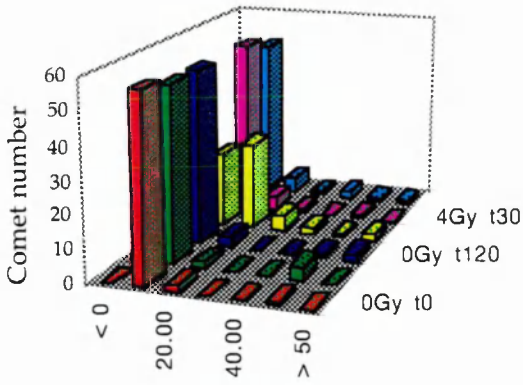

Control 12

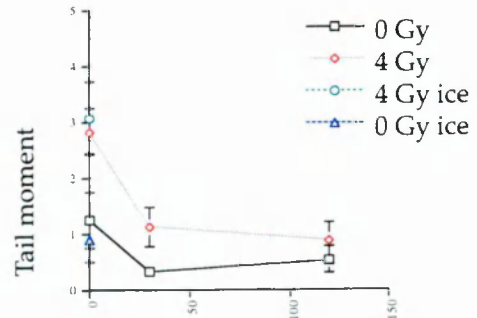

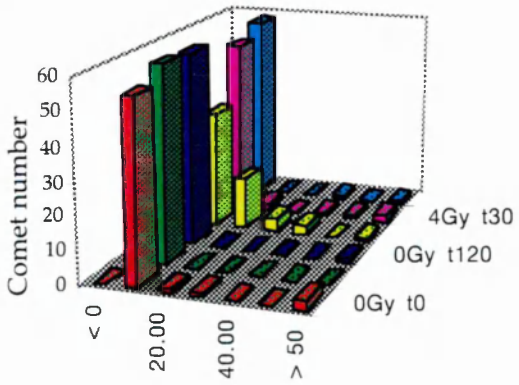

DNA damage profile

Tail DNA frequency histogram

Control 13

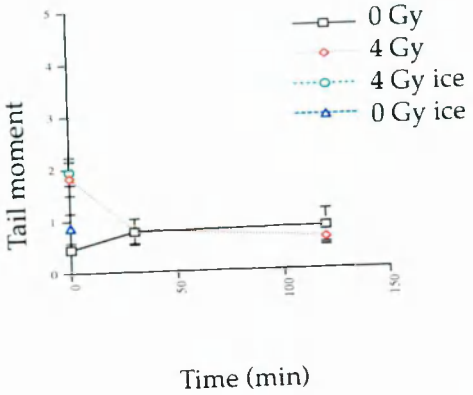

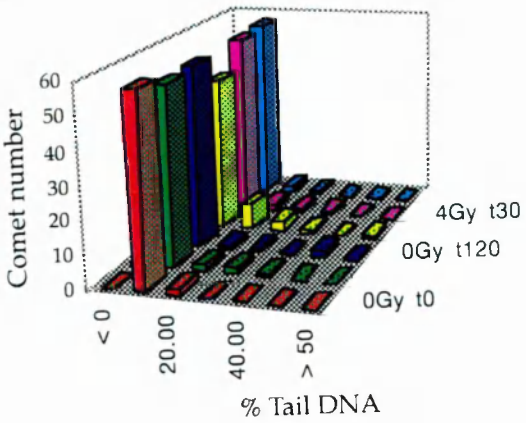

Control 14

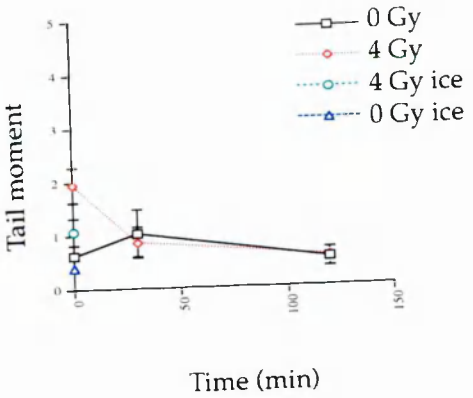

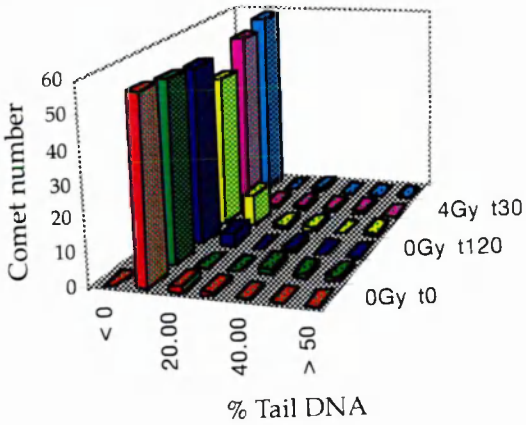

Control 15

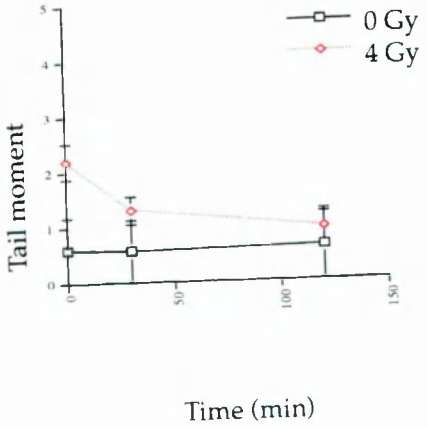

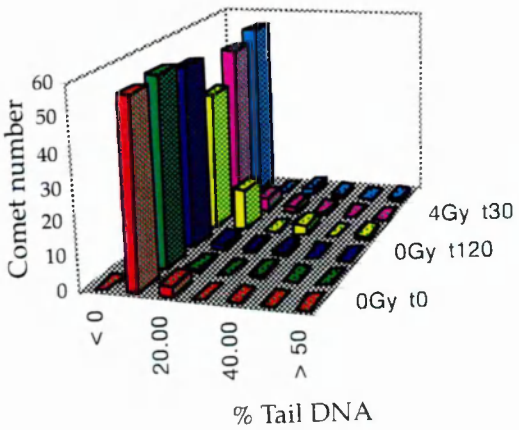

DNA damage profile

Tail DNA frequency histogram

Control 16

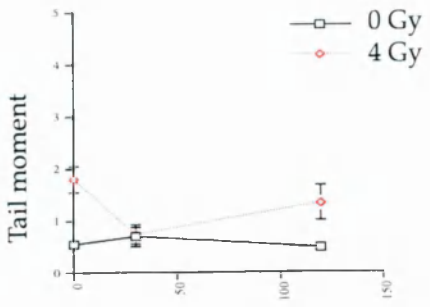

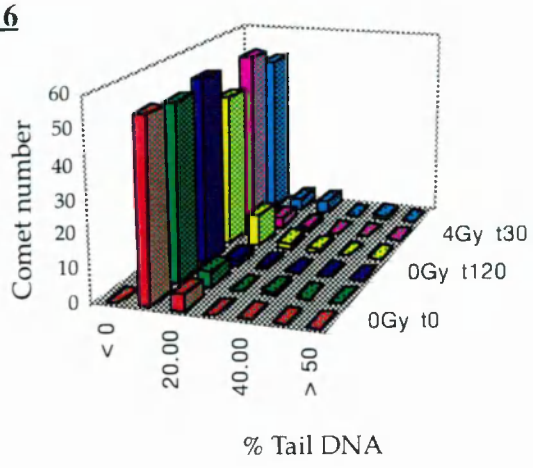

Control 17

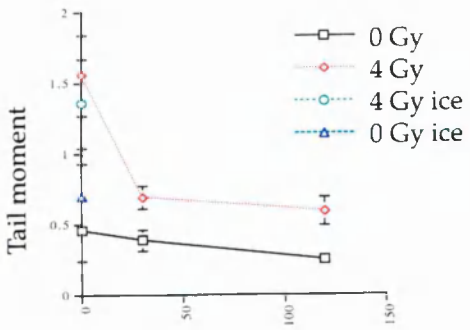

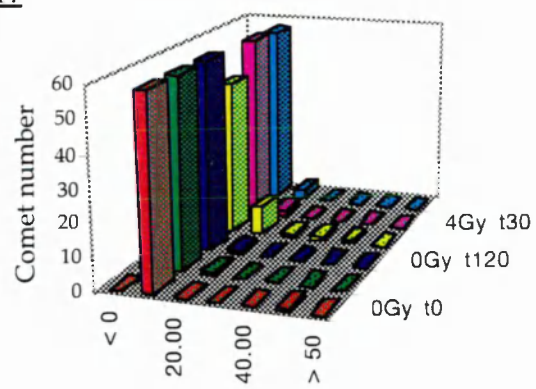

Control 18

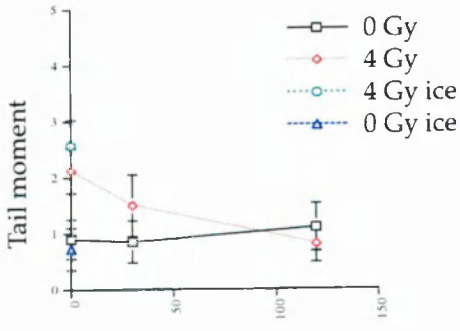

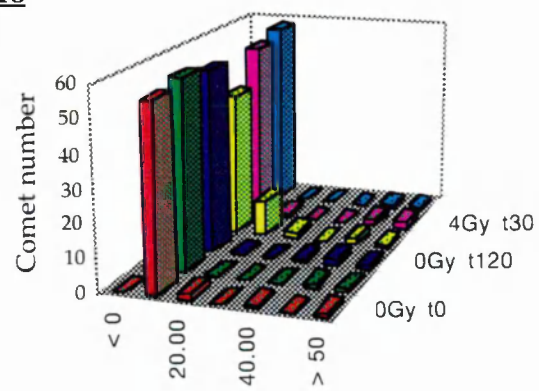

DNA damage profile

Tail DNA frequency histogram

Control 19

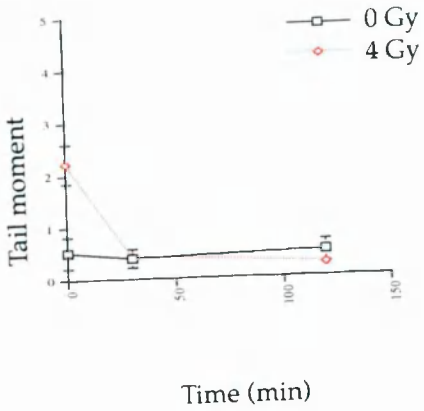

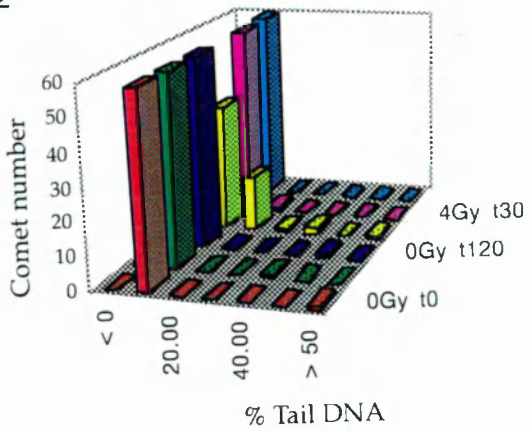

Control 20

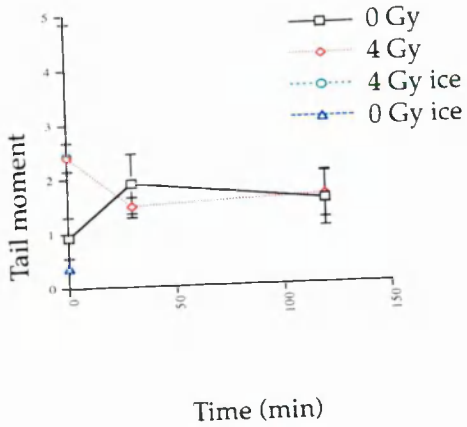

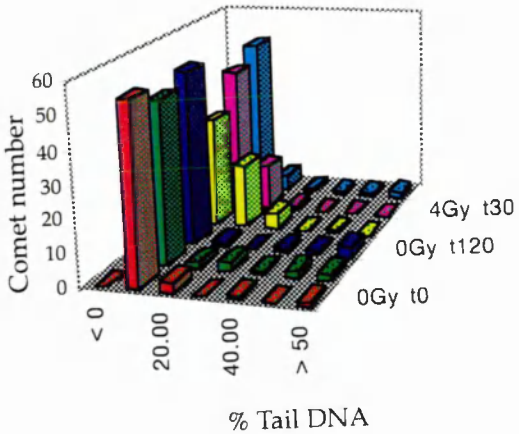

Control 21

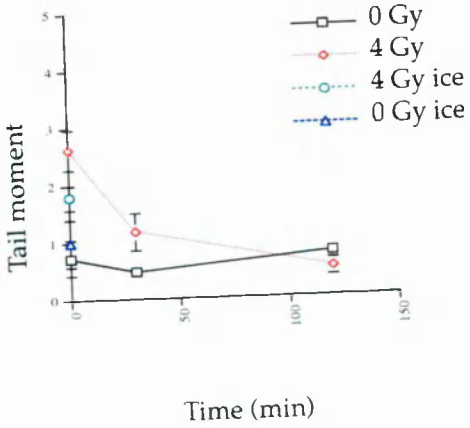

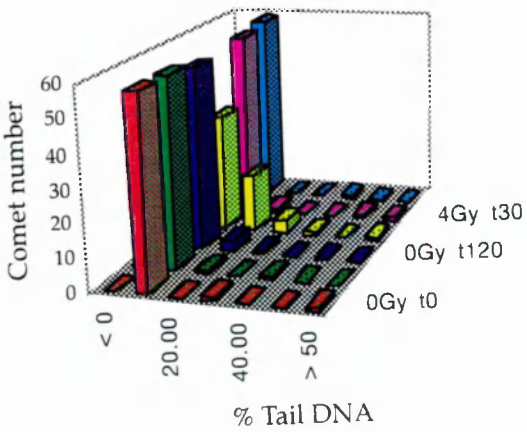

DNA damage profile

Tail DNA frequency histogram

Control 22

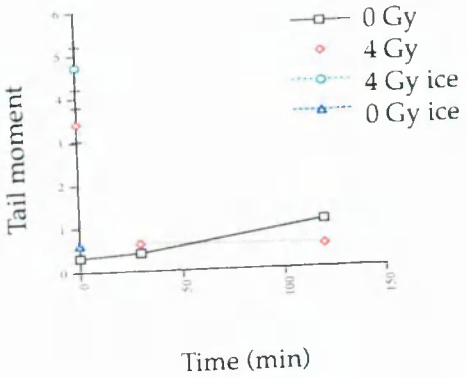

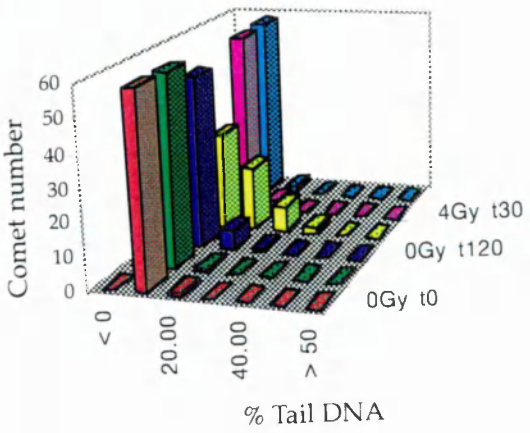

Control 23

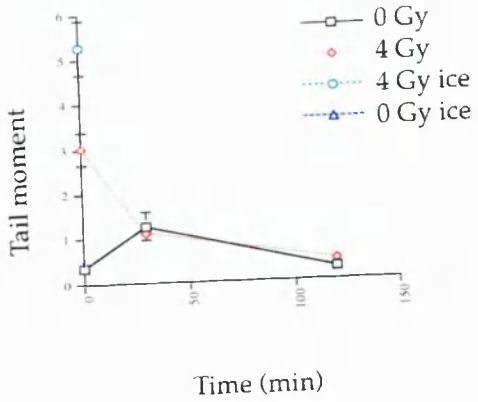

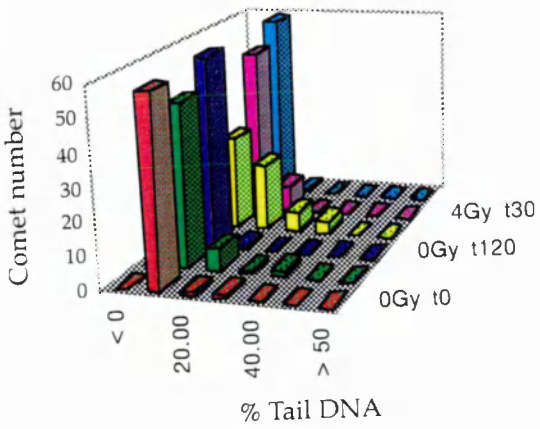

Control 24

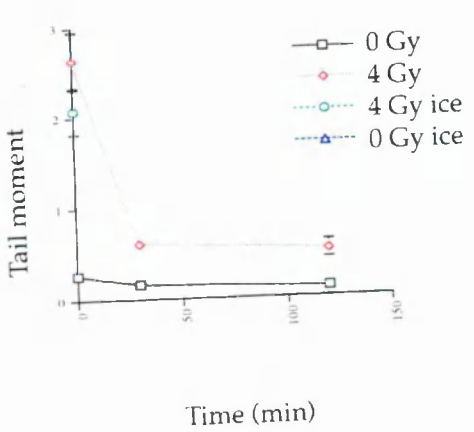

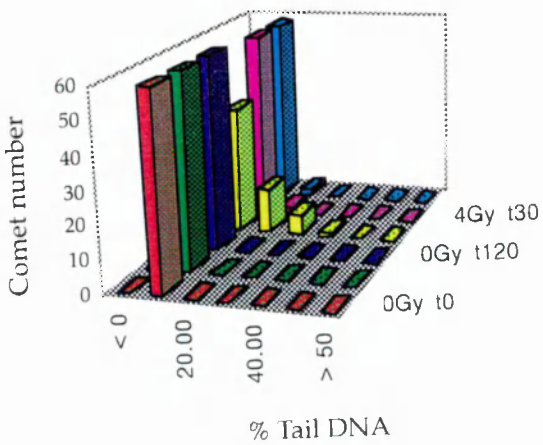

DNA damage profile

Tail DNA frequency histogram

Control 25

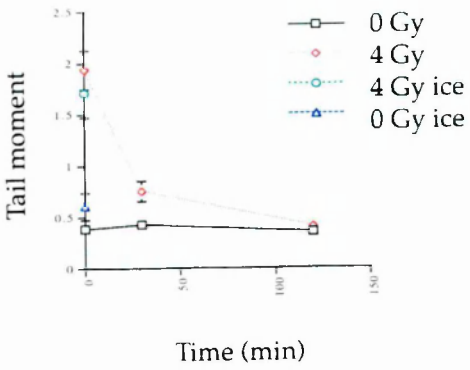

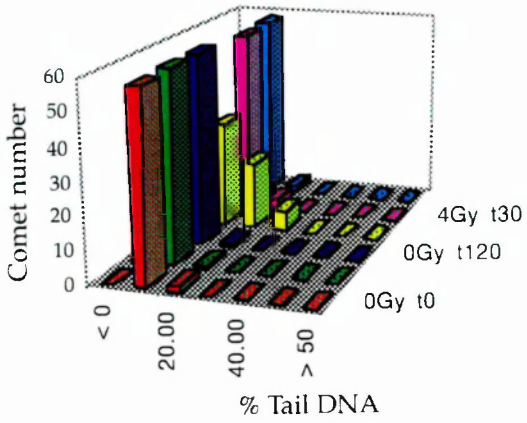

DNA damage profile

Tail DNA frequency histogram

Patient 1

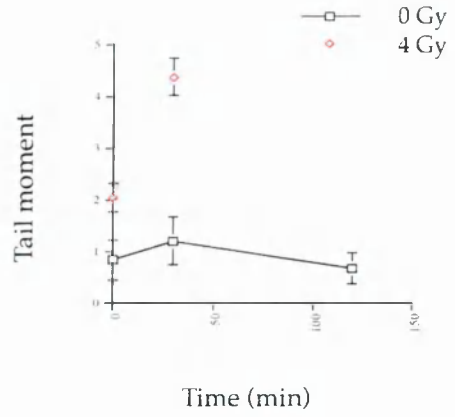

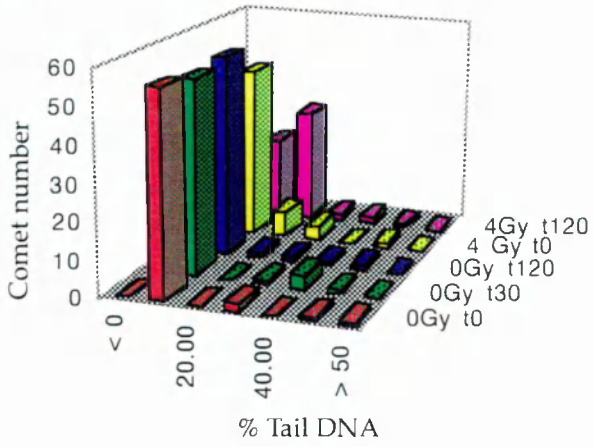

Patient 2

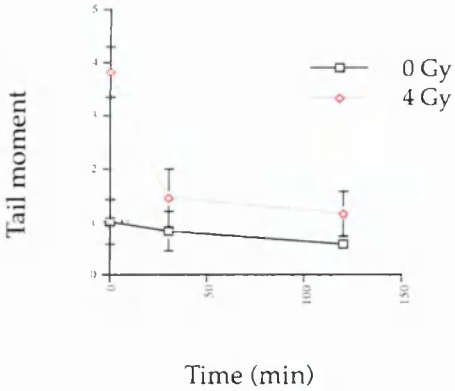

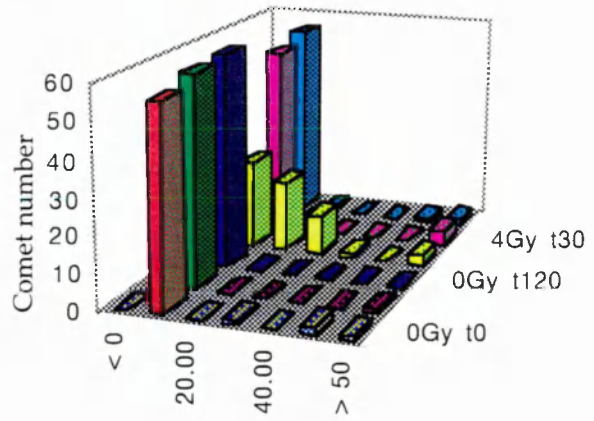

Patient 3

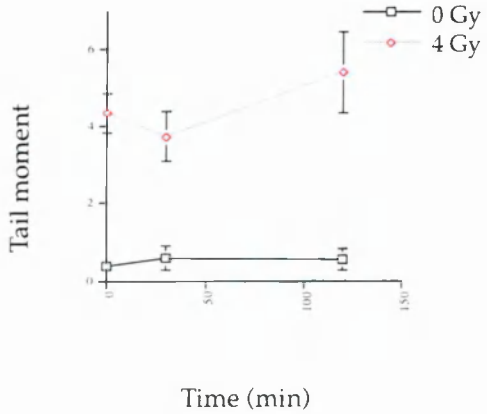

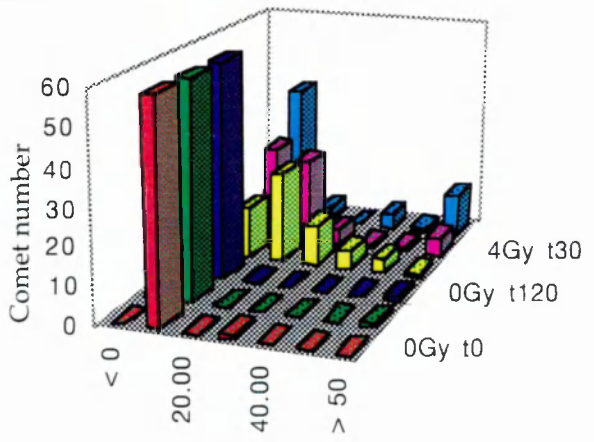

DNA damage profile

Tail DNA frequency histogram

Patient 4

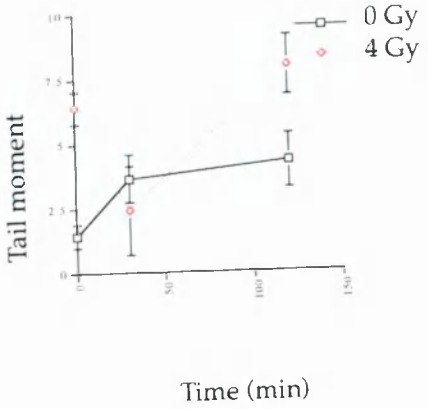

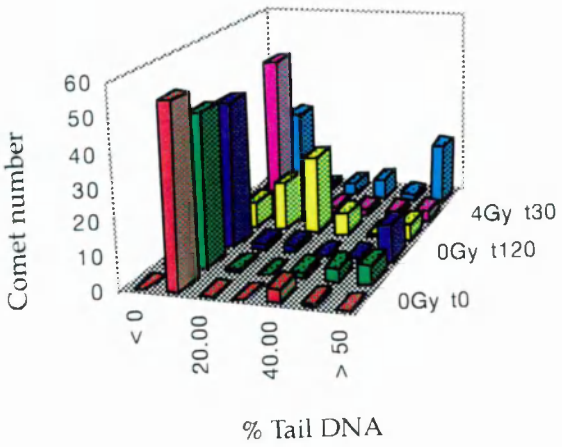

Patient 5

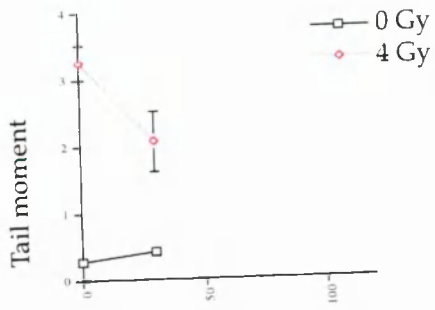

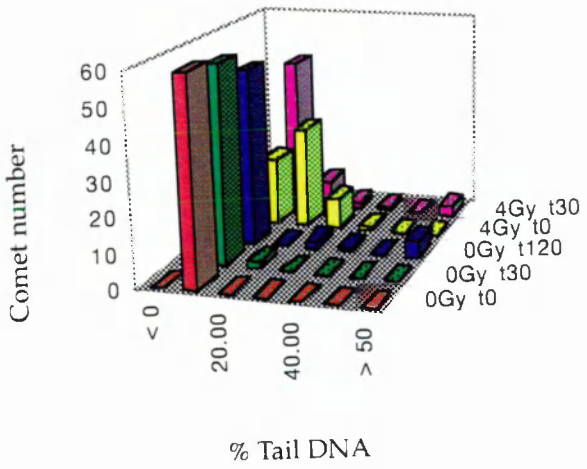

Patient 6

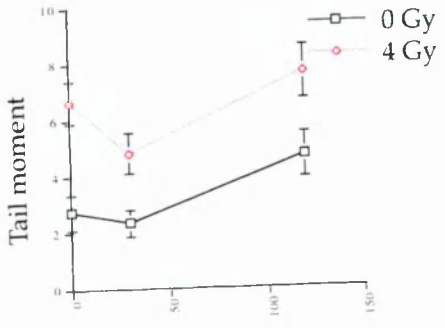

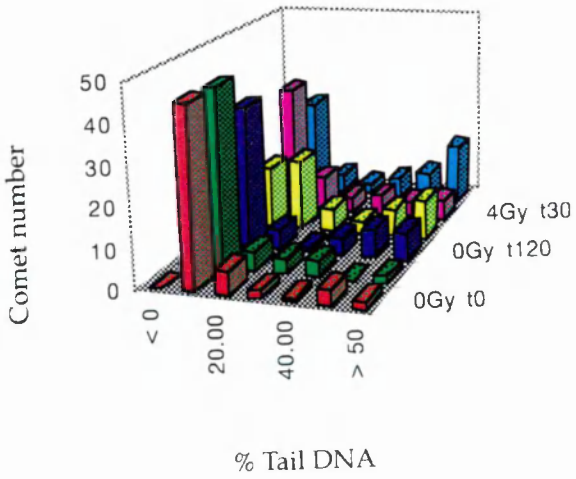

DNA damage profile

Tail DNA frequency histogram

Patient 7

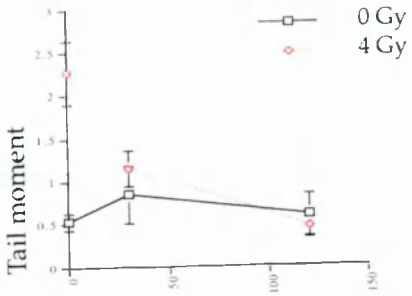

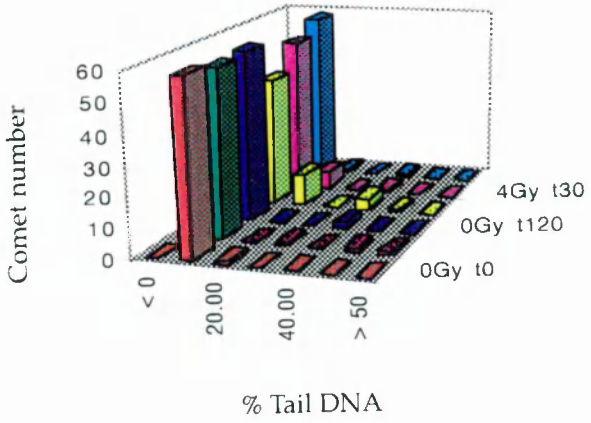

Patient 8

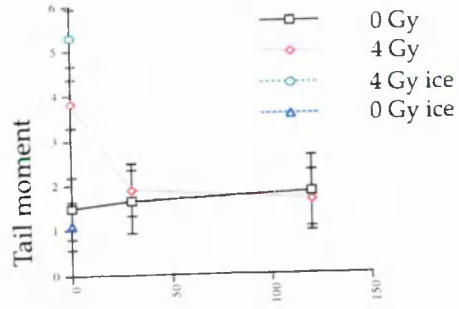

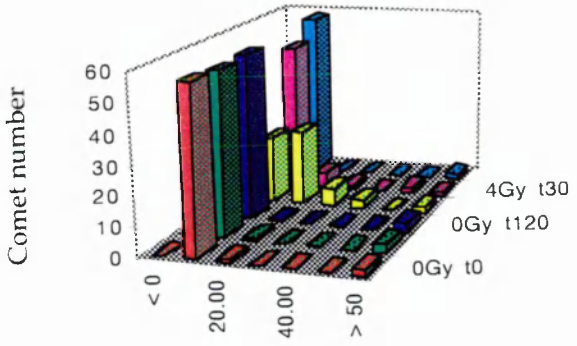

Patient 9

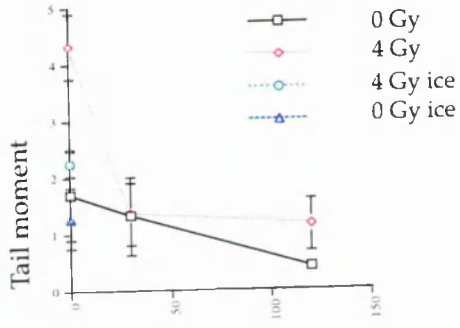

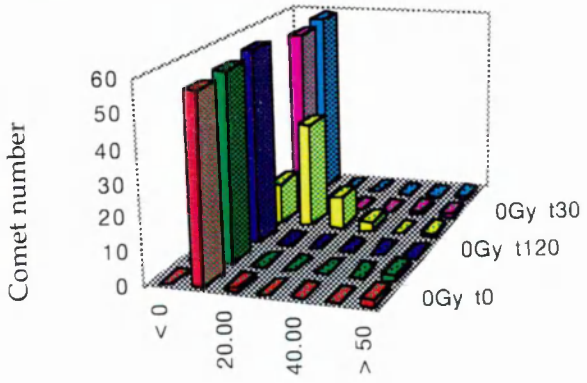

DNA damage profile

Tail DNA frequency histogram

Patient 10

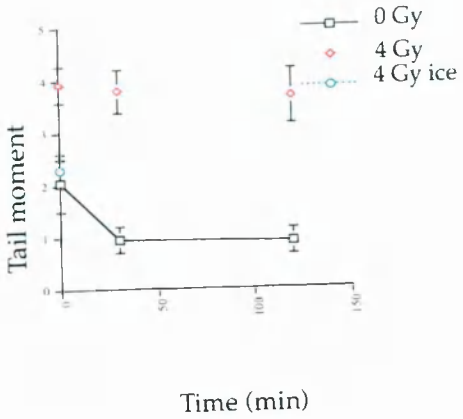

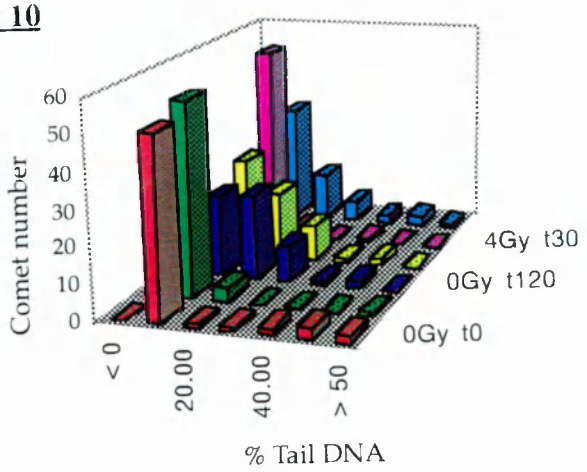

Patient 11

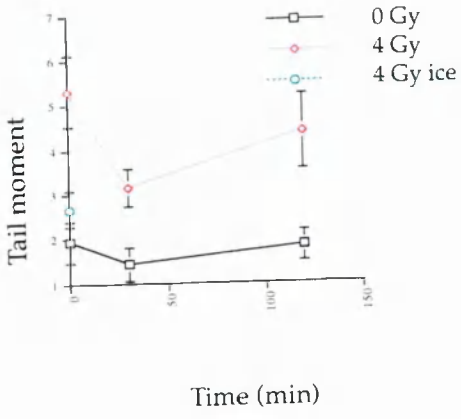

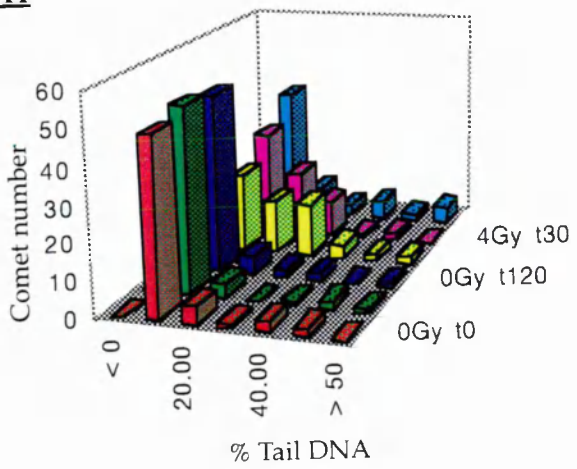

Patient 12

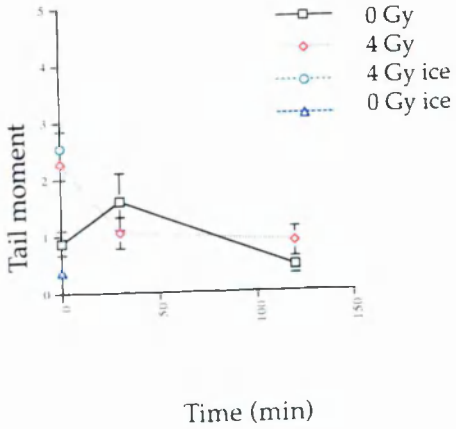

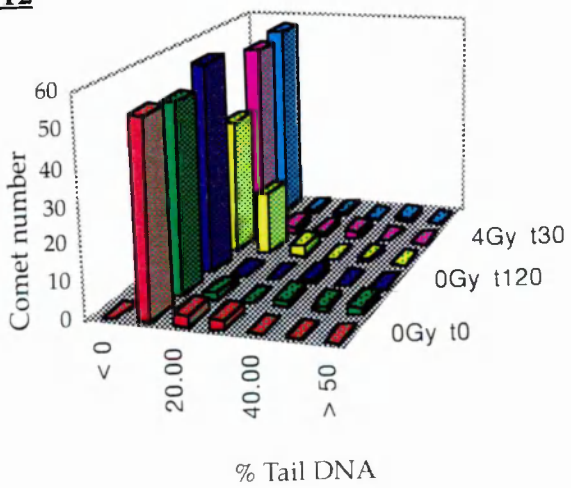

DNA damage profile

Tail DNA frequency histogram

Patient 13

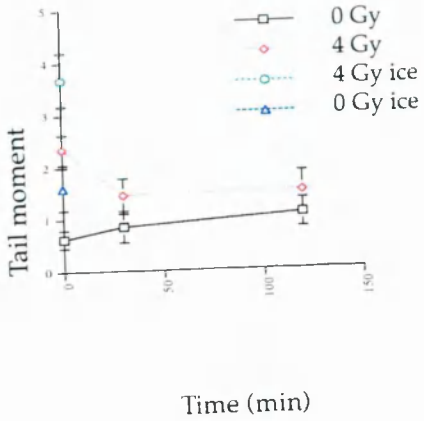

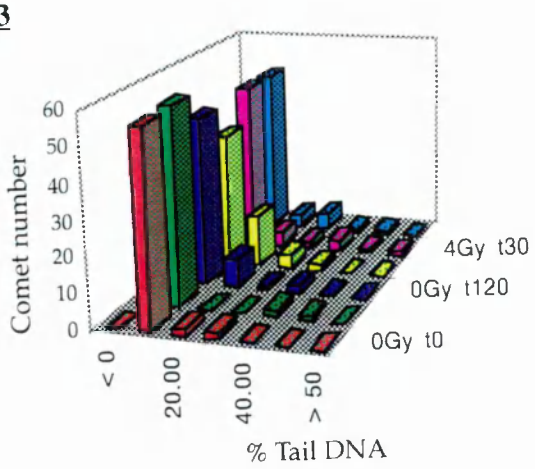

Patient 14

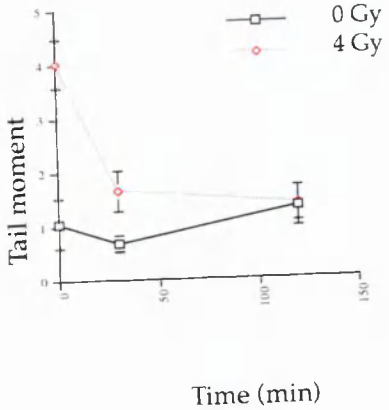

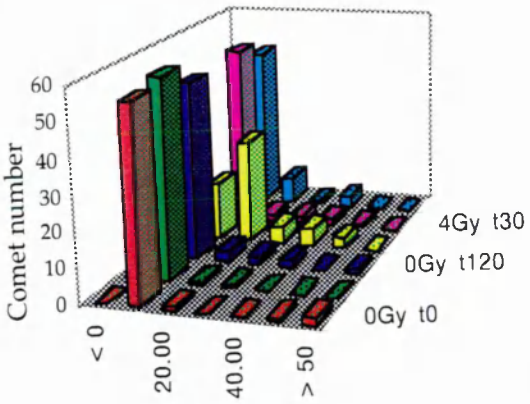

Patient 15

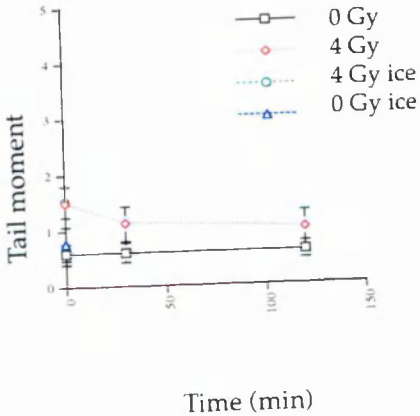

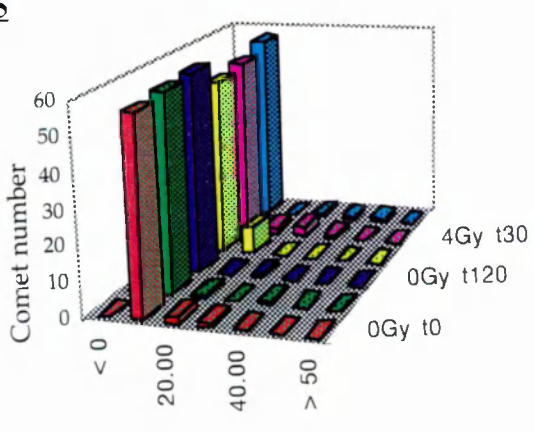

DNA damage profile **Tail DNA frequency histogram**

Patient 16

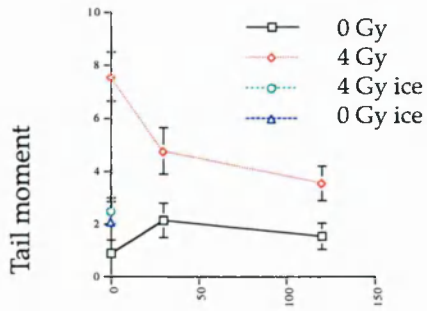

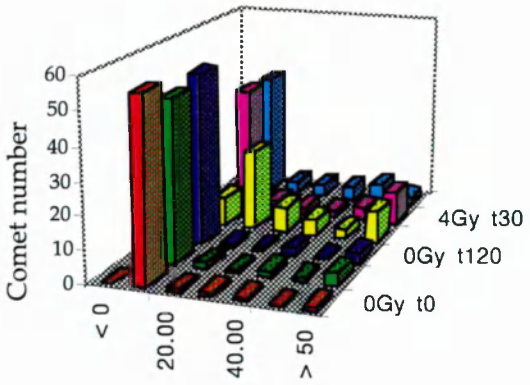

Patient 17

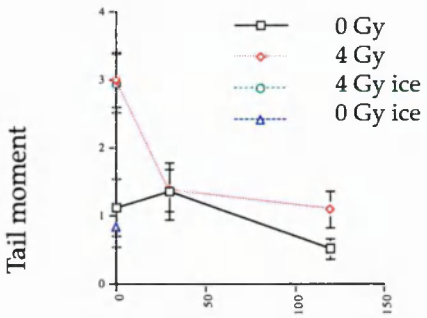

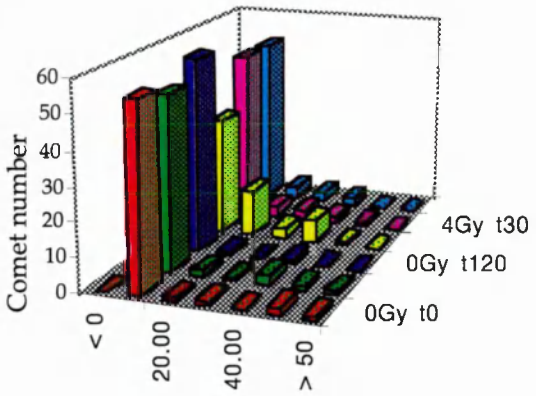

Patient 18

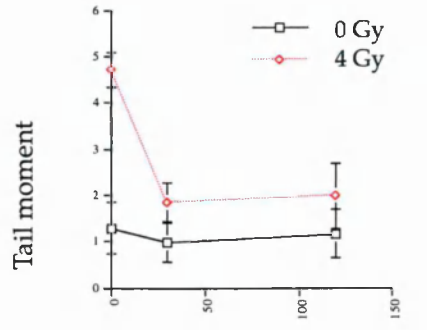

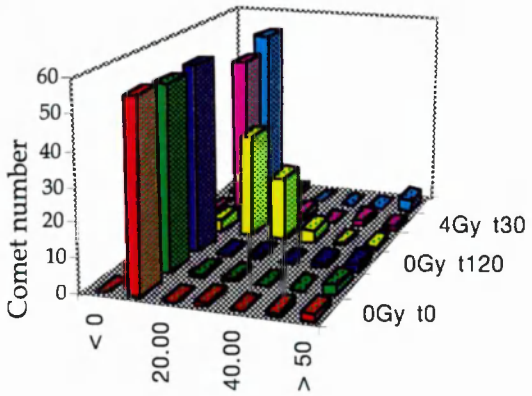

DNA damage profile

Tail DNA frequency histogram

Patient 19

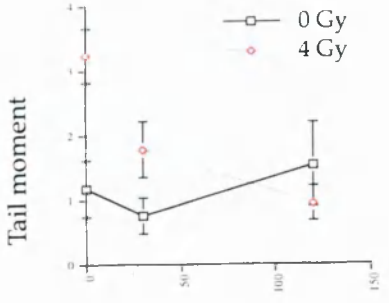

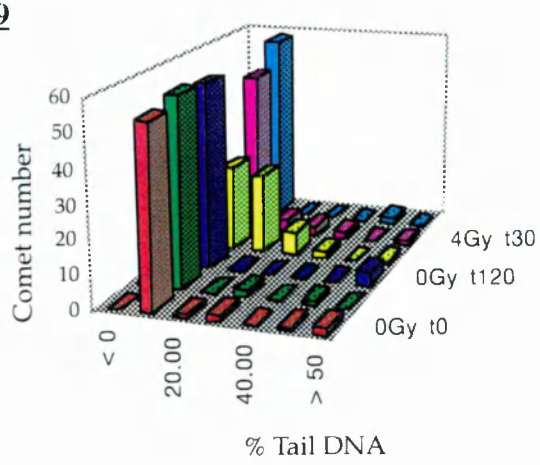

Patient 20

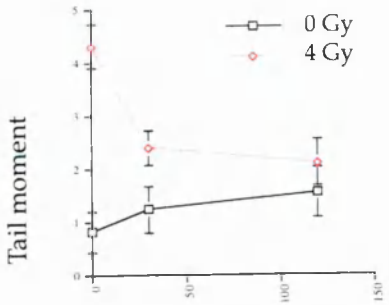

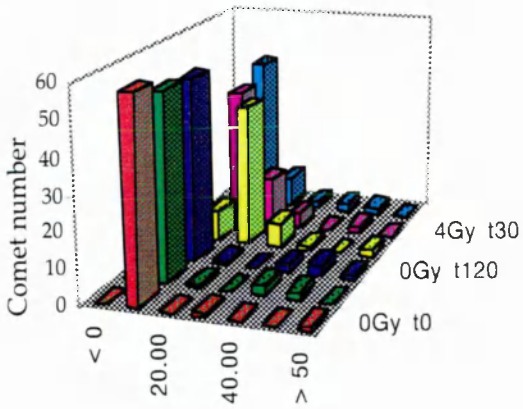

Patient 21

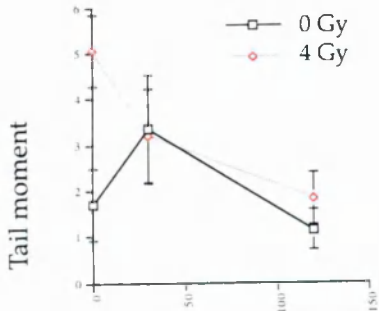

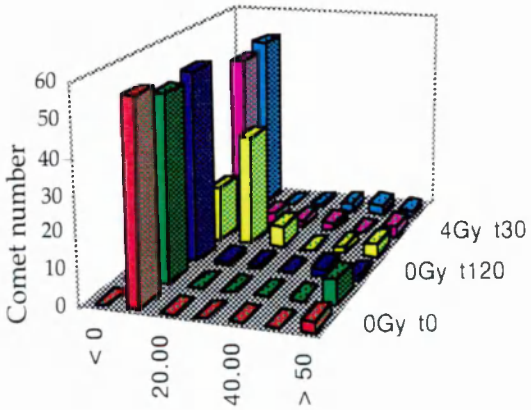

DNA damage profile

Tail DNA frequency histogram

Patient 22

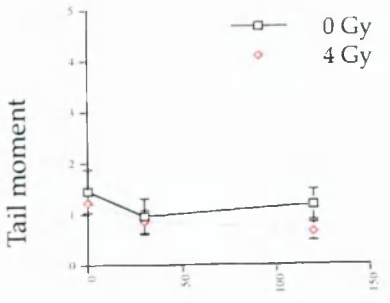

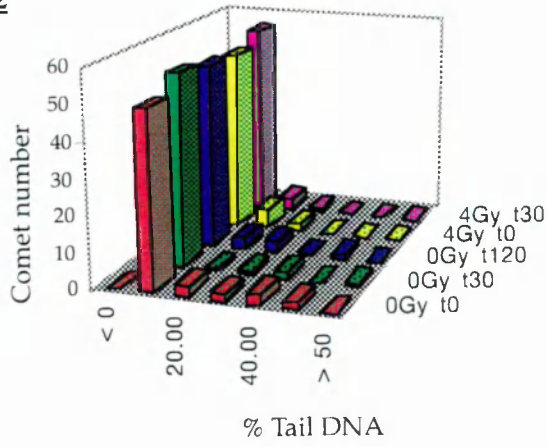

Patient 23

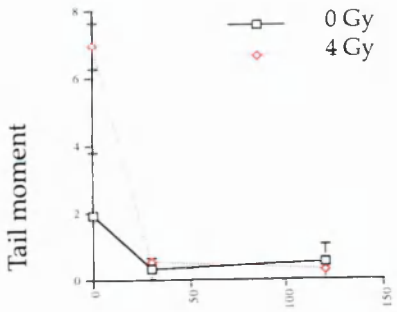

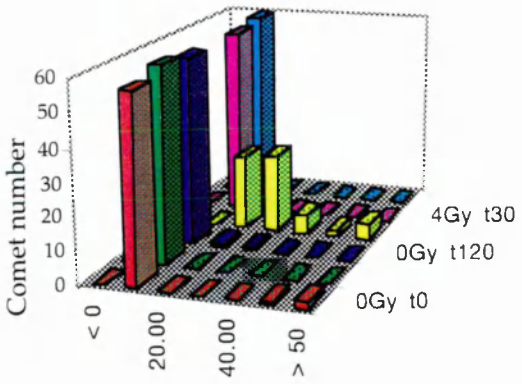

Patient 24

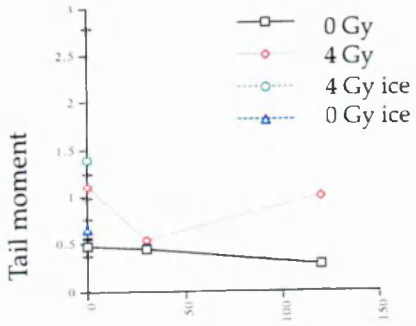

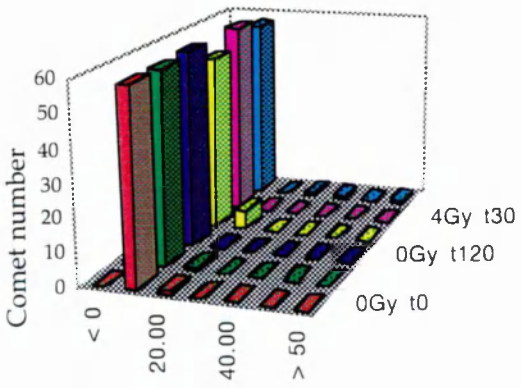

DNA damage profile **Tail DNA frequency histogram**

Patient 25

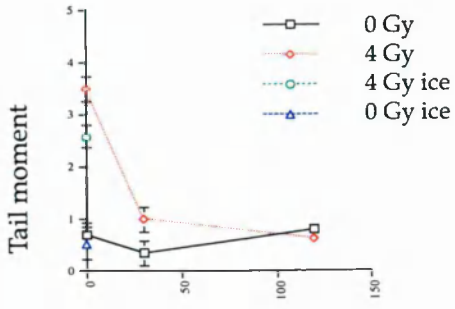

Time (min)

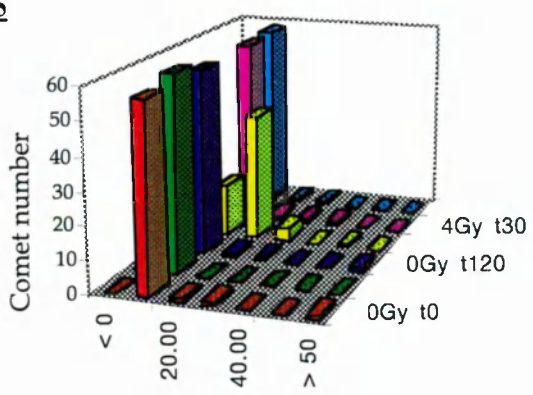

% Tail DNA

Patient 26

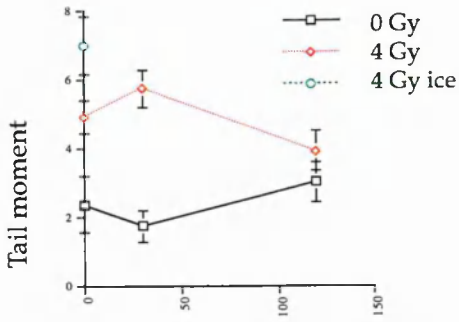

Time (min)

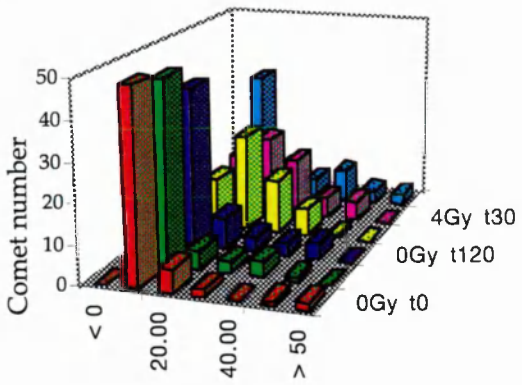

% Tail DNA

Patient 27

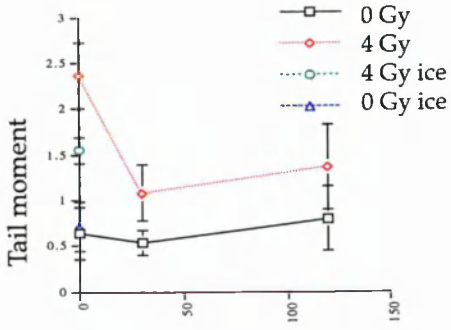

Time (min)

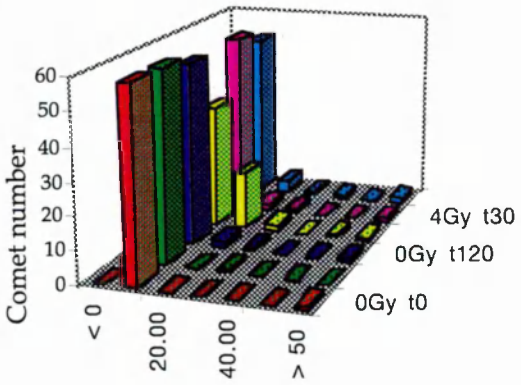

% Tail DNA

DNA damage profile

Tail DNA frequency histogram

Patient 28

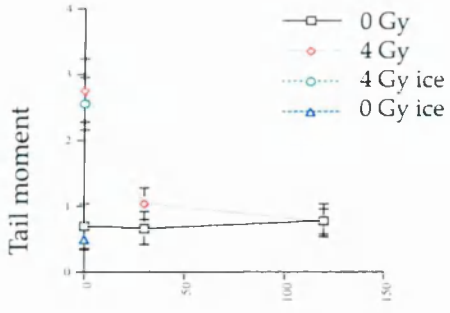

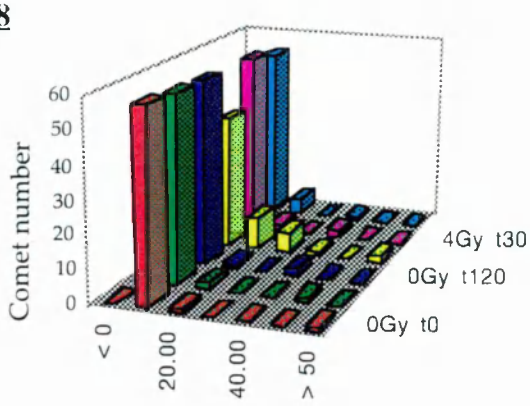

Patient 29

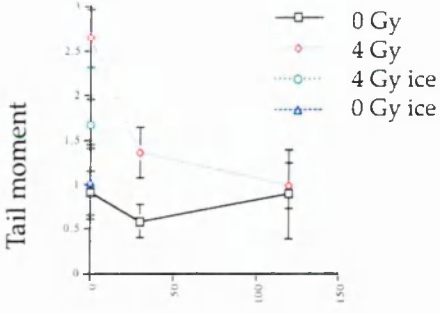

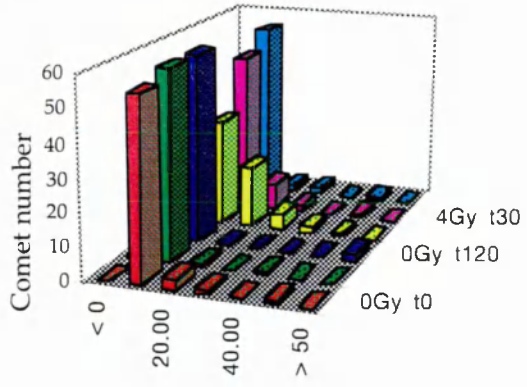

Patient 30

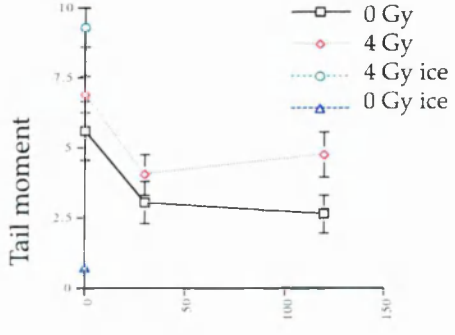

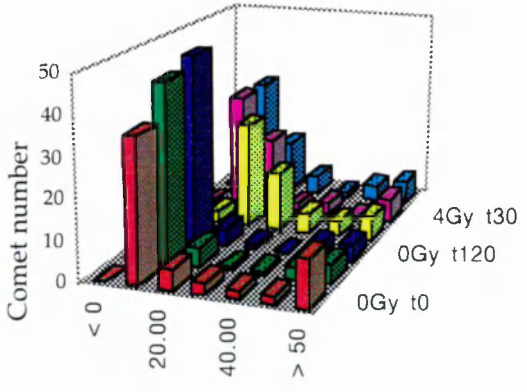

DNA damage profile **Tail DNA frequency histogram**

Patient 31

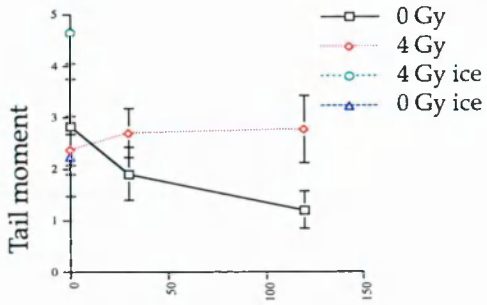

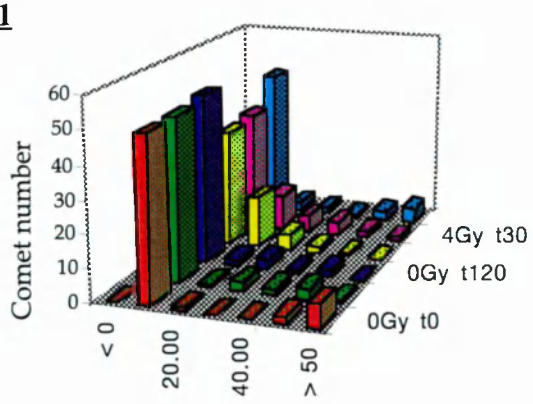

Patient 32

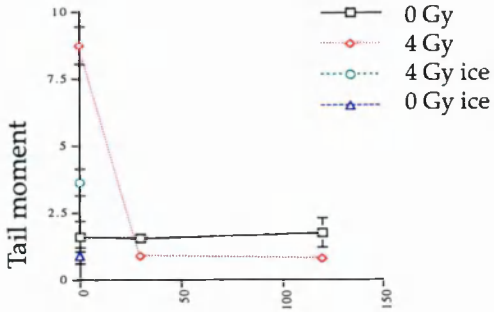

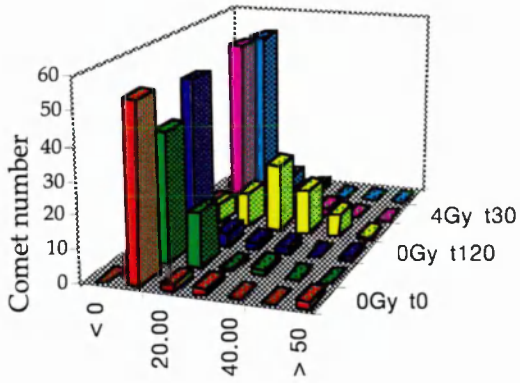

Patient 33

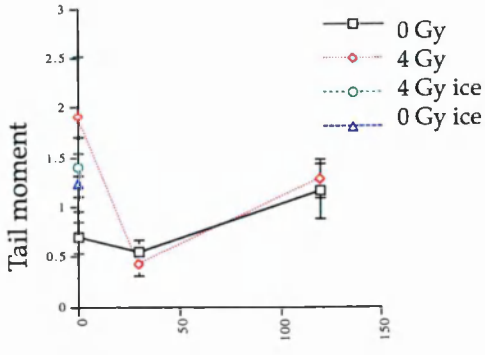

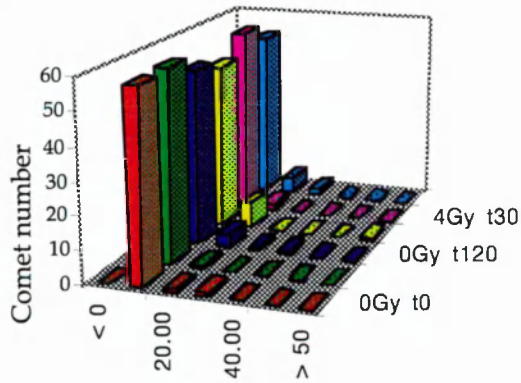

Bibliography

Aaltonen, L. A., Peltomaki, P., Leach, F. S., Sistonen, P., Pylkkanen, L., Mecklin, J.-P., Jarvinen, H., Powell, S. M., Jen, J., Hamilton, S. R., Petersen, G. M., Kinzler, K. W., Vogelstein, B., and Chapelle, A. D. L. (1993). Clues to the pathogenesis of familial colorectal cancer. Science *260*, 812-816.

Abadir, R., and Hakami, N. (1983). Ataxia telangiectasia with cancer. An indication for reduced radiotherapy and chemotherapy doses. British Journal of Radiology *56*, 343-5.

Acharya, S., Wilson, T., Gradia, S., Kane, M. F., Guerrette, S., Marsischky, G. T., Kolodner, R., and Fishel, R. (1996). hMSH2 forms specific mispair-binding complexes with hMSH3 and hMSH6. Proceedings of the National Academy of Sciences of the United States of America *93*, 13629-34.

Albers, M., Williams, R., Brown, E. J., Tanaka, A., Hall, F. L., and Schreiber, S. L. (1993). FKBP-rapamycin inhibits a cyclin-dependent kinase activity and a cyclin D1-cdk association in early G1 of an osteosarcoma cell line. Journal of Biological Chemistry *286*, 22825-22829.

Andersen, T. I. (1996). Genetic heterogeneity in breast cancer susceptibility. Acta Oncologica *35*, 407-10.

Anderson, D., Yu, T.-W., Dobrzynska, M. M., Ribas, G., and Marcos, R. (1997). Effects in the comet assay of storage conditions on human blood. Teratogenesis, Carcinogenesis and Mutagenesis *17*, 115-125.

Antoccia, A., Chessa, L., Ricordy, R., and Tanzarella, C. (1995). Modulation of radiation-induced chromosomal damage by inhibitors of DNA repair and flow cytometric analysis in ataxia telangiectasia cells with 'intermediate radiosensitivity'. Mutagenesis *10*, 523-9.

Appleby, J. M., Barber, J. B. P., Levine, E., Varley, J. M., Stankovic, T., Heighway, J., Warren, C., and Scott, D. (1997). Absence of mutations in the ATM gene in breast cancer patients with severe responses to radiotherapy. British Journal of Cancer *76*, 1546-1549.

Arlett, C. F., and Priestley, A. (1985). An assessment of the radiosensitivity of ataxia-telangiectasia heterozygotes. Kroc Foundation Series *19*, 101-9.

Athma, P., Rappaport, R., and Swift, M. (1996). Molecular genotyping shows that ataxia-telangiectasia heterozygotes are predisposed to breast cancer. Cancer Genetics & Cytogenetics *92*, 130-4.

Ausubel, F., Brent, R., Kingston, R., Moore, D. D., Seidman, J. G., Smith, J. A., and Struhl, K. (1997). Current Protocols in Molecular Biology: John Wiley and Sons Inc.).

Banin, S., Moyal, L., Shieh, S.-Y., Taya, C., Anderson, W., Chessa, L., Smorodinsky, I., Prives, C., Reiss, Y., Shiloh, Y., Ziv, Y. (1998). Enhanced phosphorylation of p53 by ATM in response to DNA damage. Science *281* 1674-1677.

Barzilay, G., and Hickson, I. D. (1995). Structure and function of apurinic /apyrimidinic endonucleases. Bioessays *17*, 713-719.

Baskaran, R., Wood, L. D., Whitaker, L. L., Canman, C. E., Morgan, S. E., Xu, Y., Barlow, C., Baltimore, D., Wynshaw-Boris, A., Kastan, M. B., and Wang, J. Y. J. (1997). Ataxia-telangiectasia mutant protein activates c-Abl tyrosine kinase in response to ionizing radiation. Nature, 516-519.

Belmaaza, A., and Chartrand, P. (1994). A review: One stranded invasion events in homologous recombination at double strand breaks. Mutation Research *314*, 199-208.

Bentley, N. J., Holtzman, D. A., Flaggs, G., Keegan, K. S., DeMaggio, A., Ford, J. C., Hoekstra, M., and Carr, A. M. (1996). The *Schizosaccharomyces pombe rad 3* checkpoint. The EMBO Journal *15*, 6641-6651.

Bieche, I., and Lidereau, R. (1995). Genetic alterations in breast cancer. Genes , Chromosomes and Cancer *14*, 227-251.

Bishop, D. T., and Hopper, J. (1997). AT-tributable risks? Nature Genetics *15*, 226-226.

Bodmer, W. (1988). Somatic cell genetics and cancer. Cancer Surveys *7*, 239-250.

Bork, P., Hoffman, K., Bucher, P., Neuwald, A. F., Altschul, S. F., and Koonin, E. V. (1997). A superfamily of conserved domains in DNA damage-responsive cell cycle checkpoint proteins. FASEB Journal *11*, 68-76.

Borresen, A. L., Andersen, T. I., Tretli, S., Heiberg, A., and Moller, P. (1990). Breast cancer and other cancers in Norwegian families with ataxia-telangiectasia. Genes, Chromosomes & Cancer 2, 339-40.

Broughton, B. C., Steingrimsdottir, H., Weber, C. A., and Lehmann, A. R. (1994). Mutations in the xeroderma pigmentosum group D DNA repair/transcription gene in patients with trichothiodystrophy. Nature Genetics *7*, 189-94.

Broughton, B. C., Thompson, A. F., Harcourt, S. A., Vermeulen, W., Hoeijmakers, J. H., Botta, E., Stefanini, M., King, M. D., Weber, C. A., Cole, J., and et al. (1995). Molecular and cellular analysis of the DNA repair defect in a patient in xeroderma pigmentosum complementation group D who has the clinical features of xeroderma pigmentosum and Cockayne syndrome. [Review] [44 refs]. American Journal of Human Genetics *56*, 167-74.

Brown, E. J., Albers, M. W., Shim, T. B., Ichikawa, K., Keith, C. T., Lane, W. S., and Schreiber, S. L. (1994). A mammalian protein targeted by a G1-arresting rapamycin-receptor complex. Nature *369*, 756-758.

Brown, E. J., Beal, P. A., Keith, C. T., Chen, J., Shin, T. B., and Schreiber, S. L. (1995). Control of p70 S6 kinase by the kinase activity of FRAP in vivo. Nature *377*, 441-446.

Brown, K. D., Ziv, Y., Sadanandan, S. N., Chessa, L., Collins, F. S., Shiloh, Y., and Tagle, D. A. (1997). The ataxia-telangiectasia gene product , a constitutively expressed nuclear protein that is not up-regulated following genome damage. Proceedings of the National Academy of Science, USA *94*, 1840-1845.

Brunn, G. J., Hudson, C. C., Sekulic, A., Williams, J. M., Hosoi, H., Houghton, P. J., Lawrence, J. C., and Abraham, R. T. (1997). Phosphorylation of the translational repressor PHAS-I by the mammalian target of Rapamycin. Science *277*, 99-101.

Buchwald, M., Joenje, H., and Auerbach, A. (1997). Fanconi anaemia. In Metabolic and molecular basis of inherited disease, B. Vogelstein and K. W. Kinzler, eds. (New York: McGraw-Hill).

Byrd, P. J., McConville, C. M., Cooper, P., Parkhill, J., Stankovic, T., McGuire, G. M., Thick, J. A., and Taylor, A. M. (1996). Mutations revealed by sequencing the 5' half of the gene for ataxia telangiectasia. Human Molecular Genetics *5*, 145-9.

Callahan, R., and Campbell, G. (1989). Mutations in human breast cancer: An overview. Journal of the National Cancer Institute *81*, 1780.

Camerini-Otero, R. D., and Hsieh, P. (1995). Homologous recombination proteins in prokaryotes and eukaryotes. Annual Reviews in Genetics *29*, 509-552.

Canman, C., Lim, D-S., Cimprich, K., Taya, Y., Tamai, K., Sakaguchi, K., Appella, E., Kastan, M., Siciliano, J. (1998). Activation of the ATM kinase by ionizing radiation and phosphorylation of p53. Science *281*, 1677-1679.

Carney, J. P., Maser, R. S., Olivares, H., Davis, E. M., Beau, M. L., III, J. R. Y., Hays, L., Morgan, W. F., and Petrini, J. H. J. (1998). The hMre11/hRad50 protein complex and Nijmegen breakage syndrome: Linkage of double-strand break repair to the cellular DNA damage response. Cell *93*, 477-486.

Carpenter, C. L., Auger, K. R., Duckworth, B. C., Hou, W.-M., Schaffhausen, B., and Cantley, L. C. (1993). A tightly associated serine/threonine protein kinase regulates phosphoinositide 3-kinase activity. Molecular Cell Biology *13*, 1657-1665.

Chan, D. W., and Lees-Miller, S. P. (1996). The DNA dependent protein kinase is inactivated by autophosphorylation of the catalytic subunit. Journal of Biological Chemistry *271*, 8936-8941.

Chapman, M. S., and Verma, I. M. (1996). Transcriptional activation by BRCA1. Nature *382*, 678-679.

Chen, G., and Lee, E. Y.-H. P. (1996). The product of the ATM gene is a 370 kDa nuclear phosphoprotein. Journal of Biological Chemistry *271*, 33693-33697.

Chen, J., Birkholtz, G. G., Lindblom, P., Rubio, C., and Lindblom, A. (1998). The role of ataxia-telangiectasia heterozygotes in familial breast cancer. Cancer Research *58*, 1376-1379.

Cleaver, J. E. (1968). Defective repair replication of DNA in xeroderma pigmentosum. Nature *218*, 652-656.

Collins, A., Dusinska, M., Franklin, M., Somorovska, M., Petrovska, H., Duthie, S., Fillion, L., Panayiotidis, M., Raslova, K., and Vaughan, N. (1997). Comet assay in human biomonitoring studies: Reliability, validation and applications. Environmental and Molecular Mutagenesis *30*, 139-146.

Collins, A. R., Dobson, V. L., Dusinska, M., Kennedy, G., and Stetina, R. (1997). The comet assay: what can it really tell us? Mutation Research *375*, 183-193.

Collins, N., McManus, R., Wooster, R., Mangion, J., Seal, S., Lakhani, S., Ormiston, W., and Daly, P. (1995). Consistent loss of the wild-type allele in breast cancer from a family linked to the BRCA2 gene on chromosome 13q12-13. Oncogene *10*, 1673-1675.

Connor, F., Bertwistle, D., Mee, P. J., Ross, G. M., Swift, S., Grigorieva, E., Tybulewicz, V. L. J., and Ashworth, A. (1997). Tumorigenesis and a DNA repair defect in mice with a truncating Brca2 mutation. Nature Genetics *17*, 423-430.

F. A. B. C. Consortium (1996). Positional cloning of the Fanconi anaemia group A gene. Nature Genetics *14*, 324-328.

Cornforth, M. N., and Bedford, J. S. (1985). On the nature of a defect in cells from individuals with ataxia-telangiectasia. Science *227*, 1589-91.

Cortessis, V., Ingles, S., Millikan, R., Diep, A., Gatti, R. A., Richardson, L., Thompson, W. D., Paganini-Hill, A., Sparkes, R. S., and Haile, R. W. (1993). Linkage analysis of DRD2, a marker linked to the ataxia-telangiectasia gene, in 64 families with premenopausal bilateral breast cancer. Cancer Research *53*, 5083-6.

Cox, R. (1982). A cellular description of the repair defect in ataxia telangiectasia. In Ataxia telangiectasia - A cellular and molecular link between cancer, neuropathology and immune deficiency, B. A. Bridges and D. G. Harnden, eds. (Chichester: Wiley), pp. 141-153.

Cunliffe, P. N., Mann, J. R., Cameron, A. H., and Roberts, K. D. (1975). Radiosensitivity in ataxia-telangiectasia. British Journal of Radiology *48*, 374-376.

Curry, C. J., O'Lague, P., Tsai, J., Hutchison, H. T., Jaspers, N. G., Wara, D., Gatti, R. A., and Hutchison, H. T. (1989). ATFresno: a phenotype linking ataxia-telangiectasia with the Nijmegen breakage syndrome [published erratum appears in Am J Hum Genet 1989 Oct;45(4):663]. American Journal of Human Genetics *45*, 270-5.

Dahlberg, W. K., and Little, B. J. (1995). Response of dermal fibroblast cultures from patients with unusually severe responses to radiotherapy and from ataxia-telangiectasia heterozygotes to fractionated radiation. Clinics in Cancer Research *1*, 785-790.

Dar, M. E., Winters, T. A., and Jorgensen, T. J. (1997). Identification of defective illegitimate recombinational repair of oxidatively-induced DNA double strand breaks in ataxia-telangiectasia cells. Mutation Research *384*, 169-179.

Digweed, M., and Sperling, K. (1996). Molecular analysis of Fanconi anaemia. [Review] [59 refs]. Bioessays *18*, 579-85.

Digweed, M., Zakrzewski-Ludcke, S., and Sperling, K. (1988). Fanconi's anaemia: correlation of genetic complementation group with psoralen/UVA response. Human Genetics *78*, 51-4.

Duckworth-Rysiecki, G., Cornish, K., Clarke, C. A., and Buchwald, M. (1985). Identification of two complementation groups in Fanconi anemia. Somatic Cell & Molecular Genetics *11*, 35-41.

Dunderdale, H. J., and West, S. C. (1994). Recombination genes and proteins. Current Opinion in Genetics and Development *4*, 221-228.

Easton, D. F. (1994). Cancer risks in A-T heterozygotes. [Review] [22 refs]. International Journal of Radiation Biology *66*, S177-82.

Ellis, N. A., Groden, J., Ye, T. Z., Straughen, J., Lennon, D. J., Ciocci, S., Proytcheva, M., and German, J. (1995). The Bloom's syndrome gene product is homologous to RecQ helicases. Cell *83*, 655-66.

Ellis, N. A., Lennon, D. J., Proytcheva, M., Alhadeff, B., Henderson, E. E., and German, J. (1995). Somatic intragenic recombination within the mutated locus BLM can correct the high sister-chromatid exchange phenotype of Bloom syndrome cells [see comments] [published erratum appears in Am J Hum Genet 1996 Jan;58(1):254]. American Journal of Human Genetics *57*, 1019-27.

Fairburn, D. W., Olive, P. L., and O'Neill, K. L. (1995). The comet assay: A comprehensive review. Mutation Research *339*, 37-59.

Fishel, R., Lescoe, M. K., Rao, M. R., Copeland, N. G., Jenkins, N. A., Garber, J., Kane, M., and Kolodner, R. (1993). The human mutator gene homolog MSH2 and its association with hereditary nonpolyposis colon cancer [published erratum appears in Cell 1994 Apr 8;77(1):167]. Cell *75*, 1027-38.

Fitzgerald, M. G., Bean, J. M., Hegde, S. J., Unsal, H., MacDonald, D. J., Harkin, D. P., Finkelstein, D. M., Isselbacher, K. J., and Haber, D. A. (1997). Heterozygous ATM mutations do not contribute to early onset of breast cancer. Nature Genetics *15*, 307-310.

Foray, N., Priestley, A., Alsbeih, G., Badie, C., Capulas, E. P., Arlett, C. F., and Malaise, E. P. (1997). Hypersensitivity of ataxia telangiectasia fibroblasts to ionizing radiation is associated with a repair deficiency of DNA double-strand breaks. International Journal of Radiation Biology *72*, 271-283.

Ford, D., Easton, D. F., Bishop, D. T., Narod, S. A., and Goldgar, D. E. (1994). The Breast Cancer Linkage Consortium, risks of cancer in BRCA1-mutation carriers. Lancet *343*, 692-695.

Gangloff, S., McDonald, J. P., Bendixen, C., Arthur, L., and Rothstein, R. (1994). The yeast type I topoisomerase Top3 interacts with SGS1 a DNA helicase homolog: a potential eukaryotic reverse gyrase. Molecular Cell Biology *14*, 8391-8398.

German, J. (1993). Bloom syndrome: a mendelian prototype of somatic mutational disease. Medicine *72*, 393-406.

German, J. (1995). Bloom's syndrome. [Review] [19 refs]. Dermatologic Clinics *13*, 7-18.

German, J., and Passarge, E. (1989). Bloom's syndrome. XII. Report from the Registry for 1987. [Review] [65 refs]. Clinical Genetics *35*, 57-69.

German, J., Roe, A. M., Leppert, M. F., and Ellis, N. A. (1994). Bloom syndrome: an analysis of consanguineous families assigns the locus mutated to chromosome band 15q26.1. Proceedings of the National Academy of Sciences of the United States of America *91*, 6669-73.

Giannelli, F., Benson, P. F., Pawsey, S. A., and Polani, P. E. (1977). Ultraviolet light sensitivity and delayed DNA-chain maturation in Bloom's syndrome fibroblasts. Nature *265*, 466-469.

Gilad, S., Chessa, L., Khosravi, R., Russell, P., Galanty, Y., Piane, M., Gatti, R. A., Jorgensen, T. J., Shiloh, Y., and Bar-Shira, A. (1998). Genotype-phenotype relationships in ataxia-telangiectasia and variants. American Journal of Human Genetics *62*, 551-561.

Gilad, S., Khosravi, R., Shkedy, D., Uziel, T., Ziv, Y., Savitsky, K., Rotman, G., Smith, S., Chessa, L., Jorgensen, T. J., Harnik, R., Frydman, M., Sanal, O.,

Portnoi, S., Goldwicz, Z., Jaspers, N. G., Gatti, R. A., Lenoir, G., Lavin, M. F., Tatsumi, K., Wegner, R. D., Shiloh, Y., and Bar-Shira, A. (1996). Predominance of null mutations in ataxia-telangiectasia. Human Molecular Genetics *5*, 433-9.

Goss, P. E., and Sierra, S. (1998). Current perspectives on radiation-induced breast cancer. Journal of Clinical Oncology *16*, 338-347.

Gotoff, S. P., Amirmokri, E., and Liebner, E. J. (1967). Ataxia telangiectasia: Neoplasia, untoward response to x-irradiation, and tuberous sclerosis. American Journal of Diseases of Children *114*, 617-25.

Gottlieb, T. M., and Jackson, S. P. (1993). The DNA-dependent protein kinase: requirement for DNA ends and association with Ku antigen. Cell *72*, 131-142.

Gradia, S., Acharya, S., and Fishel, R. (1997). The human mismatch recognition complex hMSH2-hMSH6 functions as a novel molecular switch. Cell *91*, 995-1005.

Graham, F. L., and Eb, A. J. v. d. (1973). A new technique for the assay of infectivity of human adenovirus 5 DNA. Virology *52*, 456.

Greenwell, P. W., Kronmal, S. L., Porter, S. E., Gassenhuber, J., Obermaier, B., and Petes, T. D. (1995). *TEL1*, a gene involved in controlling telomere length in S. cerevisiae, is homologous to the human ataxia telangiectasia gene. Cell *82*, 823-829.

Gudmundsson, J., Johannesdottir, G., Bergthorsson, J., Arason, A., Ingvarsson, S., Eglisson, V., and Barkadottir, R. (1995). Different tumour types from BRCA2 gene carriers show wild-type chromosome deletions on 13q12q13. Cancer Research *55*, 4830-4832.

Hall, N. R., Murday, V. A., Chapman, P., Williams, M. A. T., Burn, J., Finan, P. J., and Bishop, D. T. (1994). Genetic linkage in Muir-Torre syndrome to the same chromosomal region as cancer family syndrome. European Journal of Cancer *30A*, 180-182.

Hand, R., and German, J. (1975). A retarded rate of DNA chain growth in Bloom's syndrome. Proceedings of the National Academy of Science USA *72*, 758-762.

Hang, B., Yeung, A. T., and Lambert, M. W. (1993). A damage-recognition protein which binds to DNA containing interstrand cross-links is absent or defective in Fanconi anemia, complementation group A, cells. Nucleic Acids Research *21*, 4187-92.

Hari, K. L., Santerre, A., Sekelsky, J. J., McKim, K. S., Boyd, J. B., and Hawley, R. S. (1995). The mei-41 gene of D. melanogaster is a structural and functional homolog of the human ataxia telangiectasia gene. Cell *82*, 815-21.

Harris, C. C. (1996). Structure and function of the p53 tumour suppressor gene: Clues for rational cancer therapeutic strategies. The Journal of the National Cancer Institute *88*, 1442-1455.

Hartley, K. O., Gell, D., Smith, G. C., Zhang, H., Divecha, N., Connelly, M. A., Admon, A., Lees-Miller, S. P., Anderson, C. W., and Jackson, S. P. (1995). DNA-dependent protein kinase catalytic subunit: a relative of phosphatidylinositol 3-kinase and the ataxia telangiectasia gene product. Cell *82*, 849-56.

Hawley, R. S., and Friend, S. H. (1996). Strange bedfellows in even stranger places: the role of ATM in meiotic cells, lymphocytes, tumors, and its functional links to p53 [comment]. [Review] [49 refs]. Genes & Development *10*, 2383-8.

Helliwell, S. B., Wagner, P., Kunz, J., Deuter-Reinhard, M., Henriquez, R., and Hall, M. N. (1994). TOR1 and TOR2 are structurally and functionally similar but not identical phosphatidylinositol kinase homologues in yeast. Molecular Biology of the Cell *5*, 105-118.

Henderson, L., Wolfreys, A., Fedyk, J., Bourner, C., and Windebank, S. (1998). The ability of the comet assay to discriminate between genotoxins and cytotoxins. Mutagenesis *13*, 89-94.

Hendrickson, E. A. (1997). Cell cycle regulation of mammalian DNA double-strand-break repair. American Journal of Human Genetics *61*, 795-800.

Hodgson, S. V., and Maher, E. R. (1993). Genetics of human cancers by site of origin. Reproductive system. Breast. In A practical guide to human cancer genetics (Cambridge: Cambridge University Press), pp. 58-63.

Hoffman, K., and Bucher, P. (1995). The FHA domain: a putative nuclear signalling domain found in protein kinases and transcription factors. Trends in Biochemical Sciences *20*, 347-349.

Honchel, R., Halling, K. C., and Thibodeau, S. N. (1995). Genomic instability in neoplasia. [Review] [49 refs]. Seminars in Cell Biology *6*, 45-52.

Huschtscha, L. I., and Holliday, R. (1983). Limited an unlimited growth of SV40-transformed cells from human diploid MRC-5 fibroblasts. Journal of Cell Science *63*, 77-99.

Itin, P. H., and Pittelkow, M. R. (1990). Trichothiodystrophy: Review of sulfur-deficient brittle hair syndromes and association with the ectodermal dysplasias. Journal of the American Academy of Dermatology 22, 705-717.

Jackson, S. P. (1996). DNA damage detection by DNA dependent protein kinase and related enzymes. Cancer Surveys *28: Genetic Instability in Cancer,* 261-279.

Jaloszynski, P., Kujawski, M., Czub-Swierczek, M., Markowska, J., and Szyfter, K. (1997). Bleomycin-induced DNA damage and its removal in lymphocytes of breast cancer patients studied by comet assay. Mutation Research *385,* 223-233.

Jeggo, P. A. (1997). DNA-PK: at the cross-roads of biochemistry and genetics. Mutation Research *384,* 1-14.

Jimenez, G., Yucel, J., Rowley, R., and Subramani, S. (1992). The rad3^{+} gene of *Schizosaccharomyces pombe* is involved in multiple checkpoint functions and in DNA repair. Proceedings of the National Academy of Science, USA *89,* 4952-4956.

Joenje, H., and Oostra, A. B. (1983). Effect of oxygen tension on chromosomal aberrations in Fanconi anaemia. Human Genetics *65,* 99-101.

Joenje, H., Oostra, A. B., Wijker, M., Summa, F. M. d., Berkel, C. G. M. v., Rooimans, M. A., Ebell, W., Weel, M. v., Pronk, J. C., Buchwald, M., and Arwert, F. (1997). Evidence for at Least Eight Fanconi Anemia Genes. American Journal of Human Genetics *61,* 940-944.

Jolly, K. W., Malkin, D., Douglass, E. C., Brown, T. F., and Sinclair, A. E. (1994). Splice-site mutation of the p53 gene in a family with hereditary breast-ovarian cancer. Oncogene *9*, 97-102.

Jones, C. J., and Wood, R. D. (1993). Preferential binding of the xeroderma pigmentosum group A complementing protein to damaged DNA. Biochemistry *32*, 12096-104.

Jones, L. A., Scott, D., Cowan, R., and Roberts, S. A. (1995). Abnormal radiosensitivity of lymphocytes from breast cancer patients with excessive normal tissue damage after radiotherapy: chromosome aberrations after low dose-rate irradiation. International Journal of Radiation Biology *67*, 519-28.

Jongmans, W., Vuillaume, M., Chrzanowska, K., Smeets, D., Sperling, K., and Hall, J. (1997). Nijmegen breakage syndrome cells fail to induce the p53-mediated DNA damage response following exposure to ionizing radiation. Molecular & Cellular Biology *17*, 5016-22.

Jung, M., Kondratyev, A., Lee, S. A., Dimtchev, A., and Dritschilo, A. (1997). *ATM* gene product phosphorylates IκB-α. Cancer Research *57*, 24-27.

Jung, M., Zhang, Y., Lee, S., and Dritschilo, A. (1995). Correction of radiation sensitivity in ataxia telangiectasia cells by a truncated I kappa B-alpha. Science *268*, 1619-21.

Kappeller, R., and Kantley, L. C. (1994). Phosphatidylinositol 3-kinase. Bioessays *16*, 565-576.

Karow, J. K., Chakraverty, R. K., and Hickson, I. D. (1997). The Bloom's syndrome gene product is a 3'-5' DNA helicase. Journal of Biological Chemistry *272*, 30611-30614.

Keegan, K. S., Holtzman, D. A., Plug, A. W., Christenson, E. R., Brainerd, E. E., Flaggs, G., Bentley, N. J., Taylor, E. M., Meyn, M. S., Moss, S. B., Carr, A. M., Ashley, T., and Hoekstra, M. F. (1996). The Atr and Atm protein kinases associated with different sites along meiotically pairing chromosomes. Genes and Development *10*, 2423-2437.

Keith, C. T., and Schreiber, S. L. (1998). PIK-related kinases: DNA repair, recombination, and cell cycle checkpoints. Science *270*, 50-51.

Kerangueven, F., Eisinger, F., Noguchi, T., Allione, F., Wargniez, V., Eng, C., Padberg, G., Theillet, C., Jacquemier, J., Longy, M., Sobol, H., and Birnbaum, D. (1997). Loss of heterozygosity in human breast carcinomas in the ataxia telangiectasia, Cowden disease and BRCA1 gene regions. Oncogene *14*, 339-47.

Khanna, K. K., Yan, J., Watters, D., Hobson, K., Beamish, H., Spring, K., Shiloh, Y., Gatti, R. A., and Lavin, M. F. (1997). Defective signaling through the B cell

antigen receptor in Epstein-Barr virus-transformed ataxia-telangiectasia cells. Journal of Biological Chemistry 272, 9489-95.

Kharbanda, S., Pandey, P., Jin, S., Inoue, S., Bharti, A., Yuan, Z.-M., Weichselbaum, R., Weaver, D., and Kufe, D. (1997). Functional interaction between DNA-PK and c-Abl in response to DNA damage. Nature *386*, 732-735.

Kinzler, K. W., and Vogelstein, B. (1996). Lessons from hereditary colorectal cancer. [Review] [97 refs]. Cell *87*, 159-70.

Klaude, M., Eriksson, S., Nygren, J., and Ahnstrom, G. (1996). The comet assay: mechanisms and technical considerations. Mutation Research *363*, 89-96.

Kraemer, K. H., Lee, M. M., and Scotto, J. (1987). Xeroderma pigmentosum. Cutaneous, ocular, and neurologic abnormalities in 830 published cases. Archives of Dermatology *123*, 241-50.

Kroll, D. J., and Rowe, T. C. (1991). Phosphorylation of DNA topoisomerase II in a human tumor cell line. Journal of Biological Chemistry *266*, 7957-7961.

Kupfer, G. M., Naf, D., Suliman, A., Pulsipher, M., and D'Andrea, A. D. (1997). The Fanconi anaemia proteins, FAA and FAC, interact to form a nuclear complex. Nature Genetics *17*, 487-490.

Laemmli, U. K. (1970). Cleavage of structural proteins during the asssembly of the head of bacteriophage T4. Nature 227, 680-685.

Lakin, N. D., Weber, P., Stankovic, T., Rottinghaus, S. T., Taylor, A. M., and Jackson, S. P. (1996). Analysis of the ATM protein in wild-type and ataxia telangiectasia cells. Oncogene *13*, 2707-16.

Lambert, M. W., Tsongalis, G. J., Lambert, W. C., Hang, B., and Parrish, D. D. (1992). Defective DNA endonuclease activities in Fanconi's anemia cells, complementation groups A and B. Mutation Research *273*, 57-71.

Lavin, M. F., Khanna, K. K., Beamish, H., Spring, K., Watters, D., and Shiloh, Y. (1995). Relationship of the ataxia-telangiectasia protein ATM to phosphoinositide 3-kinase. [Review] [22 refs]. Trends in Biochemical Sciences *20*, 382-3.

Lavin, M. F., and Shiloh, Y. (1996). Ataxia-telangiectasia: a multifaceted genetic disorder associated with defective signal transduction. [Review] [47 refs]. Current Opinion in Immunology *8*, 459-64.

Lawrence, J. C., and Abraham, R. T. (1997). PHAS/4E-BPs as regulators of mRNA translation and cell proliferation. Trends in Biochemical Sciences 22, 345-349.

Leach, F. S., Nicolaides, N. C., Papadopoulos, N., Liu, B., Jen, J., Parsons, R., Peltomaki, P., Sistonen, P., Aaltonen, L. A., Nystrom-Lahti, M., and et al. (1993). Mutations of a mutS homolog in hereditary nonpolyposis colorectal cancer. Cell *75*, 1215-25.

Lehmann, A. R., Thompson, A. F., Harcourt, S. A., and al, e. (1993). Cockayne's syndrome: Correlation of clinical features with cellular sensitivity of RNA synthesis to UV irradiation. Journal of Medical Genetics *30*, 679-682.

Levinson, G., and Gutman, G. A. (1987). High frequencies of short frameshifts in poly-CA/TG tandem repeats borne by bacterial M13 in Escherichia coli K-12. Nucleic Acids Research *15*, 5323-5338.

Lindahl, T. (1996). Genetic instability in Cancer, J. Tooze, ed. (Cold Spring Harbor: Cold Spring Harbor Laboratory Press).

Little, J. B., and Nagasawa, H. (1985). Effect of confluent holding on potentially lethal damage repair, cell cycle progression, and chromosomal aberrations in human normal and ataxia-telangiectasia fibroblasts. Radiation Research *101*, 81-93.

Liu, J. M., Buchwald, M., Walsh, C. E., and Young, N. S. (1994). Fanconi anemia and novel strategies for therapy. [Review] [149 refs]. Blood *84*, 3995-4007.

Lo Ten Foe, J. R., Rooimans, M. A., Bosnoyan-Collins, L., Alon, N., Wijker, M., Parker, L., Lightfoot, J., Carreau, M., Callen, D. F., Savoia, A., Cheng, N. C., van Berkel, C. G., Strunk, M. H., Gille, J. J., Pals, G., Kruyt, F. A., Pronk, J. C., Arwert, F., Buchwald, M., and Joenje, H. (1996). Expression cloning of a cDNA for the major Fanconi anaemia gene, FAA. Nature Genetics *14*, 320-3.

Loeb, L. (1991). Mutator phenotype may be required for multistage carcinogenesis. Cancer Research *51*, 3075-3079.

Lonn, U., Lonn, S., Nylen, U., Winblad, G., and German, J. (1990). An abnormal profile of DNA replication intermediates in Bloom's syndrome. Cancer Research *50*, 3141-5.

Lu, X., and Lane, D. P. (1993). Differential induction of transcriptionally active p53 following UV or ionizing radiation: defects in chromosome instability syndromes? Cell *75*, 765-78.

Lynch, H. T., Smyrk, T. C., Watson, P., Lanspa, S. J., Lynch, J. F., Lynch, P. M., Cavalieri, R. J., and Boland, C. R. (1993). Genetics, natural history, tumor spectrum, and pathology of hereditary nonpolyposis colorectal cancer: an updated review. [Review] [123 refs]. Gastroenterology *104*, 1535-49.

Man, S., Ellis, I. O., Sibbering, M., Blamey, R. W., and Brook, J. D. (1996). High levels of allele loss at the FHIT and ATM genes in non-comedo ductal

carcinoma in situ and grade I tubular invasive breast cancers. Cancer Research *56*, 5484-5489.

Matsuura, K., Balmukhanov, T., Tauchi, H., Weemaes, C., Smeets, D., Chrzsnowska, K., Endou, S., Matsuura, S., and Komatsu, K. (1998). Radiation induction of p53 in cells from Nijmegen breakage syndrome is defective but not similar to ataxia- telangiectasia. Biochemical and Biophysical Research Communications *242*, 602-607.

Matsuura, S., Weemaes, C., Smeets, D., Takami, H., Kondo, N., Sakamoto, S., Yano, N., Nakamura, A., Tauchi, H., Endo, S., Oshimura, M., and Komatsu, K. (1997). Genetic mapping using microcell-mediated chromosome transfer suggests a locus for Nijmegen breakage syndrome at chromosome 8q21-24. American Journal of Human Genetics *60*, 1487-94.

McConville, C. M., Stankovic, T., Byrd, P. J., McGuire, G. M., Yao, Q. Y., Lennox, G. G., and Taylor, M. R. (1996). Mutations associated with variant phenotypes in ataxia-telangiectasia. American Journal of Human Genetics *59*, 320-30.

McDaniel, L. D., and Schultz, R. A. (1992). Elevated sister chromatid exchange phenotype of Bloom syndrome cells is complemented by human chromosome

15. Proceedings of the National Academy of Sciences of the United States of America *89*, 7968-72.

McKelvey-Martin, V. J., Green, M. H. L., Schmezer, P., Pool-Zobel, B. L., Meo, M. P. D., and Collins, A. (1993). The single cell gel electrophoresis (comet assay): A European review. Mutation Research *288*, 47-63.

Metcalfe, J. A., Parkhill, J., Campbell, L., Stacey, M., Biggs, P., Byrd, P. J., and Taylor, A. M. (1996). Accelerated telomere shortening in ataxia telangiectasia. Nature Genetics *13*, 350-3.

Miki, Y., Swensen, J., Shattuck-Eidens, D., Futreal, P. A., Harshman, K., Tavtigain, S., Cochran, C., Bennet, L. M., Ding, W., Bell, R., Rosenthal, J., Hussey, C., Tran, T., McClure, M., Frye, C., Hattier, T., Phelps, R., Haugen-Strano, A., Katcher, H., Yakumo, K., Gholami, Z., Shaffer, D., Stone, S., Bayer, S., Wray, C., Bogden, R., Dayanath, P., Ward, J., Tonin, P., Narod, S., Bristow, P. K., Norris, F. H., Helverling, L., Morrison, P., Rosteck, P., Lai, M., Barrett, C. J., Lewis, C., Neuhausen, S., Cannon-Albright, L., Goldgar, D., Wiseman, R., Kamb, A., and Skolnick, M. H. (1994). A strong candidate for the breast and ovarian cancer susceptibility gene BRCA1. Science *266*, 66-71.

Millis, R. R., Hanby, A. M., and Girling, A. C. (1994). The Breast. In Diagnostic Surgical Pathology, S. S. Sternberg, ed. (New York: Raven Press Ltd.), pp. 323-407.

Milner, J., Ponder, B. A. J., Hughes-Davies, L., Seltmann, M., and Kouzarides, T. (1997). Transcriptional activation functions in Brca2 (scientific correspondence). Nature *386*, 772-773.

Miyagawa, K. (1998). Genetic instability and cancer. International Journal of Hematology *67*, 3-14.

Mizuta, R., Salle, J. M. L., Cheng, H., Shinohara, A., Ogawa, H., Copeland, N., Jenkins, N. A., Lalande, M., and Alt, F. W. (1997). RAB22 and RAB163/mouse BRCA2: proteins that interact specifically with the RAD51 protein. Proceedings of the National Academy of Science USA *94*, 6927-6932.

Morgan, S. E., Lovly, C., Pandita, T. K., Shiloh, Y., and Kastan, M. B. (1997). Fragments of ATM which have dominant-negative or complementing activity. Molecular & Cellular Biology *17*, 2020-9.

Morrell, D., Cromartie, E., and Swift, M. (1986). Mortality and cancer incidence in 263 patients with ataxia telangiectasia. J Natl Cancer Inst *77*, 89.

Morrell, D., Cromartie, E., and Swift, M. (1986). Mortality and cancer incidence in 263 patients with ataxia-telangiectasia. Journal of the National Cancer Institute *77*, 89-92.

Morrow, D. M., Tagle, D. A., Shiloh, Y., Collins, F. S., and Hieter, P. (1995). TEL1, an S. cerevisiae homolog of the human gene mutated in ataxia telangiectasia, is functionally related to the yeast checkpoint gene MEC1. Cell *82*, 831-40.

Moustacchi, E., Papadopoulo, D., Diatloff-Zito, C., and Buchwald, M. (1987). Two complementation groups of Fanconi's anemia differ in their phenotypic response to a DNA-crosslinking treatment. Human Genetics *75*, 45-7.

Myung, K., Braastad, C., He, D. M., and Hendrickson, E. A. (1998). KARP-1 is indrced by DNA damage in a p53 and ataxia telangiectasia mutated-dependent fashion. Proceedings of the National Academy of Science *95*, 7664-7669.

Myung, K., He, D. M., Lee, S. E., and Hendrickson, E. A. (1997). KARP-1: a novel leucine zipper protein expressed from the Ku 86 autoantigen locus is implicated in the control of DNA-dependent protein kinase activity. The EMBO Journal *16*, 3172-3184.

Natarajan, A. T., Obe, G., vanZeeland, A. A., Palitti, F., Meijers, M., and Verdegaal-Immerzeel, E. A. (1980). Molecular mechanisms involved in the production of chromosomal aberration.II. Utilization of neurospora endonuclease for the study of aberration production by X-ray in G1 and G2 studies of cell cycle. Mutation Research *69*, 293-305.

Norman, A., Kagan, A. R., and Chan, S. L. (1988). The importance of genetics for the optimisation of radiation therapy. American Journal of Clinical Oncology *11*, 84-88.

Nowell, P. C. (1976). The clonal evolution of tumor cell populations. Science *194*, 23-28.

O'Connell, M. J., Norbury, C., and Nurse, P. (1994). Premature chromatin condensation upon accumulation of NIMA. EMBO Journal *13*, 4926-4937.

O'Connor, R. D., and Linthicum, D. S. (1980). Mitogen receptor redistribution defects and concomitant absence of blastogenesis in ataxia-telangiectasia T lymphocytes. Clinical Immunology & Immunopathology *15*, 66-75.

Olive, P. L., Banath, J. P., and Durand, R. E. (1990). Heterogeneity in radiation-induced DNA damage and repair in tumor and normal cells measured using the "comet" assay. Radiation Research *122*, 86-94.

Olive, P. L., Frazer, G., and Banath, J. P. (1993). Radiation-induced apoptosis measured in TK6 human B lymphoblastoid cells using the comet assay. Radiation Research *136*, 130-136.

Ostling, O., and Johanson, K. J. (1984). Microelectrophoretic study of radiation-induced DNA damage in individual mammalian cells. Biochemical and Biophysical Research Communications *123*, 291-298.

Ouichi, T., Monteiro, A. N. A., August, A., Aaronson, S. A., and Hanafusa, H. (1998). BRCA1 regulates p53-dependent gene expression. Proceedings of the National Academy of Science of the United States of America *95*, 2302-2306.

Papadopoulo, D., Guillouf, C., Mohrenweiser, H., and Moustacchi, E. (1990). Hypomutability in Fanconi anemia cells is associated with increased deletion frequency at the HPRT locus. Proceedings of the National Academy of Sciences of the United States of America *87*, 8383-7.

Parshad, R., Price, F. M., Bohr, V. A., Cowans, K. H., Zujewski, J. A., and Sanford, K. K. (1996). Deficient DNA repair capacity, a predisposing factor in breast cancer. British Journal of Cancer *74*, 1-5.

Parshad, R., Sanford, K. K., and Jones, G. M. (1983). Chromatid damage after G2 phase x-irradiation of cells from cancer-prone individuals implicates deficiency in DNA repair. Proceedings of the National Academy of Sciences of the United States of America *80*, 5612-6.

Parshad, R., Tarone, R. E., Price, F. M., and Sanford, K. K. (1993). Cytogenetic evidence for differences in DNA incision activity in xeroderma pigmentosum group A, C and D cells after X-irradiation during G2 phase. Mutation Research *294*, 149-55.

Patel, K. J., Yu, V. P. C. C., Lee, H., Corcoran, A., Thistlethwaite, F. C., Evans, M. J., Colledge, W. H., Friedman, L. S., Ponder, B. A. J., and Venkitaraman, A. R. (1998). Involvement of Brca2 in DNA repair. Molecular Cell *1*, 347-357.

Paterson, M. C., Anderson, A. K., Smith, B. P., and Smith, P. J. (1979). Enhanced radiosensitivity of cultured fibroblasts from ataxia telangiectasia heterozygotes manifested by defective colony-forming ability and reduced DNA repair replication after hypoxic gamma-irradiation. Cancer Research *39*, 3725-34.

Peltomaki, P., Aaltonen, L. A., Sistonen, P., Pylkkanen, L., Mecklin, J.-P., Jarvinen, H., Green, J. S., Jass, J. R., Weber, J. L., Leach, F. S., Petersen, G. M., Hamilton, S. R., Chapelle, A. d. l., and Vogelstein, B. (1993). Genetic mapping of a locus predisposing to human colorectal cancer. Science *260*, 810-812.

Perez-Vera, P., Gonzalez-del Angel, A., Molina, B., Gomez, L., Frias, S., Gatti, R. A., and Carnevale, A. (1997). Chromosome instability with bleomycin and X-ray hypersensitivity in a boy with Nijmegen breakage syndrome. American Journal of Medical Genetics *70*, 24-7.

Piperakis, S. M., Visvardis, E.-E., Sagnou, M., and Tassiou, A. M. (1998). Effects of smoking and aging on oxidative DNA damage of human lymphocytes. Carcinogenesis *19*, 695-698.

Pippard, E. C., Hall, A. J., Barker, D. J., and Bridges, B. A. (1988). Cancer in homozygotes and heterozygotes of ataxia-telangiectasia and xeroderma pigmentosum in Britain. Cancer Research *48*, 2929-32.

Plug, A. W., Peters, A. H. F. M., Xu, Y., Keegan, K. S., Hoekstra, M. F., Baltimore, D., Boer, P. d., and Ashley, T. (1997). ATM and RPA in meiotic chromosome synapsis and recombination. Nature Genetics *17*, 457-461.

Plummer, S. J., Paris, M. J., Myles, J., Tubbs, R., Crowe, J., and Casey, G. (1997). Four regions of allelic imbalance on 17q12-qter associated with high-grade breast tumours. Genes, Chromosomes and Cancer *20*, 354-362.

Ponder, B. A. J. (1990). Inherited predisposition to cancer. Trends in Genetics *6*, 213-218.

Pronk, J. C., Gibson, R. A., Savoia, A., Wijker, M., Morgan, N. V., Melchionda, S., Ford, D., Temtamy, S., Ortega, J. J., Jansen, S., and et al. (1995). Localisation of the Fanconi anaemia complementation group A gene to chromosome 16q24.3. Nature Genetics *11*, 338-40.

Prosser, J., Porter, D., Coles, C., Condie, A., Thompson, A. M., Chetty, U., Steel, C. M., and Evans, H. J. (1992). Constitutional p53 mutation in a non-Li-Fraumeni family. Br J Cancer *65*, 527-528.

Ramsay, J., Birrell, G., and Lavin, M. (1996). Breast cancer and radiotherapy in ataxia-telangiectasia heterozygotes. Lancet *347*, 1627-.

ap Rhys, C. M. J., and Bohr, V. A. (1996). Mammalian DNA repair responses and genomic instability. In Stress-inducible cellular responses, U. Feige, R. I. Morimoto, I. Yahara and B. Polla, eds. (Basel, Switzerland: Birkhauser Verlag), pp. 289-305.

Ribeiro, G. G., Magee, B., Swindell, R., Harris, M., and Banerjee, S. S. (1993). The Christie Hospital breast conservation trial: an update at 10 years from inception. Clinical Oncology *5*, 278-283.

Risinger, J. I., Umar, A., Boyd, J., Berchuck, A., Kunkel, T. A., and Barrett, J. C. (1996). Mutation of MSH3 in endometrial cancer and evidence for its functional role in heteroduplex repair. Nature Genetics *14*, 102-5.

Rotman, G., and Shiloh, Y. (1997). Ataxia-telangiectasia: is ATM a sensor of oxidative damage and stress? Bioessays *19*, 911.

Rydberg, B., and Johanson, K. J. (1978). Estimation of DNA strand breaks in single mammalian cells. In DNA Repair Mechanisms, P. C. Hanwalt and E. C. Friedberg, eds. (New York: Academic Press), pp. 465-468.

Saar, K., Chrzanowska, K. H., Stumm, M., Jung, M., Nurnberg, G., Wienker, T. F., Seemanova, E., Wegner, R. D., Reis, A., and Sperling, K. (1997). The gene for the ataxia-telangiectasia variant, Nijmegen breakage syndrome, maps to a 1-cM interval on chromosome 8q21. American Journal of Human Genetics *60*, 605-10.

Sarasin, A., and Stary, A. (1997). Human cancer and DNA repair deficient diseases. Cancer Detection and Prevention *21*, 406-411.

Savitsky, K., Bar-Shira, A., Gilad, S., Rotman, G., Ziv, Y., Vanagaite, L., Tagle, D. A., Smith, S., Uziel, T., Sfez, S., and et al. (1995). A single ataxia telangiectasia gene with a product similar to PI-3 kinase [see comments]. Science *268*, 1749-53.

Savitsky, K., Platzer, M., Uziel, T., Gilad, S., Sartiel, A., Rosenthal, A., Elroy-Stein, O., Shiloh, Y., and Rotman, G. (1997). Ataxia-telangiectasia: structural diversity of untranslated sequences suggests complex post-transcriptional regulation of ATM gene expression. Nucleic Acids Research *25*, 1678-84.

Savitsky, K., Sfez, S., Tagle, D. A., Ziv, Y., Sartiel, A., Collins, F. S., Shiloh, Y., and Rotman, G. (1995). The complete sequence of the coding region of the

ATM gene reveals similarity to cell cycle regulators in different species. Human Molecular Genetics 4, 2025-2032.

Savoia, A., Zatterale, A., Del Principe, D., and Joenje, H. (1996). Fanconi anaemia in Italy: high prevalence of complementation group A in two geographic clusters. Human Genetics *97*, 599-603.

Schaeffer, L., Moncollin, V., Roy, R., Staub, A., Mezzina, M., Sarasin, A., Weeda, G., Hoeijmakers, J. H., and Egly, J. M. (1994). The ERCC2/DNA repair protein is associated with the class II BTF2/TFIIH transcription factor. EMBO Journal *13*, 2388-92.

Schaeffer, L., Roy, R., Humbert, S., Moncollin, V., Vermeulen, W., Hoeijmakers, J. H., Chambon, P., and Egly, J. M. (1993). DNA repair helicase: a component of BTF2 (TFIIH) basic transcription factor [see comments]. Science *260*, 58-63.

Schindler, D., and Hoehn, H. (1988). Fanconi anemia mutation causes cellular susceptibility to ambient oxygen. American Journal of Human Genetics *43*, 429-35.

Schu, P. V., Takegawa, K., Fry, M. J., Stack, J. H., Waterfield, M. D., and Emr, S. D. (1993). Phosphatidylinositol 3-kinase encoded by yeast VPS34 gene essential for protein sorting. Science *260*, 88-91.

Schwartz, J. L., Jordan, R., Sedita, B. A., Swenningson, M. J., Banath, J. P., and Olive, P. L. (1995). Differential sensitivity to cell killing and chromosome mutation induction by gamma rays in two human lymphoblastoid cell lines derived from a single donor: possible role of apoptosis. Mutagenesis *10*, 227-233.

Scott, D., Barber, J. B. P., Levine, E. L., Burrill, W., and Roberts, S. A. (1998). Radiation-induced micronucleus induction in lymphocytes identifies a high frequency of radiosensitive cases among breast cancer patients: a test for predisposition? British Journal of Cancer *77*, 614-620.

Scott, D., Spreadborough, A., Levine, E., and Roberts, S. A. (1994). Genetic predisposition in breast cancer [letter]. Lancet *344*, 1444.

Scott, S. P., Zhang, N., Khanna, K. K., Khromykh, A., Hobson, K., Watters, D., and Lavin, M. F. (1998). Cloning and expression of the ataxia-telangiectasia gene in baculovirus. Biochemical and Biophysical Research Communications *245*, 144-148.

Scully, R., Anderson, S. F., Chao, D. M., Wei, W. J., Ye, L. Y., Young, R. A., Livingston, D. M., and Parvin, J. D. (1997). BRCA1 is a component of the RNA polymerase II holoenzyme. Proceedings of the National Academy of Science USA *94*, 5605-5610.

Scully, R., Chen, J., Ochs, R. L., Keegan, K., Hoekstra, M., Feunteun, J., and Livingston, D. M. (1997). Cell *90*, 425-435.

Scully, R., Chen, J., Plug, A., Xiao, Y., Weaver, D., Feunteun, J., Ashley, T., and Livingston, D. M. (1997). Association of BRCA1 with Rad51 in mitotic and meiotic cells. Cell *88*.

Seaton, B. L., Yucel, J., Sunnerhagen, P., and Subramani, S. (1992). Isolation and characterization of the *Schizosaccharomyces pombe rad3* gene, involved in the DNA damage and DNA synthesis checkpoints. Gene *119*, 83-89.

Shafman, T., Khanna, K. K., Kedar, P., Spring, K., Kozlov, S., Yen, T., Hobson, K., Gatei, M., Zhang, N., Watters, D., Egerton, M., Shiloh, Y., Kharbanda, S., Kufe, D., and Lavin, M. F. (1997). Interaction between ATM protein and c-Abl in response to DNA damage [see comments]. Nature *387*, 520-3.

Sharan, S. K., Morimatsu, M., Albrecht, U., Lim, D., Regel, E., Dinh, C., Sands, A., Eichele, G., Hasty, P., and Bradley, A. (1997). Embyonic lethality and radiation hypersensitivity mediated by Rad51 in mice lacking Brca2. Nature *386*, 804-810.

Sheng, Y. Z., Pero, R. W., Olsson, A. R., Bryngelsson, C., and Hua, J. Y. (1998). DNA repair enhancement by a combined supplement of carotenoids, nicotinamide and zinc. Cancer Detection and Prevention *22*, 284-292.

Shieh, S.-Y., Ikeda, M., Taya, Y., and Prives, C. (1997). DNA damage-induced phosphorylation of p53 alleviates inhibition by MDM2. Cell *91*, 325-334.

Sideransky, D., Tokino, T., and Helzisouer, K. (1992). Inherited p53 mutations in breast cancer. Cancer Research *52*, 2984-2986.

Singh, N. P. (1996). Microgel electrophoresis of DNA from individual cells: Principles and methodology. In Technologies for detection of DNA damage and mutations, G. P. Pfeifer, ed. (New York: Plenum Press), pp. 3-24.

Singh, N. P., McCoy, M. T., and Tice, R. R. (1988). A simple technique for quantitation of low levels of DNA damage in individual cells. Experimental Cell Research *175*, 184-191.

Singh, N. P., and Stephens, R. E. (1986). A novel technique for viable cell determinations. Stain Technology *61*, 315-318.

Somasundaram, K., Zang, H., Zeng, Y.-X., Houvras, Y., Peng, Y., Zhang, H., Wu, G. S., Licht, J., Weber, B. L., and El-Deiry, W. S. (1997). Arrest of the cell cycle by the tumour-suppressor BRCA1 requires the CDK-inhibitor p21 WAF1/CIP1. Nature *389*, 187-190.

Sprung, C. N., Bryan, T. M., Reddel, R. R., and Murnane, J. P. (1997). Normal telomere maintenance in immortal ataxia-telangiectasia cell lines. Mutation Research *379*, 177-184.

Stack, J. H., DeWald, D. B., Takegawa, K., and Emr, S. D. (1995). Vesicle-mediated protein transport: Regulatory interactions between the Vps15 protein kinase and the Vps34 PtdIns 3-kinase essential for protein sorting to the vacuole in yeast. The Journal of Cell Biology *129*, 321-334.

Stack, J. N., and Emr, S. D. (1994). Vps34 required for yeast vacuolar protein sorting is a multispecificity kinase that exhibits both protein and phophatidylinositol specific PI 3-kinase activities. Journal of Biological Chemistry *269*, 31552-31562.

Stankovic, T., Kidd, A. M. J., Sutcliffe, A., McGuire, G. M., Robinson, P., Weber, P., Bedenham, T., Bradwell, A. R., Easton, D. F., Lennox, G. G., Haites, N., Byrd, P. J., and Taylor, A. M. R. (1998). ATM mutations and phenotypes in ataxia-telangiectasia families in the British Isle: Expression of mutant ATM and

the risk of leukaemia, lymphoma and breast cancer. American Journal of Human Genetics *62*, 334-345.

Stern, M. H., Soulier, J., Rosenzwajg, M., Nakahara, K., Canki-Klain, N., Aurias, A., Sigaux, F., and Kirsch, I. R. (1993). MTCP-1: a novel gene on the human chromosome Xq28 translocated to the T cell receptor alpha/delta locus in mature T cell proliferations. Oncogene *8*, 2475-83.

Strathdee, C. A., Duncan, A. M., and Buchwald, M. (1992). Evidence for at least four Fanconi anaemia genes including FACC in chromosome 9. Nature Genetics *1*, 196-198.

Strathdee, C. A., Gavish, H., Shannon, W. R., and Buchwald, M. (1992). Cloning of cDNAs for Fanconi's anaemia by functional complementation. Nature *358*, 434.

Stratton, M. R. (1996). Recent advances in understanding of genetic susceptibility to breast cancer. Human Molecular Genetics *5*, 1515-1519.

Straughen, J., Ciocci, S., Ye, T. Z., Lennon, D. N., Proytcheva, M., Alhadeff, B., Goodfellow, P., German, J., Ellis, N. A., and Groden, J. (1996). Physical mapping of the Bloom syndrome region by the identification of YAC and P1 clones from human chromosome 15 band q26.1. Genomics *35*, 118-28.

Sullivan, K. E., Veksler, E., Lederman, H., and Lees-Miller, S. P. (1997). Cell cycle checkpoints and DNA repair in Nijmegen breakage syndrome. Clinical Immunology & Immunopathology *82*, 43-8.

Sung, P., Bailly, V., Weber, C., Thompson, L. H., Prakash, L., and Prakash, S. (1993). Human xeroderma pigmentosum group D gene encodes a DNA helicase. Nature *365*, 852-5.

Swift, M. (1971). Fanconi's anaemia in the genetics of neoplasia. Nature *230*, 370-373.

Swift, M. (1994). Ionizing radiation, breast cancer, and ataxia-telangiectasia [editorial; comment]. Journal of the National Cancer Institute *86*, 1571-2.

Swift, M., Morrell, D., Cromartie, E., Chamberlin, A. R., Skolnick, M. H., and Bishop, D. T. (1986). The incidence and gene frequency of ataxia-telangiectasia in the United States. American Journal of Human Genetics *39*, 573-83.

Swift, M., Morrell, D., Massey, R. B., and Chase, C. L. (1991). Incidence of cancer in 161 families affected by ataxia-telangiectasia [see comments]. New England Journal of Medicine *325*, 1831-6.

Swift, M., Reitnauer, P. J., Morrell, D., and Chase, C. L. (1987). Breast and other cancers in families with ataxia-telangiectasia. New England Journal of Medicine *316*, 1289-94.

Swift, M., Sholman, L., Perry, M., and Chase, C. (1976). Malignant neoplasms in the families of patients with ataxia-telangiectasia. Cancer Research *36*, 209-15.

Taalman, R. D., Jaspers, N. G., Scheres, J. M., de Wit, J., and Hustinx, T. W. (1983). Hypersensitivity to ionizing radiation, in vitro, in a new chromosomal breakage disorder, the Nijmegen Breakage Syndrome. Mutation Research *112*, 23-32.

Taj, S., and Nagarajan, B. (1994). Induction of genotoxicity by salted deep-fried fish and mutton. Mutation Research *322*, 45-54.

Takayama, K., Salazar, E. P., Broughton, B. C., Lehmann, A. R., Sarasin, A., Thompson, L. H., and Weber, C. A. (1996). Defects in the DNA repair and transcription gene ERCC2 (XPD) in trichothiodystrophy. American Journal of Human Genetics *58*, 263-270.

Takayama, K., Salazar, E. P., Lehmann, A., Stefanini, M., Thompson, L. H., and Weber, C. A. (1995). Defects in the DNA repair and transcription gene ERCC2 in the cancer-prone disorder xeroderma pigmentosum group D. Cancer Research *55*, 5656-63.

Tavtigian, S. V., Simard, J., Rommens, J., Couch, F., Shattuck-Eidens, D., Neuhausen, S., Merajver, S., Thorlacius, S., Offit, K., Stoppa-Lyonnet, D., Belanger, C., Bell, R., Berry, S., Bogden, R., Chen, Q., Davis, T., Dumont, M.,

Frye, C., Hattier, T., Jammulapati, S., Janecki, T., Jiang, P., Kehrer, R., Leblanc, J. F., Mitchell, J. T., McArthur-Morrison, J., Nguyen, K., Peng, Y., Samson, C., Schreder, M., Snyder, S. C., Steele, L., Stringfellow, M., Stroup, C., Swedlund, B., Swensen, J., Teng, D., Thomas, A., Tran, T., Tranchant, M., Weaver-Feldhaus, J., Wong, A. K. C., Shizuya, H., EyFjord, J. E., Cannon-Albright, L., Labrie, F., Skolnick, M. H., Weber, B., Kamb, A., and Goldgar, D. E. (1996). The complete BRCA2 gene and mutations in chromosome 13q-linked kindreds. Nature Genetics *12*, 333-337.

Taylor, A. M. (1992). Ataxia telangiectasia genes and predisposition to leukaemia, lymphoma and breast cancer [editorial]. [Review] [42 refs]. British Journal of Cancer *66*, 5-9.

Taylor, A. M. (1978). Unrepaired DNA strand breaks in irradiated ataxia telangiectasia lymphocytes suggested from cytogenetic observations. Mutation Research *50*, 407-18.

Taylor, A. M., Metcalfe, J. A., Thick, J., and Mak, Y. F. (1996). Leukemia and lymphoma in ataxia telangiectasia. [Review] [110 refs]. Blood *87*, 423-38.

Taylor, A. M. R. (1998). What has the cloning of the *ATM* gene told us about ataxia telangiectasia. International Journal of Radiation Biology *73*, 365-371.

Taylor, S. S., Knighton, D. R., Zheng, J. H., Teneyck, L. F., and Sowadski, J. M. (1992). Structural framework for the protein kinase family. Annual reviews in Cell Biology *8*, 429-462.

Tlsty, T. D., Briot, A., Gualberto, A., Hall, I., Hess, S., Hixon, M., Kuppuswamy, D., Romanov, S., Sage, M., and White, A. (1995). Genomic instability and cancer. Mutation Research 337, 1-7.

Uziel, T., Savitsky, K., Platzer, M., Ziv, Y., Helbitz, T., Nehls, M., Boehm, T., Rosenthal, A., Shiloh, Y., and Rotman, G. (1996). Genomic Organization of the ATM gene. Genomics 33, 317-20.

Varon, R., Vissinga, C., Platzer, M., Cerosaletti, K. M., Chrzanowska, K. H., Saar, K., Beckman, G., Nowak, N. J., Stumm, M., Weemaes, C. M. R., Gatti, R. A., Wilson, R. K., Digweed, M., Rosenthal, A., Sperling, K., Concannon, P., and Reis, A. (1998). Nibrin, a novel DNA double-strand break repair protein, is mutated in Nijmegen breakage syndrome. Cell 93, 467-476.

Vasen, H. F., Mecklin, J. P., Khan, P. M., and Lynch, H. T. (1991). The International Collaborative Group on Hereditary Non-Polyposis Colorectal Cancer (ICG-HNPCC). Diseases of the Colon & Rectum 34, 424-5.

Verlander, P. C., Lin, J. D., Udono, M. U., Zhang, Q., Gibson, R. A., Mathew, C. G., and Auerbach, A. D. (1994). Mutation analysis of the Fanconi anemia gene FACC. American Journal of Human Genetics *54*, 595-601.

Virgilio, L., Narducci, M. G., Isobe, M., Billips, L. G., Cooper, M. D., Croce, C. M., and Russo, G. (1994). Identification of the TCL1 gene involved in T cell malignancies. Proceedings of the National Academy of Science, USA *91*, 12530.

Visvardis, E. E., Tassiou, A. M., and Piperakis, S. M. (1997). Study of DNA damage induction and repair capacity of fresh and cryopreserved lymphocytes exposed to H_2O_2 and γ-irradiation with the alkaline comet assay. Mutation Research *383*, 71-80.

Vorechovsky, I., Luo, L., Dyer, M. J. S., Catovsky, D., Amlot, P. L., Yaxley, J. C., Foroni, L., Hammarstrom, L., Webster, A. D. B., and Yuille, M. A. R. (1997). Clustering of missense mutations in the ataxia-telangiectasia gene in a sporadic T cell leukaemia. Nature Genetics *17*, 96-99.

Wang, L., Cui, L., Lord, B. I., Roberts, S. A., Potten, C. S., Hendry, J. H., and Scott, D. (1996). Gamma-ray-induced cell killing and chromosome abnormalities in the bone marrow of p53 deficient mice. Radiation Research *196*, 259-266.

Waterman, M. J. F., Stavridi, E. S., Waterman, J. L. F., and Halazonetis, T. D. (1998). ATM-dependent activation of p53 involves dephosphorylation and association with 14-3-3 proteins. Nature Genetics *19*, 175-178.

Watt, P. M., Hickson, I. D., Borts, R. H., and Louis, E. J. (1996). SGS1, a homologue of the Bloom's and Werner's syndrome genes, is required for maintenance of genome stability in Saccharomyces cerevisiae. Genetics *144*, 935-45.

Watt, P. M., Louis, E. J., Borts, R. H., and Hickson, I. D. (1995). Sgs-1: eukaryotic homolog of E. coli RecQ that interacts with topoisomerase II in vivo and is required for faithful chromosome segregation. Cell *81*, 253-260.

Watters, D., Khanna, K. K., Beamish, H., Birrell, G., Spring, K., Kedar, P., Gatei, M., Stenzel, D., Hobson, K., Kozlov, S., Zhang, N., Farrell, A., Ramsay, J., Gatti, R., and Lavin, M. (1997). Cellular localisation of the ataxia-telangiectasia (ATM) gene product and discrimination between mutated and normal forms. Oncogene *14*, 1911-21.

Weemaes, C. M., Hustinx, T. W., Scheres, J. M., van Munster, P. J., Bakkeren, J. A., and Taalman, R. D. (1981). A new chromosomal instability disorder: the Nijmegen breakage syndrome. Acta Paediatrica Scandinavica *70*, 557-64.

Wegner, R. D., Chrzanowska, K. H., Sperling, K., and Stumm, M. (1998). Ataxia-telangiectasia variants. In Primary immunodeficiency diseases, a

molecular and genetic approach, H. D. Ochs, E. Smith and G. Puck, eds. (Oxford: Oxford University Press).

Wei, Q., and Spitz, M. R. (1997). The role of DNA repair capacity in susceptibility to lung cancer. Cancer and Metastasis Reviews *16*, 295-307.

Whitney, M., Thayer, M., Reifsteck, C., Olson, S., Smith, L., Jakobs, P. M., Leach, R., Naylor, S., Joenje, H., and Grompe, M. (1995). Microcell mediated chromosome transfer maps the Fanconi anaemia group D gene to chromosome 3p. Nature Genetics *11*, 341-3.

Whitney, M. A., Saito, H., Jakobs, P. M., Gibson, R. A., Moses, R. E., and Grompe, M. (1993). A common mutation in the FACC gene causes Fanconi anaemia in Ashkenazi Jews. Nature Genetics *4*, 202-5.

Wong, A. K. C., Pero, R., Ormonde, P. A., Tavtigian, S. V., and Bartel, P. L. (1997). RAD51 interacts with the evolutionary conserved BRC motifs in the human breast cancer susceptibility gene Brca2. Journal of Biological Chemistry *272*, 31941-31944.

Woods, C. G., Bundey, S. E., and Taylor, A. M. R. (1990). Unusual features in the inheritance of ataxia telangiectasia. Human Genetics *84*, 555-562.

Wooster, R., Bignell, G., Lancaster, J., Swift, S., Seal, S., Manglon, J., Collins, N., Gregory, S., Gumbs, C., Micklem, G., Barfoot, R., Hamoudi, R., Patel, S., Rice, C., Biggs, P., Hashim, Y., Smith, A., Connor, F., Arason, A., Gudmundsson, J., Ficenec, D., Keisell, D., Ford, D., Tonin, P., Bishop, D. T., Spurr, N. K., Ponder, B. A. J., Eels, R., Peto, J., Devilee, P., Cornelisse, C., Lynch, H., Narod, S., Lenoir, G., Eglisson, V., Barkadottir, R. B., Easton, D. F., Bentley, D. R., Futreal, P. A., Ashworth, A., and Stratton, M. R. (1995). Identification of the breast cancer susceptibility gene BRCA2. Nature *378*, 789-792.

Wooster, R., Ford, D., Mangion, J., Ponder, B. A., Peto, J., Easton, D. F., and Stratton, M. R. (1993). Absence of linkage to the ataxia telangiectasia locus in familial breast cancer. Human Genetics *92*, 91-4.

Wright, J. A., Keegan, K. S., Herendeen, D. R., Bentley, N. J., Carr, A. M., Hoekstra, M. F., and Concannon, P. (1998). Protein kinase mutants of human ATR increase sensitivity to UV and ionizing radiation and abrogate cell cycle checkpoint control. Proceedings of the National Academy of Science, USA *95*, 7445-7450.

Young, B. R., and Painter, R. B. (1989). Radioresistant DNA synthesis and human genetic diseases. Human Genetics *82*, 113-7.

Yuille, M. A. R., Coignet, L. J. A., Abraham, S. M., Yaqub, F., Luo, L., Matutes, E., Brito-Babapulle, V., Vorechovsky, I., Dyer, M. J. S., and Catovsky, D. (1998). ATM is usually rearranged in T-cell prolymphocytic leukaemia. Oncogene *16*, 789-796.

Zakian, V. A. (1995). ATM-related genes: what do they tell us about functions of the human gene?. [Review] [30 refs]. Cell *82*, 685-7.

Zuppan, P., Hall, J. M., Lee, M. K., Ponglikitmongkol, M., and King, M.-C. (1991). Possible linkage of the estrogen receptor gene to breast cancer in a family with late-onset disease. American Journal of Human Genetics *48*, 1065-1068.